A Practical Guide to Soil-Structure Interaction

FEMA P-2091 / December 2020

FEMA

nehrp

A Practical Guide to Soil-Structure Interaction

Prepared by

APPLIED TECHNOLOGY COUNCIL
201 Redwood Shores Parkway, Suite 240
Redwood City, California 94065
www.ATCouncil.org

Prepared for

FEDERAL EMERGENCY MANAGEMENT AGENCY
Michael Mahoney, Project Officer
Robert D. Hanson, Subject Matter Expert
Washington, D.C.

APPLIED TECHNOLOGY COUNCIL
Jon A. Heintz, Program Executive, Program Manager
Ayse Hortacsu, Project Manager

PROJECT TECHNICAL COMMITTEE
Bret Lizundia (Project Technical Director)
C.B. Crouse
Steve Harris
Boris Jeremic
Jonathan P. Stewart
Michael Valley

PROJECT REVIEW PANEL
Peter Lee
Sissy Nikolaou*
Robert Pekelnicky
Payman Khalili Tehrani

*ATC Board Representative

WORKING GROUP MEMBERS
Timothy D. Ancheta
Laurel Jiang
Ricardo Henoch
Gyimah Kasali
Lisa M. Star
Christos Tokas
Jiejing Zhou

FEMA

nehrp

Notice

Any opinions, findings, conclusions, or recommendations expressed in this publication do not necessarily reflect the views of the Applied Technology Council (ATC), the Department of Homeland Security (DHS), or the Federal Emergency Management Agency (FEMA). Additionally, neither ATC, DHS, FEMA, nor any of their employees, makes any warranty, expressed or implied, nor assumes any legal liability or responsibility for the accuracy, completeness, or usefulness of any information, product, or process included in this publication. Users of information from this publication assume all liability arising from such use. The contents of this document do not have the force and effect of law and are not meant to bind the public in any way. This document is intended only to provide clarity to the public regarding existing requirements under the law or agency policies.

Cover image – Photo of project site showing soil conditions and foundation and superstructure under construction.

Preface

Modern building codes include criteria for how ground motions enter a structure's foundation and affect the building response. This soil-structure interaction (SSI) can make a substantial difference in how buildings behave during earthquake shaking and how they should be designed, yet there is relatively little implementation of SSI effects by practicing structural engineers. Provisions are available in ASCE/SEI 7-16 and in ASCE/SEI 41-17 that can be used to address SSI. In addition, a research report prepared by the National Institute of Standards and Technology (NIST) published in 2012 is also a valuable resource.

In 2019, the Applied Technology Council (ATC), with funding from FEMA under Task Order Contract HSFE60-17-D-1005, commenced the ATC-144 project. The objective of this project was to develop this document, *A Practical Guide to Soil-Structure Interaction*, to present information regarding SSI as implemented in code provisions but in an easy-to-understand, concise format targeted toward practicing engineers to help them determine when SSI effects are of importance and show them examples of how to implement them in design.

ATC is indebted to the leadership of Bret Lizundia, Project Technical Director, and to the members of the ATC-144 Project Team for their efforts in developing this *Guide*. The Project Technical Committee, consisting of C.B. Crouse, Steve Harris, Boris Jeremic, Bret Lizundia (Chair), Jonathan Stewart, and Michael Valley, performed the technical development efforts and served as primary authors. Tim Ancheta, Laurel Jiang, Gyimah Kasali, and Lisa Star assisted in the development of the design examples, and Ricardo Henoch and Jiejing Zhou provided detailed review of the design examples as members of the Project Working Group. Chris Tokas developed many of the figures in the document. The Project Review Panel, consisting of Peter Lee, Sissy Nikolaou, Robert Pekelnicky, and Payman Khalili Tehrani provided technical review, advice, and consultation at key stages of the work. The names and affiliations of all who contributed to this report are provided in the list of Project Participants.

ATC also gratefully acknowledges Michael Mahoney (FEMA Project Officer), and Robert D. Hanson (FEMA Subject Matter Expert) for their input and guidance in the preparation of this document. Carrie J. Perna (ATC) provided report production services.

Ayse Hortacsu
ATC Director of Projects

Jon A. Heintz
ATC Executive Director

Table of Contents

Preface iii

List of Figures ix

List of Tables xv

1. Introduction 1-1
- 1.1 Overview 1-1
- 1.2 Types of Soil-Structure Interaction Modeling 1-1
- 1.3 Purpose of the *Guide* 1-2
- 1.4 Scope of the *Guide* 1-2
- 1.5 Target Audience for the *Guide* 1-2
- 1.6 Key SSI Terminology 1-3
- 1.7 Tips for Understanding and Implementing SSI 1-4
- 1.8 Organization of the *Guide* 1-5

2. Situations Where SSI is Important 2-1
- 2.1 Overview 2-1
- 2.2 Large Building Footprint Reduces Design Forces 2-1
- 2.3 Substantial Foundation Embedment Reduces Design Forces 2-2
- 2.4 High Structure-to-Soil Stiffness Ratios Will Lengthen Period and Change Design Forces 2-2
- 2.5 Foundation Rocking Impacts Superstructure Behavior 2-4

3. Rule of Thumb Test for Inertial SSI Significance 3-1
- 3.1 Overview 3-1
- 3.2 Key Equation 3-1
- 3.3 Determining Average Effective Shear Wave Velocity 3-2
- 3.4 Determining Fundamental Period of the Structure 3-3
- 3.5 Example 3-4
  - 3.5.1 Building Description 3-4
  - 3.5.2 Average Effective Shear Wave Velocity 3-6
  - 3.5.3 Fundamental Period of the Structure 3-7
  - 3.5.4 Structure-to-Soil Stiffness Ratio 3-7
- 3.6 Comparisons Using Site Class 3-7

4. Base Slab Averaging 4-1
- 4.1 Overview 4-1
- 4.2 Key Equations 4-2
- 4.3 Determining Effective Foundation Size 4-3
- 4.4 Determining whether Base Slab Averaging Applies 4-3
- 4.5 Limitations and Issues 4-4
- 4.6 Example 4-5

5. Embedment Effects 5-1
5.1 Overview 5-1
5.2 Key Equation 5-1
5.3 Determining Depth of Embedment 5-2
5.4 Limitations and Issues 5-6
5.5 Example 5-7

6. Foundation and Soil Flexibility 6-1
6.1 Overview 6-1
6.2 Soil Properties for Flexibility Calculations 6-2
6.3 Vertical and Rotational Springs 6-3
6.3.1 Method 1 – Rigid Foundation and Flexible Soil 6-3
6.3.2 Method 2 – Flexible Foundation and Nonlinear Flexible Soil 6-8
6.3.3 Method 3 – Flexible Foundation and Linear Flexible Soil 6-8
6.4 Horizontal Springs 6-9
6.4.1 Method 1 6-10
6.4.2 Resistance due to Passive Pressure 6-12
6.4.3 Resistance due to Friction or Cohesion 6-13
6.5 Bounding Analyses 6-14
6.6 Vertical and Rotational Spring Example 6-14
6.6.1 Method 1 6-15
6.6.2 Method 3 6-15
6.7 Horizontal Spring Example 6-16
6.7.1 Method 1 6-16
6.7.2 Passive Pressure and Friction 6-17

7. Period Lengthening 7-1
7.1 Overview 7-1
7.2 Key Equation 7-2
7.3 Examples to Illustrate Dynamic Response 7-5
7.4 Example Using Code Equations 7-11
7.4.1 Calculations for the Fixed-Base Condition 7-12
7.4.2 Calculations for the Flexible-Base Condition 7-13
7.4.3 Summary of Design Demands 7-15

8. Foundation Damping 8-1
8.1 Overview 8-1
8.2 Foundation Damping Requirements 8-2
8.3 Effective Damping Ratio 8-4
8.4 Soil Damping 8-5
8.4.1 Discussion 8-5
8.4.2 Soil Damping Example 8-6
8.5 Radiation Damping 8-8
8.5.1 Discussion 8-8
8.5.2 Radiation Damping Example 8-9
8.6 Limitations and Issues 8-16
8.6.1 Limitations on the Influence of Radiation Damping 8-16
8.6.2 Potential Code Changes Related to Foundation Damping 8-16

9. How to Model a Basement 9-1
9.1 Overview 9-1
9.2 Past Analytical Comparisons of Different Models 9-1
9.2.1 Models Studied 9-1
9.2.2 Recommended Models 9-4
9.3 Models for Buildings on Relatively Level Grade 9-5
9.3.1 Example Building 9-5
9.3.2 Model 1 for Example Building on Level Grade 9-5
9.3.3 Model 2 for Example Building on Level Grade 9-7
9.4 Models for Buildings on Sloping Grade 9-9
9.4.1 Example Building 9-9
9.4.2 Model 2 for Example Building 9-10

10. Conclusions and Recommendations 10-1
10.1 Overview 10-1
10.2 Conclusions 10-1
10.3 Other Helpful Resources 10-2
10.4 Comparison of SSI Provisions 10-2
10.5 Recommendations 10-2
10.5.1 Recommendations for Code Developers 10-2
10.5.2 Recommendations for Further Study 10-6

Appendix A: Two-Story Building Example A-1
A.1 Overview A-1
A.1.1 Outline of the Example A-2
A.1.2 Limitations in ASCE/SEI 7-16 Chapter 19 ..... A-2
A.2 Site Description A-2
A.3 Building Description A-5
A.3.1 Gravity Framing A-5
A.3.2 Lateral Framing A-5
A.3.3 Gravity Loads and Seismic Weight A-6
A.3.4 Foundation System A-7
A.4 Initial Design A-9
A.4.1 Base Shear per ASCE/SEI 7-16 Chapter 12 Equivalent Lateral Force Procedure A-9
A.4.2 Brace Design A-10
A.4.3 Foundation Design A-11
A.4.4 Fixed-base Modal Analysis A-15
A.5 Flexible-base Analysis A-15
A.5.1 Vertical Springs A-16
A.5.2 Lateral Springs A-17
A.5.3 Flexible-base Modal Analysis A-20
A.6 Foundation Damping A-21
A.6.1 Soil Hysteretic Damping A-22
A.6.2 Radiation Damping A-22
A.6.3 Adjusted Base Shear A-26
A.6.4 Code-limited Adjusted Base Shear A-27
A.7 Design for SSI-Reduced Base Shear per ASCE/SEI 7-16 Chapter 19 ..... A-27
A.7.1 Brace Design A-27
A.7.2 Foundation Design A-28
A.7.3 Fixed-base Modal Analysis A-28
A.7.4 Flexible-base Modal Analysis A-29

A.7.5 Check of Base Shear A-29
A.8 Design for Full Theoretical SSI-Reduced Base Shear A-30
A.8.1 Base Slab Averaging A-30
A.8.2 Brace Design A-32
A.8.3 Foundation Design A-33
A.8.4 Fixed-base Modal Analysis A-33
A.8.5 Flexible-base Modal Analysis A-33
A.8.6 Check of Base Shear A-34
A.8.7 Redesign (Iteration) A-34
A.8.8 Reanalysis A-34
A.8.9 Check of Base Shear A-35

Appendix B: Twelve-Story Building Example B-1
B.1 Overview B-1
B.1.1 Outline of the Example B-1
B.2 Site Description B-2
B.2.1 Geotechnical Properties B-2
B.2.2 Seismic Ground Motion Parameters B-3
B.3 Building Description B-3
B.3.1 Framing Systems B-3
B.3.2 Material Properties and Modeling Criteria B-8
B.3.3 Gravity Loads and Seismic Mass B-9
B.4 Initial Design for Model 1 ..... B-10
B.4.1 Base Shear per ASCE/SEI 7-16 Chapter 12 Equivalent Lateral Force Procedure B-10
B.4.2 Fixed-base Modal Analysis B-13
B.4.3 Story Shears and Moments B-13
B.4.4 Story Drifts B-13
B.4.5 Foundation Design B-13
B.5 Spectral Modifications for Kinematic SSI B-17
B.5.1 Base Slab Averaging B-17
B.5.2 Embedment B-18
B.6 SSI Adjusted Structural Demands B-20
B.6.1 Period Elongation Due to Flexible Base B-20
B.6.2 Foundation Damping B-21
B.6.3 ELF Base Shear Adjusted for SSI B-23
B.6.4 Story Shears, Moments, and Drifts B-24
B.7 Design Variations B-27
B.7.1 Building Without Basement, Fixed Base7 (Model 3) B-27
B.7.2 Building Without Basement, Flexible Base (Model 4) B-27
B.7.3 Sensitivity to Lower-Bound and Upper-Bound Spring Stiffnesses B-29

Appendix C: Helpful Resources C-1

References D-1

Glossary E-1

Symbols F-1

Project Participants G-1

List of Figures

Figure 1-1 Types of soil-structure interaction modeling and scope of the *Guide* 1-2

Figure 1-2 Illustration of free-field motion and its relationship to kinematic interaction and inertial interaction..... 1-3

Figure 2-1 The building on the left with the larger footprint size will have lower design forces than the building with the smaller footprint on the right 2-1

Figure 2-2 The building on the left with a deeper foundation embedment will typically have a greater reduction in design forces than the building on the right..... 2-2

Figure 2-3 A structure where soil flexibility will have a significant impact on the lateral displacement and fundamental period of the structure 2-3

Figure 2-4 Significant impacts of period lengthening and foundation damping on spectral response. The solid black line is the fixed-based spectral response; the dashed black line is the reduction due to the addition of foundation damping to the overall damping ratio..... 2-4

Figure 2-5 The significant impact of soil flexibility on a coupled braced frame system. Utilization ratio is the acceptance ratio as defined in FEMA (2018) and is similar to the demand-to-capacity ratio 2-5

Figure 2-6 The significant impact of soil flexibility on a reinforced concrete shear wall system..... 2-6

Figure 3-1 Example building for rule of thumb test..... 3-4

Figure 3-2 Low strain shear wave velocity at example building site..... 3-5

Figure 4-1 Example building base configurations, showing differing degrees of interconnectivity..... 4-4

Figure 4-2 Example building foundation plan, representative of Condition b in Figure 4-1..... 4-5

Figure 4-3 RRS_{bsa} reduction as a function of period..... 4-7

Figure 4-4 Example resulting response spectrum for S_{DS} =1.0 and S_{D1} = 0.6 4-7

Figure 5-1 Depth of embedment for a building on a mat foundation 5-2

Figure 5-2 Depth of embedment for a building on grade beams and spread footings 5-3

Figure 5-3 Depth of embedment for a building with a basement on perimeter strip footings and interior spread footings 5-3

Figure 5-4 Maximum depth of embedment 5-4

Figure 5-5 Depth of embedment for a smaller partial basement 5-5

Figure 5-6 Depth of embedment for a larger partial basement 5-5

Figure 5-7 Depth of embedment on a sloping site 5-6

Figure 5-8 Example building for embedment effects 5-7

Figure 5-9 Shear wave velocity at example building 5-8

Figure 5-10 Site-specific response spectral acceleration modification factor for foundation embedment, RRS_e 5-11

Figure 5-11 Response spectra for example building, with and without embedment SSI 5-11

Figure 6-1 Three methods for foundation modeling approaches with vertical and rotational springs presented in ASCE/SEI 41 6-4

Figure 6-2 Definitions and orientations of dimensions and axes 6-5

Figure 6-3 Variation of vertical stiffness with foundation dimensions 6-5

Figure 6-4 Variation of rotational stiffness with foundation dimensions 6-6

Figure 6-5 Variation of the embedment modifier vertical stiffness with foundation dimensions 6-7

Figure 6-6 Variation of embedment modifiers for rotational stiffness with foundation dimensions 6-7

Figure 6-7 Vertical stiffness per unit length computed via Method 1, for various foundation half-lengths and half-widths, with stiffness computed by Method 3 for comparison 6-9

Figure 6-8 Variation of horizontal stiffness with foundation dimensions 6-11

Figure 6-9 Variation of the embedment modifier horizontal stiffness with foundation dimensions 6-12

Figure 6-10 Passive pressure mobilization curve 6-13

Figure 7-1 Example acceleration and displacement spectra 7-2

Figure 7-2 Example acceleration and displacement spectra, including points for each example building 7-6

Figure 7-3 Story shears for example buildings 7-8

Figure 7-4 Story moments for example buildings 7-9

Figure 7-5 Story drift ratios for example buildings 7-10

Figure 7-6 Displaced shape for flexible-base, 10-story RCSW building 7-11

Figure 7-7 Design response spectrum for the example building 7-12

Figure 8-1 Example of a foundation and superstructure where foundation damping is not permitted because the unconnected footings are too close 8-3

Figure 8-2 Determining slab-on-grade in-plane flexibility 8-4

Figure 9-1 Illustration of an embedded building configuration with a basement surrounded by soil and a level grade on all sides. u_g represents the free field motion 9-1

Figure 9-2 Modeling approaches for buildings with basements. u_g represents the free field motion, and u_{FIM} represents the foundation input motion. In Model 3 and the full substructure model, the little boxcars are sliders to which the free-field motion is applied. They do not have mass. The mass of the soil is included in the calculation of the free-field motions (and, as applicable, its depth-dependence) 9-2

Figure 9-3 Simplified version of Model 4 in Figure 9-2. u_g represents the free field motion, and u_{FIM} represents the foundation input motion 9-2

Figure 9-4 Example building with basement and relatively level grade 9-5

Figure 9-5 Model 1 distribution of forces for example building 9-7

Figure 9-6 Model 2 distribution of forces for example building 9-9

Figure 9-7 Example building on a sloping site 9-10

Figure 9-8 Model 2 distribution for example building on a slope 9-11

Figure A-1 Generalized soil profile for the Loma Linda Site A-4
Figure A-2 Design acceleration response spectrum per ASCE/SEI 7-16 Chapters 11 and 12 ..... A-5
Figure A-3 Overall view A-7
Figure A-4 Typical floor framing plan (roof framing similar) A-8
Figure A-5 Foundation plan A-8
Figure A-6 Free-body diagram of a typical transverse frame showing the 25%-reduced overturning demands and the maximum factored gravity loads A-13
Figure A-7 Passive pressure mobilization curve A-17
Figure A-8 First-mode displaced shape of a typical frame with foundation flexibility included A-21
Figure A-9 Reductions for base slab averaging relative to building period for three values of effective foundation size A-32
Figure B-1 Design response spectra for the example building B-3
Figure B-2 Typical floor plan of the example building B-4
Figure B-3 Typical sections of the example building B-5
Figure B-4 Analytical model for base case building (Model 1) B-6
Figure B-5 Foundation plan for the example building B-7
Figure B-6 Arrangement of piles and columns or boundary elements at each pile group B-8
Figure B-7 Story shears and moments for Model 1, ELF vs. MRSA B-14
Figure B-8 Story drifts for Model 1, ELF vs. MRSA B-15
Figure B-9 Lateral pile analysis results vs. depth B-17
Figure B-10 Pile group lateral stiffness for Models 1 and 2 ..... B-18
Figure B-11 Kinematic SSI spectral modification factors and design response spectra for the example building B-19
Figure B-12 Analytical model for the example building, with spring supports (Model 2) B-21
Figure B-13 Story shears and moments for Models 1 and 2 ..... B-25
Figure B-14 Story drifts for Models 1 and 2 ..... B-26

Figure B-15 Analytical model of the example building, with basement removed and fixed base (Model 3) B-27

Figure B-16 Analytical model of the example building, with basement removed and flexible base (Model 4) B-28

Figure B-17 Pile group lateral stiffness for Models 3 and 4 .....B-29

List of Tables

Table 3-1 Measured Shear Wave Velocity, v_{si}, at Example Building 3-5

Table 3-2 Structure-to-Soil Stiffness Ratio, $h' / (v_s T)$, for $r = e + z_p = 33$ ft 3-9

Table 3-3 Structure-to-Soil Stiffness Ratio, $h' / (v_s T)$, for $r = e + z_p = 52.5$ ft 3-10

Table 4-1 Values of RRS_{bsa} at Selected Periods for $b_e = 200$ ft 4-6

Table 5-1 Measured Shear Wave Velocity at Example Building 5-8

Table 5-2 Response Spectral Ordinates with and without Embedment Effects 5-10

Table 7-1 Fundamental Mode Dynamic Properties for Example Buildings 7-5

Table 7-2 Summary of Design Demands for Example Building 7-16

Table 8-1 Soil Hysteretic Damping Ratio, β_s 8-6

Table 9-1 Model 1 Distribution of Forces 9-6

Table 9-2 Model 2 Distribution of Forces 9-8

Table 10-1 Comparison of SSI Provisions 10-3

Table A-1 Flat Loads on Roof A-6

Table A-2 Flat Loads on Second Floor A-6

Table A-3 Summary of Seismic Weights A-7

Table A-4 Vertical Distribution of Seismic Forces A-10

Table A-5 Transverse Brace Core Areas A-10

Table A-6 Longitudinal Brace Core Areas A-10

Table A-7 Resisting Moments A-13

Table A-8 Soil Pressures A-14

Table A-9 Resisting Moments A-14
Table A-10 Soil Pressures A-15
Table A-11 Total Lateral Resistance - Transverse Direction at Displacement of 0.015 in A-19
Table A-12 Total Lateral Resistance - Longitudinal Direction at Displacement of 0.035 in A-19
Table A-13 Spring Values A-20
Table A-14 Fundamental Periods for Fixed- and Flexible-Base Models A-21
Table A-15 Tabulation of Reduced Seismic Response A-27
Table A-16 Transverse Brace Core Areas A-28
Table A-17 Longitudinal Brace Core Areas A-28
Table A-18 Updated Spring Values A-29
Table A-19 Updated Fundamental Periods for Fixed-base and Flexible-base Models A-29
Table A-20 Tabulation of Reduced Seismic Response A-29
Table A-21 Tabulation of Reduced Seismic Response with and without Base Slab Averaging A-31
Table A-22 Transverse Brace Core Areas A-33
Table A-23 Longitudinal Brace Core Areas A-33
Table A-24 Updated Fundamental Periods for Fixed-base and Flexible-base Models A-33
Table A-25 Tabulation of Reduced Seismic Response A-34
Table A-26 Updated Fundamental Periods for Fixed-base and Flexible-base Models A-34
Table A-27 Tabulation of Reduced Seismic Response A-35
Table B-1 Site Characteristics B-2
Table B-2 Response Modification Coefficient, Overstrength Factor, and Deflection Amplification Factor for Structural Systems Used B-6
Table B-3 Story Weights and Masses B-10

Table B-4 Fundamental Periods for Model 1 (Fixed-Base) and Model 2 (Flexible-Base) B-21

Table B-5 Design Base Shear for Model 1 (Fixed-Base) and Model 2 (Flexible-Base), Using Best-Estimate Springs .. B-24

Table B-6 Summary of Periods and Base Shears for All Models, E-W Direction B-31

Chapter 1
Introduction

1.1 Overview

Soil-structure interaction (SSI) can make a substantial difference in how buildings behave during earthquake shaking and how they should be designed, and yet there is relatively little implementation of SSI effects by practicing engineers. Provisions are available in Chapter 19 of ASCE/SEI 7-16 *Minimum Design Loads and Associated Criteria for Buildings and Other Structures* (ASCE, 2017a) and in Chapter 8 of ASCE/SEI 41-17 *Seismic Evaluation and Retrofit of Existing Buildings* (ASCE, 2017b) that can be used to address SSI. Another valuable resource that was developed to synthesize fundamental principles and procedures of SSI for application to buildings is *Soil-Structure Interaction for Building Structures* (NIST, 2012a). The overall goal of this *Guide* is to present information regarding SSI as implemented in code provisions but in an easy-to-understand, concise format targeted towards practicing engineers to help them determine when SSI effects are of importance and show them examples of how to implement them in design. Relevant recent research findings that help clarify implementation are provided.

1.2 Types of Soil-Structure Interaction Modeling

There are two common approaches to modeling the interrelationships between a structure, its foundation, and the soil that supports it, including the flexibility and damping of the soil.

One approach is called the **substructure approach** where the soil is represented with springs. The springs are typically vertically oriented to capture foundation rotations, which are often the dominant contributor to SSI effects. Often, the foundation is fixed against horizontal translation. However, horizontal springs can be used to capture the ability of the foundation to displace horizontally relative to the free-field, and dampers can be included to capture foundation damping.

A second approach, called the **direct analysis approach**, is where the soil and the structure are both modeled using finite elements. The soil modeling extends sufficiently around and beneath the building to account for site properties, and seismic waves are imparted at the boundary of the soil and

excite the soil elements which in turn excite the structure. The structure, with its inertial weight and other properties, will in turn affect the behavior of the soil. In current practice, the direct method approach is typically only undertaken on large, critical projects like nuclear power plants or large infrastructure projects such as major bridges, tunnels, subway stations, tanks and marine structures, and requires specialist expertise.

This *Guide* covers the substructure approach with equivalent springs. Some simple SSI techniques do not require development and modeling with springs but rather use calculations of building and site properties to make adjustments in seismic demands. The *Guide* also covers these topics. Figure 1-1 provides a summary of modeling approaches and what is covered by the *Guide.*

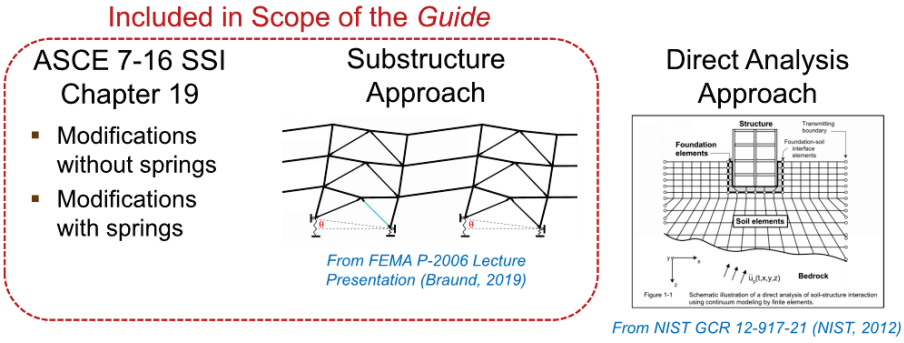

Figure 1-1 Types of soil-structure interaction modeling and scope of the *Guide*.

1.3 Purpose of the *Guide*

The purpose of the *Guide* is (1) to help practicing engineers know when incorporating SSI would be important and (2) to show examples of how to implement different SSI techniques.

1.4 Scope of the *Guide*

The *Guide* covers the SSI topics in ASCE/SEI 7-16 Section 12.13 and Chapter 19, including base slab averaging, foundation embedment, foundation and soil flexibility, period lengthening, and foundation damping. It also provides advice on modeling of basements and gives easy-to-use rules-of-thumb on when SSI is likely to be of significance. The focus is on techniques that practicing engineers can use. As such, soil flexibility is addressed through the use of springs, rather than by finite element modeling.

1.5 Target Audience for the *Guide*

The primary target audience for the *Guide* is practicing engineers who are familiar with seismic design using ASCE/SEI 7 but who have little to no experience with SSI. A secondary audience is engineers who have some

experience with some SSI techniques, such as using springs, but may need advice on other SSI techniques they have not utilized.

1.6 Key SSI Terminology

It is helpful to understand some key SSI terms that are used in ASCE/SEI 7-16 and ASCE/SEI 41-17. The terms are also illustrated in Figure 1-2. Motion at the ground surface in the absence of a structure and its foundation is called **free-field motion**. It is typically larger than the **foundation input motion** that effectively excites the structure and its foundation. The modification of free-field motion into the foundation input motion comes from **kinematic interaction**. The foundation input motion can be viewed as the motion applied to the ends of horizontal foundation springs; it differs from the actual motion of the foundation due to the inertial response of the structure and the deflections that response produces in foundation springs. That response is referred to as **inertial interaction**.

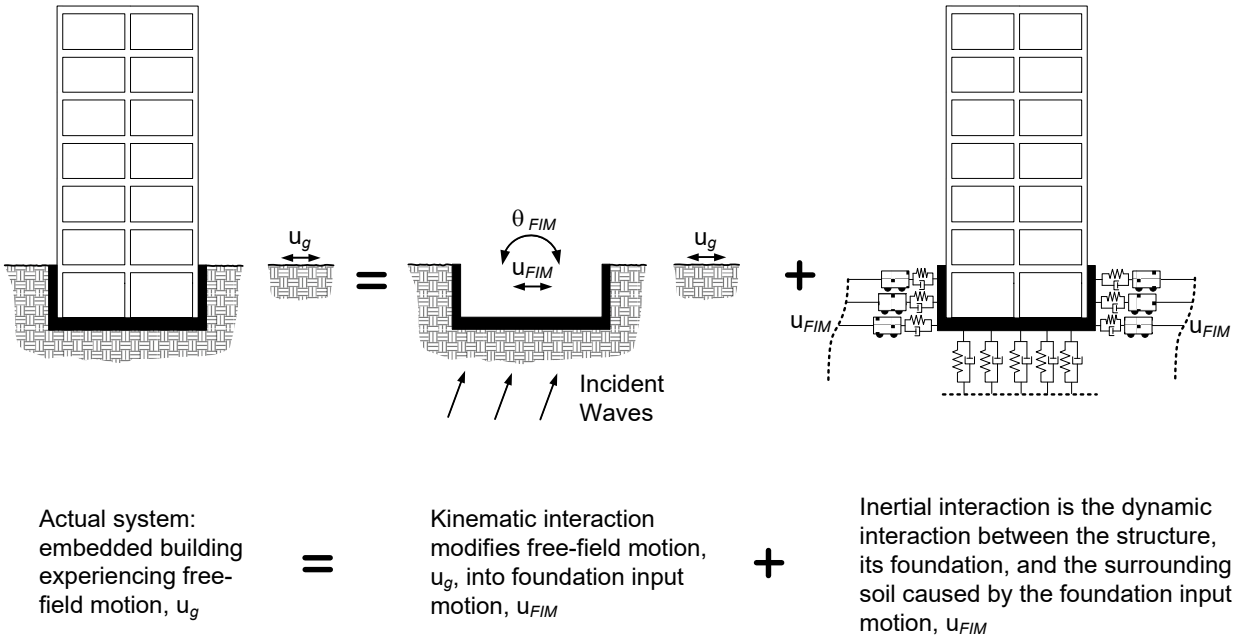

Figure 1-2 Illustration of free-field motion and its relationship to kinematic interaction and inertial interaction (modified from Figure 1-2 in NIST, 2012a).

Kinematic interaction modifies the free-field ground motion to a foundation input motion as a result of spatial variability in the free-field ground motions. Those spatially variable motions are averaged within the building envelope and over the foundation depth within the foundation footprint due to the stiffness and strength of the foundation system. The two kinematic SSI effects are (1) **base slab averaging** of shallow (nonembedded) foundations caused primarily by wave incoherence over the base area and secondarily by incoming seismic waves at non-vertical incidence; and (2) **embedment**

effects in which foundation-level motions are reduced as a result of ground motion reduction with depth below the free surface in structures with embedded foundations. **Base slab averaging** and **embedment effects** can be combined.

Inertial interaction is the dynamic interaction between the structure, its foundation, and the surrounding soil caused by the foundation input motion, and includes: (1) **period lengthening**, the increase in the building period due to foundation flexibility; (2) **radiation damping**, the damping in the soil-structure system caused by the generation and propagation of waves away from the foundation, which are caused by dynamic displacements of the foundation relative to the free-field displacements; and (3) **soil damping**, the hysteretic (material) damping of the soil, similar to inherent viscous damping in the superstructure, but it is independent of the flexible-base period of the structure.

1.7 Tips for Understanding and Implementing SSI

Blue comment boxes are used in the *Guide* to highlight useful tips and summarize key points.

Based on experience in performing SSI analyses, the following general observations are offered. These observations are discussed in detail in the *Guide*. Blue comment boxes are used to highlight useful tips and to summarize key points in the *Guide*.

- SSI is not that difficult to implement.
- SSI is typically iterative, so it may require additional rounds of analysis, as compared to a fixed base analysis, to converge on the final solution.
- SSI typically reduces the seismic demands that are used for design, but there are unusual cases with site-specific response spectra where demands can increase because period elongation may lead to climbing up the response spectrum with increasing levels of spectral acceleration.
- Adding foundation flexibility to a model can change deformation patterns in the superstructure, which can stress particular elements in a different way than in a fixed base model. For example, adding foundation flexibility can lead to rocking of shear walls or braced frames and increased demands on couple beams connecting rocking elements.
- Effective shear wave velocity, v_s, is a key parameter in several SSI equations and techniques. The effective shear wave velocity differs from the low-strain shear wave velocity, v_{so}, used for site classification in ASCE/SEI 7-16 Chapter 20. The parameter, v_s, depends on soil type, site spectral acceleration, and the depth of importance. The *Guide* provides detailed guidance on the subtle, but important, differences between v_s and v_{so}.

- There are a number of code provisions, both in ASCE/SEI 7-16 Chapter 12 and Chapter 19, that can limit the extent of SSI reductions that can be utilized.
- Although ASCE/SEI 7-16 is the standard that is referenced and used in the *Guide*'s design examples, ASCE/SEI 41-17 has a similar set of SSI provisions. In some cases, ASCE/SEI 41-17 has more relaxed requirements and limitations regarding the use of SSI. The *Guide* highlights these differences, typically in a green comment box.

ASCE/SEI 41-17

Although ASCE/SEI 7-16 is the standard that is referenced and used in the design examples in the *Guide*, key differences between the SSI provisions in ASCE/SEI 41-17 and those in ASCE/SEI 7-16 are noted in green comment boxes.

1.8 Organization of the *Guide*

The remainder of the *Guide* is organized into the following chapters.

- **Chapter 2, Situations Where SSI is Important,** provides a series of example images and related discussion of situations that engineers commonly encounter where SSI can impact the forces used in design and the way the structure responds to earthquake shaking.
- **Chapter 3, Rule-of-Thumb Test for SSI Importance,** describes a simple test that can be used at the start of a project when only very limited information is available to help determine if using SSI will likely make a difference in results. The rule of thumb is targeted at inertial interaction and does not provide information about the potential significance of kinematic interaction.
- **Chapter 4, Base Slab Averaging,** addresses how the interconnectivity of the foundation can help reduce the demands into the structure. It provides examples of common foundation situations and whether base slab averaging can be used.
- **Chapter 5, Embedment Effects,** discusses how foundation embedment can reduce the demands on the structure.
- **Chapter 6, Foundation and Soil Flexibility,** reviews different methods for adding vertical and horizontal springs to represent soil flexibility.
- **Chapter 7, Period Lengthening,** covers provisions for how soil flexibility leads to period lengthening in the structural response and the resulting impact on seismic demands.
- **Chapter 8, Foundation Damping,** shows how and when to apply two types of foundation damping—called radiation damping and soil damping—that can reduce demands on the structure.
- **Chapter 9, How to Model a Basement,** discusses different simple but accurate analytical approaches to modeling basements.

- **Chapter 10, Conclusions and Recommendations,** summarizes key points regarding SSI discussed in the *Guide* and provides recommendations on revisions needed to code SSI provisions and further SSI studies that should be undertaken.
- **Appendix A, Two-Story Building Example,** provides a detailed example of applying different SSI techniques for a two-story steel buckling-restrained braced frame building supported by spread footings. SSI topics include implementation of soil springs and reduction in seismic demands due to foundation and soil flexibility, foundation damping, and base slab averaging.
- **Appendix B, Twelve-Story Building Example,** provides a detailed example of applying different SSI techniques for a 12-story concrete building that has a moment frame in one direction and a dual system with a moment frame and shear wall in the other direction. It is pile supported and includes variations with and without a basement. SSI topics covered include reduction in design demands due to base slab averaging and foundation embedment, adjustments to demands from period elongation and foundation damping, and impacts of limitations imposed by ASCE/SEI 7-16 provisions.

The *Guide* also includes lists of helpful resources for SSI and references cited, as well as a glossary of key terms, a list of symbols used, and a list of project participants.

Computer output is shown in some design examples. FEMA, the authors, and the project participants do not endorse any particular computer software program or vendor.

Chapter 2
Situations Where SSI is Important

2.1 Overview

In some situations, soil-structure interaction (SSI) can make a substantial difference in how buildings behave during earthquake shaking and in the forces used in their design. This chapter shows qualitative, graphic examples of such situations that can arise in practice. Quantitative, detailed discussion is covered in subsequent chapters.

Topics Covered

This chapter shows graphic examples of situations that arise in practice where SSI can make a substantial difference in how the building behaves and in the forces used in their design. Examples include:

- Large building footprint.
- Substantial foundation embedment.
- Period lengthening changes design forces.
- Soil flexibility induces rocking of the superstructure and impacts behavior.

2.2 Large Building Footprint Reduces Design Forces

Building footprint size has been shown to correlate with spectral demands, primarily in the shorter period range. The larger the building footprint, the greater the reduction in short period spectral response. This is due to the kinematic interaction effects of base slab averaging. Chapter 4 of this *Guide* discusses base slab averaging in detail.

Figure 2-1 shows an example of a large building where the reduction will be greater and a smaller building where the reduction will be smaller.

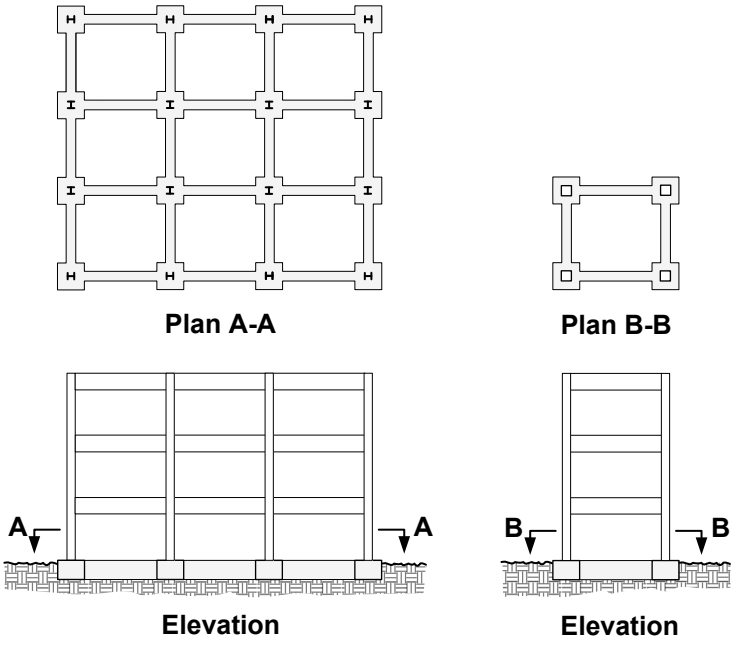

Figure 2-1 The building on the left with the larger footprint size will have lower design forces than the building with the smaller footprint on the right.

2.3 Substantial Foundation Embedment Reduces Design Forces

Combining SSI Effects

The reduction in design forces from large building footprints and foundation embedment can be and often are combined.

Foundation embedment has been shown to correlate with spectral demands, primarily in the shorter period range. Typically, the deeper the embedment, the greater the reduction in short period spectral response. This is due to the decrease of ground motion amplitudes with depth, which is a typical feature of site response. Chapter 5 of this *Guide* discusses kinematic interaction effects from embedment effects in detail.

Figure 2-2 shows an example of a building with a basement where the reduction in demand is expected to be greater and a building without a basement where there is no reduction.

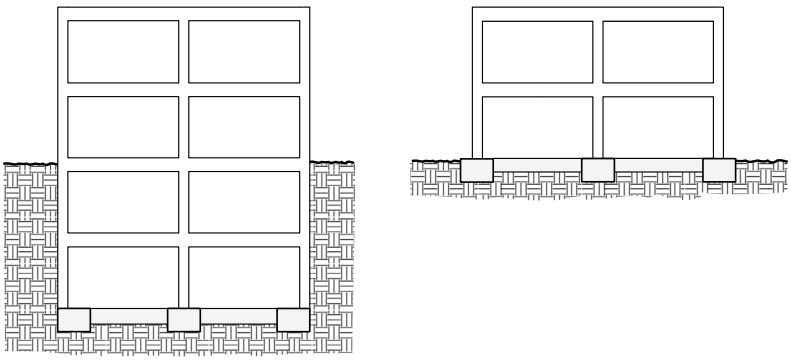

Figure 2-2 The building on the left with a deeper foundation embedment will typically have a greater reduction in design forces than the building on the right.

2.4 High Structure-to-Soil Stiffness Ratios Will Lengthen Period and Change Design Forces

When the structure is relatively stiff compared to the soil, foundation rotation and translation relative to the free-field motion can occur adding to structural displacements and increasing or lengthening the fundamental period of the structure. The increase in period can affect the associated spectral accelerations used in design. This effect commonly occurs in buildings with a concentrated lateral force-resisting system, such as reinforced concrete shear walls and steel braced frames that are supported on localized foundation elements on flexible soils. Conversely, for a building with wide, stiff foundations on very stiff soils and relatively flexible superstructures, the impact of soil flexibility on the building response is typically relatively small.

Figure 2-3 shows an example of a concentrated cantilever shear wall and foundation system where including soil flexibility will increase the fundamental period of vibration. The roof displacement of the shear wall

itself is shown in the left as Δ_w. In the figure on the right, the vertical flexibility of the soil is represented by a set of springs. During lateral displacement of the superstructure, there will be vertical displacement of the springs and foundation rotation. The drift from foundation rotation is shown in the figure on the right as Δ_r. The increase in displacement correlates with an increase in fundamental period for the structure. Figure 2-3 is shown at the shear wall level of detail to provide a scale to illustrate the impact of rotation more clearly and easily. If there are additional walls and other structural elements, they can impact the overall fundamental period. Development of springs is covered in detail in Chapter 6 of this *Guide*.

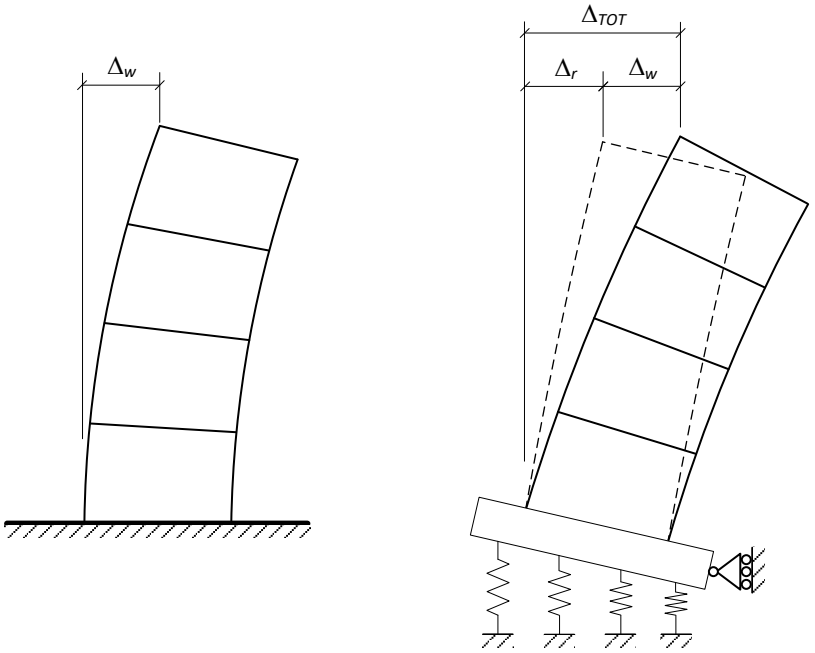

Figure 2-3 A structure where soil flexibility will have a significant impact on the lateral displacement and fundamental period of the structure.

Figure 2-4 shows the potential impact of changing the period in a response spectrum analysis. The period with the fixed base model is denoted as T, and the period with soil flexibility is denoted as $\tilde{T}$. Two cases are shown. In the short period case, the structure is very stiff, and the increase from T to $\tilde{T}$ results in climbing up the response spectrum and an increase in spectral acceleration. In the long period case, the structure is more flexible, and the increase in period results in a reduction in spectral acceleration. Period lengthening is discussed in detail in Chapter 7 of this *Guide*. Figure 2-4 also shows how the addition of foundation damping to the overall damping ratio reduces the spectral acceleration at most periods. Foundation damping is discussed in detail in Chapter 8 of the *Guide*.

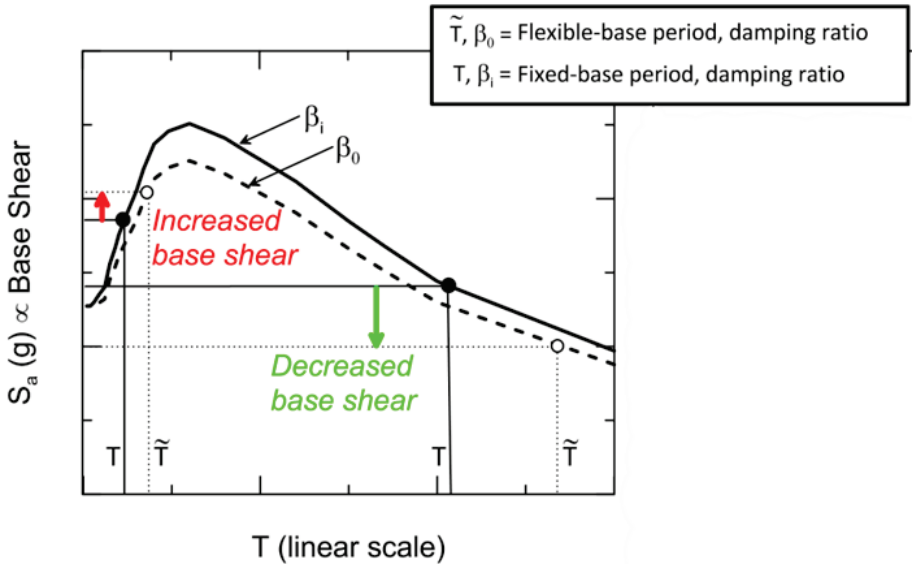

Figure 2-4 Significant impacts of period lengthening and foundation damping on spectral response. The solid black line is the fixed-based spectral response; the dashed black line is the reduction due to the addition of foundation damping to the overall damping ratio. (Adapted from Figure 2-3 in NIST, 2012a).

2.5 Foundation Rocking Impacts Superstructure Behavior

Structures with concentrated coupled vertical lateral force-resisting systems can behave much differently when soil flexibility is introduced. Figure 2-5 shows a nonlinear static (pushover) analysis example. In the fixed-base model shown on top, the mechanism is buckling of the compression brace in the lowest story, and the brace is highly overstressed. In the flexible-base model shown on the bottom where vertical springs are located under each column, the braced frames rock, and the system has sufficient capacity to resist the demands. Note that, in the flexible-base model, the ends of the beams linking the frames have higher rotations than they do in the fixed-base model.

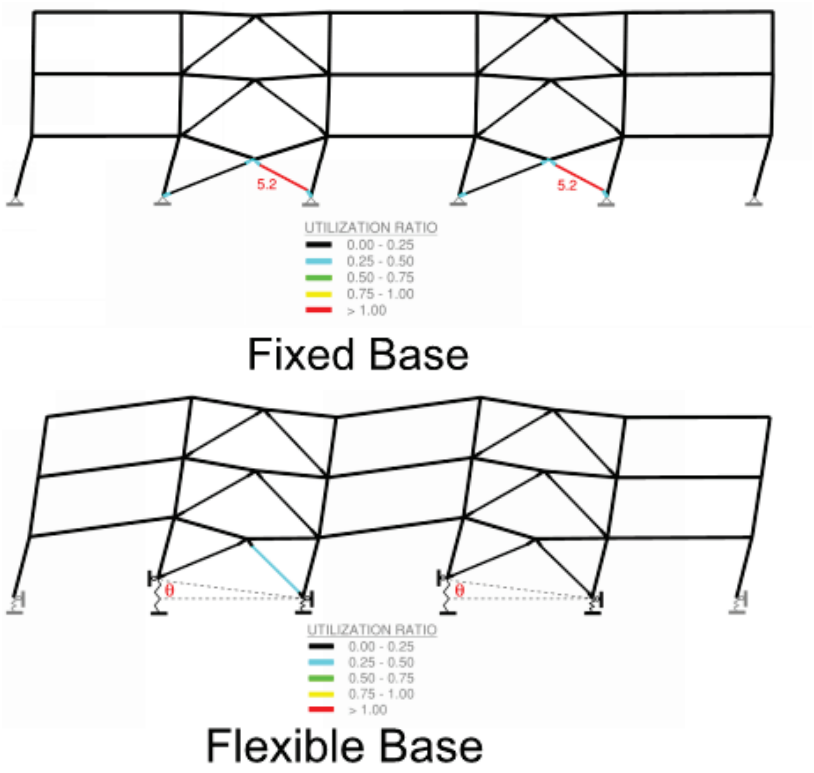

Figure 2-5 The significant impact of soil flexibility on a coupled braced frame system (from FEMA, 2019). Utilization ratio is the acceptance ratio as defined in FEMA (2018) and is similar to the demand-to-capacity ratio.

Figure 2-6 shows a reinforced concrete cantilever shear wall coupled to an adjacent gravity frame of beams and columns. The upper figure shows that a stiff, strong foundation system (represented as a fixed-base condition) can reduce superstructure displacement and protect the adjacent frame from damage, but damage will concentrate in the shear wall base. The lower figure has a more flexible foundation system, which leads to rocking of the shear wall. This increases displacement and damage in the adjacent frame but potentially reduces damage to the shear wall. The response in the lower figure could be modeled with vertical soil springs, similar to those in Figure 2-3. Soil flexibility modeling is discussed in detail in Chapter 6 of this *Guide*.

Foundation stiffness and strength affect various structural components differently.

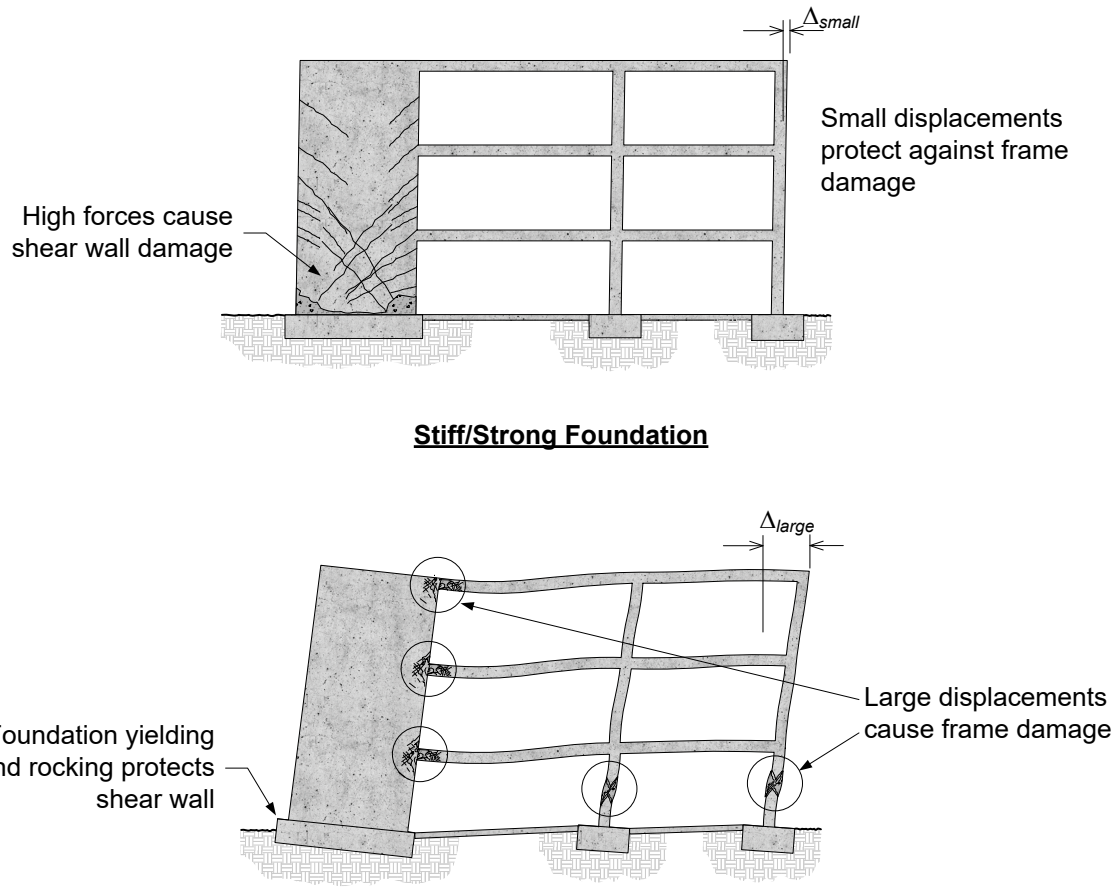

Stiff/strong is not always favorable; nor is flexible/weak always conservative.

Figure 2-6 The significant impact of soil flexibility on a reinforced concrete shear wall system (from ATC, 1996).

Chapter 3
Rule of Thumb Test for Inertial SSI Significance

3.1 Overview

A rule of thumb test to determine if inertial soil-structure interaction (SSI) inertial effects are likely to be significant was developed in *Soil-Structure Interaction for Building Structures* (NIST, 2012a). This test combines three simple parameters that are relatively easy to obtain—building height, fundamental period of the structure, and shear wave velocity—into a term called the **structure-to-soil stiffness ratio** and correlates the ratio with the likelihood that SSI inertial effects will be significant. This test is not contained in ASCE/SEI 7-16 (ASCE, 2017a) or ASCE/SEI 41-17 (ASCE, 2017b). SSI inertial effects include period lengthening addressed in Chapter 7 and foundation damping addressed in Chapter 8 of this *Guide*.

Rule of Thumb Test

Description: Provides an indication before substantial design effort of whether SSI inertial effects may be significant.

Requirements:

- Building height, h_n
- Fundamental fixed-based period of the structure, T
- Average low strain shear wave velocity over the rocking depth, v_{so}
- Footprint dimensions for the width, $2B$, and length, $2L$ of the building
- Depth of embedment of the foundation, e
- Design spectral response acceleration parameter at short periods, S_{DS}
- Site class

3.2 Key Equation

The structure-to-soil stiffness ratio is defined as $h'/(v_s T)$. The equation for the rule of thumb test is the following inequality:

If $h'/(v_s T) > 0.1$, then inertial SSI effects are likely to be significant.

where:

h' = effective structure height, measured from base of foundation to the center of mass of the fundamental mode (in ft). It can be approximated as 2/3 h_n, where h_n is the structure height as defined in ASCE/SEI 7-16 Section 11.2, plus the depth from grade to the bottom of the foundation.

v_s = the average effective shear wave velocity (ft/s) for site soil conditions, taken as the average value of velocity over the effective depth for foundation rotation determined using v_{so} and a velocity reduction factor from ASCE/SEI 7-16 Table 19.3-1 or a site-specific study. Calculation of v_{so} is discussed in Section 3.3 of this *Guide*.

T = fundamental mode of the structure assuming a fixed base at grade (in seconds). Calculation of T is discussed in Section 3.4 of this *Guide*.

3.3 Determining Average Effective Shear Wave Velocity

Site classification is based on the average low strain shear wave velocity, v_{so}, over the top 100 ft (or 30 m) of soil from grade. The average effective shear wave velocity, v_s, is a reduced value that accounts for the larger strains that occur during earthquake shaking. For the rule of thumb test, the depth of significance is not the same as that used for site soil classification. Calculation of the average low strain shear wave velocity over the effective depth for foundation rotation is determined as follows.

Step 1: Determine footing embedment depth, *e*.

The footing embedment depth, e, is the depth to from grade to the bottom of the footing.

Step 2: Determine the effective profile depth, z_p.

The effective profile depth per Equation 2-18c of NIST (2012a) is the parameter, z_p, as determined from the footing width and length as follows.

$$z_p = (B^3 L)^{0.25}$$

where:

B = overall foundation half width (ft). B is measured parallel to the direction of loading

L = overall foundation half width (ft). L is measured perpendicular to the direction of loading

Step 3: Determine the effective depth for foundation rotation, $e + z_p$.

The depth of interest for calculation of the average effective shear wave velocity is the effective depth for foundation rotation which is the sum of the foundation embedment depth and the effective profile depth or $e + z_p$.

Step 4: Determine the average low strain shear wave velocity, v_{so}, over the effective depth for foundation rotation.

Low strain shear wave velocity measurements are those measured for site classification. Typically, they are reported or graphed in layers. The average is determined using the same formula as ASCE/SEI 7-16 Equation 20.4-1.

$$v_{so} = \Sigma d_i / \Sigma (d_i / v_{si})$$

where:

d_i = thickness of any layer between grade and the effective depth for foundation rotation

v_{si} = low strain shear wave velocity in ft/s

Step 5: Determine the effective shear wave velocity ratio, v_s / v_{so}.

Low strain shear wave velocities are converted to the effective shear wave velocities using the effective shear wave velocity ratio in ASCE/SEI 7-16 Table 19.3-1. It varies by site class and short period design spectral acceleration, S_{DS}.

Step 6: Determine the average effective shear wave velocity, v_s.

The average effective shear wave velocity from the ground surface to depth $e + z_p$ is computed as follows:

$$v_s = [v_s / v_{so}] \, (v_{so})$$

where:

v_s = average effective shear wave velocity (ft/s) for site soil conditions

v_{so} = average low strain shear wave velocity (ft/s) for site soil conditions, computed as described in Step 4

$[v_s / v_{so}]$ = effective shear wave velocity ratio from ASCE/SEI 7-16 Table 19.3-1, as identified in Step 6.

Note that in ASCE/SEI 7-16 Section 19.3.3, the definition of v_s uses a depth measured from ground surface to depth e, not $e + z_p$.

Overburden Corrections

NIST (2012a) Section 2.2.2 also includes a procedure for modifying the effective shear wave velocity to account for the increase due to the building weight on the soil. This calculation involves several steps. With an increase in the shear wave velocity, the structure-to-soil stiffness ratio would go down and may be less likely to exceed the threshold value for the rule of thumb test. The refinement is typically relatively minor and not necessary for the rule of thumb calculation.

3.4 Determining Fundamental Period of the Structure

The fundamental period of the structure can be obtained from a computer model or by using the approximate fundamental period from ASCE/SEI 7-16 Equation 12.8-7.

$$T = T_a = C_t \, h_n^{\,x}$$

where:

h_n = structure height as defined in ASCE/SEI 7-16 Section 11.2 plus depth of footing

C_t = coefficient from ASCE/SEI 7-16 Table 12.8-2 that depends on the structural system

x = coefficient from ASCE/SEI 7-16 Table 12.8-2 that depends on the structural system

3.5 Example

3.5.1 Building Description

Figure 3-1 shows an example building to illustrate the rule of thumb test. It is a three-story special concentric braced frame building with one bay of chevron bracing on each perimeter line supported by spread footings linked by grade beams. It is on Site Class D soil, with S_{DS} = 1.0g and S_{D1} = 0.6g from a site-specific investigation. The rule of thumb test will be evaluated in the short direction of the building or parallel to the 2B dimension.

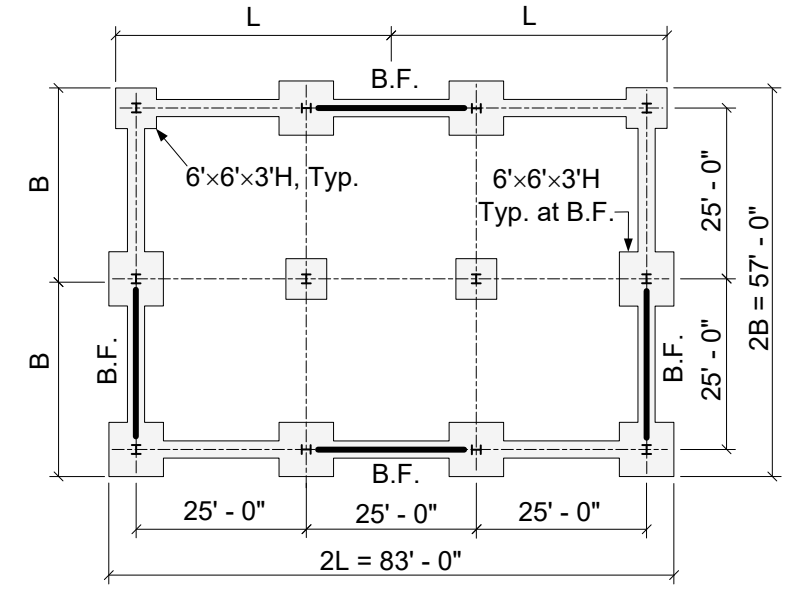

Plan A-A

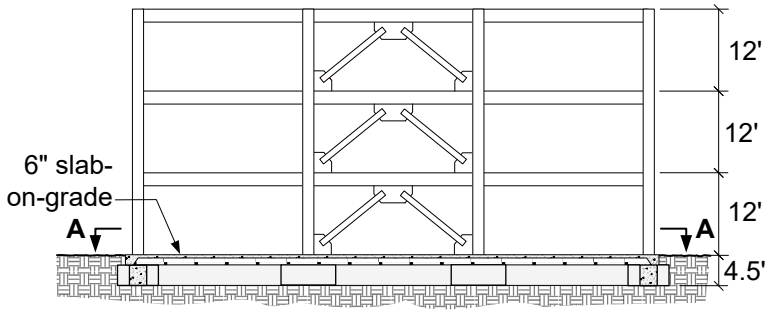

Elevation

Figure 3-1 Example building for rule of thumb test.

For site classification, the low strain shear wave velocity has been measured at the site and is shown in Figure 3-2. The measured velocity for each layer is shown in Table 3-1.

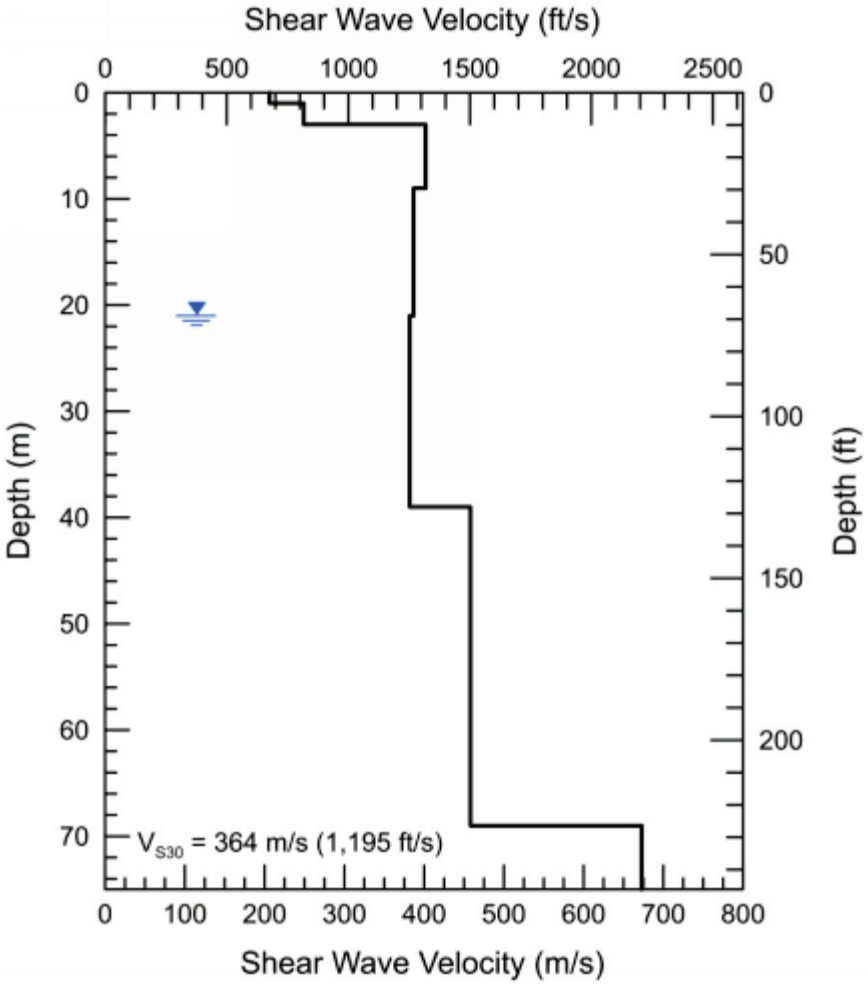

Figure 3-2 Low strain shear wave velocity at example building site.

Table 3-1 Measured Shear Wave Velocity, v_{si} , at Example Building

Depth to Top of Layer (ft)	Layer Thickness (ft)	Shear Wave Velocity, v_{si} (ft/s)
0.0	3.28	676
3.28	6.56	817
9.84	19.69	1,319
29.53	39.37	1,269
68.90	59.10	1,253
128.0	98.40	1,503

Shear Wave Velocity

There are several similar shear wave velocity parameters. ASCE/SEI 7-16 is not consistent with the terms:

In Chapter 20, $\overline{v}_s$ is the "average shear wave velocity." It is taken over the top 100 ft of soil. This is often designated as V_s^{30} for 30 m. Both $\overline{v}_s$ and Vs30 are the low strain shear wave velocity, though this is never stated in Chapter 20.

In Chapter 19, v_{so}, for inertial SSI is the "average low strain shear wave velocity over a depth of *B* below the base of the structure." If the depth *B* were 100 ft it would be the same as $\overline{v}_s$.

In Chapter 19, the low strain shear wave velocity needs to be modified by Table 19.3-1 to obtain the average effective shear wave velocity, v_s.

3.5.2 Average Effective Shear Wave Velocity

Since shear wave velocity data exist for the site, then the average effective shear wave velocity can be calculated directly as follows.

Step 1: Determine footing embedment depth, *e*.

The footing embedment depth, *e*, is calculated per ASCE/SEI 7-16 Section 19.4.2 as described in Chapter 5 of this *Guide*. As the area of the bottom of the grade beams and spread footings does not exceed 75% of the footprint area, the bottom of the grade beams and spread footings does not qualify as the embedment depth, so the embedment depth is taken at the bottom of the slab-on-grade or 0.5 ft.

Step 2: Determine the effective profile depth, z_p.

$$z_p = (B^3 L)^{0.25} = (28.5^3 \times 41.5)^{0.25} = 31.31 \text{ ft}$$

where:

B = overall foundation half width, 57 ft /2 = 28.5 ft. B is in the parallel to the direction of loading

L = overall foundation half width, 83 ft / 2 = 41.5 ft. L is perpendicular to the direction of loading

Step 3: Determine the effective depth for foundation rotation, *r*.

The effective depth for foundation rotation is $r = e + z_p = 0.5 + 31.31 = 31.81$ ft.

Step 4: Determine the average low strain shear wave velocity, v_{so}, over the rocking depth.

$$v_{so} = \Sigma d_i / \Sigma(d_i / v_{si})$$
$$= (31.81 / [(3.28 / 676) + (6.56 / 817) + (19.69 / 1{,}319) + ((31.81 - 29.53) / 1{,}269)]$$
$$= 1{,}074 \text{ ft/s}$$

Step 5: Determine the effective shear wave velocity ratio, v_s / v_{so}.

With S_{DS} / 2.5 = 1.00 /2.5 = 0.4 and Site Class D, then the effective shear wave velocity ratio, [v_s / v_{so}], is 0.71 per ASCE/SEI 7-16 Table 19.3-1.

Step 6: Determine the average effective shear wave velocity, v_s.

Thus, the average effective shear wave velocity over the depth of embedment is $v_s = v_{so} \times [v_s / v_{so}] = 1{,}074$ ft/s $\times$ 0.71 = 763 ft/s.

3.5.3 Fundamental Period of the Structure

A computer model has not yet been created for the structure. ASCE/SEI 7-16 Equation 12.8-7 is used to determine the fundamental period of the structure.

$$T = T_a = C_t\, h_n^x = 0.020 \times 36^{0.75} = 0.294 \text{ s}$$

where:

h_n = 36 ft

C_t = 0.020 (coefficient from ASCE/SEI 7-16 Table 12.8-2 for all other structural systems)

x = 0.75 (coefficient from ASCE/SEI 7-16 Table 12.8-2 for all other structural systems)

3.5.4 Structure-to-Soil Stiffness Ratio

The structure-to-soil stiffness ratio is then calculated as follows.

$$h' / (v_s\, T) = 24.3 \text{ ft} / (763 \text{ ft/s} \times 0.294 \text{ s}) = 0.11 > 0.10$$

where:

h' = This is approximated as 2/3 h_n = 2/3 × (36 ft + e) = 2/3 × (36 + 0.5)

= 24.3 ft

v_s = 763 ft/s, as shown in Section 3.5.2

T = 0.294 s, as shown in Section 3.5.3

Since $h' / (v_s\, T) = 0.11 > 0.10$, SSI inertial effects are likely to have significance.

3.6 Comparisons Using Site Class

When shear wave velocity measurements are not available, the ASCE/SEI 7-16 site classifications can be used instead. Site classifications are defined by the low strain shear wave velocity over the top 100 ft of soil. Table 3-2 compares four common seismic force-resisting systems: steel moment-resisting frame (SMRF), buckling-restrained braced frame (BRBF), special steel concentrically braced frame (SCBF), and reinforced concrete shear wall (RCSW). For each system, five heights are evaluated: 12 ft (for a one-story building), 36 ft (three-story), 60 ft (five-story), 120 ft (ten stories), and 240 ft (20 stories). The approximate fundamental period is calculated for each system at each height using ASCE/SEI 7-16 Equation 12.8-7 (as shown in Section 3.4).

The low shear strain shear wave velocity values, v_{so}, in ASCE/SEI 7-16 Table 20.3-1 for each of the five site classifications are assumed as follows. For Site Class A, the minimum value of 5,000 ft/s is assigned. For Site Classes B, C, and D, the average of the range in Table 20.3-1 is used. For Site Class D, for example, it is (600 ft/s + 1,200 ft/s) /2 = 900 ft/s. For Site Class E, the maximum value of 600 ft/s is used. Shear wave velocity typically increases with depth. Thus, the velocity at the base for effective depth for foundation rotation will be lower than the low shear strain shear wave velocity used in ASCE/SEI 7-16 Table 20.3-1 which is based on a 30 m depth weight average. Boore et al. (2011) provided regression equations to estimate shear wave velocities at depths shallower than 30 m. These have been calculated and added into Table 3-2 as the ratio of v_{so_r}/v_{so}, where v_{so_r} is the v_{so} at the effective depth for foundation rotation, $r = e + z_p$. The average low shear strain shear wave velocity at the effective depth is then converted to the average effective shear wave velocity using the ratios in ASCE/SEI 7-16 Table 19.3-1. For simplicity, a short period spectral acceleration of S_{DS} = 1.0g is assumed. Table 3-2 is for the shallow embedment depth, e = 0.5 ft, in the example. Table 3-3 shows the difference for a much deeper embedment depth of e = 20 ft, which could be for a 16 ft deep basement on a 4 ft mat. Values in red in the tables have $h'/(v_s\ T) > 0.1$ indicating SSI inertial effects are likely to be significant.

Tables 3-2 and 3-3 show several trends.

- The structure-to-soil stiffness ratio, $h'/(v_s T)$, is higher for stiffer structures, so that the RCSW and SCBF structures have the highest ratio, then the BRBF, and then the SMRF with the lowest ratio.
- The structure-to-soil stiffness ratio is higher with the softer site classes because they have the lower average effective shear wave velocity.
- The structure-to-soil stiffness ratio increases with height because of the scaling of period with height in the code equations.
- The structure-to-soil ratio only goes over the 0.10 threshold (indicating inertial SSI effects are potentially significant) for Site Classes D and E with the assigned shear wave velocity, except for taller SCBF and RCSW buildings on Site Class C.

Table 3-2 Structure-to-Soil Stiffness Ratio, $h'/(v_s T)$, for $r = e + z_p = 33$ ft

Example Inputs $e = 0.5$ ft $z_p = 32.5$ ft $r = e + z_p = 33$ ft				Site Class, Shear Wave Velocity and Structure-to-Soil Stiffness Ratio					
					A_{min}	B_{ave}	C_{ave}	D_{ave}	E_{max}
				v_{so}:	5000	3750	1750	900	600
				v_{so_r} / v_{so}:	0.86	0.76	0.63	0.60	0.60
				v_s / v_{so_r}:	1.0	0.97	0.87	0.71	0.22
System	h_n (ft)	$h'=2/3(h_n+e)$ (ft)	T (s)	v_s:	(ft/s)	(ft/s)	(ft/s)	(ft/s)	(ft/s)
SMRF	12	8	0.20		0.009	0.015	0.043	0.106	0.515
	36	24	0.49		0.011	0.018	0.052	0.129	0.624
	60	40	0.74		0.013	0.020	0.057	0.142	0.687
	120	80	1.29		0.014	0.023	0.065	0.162	0.786
	240	160	2.25		0.017	0.026	0.074	0.186	0.902
BRBF	12	8	0.19		0.010	0.016	0.045	0.112	0.544
	36	24	0.44		0.013	0.020	0.058	0.144	0.697
	60	40	0.65		0.015	0.023	0.065	0.163	0.787
	120	80	1.09		0.017	0.027	0.077	0.193	0.933
	240	160	1.83		0.020	0.032	0.091	0.229	1.107
SCBF	12	8	0.13		0.015	0.023	0.067	0.169	0.816
	36	24	0.29		0.019	0.030	0.086	0.216	1.045
	60	40	0.43		0.022	0.034	0.098	0.244	1.181
	120	80	0.73		0.026	0.040	0.116	0.289	1.399
	240	160	1.22		0.031	0.048	0.137	0.343	1.660
RCSW	12	8	0.13		0.015	0.023	0.067	0.169	0.816
	36	24	0.29		0.019	0.030	0.086	0.216	1.045
	60	40	0.43		0.022	0.034	0.098	0.244	1.181
	120	80	0.73		0.026	0.040	0.116	0.289	1.399
	240	160	1.22		0.031	0.048	0.137	0.343	1.660

Notes:

1. v_{so} = average shear wave velocity for small strains over upper 100 ft (30 m) of the site profile from ASCE/SEI 7-16 Table 20.3-1.
2. v_{s_r} / v_{so} = reduction ratio at effective depth for foundation rotation, $r = e + z_p$.
3. v_s / v_{so_r} = ASCE/SEI 7-16 Table 19.3-1 reduction ratio from low strain shear wave velocity to effective shear wave velocity.
4. $v_s = v_{so} \times (v_{s\_r} / v_{so}) \times (v_s / v_{so\_r})$ = effective shear wave velocity at the effective depth for foundation rotation.
5. $S_{DS} = 1.0$g, so $S_{DS}/2.5 = 0.4$.
6. T is per ASCE/SEI 7-16 Equation 12.8-7, $T = C_t h_n^x$.
7. For SMRF, $C_t = 0.028$ and $x = 0.80$, per ASCE/SEI 7-16 Table 12.8-2.
8. For BRBF, $C_t = 0.030$ and $x = 0.75$, per ASCE/SEI 7-16 Table 12.8-2.
9. For SCBF and RCSW, $C_t = 0.020$ and $x = 0.75$, per ASCE/SEI 7-16 Table 12.8-2.

Table 3-3 Structure-to-Soil Stiffness Ratio, $h' / (v_s T)$, for $r = e + z_p = 52.5$ ft

Example Inputs $e = 20$ ft $z_p = 32.5$ ft $r = e + z_p = 52.5$ ft				Site Class, Shear Wave Velocity and Structure-to-Soil Stiffness Ratio					
					A_{min}	B_{ave}	C_{ave}	D_{ave}	E_{max}
				v_{so}:	5000	3750	1750	900	600
				v_{so_r} / v_{so}:	0.88	0.83	0.76	0.75	0.76
				v_s / v_{so_r}:	1.0	0.97	0.87	0.71	0.22
System	h_n (ft)	$h'=2/3(h_n+e)$ (ft)	T (s)	v_s:	4400 (ft/s)	3019 (ft/s)	1157 (ft/s)	479 (ft/s)	100 (ft/s)
SMRF	12	8	0.20		0.024	0.014	0.035	0.085	0.406
	36	24	0.49		0.017	0.016	0.043	0.103	0.493
	60	40	0.74		0.016	0.018	0.047	0.114	0.543
	120	80	1.29		0.016	0.021	0.054	0.130	0.621
	240	160	2.25		0.018	0.024	0.062	0.149	0.712
BRBF	12	8	0.19		0.025	0.014	0.037	0.090	0.429
	36	24	0.44		0.019	0.018	0.048	0.115	0.550
	60	40	0.65		0.019	0.021	0.054	0.130	0.622
	120	80	1.09		0.020	0.024	0.064	0.154	0.736
	240	160	1.83		0.022	0.029	0.076	0.183	0.874
SCBF	12	8	0.13		0.038	0.021	0.056	0.135	0.644
	36	24	0.29		0.029	0.027	0.072	0.173	0.825
	60	40	0.43		0.028	0.031	0.081	0.195	0.932
	120	80	0.73		0.029	0.037	0.096	0.231	1.104
	240	160	1.22		0.032	0.044	0.114	0.274	1.311
RCSW	12	8	0.13		0.038	0.021	0.056	0.135	0.644
	36	24	0.29		0.029	0.027	0.072	0.173	0.825
	60	40	0.43		0.028	0.031	0.081	0.195	0.932
	120	80	0.73		0.029	0.037	0.096	0.231	1.104
	240	160	1.22		0.032	0.044	0.114	0.274	1.311

Notes:

1. v_{so} = average shear wave velocity for small strains over upper 100 ft (30 m) of the site profile from ASCE/SEI 7-16 Table 20.3-1.
2. v_{s_r} / v_{so} = reduction ratio at effective depth for foundation rotation, $r = e + z_p$.
3. v_s / v_{so_r} = ASCE/SEI 7-16 Table 19.3-1 reduction ratio from low strain shear wave velocity to effective shear wave velocity.
4. $v_s = v_{so} \times (v_{s\_r} / v_{so}) \times (v_s / v_{so\_r})$ = effective shear wave velocity at the effective depth for foundation rotation.
5. $S_{DS} = 1.0$g, so $S_{DS}/2.5 = 0.4$.
6. T is per ASCE/SEI 7-16 Equation 12.8-7, $T = C_t h_n^x$.
7. For SMRF, $C_t = 0.028$ and $x = 0.80$, per ASCE/SEI 7-16 Table 12.8-2.
8. For BRBF, $C_t = 0.030$ and $x = 0.75$, per ASCE/SEI 7-16 Table 12.8-2.
9. For SCBF and RCSW, $C_t = 0.020$ and $x = 0.75$, per ASCE/SEI 7-16 Table 12.8-2.

Chapter 4
Base Slab Averaging

4.1 Overview

Seismic input motions for buildings with large base areas are reduced due to incoherence of the ground motions that occur over the base area. Incoherent motions are those that vary from each other in some way. These variations can be due simply to the time of seismic wave arrival across the building base; they may also be due to local variations in soil properties that modify the waves as they travel across the site. The result of this incoherence is that various portions of the building will experience disparate ground motions. When the ground under one corner of a building is being moved in a particular direction, the ground at the opposite corner may be moving in another direction – these motions will partially offset one another, resulting in a smaller net motion. This effect is most pronounced at short periods, since longer period motions are more coherent (i.e., less likely to vary across the site). As a result, stiff buildings with large base areas and rigidly connected foundations will experience reductions in the ground motions transmitted to their superstructures.

Base Slab Averaging

Description: Kinematic SSI reduction of demands on structure due to variations in ground motion across large foundations.

Requirements:

- Foundation base area, A_{base}.
- Average effective shear wave velocity, v_s.

Base slab averaging is a kinematic interaction effect – these are effects that depend only on the building and foundation geometry and the frequency content and spatial variability of the earthquake wave field. These effects are distinct from foundation damping and period lengthening effects, which also depend upon the local soil properties under the foundations and the dynamic characteristics of the seismic system and its foundations.

Base slab averaging results in modified foundation input motions, the effects of which are most accurately described in the frequency domain (i.e., through the Fourier amplitudes and phase angles of the ground motions). However, to make the models more useful to practitioners, NIST (2012a) presents a relationship that is only a function of the building period and the average shear wave velocity, v_s. In ASCE/SEI 7-16 (ASCE, 2017a), the functional dependence on v_s was eliminated. This relationship reduces the ordinates of the response spectrum and is computed using formulas that are dependent only on the effective size of the building footprint.

The only parameters needed are the foundation base area, A_{base}, and the average effective shear wave velocity, v_s, over an effective profile depth

below the foundation. Section 2.2.2 of NIST (2012a) indicates that this depth may be taken as equal to half of the equivalent building footprint size, computed as A_{base} 2 . Although the average effective shear wave velocity is not required explicitly to compute the reductions, the pertinent equations are only applicable for v_s in the range of 650 to 1,650 ft/s. This is not to say that base slab averaging is not applicable to sites outside of this range, only that the equations in ASCE/SEI 7-16 Section 19.4 have not been demonstrated as applicable outside of this range.

4.2 Key Equations

ASCE/SEI 41-17 Equations

The equations for base slab averaging in ASCE/SEI 41-17 Section 8.5.1.1 (ASCE, 2017b) are the same as those in ASCE/SEI 7-16, with the exception of ASCE/SEI 41-17 Equation 8-17 for b_0, which incorporates a factor of $0.0001 \times 2\pi$, in lieu of the value of 0.00071 in ASCE/SEI 7-16.

ASCE/SEI 41-17 includes only the equation for foundation size in feet, not a companion equation in meters.

The starting point for base slab averaging is determination of the equivalent foundation size, b_e, according to ASCE/SEI 7-16 Equation 19.4-4, as $b_e =$ A_{base} , which shall not be taken as more than 260 ft. The dimensional limit occurs because the base slab averaging equation has been calibrated using data from actual sites, and the limit corresponds to the maximum foundation dimension at those sites (Kim and Stewart, 2003). A conservative estimate of base slab averaging for larger foundation footprints can be obtained by using the limiting distance.

The next step is to compute b_0 according to ASCE/SEI 7-16 Equation 19.4-3 as follows:

$$b_0 = 0.00071\left(\frac{b_e}{T}\right), \text{ where } b_e \text{ is in feet and } T \text{ is in seconds}$$

$$(\text{or } b_0 = 0.0023\left(b_e\right), \text{ where } b_e \text{ is in meters and } T \text{ is in seconds})$$

This quantity is a function of the response spectrum period, T, which shall not be taken as less than 0.2 sec. With b_0 determined, B_{bsa} is computed according to ASCE/SEI 7-16 Equation 19.4-2 as follows:

$$B_{bsa} = 1 + b_0^2 + b_0^4 + \frac{b_0^6}{2} + \frac{b_0^8}{4} + \frac{b_0^{10}}{12} \text{ for } b_0 \le 1$$

$$B_{bsa} = \exp\left(2b_0^2\right)\left[\frac{1}{\sqrt{\pi b_0}}\left(1 - \frac{1}{16b_0^2}\right)\right] \text{ for } b_0 > 1$$

When considering the upper limit on the effective foundation size (260 ft) and the lower limit on the period (0.2 s), the value of b_0 will never exceed 1.0, so the second equation will not apply. (However, if these limits are relaxed in future editions of ASCE/SEI 7, the second equation may apply.)

The modification factor for base slab averaging, RRS_{bsa} is computed according to ASCE/SEI 7-16 Equation 19.4-1 as follows:

$$RRS_{bsa} = 0.25 + 0.75\left\{\frac{1}{b_0^2}\left[1 - \left(\exp\left(-2b_0^2\right)\right)B_{bsa}\right]\right\}$$

Note that the theoretical reduction (within the braces) is multiplied by 0.75 and added to an unreduced factor of 0.25. This code-specific language diminishes the computed reduction relative to the value provided by the underlying semi-empirical model in Chapter 3 of NIST (2012a). This limitation was applied because the reduction due to RRS_{bsa} can become quite significant and because studies of these phenomena have indicated variability between the theoretically predicted modifications and actual measured modifications.

4.3 Determining Effective Foundation Size

The key parameter needed to apply base slab averaging SSI effects is the effective foundation size, b_e. ASCE/SEI 7-16 provides no guidance on this parameter other than defining it as the square root of the area of the base of the structure. The effective foundation size is then simply the equivalent width of the building base area, considering that the foundation was square in plan.

The definition of the base area should be considered as the out-to-out dimensions of the extent of the building foundation, or it may be taken conservatively as the building extent based on the overall column-grid dimensions.

4.4 Determining whether Base Slab Averaging Applies

ASCE/SEI 7-16 Section 19.4.1 allows base slab averaging to be employed only when the foundations of the structure are interconnected. This condition can be met with a continuous mat foundation, or with individual footings that are interconnected by slabs or grade beams providing sufficient stiffness so as not to be classified as a flexible diaphragm. The building base must be sufficiently stiff to permit the base to move as a unit, which allows the filtering of high-frequency motions to occur. Such filtering may still occur in structures with a more flexible base, but this has not yet been studied in sufficient detail.

Figure 4-1 shows four different building base conditions, illustrating various degrees of interconnectivity.

- Condition a, with a slab-on-grade that is not positively connected to the footings would not generally develop interconnectivity sufficient to cause the building base to move as a unit. Base slab averaging should not be considered for this case.

- Condition b, with the slab thickened and connected to the footings with reinforcing dowels, would likely produce sufficient interconnectivity, provided that the thickness of the slab provides sufficient axial and shear stiffness. Base slab averaging can be considered for this case if the slab is sufficiently thick.
- Condition c has a slab similarly constructed to Condition a, but it also includes a grid of tie beams. This condition would likely produce sufficient interconnectivity but only if there are diagonal tie beams to provide shear transfer between the parallel lines of footings. Base slab averaging can be considered for this case if diagonal tie beams are included.
- Condition d, with a continuous mat foundation, almost certainly provides sufficient interconnectivity, but its in-plane stiffness should still be verified. The mat must be stiff enough not to be characterized as a flexible diaphragm according to ASCE/SEI 7-16 Section 12.3.1.3. If this condition is met, then base slab averaging can be considered.

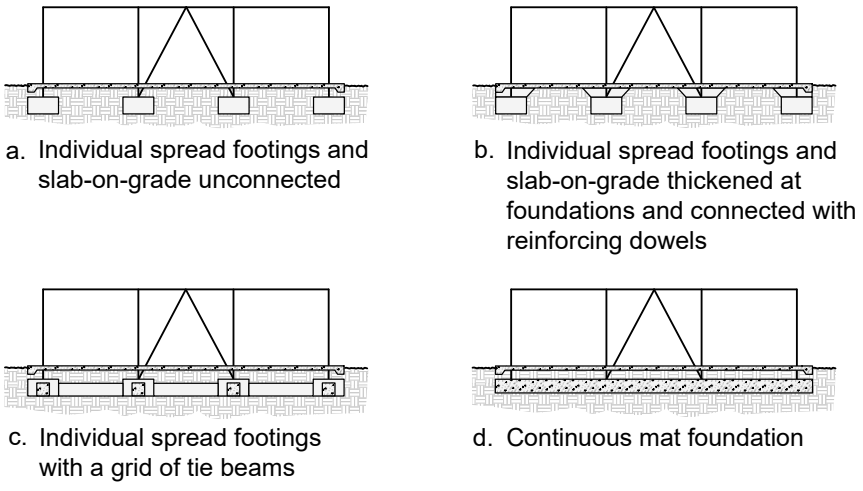

Figure 4-1 Example building base configurations, showing differing degrees of interconnectivity.

4.5 Limitations and Issues

There are several limitations to using base slab averaging effects in ASCE/SEI 7-16. They include:

- ASCE/SEI 7-16 Section 19.1.1: SSI does not apply on Site Class A or B. The analytical model for the structure must include foundation flexibility.
- ASCE/SEI 7-16 Section 19.4.1: The pertinent equations are only applicable for sites with v_s measured over the pertinent depth within the

range of 650 to 1,650 ft/sec. Note that a code change proposal for the next edition of ASCE/SEI 7 is under review to eliminate this provision.

- ASCE/SEI 7-16 Section 19.4: Modifications of the response spectrum for kinematic SSI, including base slab averaging, are only permitted when nonlinear response history analysis is used per ASCE/SEI 7-16 Chapter 16.
- ASCE/SEI 7-16 Section 19.4: There is a limit on the amount of reduction that can be taken from kinematic effects, such that the product of $RRS_{bsa} \times RRS_e$ shall not be less than 0.7.
- ASCE/SEI 7-16 Section 19.2.3: The site-specific response spectra modified for kinematic interaction shall not be taken as less than 0.7 of the design earthquake and MCE_R spectra determined from ASCE/SEI 7-16 Sections 11.4.6.
- ASCE/SEI 7-16 Section 19.2.1 limits the reduced base shear to be no less than α times the base shear as computed according to ASCE/SEI 7-16 Section 12.8.1 for the fixed-base structure. The value of α is 0.7 for $R \leq 3$, is 0.9 for $R \geq 6$ and varies linearly between.

ASCE/SEI 41-17 Limitations

The limitations in ASCE/SEI 41-17 Section 8.5.1 are generally more relaxed than those in ASCE/SEI 7-16.

- Kinematic SSI modifications, including base slab averaging, are permitted for any analysis method. However, for linear procedures, the reduction must be computed based on flexible-base building periods multiplied by 1.5.
- There is no limitation on the shear wave velocity for the site.
- The product of $RRS_{bsa} \times RRS_e$ shall not be less than 0.5.
- Foundations must be stronger than the vertical elements of the lateral-force-resisting system.

4.6 Example

An example application is used to illustrate the response spectrum reductions due to base slab averaging per ASCE/SEI 7-16 Section 19.4.1. The example building has base-level plan dimensions of 100 ft by 400 ft and is shown in Figure 4-2. The site is classified as Site Class D with a soil shear wave velocity of 900 ft/s, which is within the specified range for applicability of the equations.

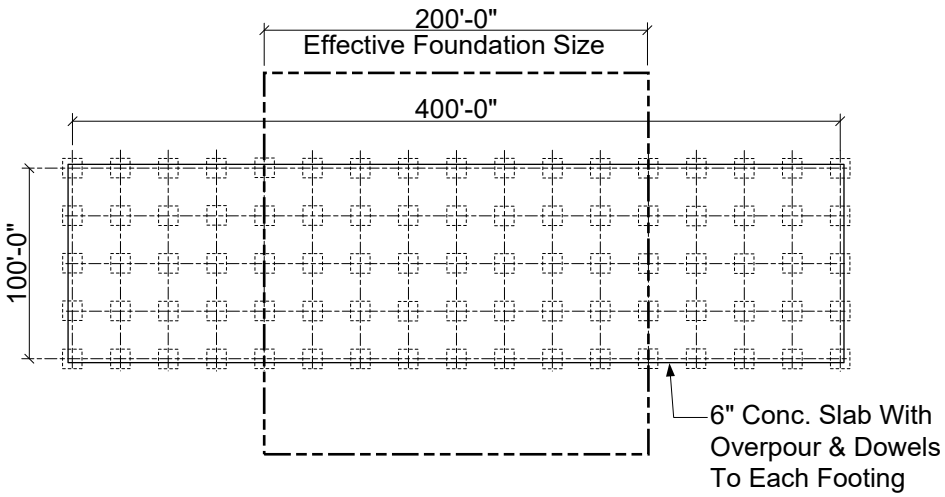

Figure 4-2 Example building foundation plan, representative of Condition b in Figure 4-1.

The area of the structure base is taken from the grid-to-grid dimensions as

$$A_{base} = (100 \text{ ft})(400 \text{ ft}) = 40{,}000 \text{ ft}^2$$

The effective foundation size is then computed in accordance with ASCE/SEI 7-16 Equation 19.4-4:

$$b_e = \sqrt{A_{base}} = \sqrt{40{,}000 \text{ ft}^2} = 200 \text{ ft}$$

This dimension is less than 260 ft and therefore may be used as computed. For equivalent dimensions exceeding 260 ft, the following computations must be based on 260 ft.

The response spectrum reductions are period-dependent and most easily computed in a spreadsheet. The following calculations pertain to the minimum period allowed to be considered, 0.2 s, in accordance with ASCE/SEI 7-16 Equation 19.4-3:

$$b_0 = 0.00071\left(\frac{b_e}{T}\right) = 0.00071\left(\frac{200 \text{ ft}}{0.2 \text{ sec}}\right) = 0.71$$

This value is confirmed to be less than 1.0, so the applicable equation for B_{bsa} is ASCE/SEI 7-16 Equation 19.4-2(a):

$$B_{bsa} = 1 + b_0^2 + b_0^4 + \frac{b_0^6}{2} + \frac{b_0^8}{4} + \frac{b_0^{10}}{12} = 1.841$$

Then, the response spectral modification factor, RRS_{bsa}, is computed in accordance with ASCE/SEI 7-16 Equation 19.4-1:

$$RRS_{bsa} = 0.25 + 0.75\left\{\frac{1}{b_0^2}\left[1 - \left(\exp\left(-2b_0^2\right)\right)B_{bsa}\right]\right\} = 0.855$$

This value is greater than the required lower limit of 0.7.

Table 4-1 provides values of RRS_{bsa}, the response spectral modification factor, at several periods of interest.

Table 4-1 Values of RRS_{bsa} at Selected Periods for b_e = 200 ft

Response Spectrum Period, T (s)	RRS_{bsa} for b_e=200 ft
0.2	0.855
0.3	0.925
0.4	0.956
0.5	0.971
1.0	0.993

Figure 4-3 shows RRS_{bsa} for b_e = 200 ft plotted vs. building period. Figure 4-4 shows example resulting response spectra (with and without the reduction applied) for S_{DS} = 1.0 and S_{D1} = 0.6. Note that the spectrum shown includes the increased value of the corner period from T_s to $1.5T_s$ for Site Class D, per ASCE/SEI 7-16, Section 11.4.8.

Note that when Method 1 of ASCE/SEI 7-16 Chapter 16 is used, which requires an MCE_R response spectrum, RRS_{bsa} can be applied to a smooth site-specific MCE_R response spectrum derived from ASCE/SEI 7-16 Chapter 21 or 2/3 of that spectrum for the Design Earthquake.

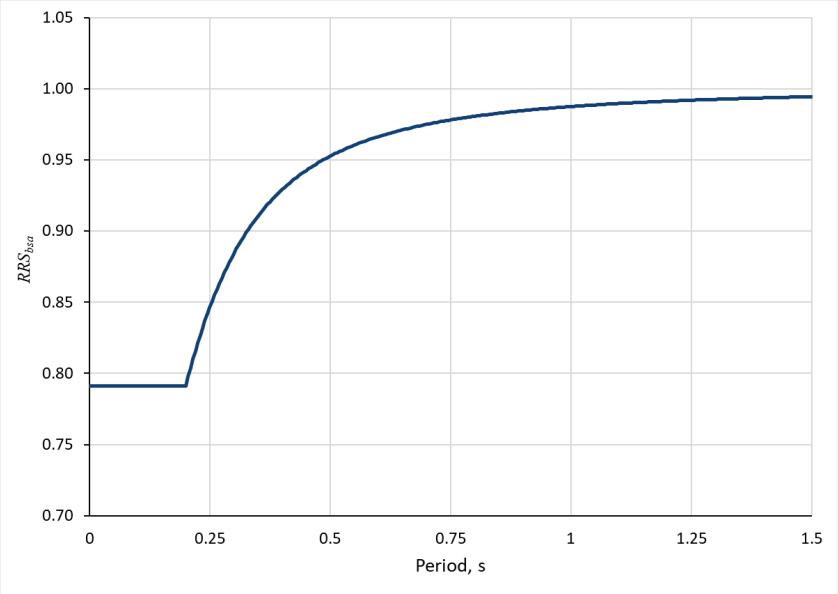

Figure 4-3 RRS_{bsa} reduction as a function of period.

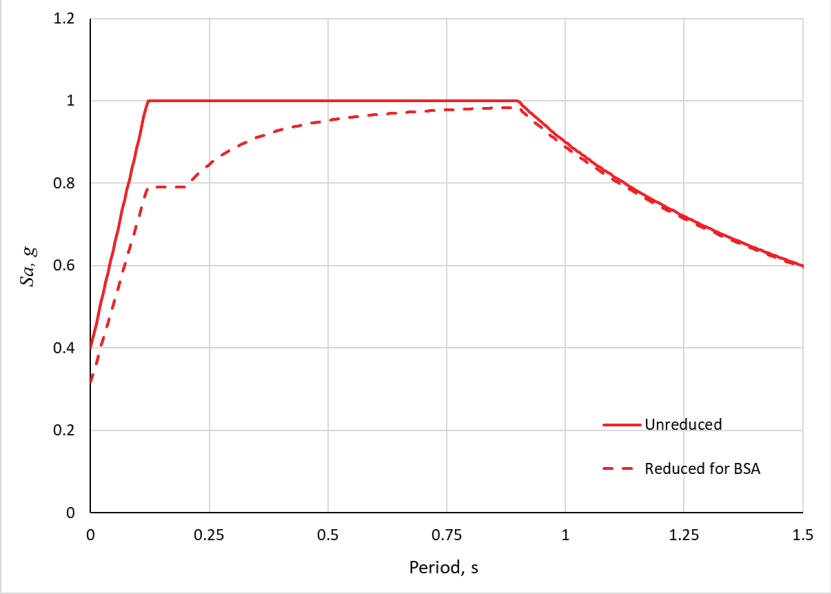

Figure 4-4 Example resulting response spectrum for S_{DS} = 1.0 and S_{D1} = 0.6.

Chapter 5
Embedment Effects

5.1 Overview

Chapter 4 of this *Guide* discussed base slab averaging, which is one kinematic soil-structure interaction (SSI) effect. This chapter discusses the second kinematic SSI effect, which is related to the reduction of ground motions with depth, and is known as embedment effects. Similar to the requirements for base slab averaging, embedment effects can only be considered for soil sites and do not apply to Site Classes A or B. Foundation embedment modifies the free field motion, assumed to be developed at the ground surface, and reduces the foundation input motion and the resulting demands on the structure. This is characterized by a reduction in the ordinates of the response spectrum. The deeper the foundation is embedded, the greater the reduction in response spectrum values. Soil flexibility modeling is not required. The parameters needed are the foundation embedment depth, e, and the average low strain shear wave velocity over the embedment depth, v_{so}, and parameters used to reduce v_{so} for the effects of nonlinearity (site class and S_{DS}). If the free field motion is determined at the embedded foundation level, then reduction of this motion for embedment effects described below cannot be taken. If the free field motion is defined at some depth between the ground surface and the embedment depth, then embedment effects can be considered provided the embedment depth is computed from the depth where the free field motion is defined.

Embedment Effects

Description: Kinematic SSI reduction of demands on structure due to embedment of building foundation.

Requirements:

- Foundation embedment depth, e
- Average low strain shear wave velocity over the embedment depth, v_{so}
- Design spectral response acceleration parameter at short periods, S_{DS}
- Site class

5.2 Key Equation

ASCE/SEI 7-16 Equation 19.4-5 determines the modification for embedment, RRS_e.

$$RRS_e = 0.25 + 0.75 \times \cos\left(2\pi e / Tv_s\right)$$

where:

e = foundation embedment depth, not greater than 20 ft. A minimum of 75% of the foundation footprint shall be present at the embedment depth. The foundation embedment for structures located on sloping sites shall be the shallowest embedment.

v_s = the average effective shear wave velocity for site soil conditions, taken as the average value of velocity over the embedment depth

of the foundation determined using v_{so} and ASCE/SEI 7-16 Table 19.3-1 or a site-specific study. It shall not be less than 650 ft/s.

v_{so} = the average low strain shear wave velocity over the embedment depth of the foundation.

T = response spectra ordinate period, which shall not be taken as less than 0.20 s.

5.3 Determining Depth of Embedment

ASCE/SEI 41-17 Embedment

ASCE/SEI 41-17 Section 8.5.1.2 (ASCE, 2017b) adds more specific requirements to use embedment effects than ASCE/SEI 7-16.

- Structures must have structural mats or foundation elements interconnected with concrete slabs or that are continuously connected with grade beams or other foundation elements of sufficient lateral stiffness so as not to be characterized as a flexible diaphragms.
- The foundation elements are stronger than the vertical elements of the lateral force-resisting system.

The key parameter needed to apply embedment effects is the foundation embedment depth, *e*. ASCE/SEI 7-16 (ASCE, 2017a) provides no guidance on this parameter other than to say in Section 19.4.2: "A minimum of 75% of the foundation footprint shall be present at the embedment depth. The foundation embedment for structures located on sloping sites shall be the shallowest embedment."

Figure 5-1 shows a building supported by a mat. The depth of embedment goes to the bottom of the mat, as the area of the foundation at this elevation covers 100% of the foundation footprint, or more than 75% of the foundation footprint threshold in ASCE/SEI 7-16 Section 19.4.2.

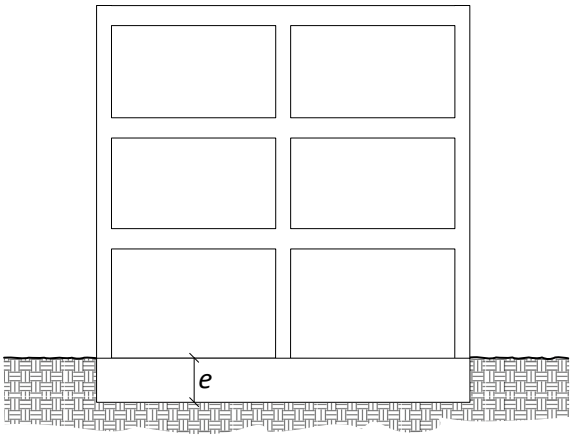

Figure 5-1 Depth of embedment for a building on a mat foundation.

Figure 5-2 shows a building with an orthogonal set of grade beams with spread footings at the intersections supporting a steel moment frame system. At the base of the footings, or e_1 below the top of slab, the footing area is only 32% of the total footprint area or well under the 75% threshold in ASCE/SEI 7-16 Section 19.4.1. Thus, the embedment depth, *e*, is the depth of the slab-on-grade, e_2, which is negligible. This example shows it is typically not possible for the depth of embedment to go to the base of the foundation, except for a mat.

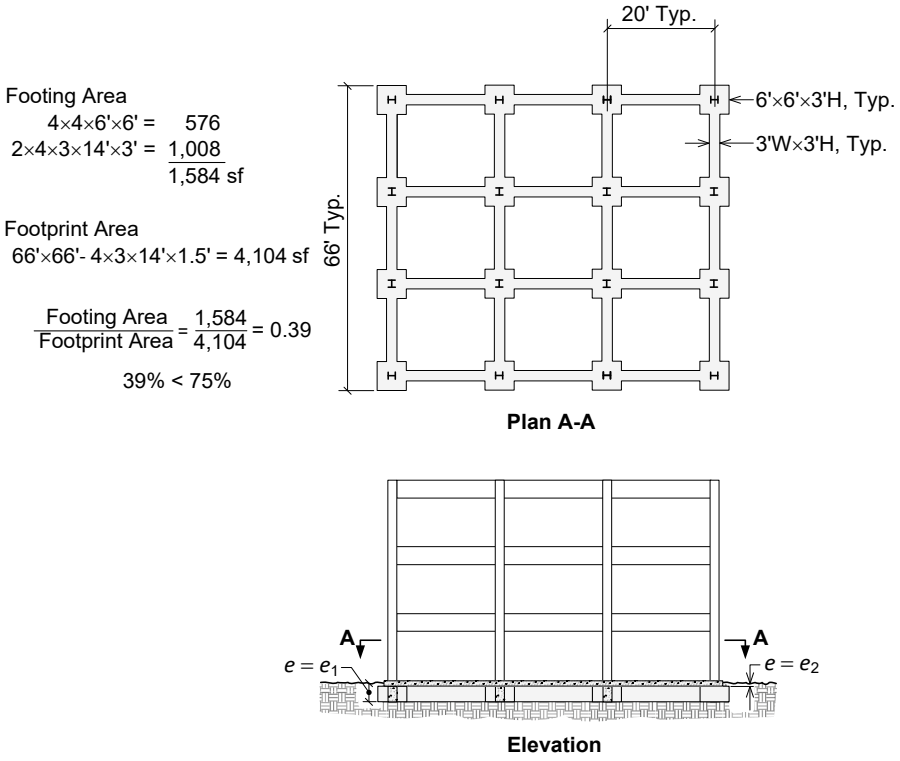

Figure 5-2 Depth of embedment for a building on grade beams and spread footings.

Figure 5-3 shows a building with a one-story basement with a perimeter strip footing and interior strip or spread footings. The depth of embedment, $e = e_2$, is from grade to the top of the basement slab, because, like the situation in Figure 5-2, the area at the base of the footings is much less than the 75% threshold in ASCE/SEI 7-16 Section 19.4.1.

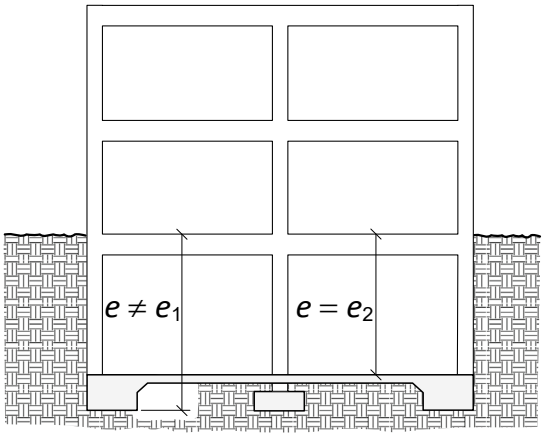

Figure 5-3 Depth of embedment for a building with a basement on perimeter strip footings and interior spread footings.

Figure 5-4 shows a situation with a two-story basement where the depth of the lowest basement floor is 24 ft below grade, or more than the 20 ft limit of ASCE/SEI 7-16 Section 19.4.1. In this case, the embedment depth, *e*, is capped at 20 ft.

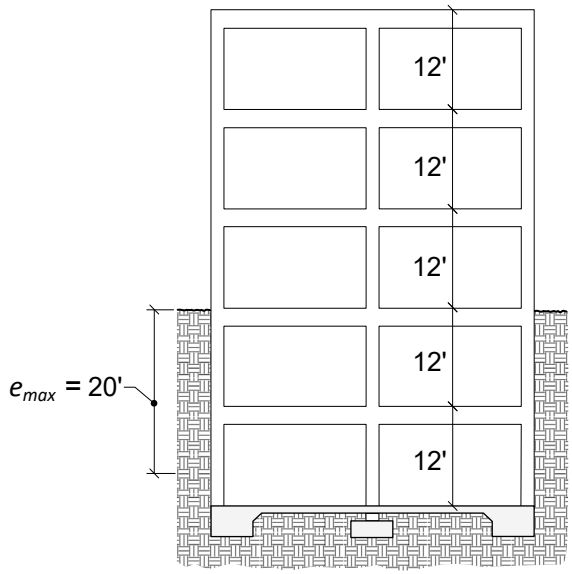

Figure 5-4 Maximum depth of embedment.

Figure 5-5 shows a situation with a partial basement. The area of the basement is less than 75% of the area of the overall building footprint, so the depth of embedment is limited to the slab-on-grade depth which is negligible. Figure 5-6, on the other hand, shows a situation where the partial basement is large enough to exceed the 75% threshold, and the depth of embedment is the from grade to the top of the basement slab.

Basement Footing Area
23'×40' = 920 sf

Footprint Area
40'×40' = 1,600 sf

$$\frac{\text{Basement Footing Area}}{\text{Footprint Area}} = \frac{920}{1{,}600} = 0.58$$

58% < 75%

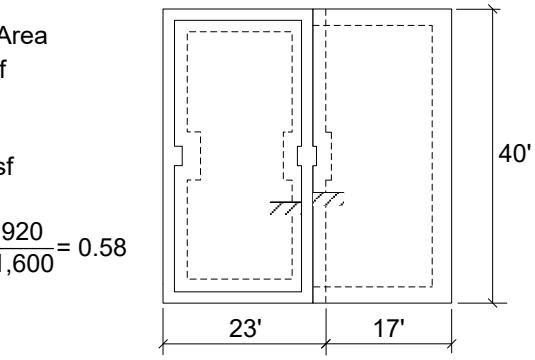

Plan A-A

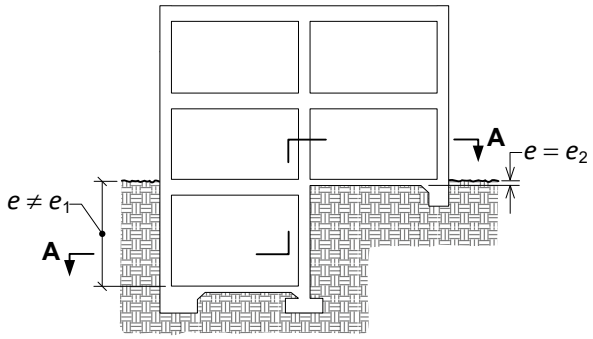

Elevation

Figure 5-5 Depth of embedment for a smaller partial basement.

Basement Footing Area
63'×40' = 2,520 sf

Footprint Area
80'×40' = 3,200 sf

$$\frac{\text{Basement Footing Area}}{\text{Footprint Area}} = \frac{2{,}520}{3{,}200} = 0.79$$

79% > 75%

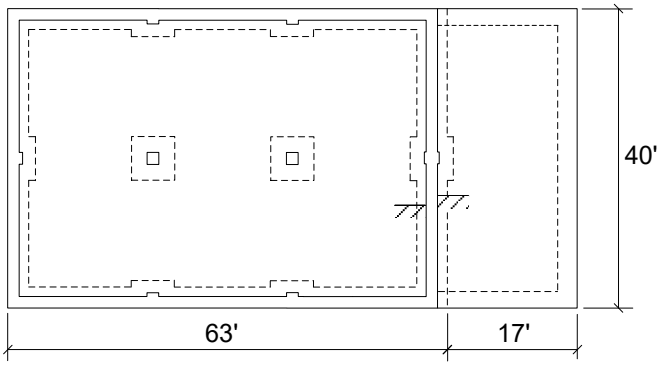

Plan A-A

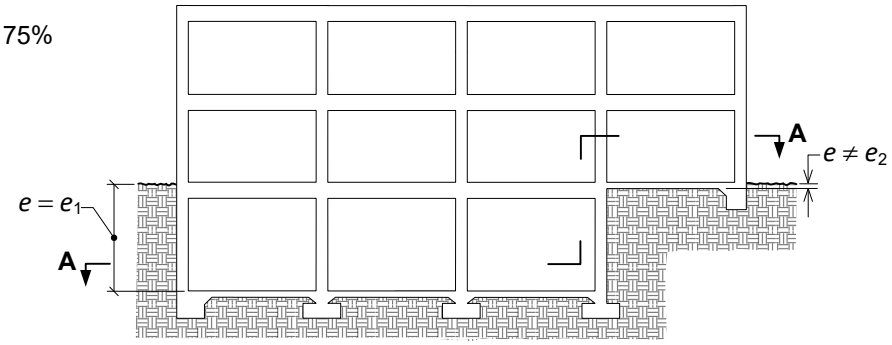

Elevation

Figure 5-6 Depth of embedment for a larger partial basement.

Figure 5-7 shows a building with a full basement on a sloping site. Per ASCE/SEI 7-16 Section 19.4.1, the depth of embedment is taken at the shallowest point of embedment, where $e = e_1$.

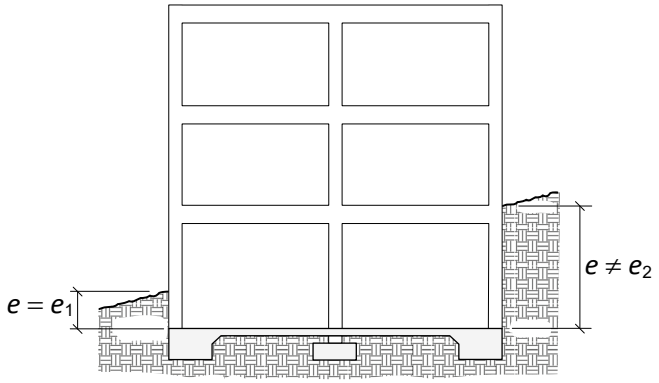

Figure 5-7 Depth of embedment on a sloping site.

5.4 Limitations and Issues

ASCE/SEI 41-17 Limitations

The limitations in ASCE/SEI 41-17 Section 8.5.1 are more relaxed than those in ASCE/SEI 7-16:

- Kinematic SSI modifications, including those for embedment effects, are permitted for any analysis method.
- The product of $RRS_{bsa} \times RRS_e$ shall not be less than 0.5.
- ASCE/SEI 41-17 does not have minimum base shear requirements.

There are several limitations to using embedment effects in ASCE/SEI 7-16 in addition to those already noted. They include:

- ASCE/SEI 7-16 Section 19.4: Modifications of the response spectrum for kinematic SSI, including embedment, are only permitted when nonlinear response history analysis is used per ASCE/SEI 7-16 Chapter 16. ASCE/SEI 41-17 does not have this restriction.
- ASCE/SEI 7-16 Section 19.4: There is a floor on the amount of reduction that can be taken for kinematic effects, such that the product of $RRS_{bsa} \times RRS_e$ shall not be less than 0.7. ASCE/SEI 41-17 has a less restrictive floor of 0.5.
- ASCE/SEI 7-16 Section 19.4.2: There is a maximum limit of 20 ft on the depth embedment, e, that can be used. NIST (2012a) does not have a similar limit.
- ASCE/SEI 7-16 Section 19.2.3: The site-specific response spectra modified for kinematic interaction shall not be taken as less than 0.7 of the design earthquake and MCE_R spectra determined from ASCE/SEI 7-16 Section 11.4.6. The modified spectra shall not be taken as less than 0.8 of the site-specific spectra are determined per ASCE/SEI 7-16 Section 21.3.

Besides limitations in ASCE/SEI 7-16 Chapter 19, there are also minimum base shear limitations in ASCE/SEI 7-16 Chapter 12 that may govern.

5.5 Example

An example application is used to illustrate the ASCE/SEI 7-16 Section 19.4.2 embedment effect equation. The example building is a three-story concrete shear wall building with a two-story basement. It is shown in Figure 5-8. The foundation uses perimeter strip footings and interior spread footings. The building is on a sloped site. Embedment on the high side of grade is 24 ft from grade to the top of the basement slab, and it is 22 ft on the low side of grade from grade to the top of the basement slab. The shallower embedment is used. However, embedment depth is capped at 20 ft per ASCE/SEI 7-16 Section 19.4.2.

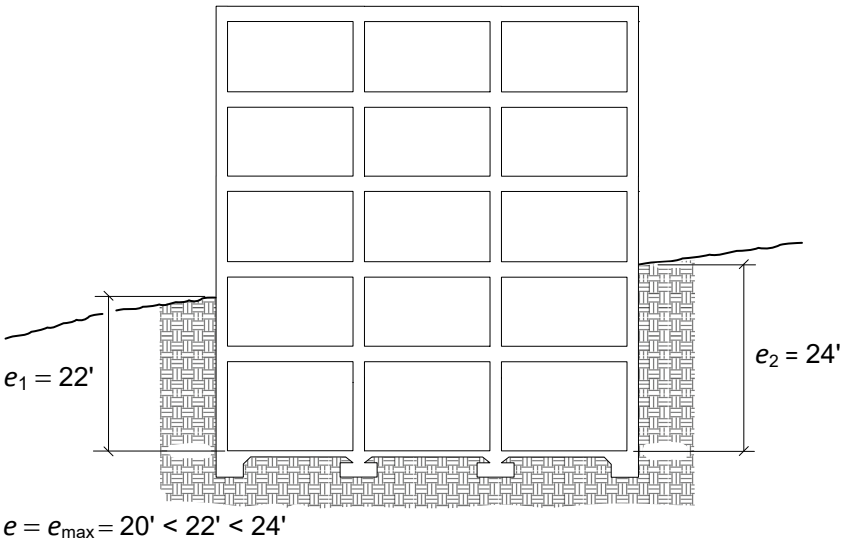

Figure 5-8 Example building for embedment effects.

For site classification, the shear wave velocity has been measured at the site and is shown in Figure 5-9. The measured velocity for each layer is shown in Table 5-1.

Shear Wave Velocity

There are several similar shear wave velocity parameters. ASCE/SEI 7-16 is not consistent with the terms.

In Chapter 20, $\overline{v}_s$ is the "average shear wave velocity." It is taken over the top 100 ft of soil. This is often designated as V_s^{30} for 30 m. Both $\overline{v}_s$ and V_s^{30} are the low strain shear wave velocity, though this is never stated in Chapter 20.

In Section 19.4.2 of Chapter 19, v_{so}, is the "average low strain shear wave velocity over the embedment depth." If the embedment depth were 100 ft it would be the same as $\overline{v}_s$.

In Chapter 19, the low strain shear wave velocity needs to be modified by Table 19.3-1 to obtain the average effective shear wave velocity, v_s, which cannot be less than 650 ft/sec.

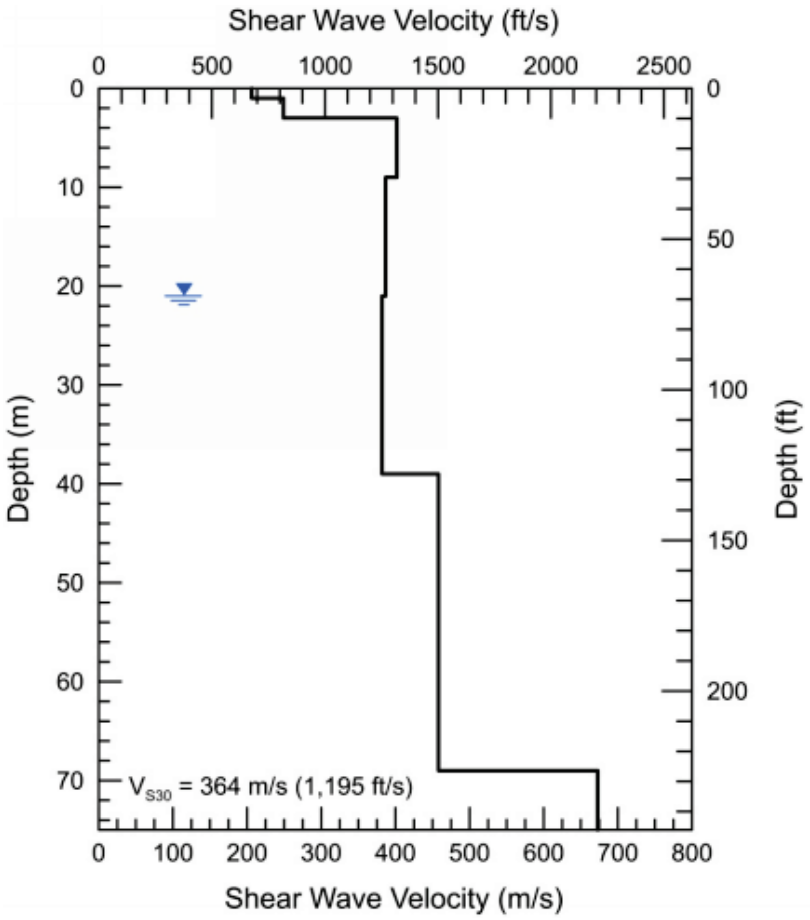

Figure 5-9 Shear wave velocity at example building.

Table 5-1 Measured Shear Wave Velocity at Example Building

Depth to Top of Layer (m)	Layer Thickness (m)	Shear Wave Velocity (m/s)	Depth to Top of Layer (ft)	Layer Thickness (ft)	Shear Wave Velocity (ft/s)
0.0	0	206	0.0	3.28	676
1	2	249	3.28	6.56	817
3	6	402	9.84	19.69	1,319
9	12	387	29.53	39.37	1,269
21	18	382	68.90	59.10	1,253
39	30	458	128.0	98.40	1,503
69	>6	673	226.38	>19.68	2,207

The average shear wave velocity $\overline{v}_s$ is calculated per ASCE/SEI 7-16 Equation 20.4.1 for the top 30 m or 100 ft. In typical current geotechnical practice, measurements are usually made in depths using meters and calculated using metric layer depths and then converted to imperial units at the end. Since 30 m and 100 ft are not identical, this means calculations

using layers up to 30 m and layers up to 100 ft would result in slightly different average shear wave velocities. The typical practice is followed here:

$$v_s = \Sigma d_i / \Sigma(d_i / v_{si})$$

where:

d_i = the thickness of any layer between 0 and 100 ft

v_{si} = the shear wave velocity in ft/s

v_s = 30 / [(1 / 206) + (2 / 249) + (6 / 402) + (12 / 387) + ((30 – 21) / 382)] = 365 m/s or 1,195 ft/s

Per ASCE/SEI 7-16 Table 20.3-1, this is just within the 600 ft/s to 1,200 ft/s range for Site Class D, Stiff Soil.

For embedment effects, the shear wave velocity calculation is not the same it is for site classification. Per ASCE/SEI 7-16 Section 19.4.2, the shear wave velocity is taken over the depth of the embedment, which is 20 ft in this case. ASCE/SEI 7-16 Section 19.4.2 does not provide explicit guidance on the formula to use for calculating the average low strain shear wave velocity over the depth of embedment, but the formulation in ASCE/SEI 7-16 Equation 20.4.1 is used here.

v_{so} = 20 / [(3.28 / 676) + (6.56 / 817) + ((20 – 9.84) / 1,319)] = 972 ft/s

The building is located in a high seismic zone with S_{DS} = 1.06 and S_{D1} = 1.45.

The average low strain shear wave velocity is converted to the average effective shear wave velocity per ASCE/SEI 7-16 Table 19.3-1. With S_{DS} / 2.5 = 1.06 /2.5 = 0.42 and Site Class D, and then using linear interpolation, the effective shear wave velocity ratio, [v_s / v_{so}], is 0.687. Thus, the average effective shear wave velocity over the depth of embedment is $v_s \times [v_s / v_{so}]$ = 972 ft/s × 0.687 = 668 ft/s.

The modification factor for embedment, RSS_e, can now be calculated. Per ASCE/SEI 7-16 Section 19.4.2, the lowest response spectra period shall not be taken as less than 0.20. For this example calculation, T = 0.20 s is used.

$$RRS_e = 0.25 + 0.75 \times \cos(2\pi e / Tv_s)$$

RRS_e = 0.25 + 0.75 × cos [2π × 20 ft / (0.20s × 668 ft/s)] = 0.692

The maximum reduction for $RRS_{bsa} \times RRS_e$ = 0.70. For this example, we will assume RRS_{bsa} = 1.0. Thus, RRS_e cannot go below 0.70.

Table 5-2 provides the remaining spectral ordinates for comparison, and Figure 5-10 plots the site-specific response spectral modification factor, RRS_e (with the floor of 0.70). Figure 5-11 plots the response spectra, with and without the modification for embedment. For example, for a period of 0.30 s, the embedment effects would permit reduction of the spectral acceleration down to 0.86 of the value without SSI.

Table 5-2 Response Spectral Ordinates with and without Embedment Effects

Period (s)	S_a without SSI (g)	RRSe	S_a with SSI (g)
0	0.42	0.700	0.30
0.05	0.54	0.700	0.38
0.1	0.66	0.700	0.46
0.16	0.80	0.700	0.56
0.2	0.89	0.700	0.62
0.225	0.95	0.753	0.71
0.27	1.06	0.829	0.88
0.3	1.06	0.857	0.91
0.4	1.06	0.919	0.97
0.5	1.06	0.948	1.00
0.6	1.06	0.963	1.02
0.8	1.06	0.979	1.04
1	1.06	0.987	1.05
1.2	1.06	0.991	1.05
1.37	1.06	0.993	1.05
1.4	1.04	0.993	1.03
1.5	0.97	0.994	0.96
2	0.73	0.997	0.72
2.5	0.58	0.998	0.58
3	0.48	0.999	0.48
3.5	0.41	0.999	0.41
4	0.36	0.999	0.36
4.5	0.32	0.999	0.32
5	0.29	0.999	0.29

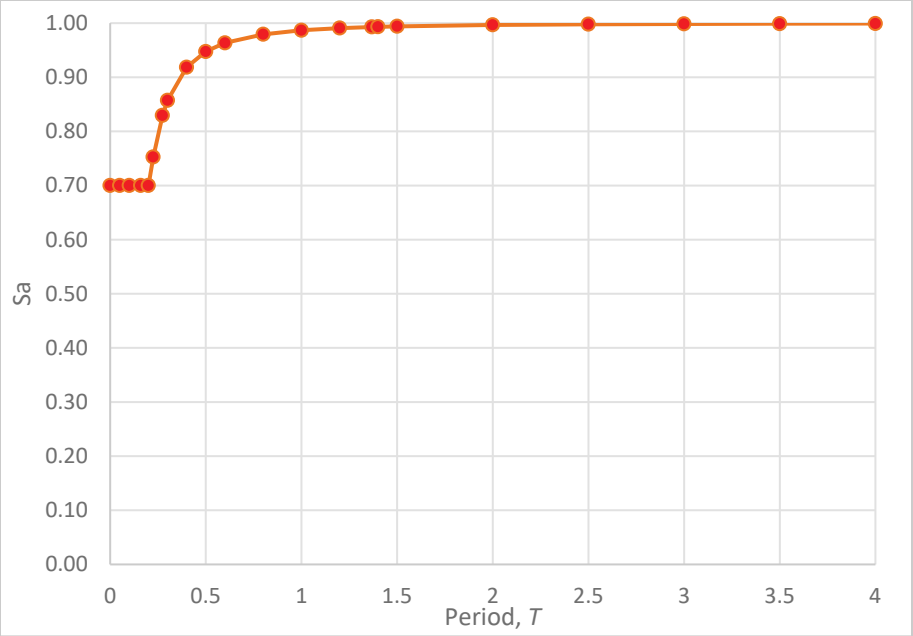

Figure 5-10 Site-specific response spectral acceleration modification factor for foundation embedment, RRS_e.

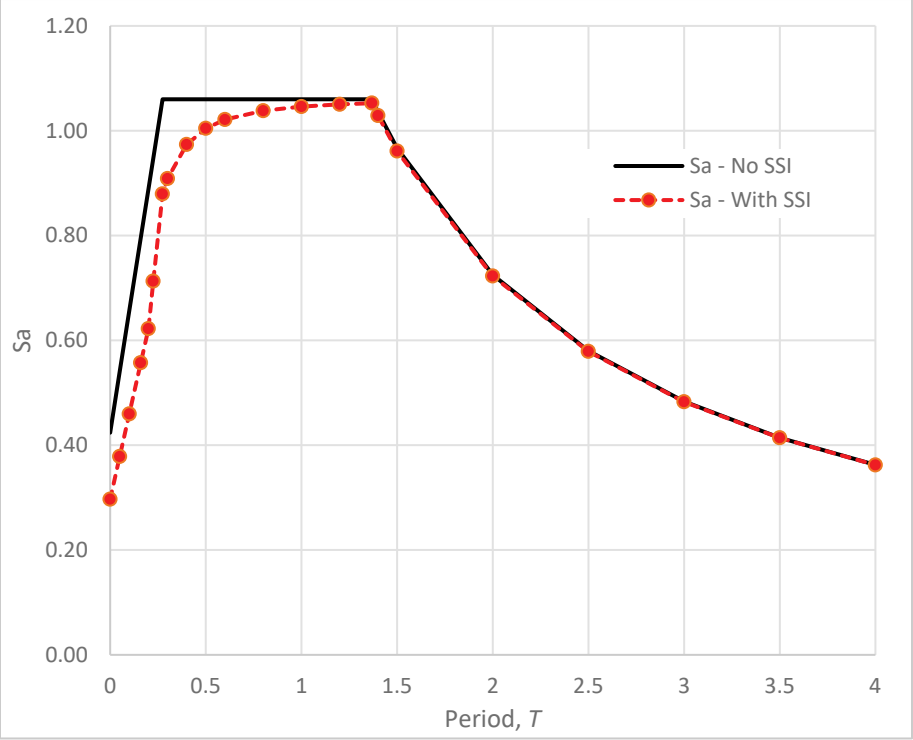

Figure 5-11 Response spectra for example building, with and without embedment SSI.

Chapter 6
Foundation and Soil Flexibility

6.1 Overview

Conventional building design is most often performed based on the assumptions that the building is fixed to the ground at its base and the ground itself is rigid. These assumptions are not strictly true but are often considered to be acceptable and conservative. The flexibility of the foundation system, including both the foundation's structural components and the supporting soil, can have a significant effect on the building's dynamic properties and its overall response. When incorporating soil-structure interaction (SSI) in the design of a building, ASCE/SEI 7-16 Section 19.1.1 (ASCE, 2017a) requires that the analytical model of the structure incorporate vertical, horizontal, and rotational flexibility of the foundation and the soil. The flexibility of the foundation elements themselves (usually reinforced concrete) can be determined using conventional methods. However, ASCE/SEI 7-16 does not provide specific guidance on determining the finite stiffness of the soil itself. This chapter is intended to provide that guidance, based on the provisions included in ASCE/SEI 41-17 (ASCE, 2017b) and NIST (2012a).

Foundation and Soil Flexibility

Description: Computation of the flexibility of soil supporting building foundations, which must be incorporated in analyses when SSI is considered.

Requirements:

- Site class
- Design spectral response acceleration parameter at short periods, S_{DS}
- The foundation geometry
- The effective soil shear modulus, G, computed from the measured shear wave velocity, v_{s0}
- Poisson's ratio for the soil, ν

The flexibility of soil in the analytical model of a building is generally accounted for through modeling the connection of structural elements to fixed supports with spring elements. These may be point springs, modeling each degree of freedom at the base with a single spring, or may be distributed springs representing the soil support as a discretized continuous medium, known as a Winkler foundation.

Vertical and rotational springs can model similar behavior. They affect the structure rocking on its base due to elastic vertical compression of the soil—either through vertical movement of the ends of a frame, or rotation at the base of a wall or core. This behavior can have a dramatic effect of the building's fundamental period and displaced shape.

Horizontal springs model the foundation displacement relative to the free-field soil displacement or resistance of the soils against basement walls or other vertical faces. Spring stiffness is limited by frictional and passive pressure resistance.

ASCE/SEI 7-16 Section 12.13.3 requires consideration of both upper and lower bound estimates of the foundation soil flexibility by requiring a 50% increase and decrease in soil stiffness. This is to account for the inherent uncertainty and variability of soil, as well as a recognition that representing the soil's actual nonlinear behavior as linear is an approximation.

Chapter 2 of NIST (2012a) presents a discussion of inertial interaction, including both foundation flexibility and damping. The foundation system flexibility sections include two similar techniques, one developed by Pais and Kausel (1988) and one by Gazetas (1991), expanded by Mylonakis et al. (2006). Both of these techniques are applicable to rigid foundation elements supported by flexible soils. Both present equations to model six degrees of potential flexibility (three translations and three rotations) based on the foundation geometry and the soil stiffness, as expressed by the shear modulus, G. Both techniques include the effects of increased stiffness due to embedment of the foundation in the soil. Because these techniques address the degrees of flexibility assigned to a single point, they do not lend themselves well to conditions where the structural foundation elements are also a source of flexibility without enhancements that address such flexibility, as included in NIST (2012a) Section 2.2.3.

ASCE/SEI 41-17 also provides recommendations for computing the effects of foundation flexibility. These include the methods outlined in NIST as well as methods that allow consideration of the flexibility of the structural foundation elements.

ASCE/SEI 41-17

NIST (2012a) defines L as half the foundation length and B as half the foundation width, which is consistent with the way these dimensions are treated in the source documents.

ASCE/SEI 41-17 defines L as the full foundation length and B as the full foundation width for springs, which is consistent with the nomenclature used by most structural engineers.

As a result of this discrepancy, the equations in the two documents incorporate different coefficients to produce the same results.

6.2 Soil Properties for Flexibility Calculations

In addition to foundation geometry, soil properties are required to compute the flexibility of the soil. These properties include the measured shear wave velocity, v_{so}, the effective soil shear modulus, G, and Poisson's ratio for the soil, ν.

The shear wave velocity, v_{so}, is determined based on the average measured value over an effective depth interval. The depth interval is defined slightly differently in the various documents. Both ASCE/SEI 41-17 and NIST describe a depth below the footing-soil interface of the half-dimension of an equivalent rectangular foundation matching the area of the actual foundation. NIST goes on to indicate that for a rocking foundation it may be more appropriate to consider the half-dimension of an equivalent square foundation matching the moment of inertia of the actual foundation. ASCE/SEI 41-17 notes that the soil that is one or two footing widths below the soil-footing interface should be considered.

The small-strain soil shear modulus, G_o, is computed according to the ASCE/SEI 41-17 Equation 8-4, which is also repeated in the definitions of ASCE/SEI 7-16 Section 19.3.3 as follows:

$$G_o = \frac{\gamma v_{so}^2}{g}$$

where γ is the soil unit weight and g is the acceleration of gravity.

Note that the shear wave velocity here, v_{so}, is not the effective value including the modification per ASCE/SEI 7-16 Table 19.3-1, but the measured value. The effective shear modulus, G, is then determined by modifying G_o by the applicable factor from ASCE/SEI 7-16 Table 19.3-2.

ASCE/SEI 7-16 and NIST indicate that Poisson's ratio, ν, may be taken as 0.3 for sandy soils and 0.45 for clayey soils. ASCE/SEI 41-17 indicates that ν may be taken as 0.5 for saturated clays and 0.25 for other soils.

6.3 Vertical and Rotational Springs

In this section, the discussion of vertical springs pertains to vertical stiffness of foundations that affect the rotation of a frame or wall about its base, not to rigid-body vertical movement of a building or portion of a building excited by vertical ground motion.

ASCE/SEI 7-16 provides no guidance regarding the development of vertical and rotational springs to compute the rotational stiffness of a foundation about an axis perpendicular to its length. There is rotational spring formula in ASCE/SEI 7-16 Section 19.3 as part of the radiation damping calculations. However, this formula is for rotation about an axis parallel to its length. ASCE/SEI 41-17 Chapter 8 presents provisions for three methods, described in the sections below. The three methods are depicted graphically in Figure 6-1.

6.3.1 Method 1 – Rigid Foundation and Flexible Soil

This method defines point springs, modeling each degree of freedom at the base of a foundation with an uncoupled spring. This method is recommended for foundations considered to be rigid relative to the soil. The equations in ASCE/SEI 41-17 include all six degrees of freedom and are taken from NIST, but with the foundation length and width parameters defined differently, as discussed in the margin box above. The definitions of L (half-length) and B (half-width) in the NIST document are the same as those in ASCE/SEI 7-16 Chapter 19.

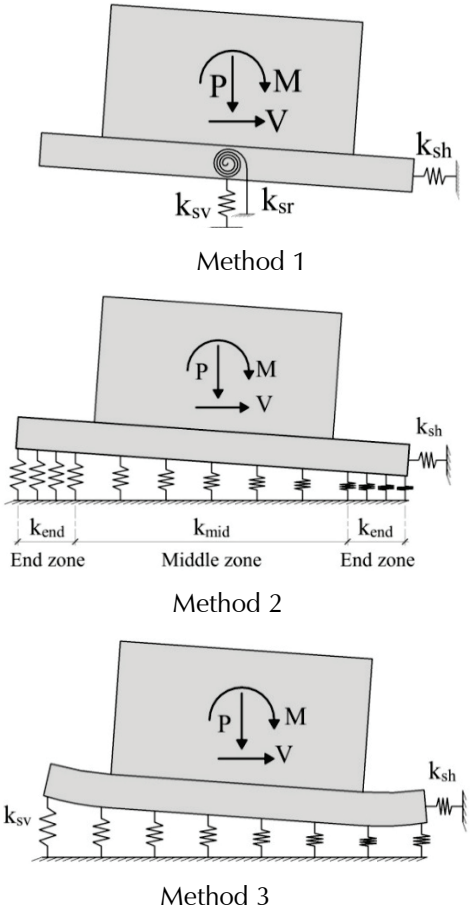

Figure 6-1 Three methods for foundation modeling approaches with vertical and rotational springs presented in ASCE/SEI 41 from FEMA (2018).

NIST (2012a) provides two sources for these elastic solutions for spring values, as discussed above. The coordinate system employed in these equations specifies the x-axis as parallel to the longer footing dimension, the y-axis parallel to the shorter dimension, and the z-axis vertically down (right-hand rule). The more widely used equations from Pais and Kausel (1988) for foundations at the ground surface for vertical (*z*-axis) stiffness and strong-axis (*yy*) rotation are presented below. The definitions and orientations of the foundation dimensions and axes are shown in Figure 6-2.

$$K_{z,sur} = \frac{GB}{1-\nu}\left[3.1\left(\frac{L}{B}\right)^{0.75} + 1.6\right]$$

$$K_{yy,sur} = \frac{GB^3}{1-\nu}\left[3.73\left(\frac{L}{B}\right)^{2.4} + 0.27\right]$$

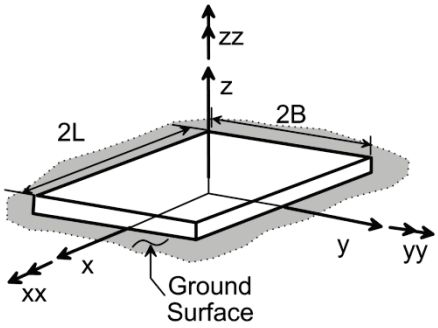

Figure 6-2 Definitions and orientations of dimensions and axes.

Figure 6-3 shows the variation of vertical stiffness, $K_{z,sur}$, with foundation dimensions. The figure includes stiffness computed for example values of L (half-length) = 10 ft, 15 ft, and 20 ft, B (half width) = 1 ft to 10 ft, G = 500 kip/ft^2 and ν = 0.3. As the width increases by 10, the stiffness increases by approximately 2. As the length increases by a 2, the stiffness increases by approximately 1.5. Note that these particular values are dependent on the value of Poisson's ratio.

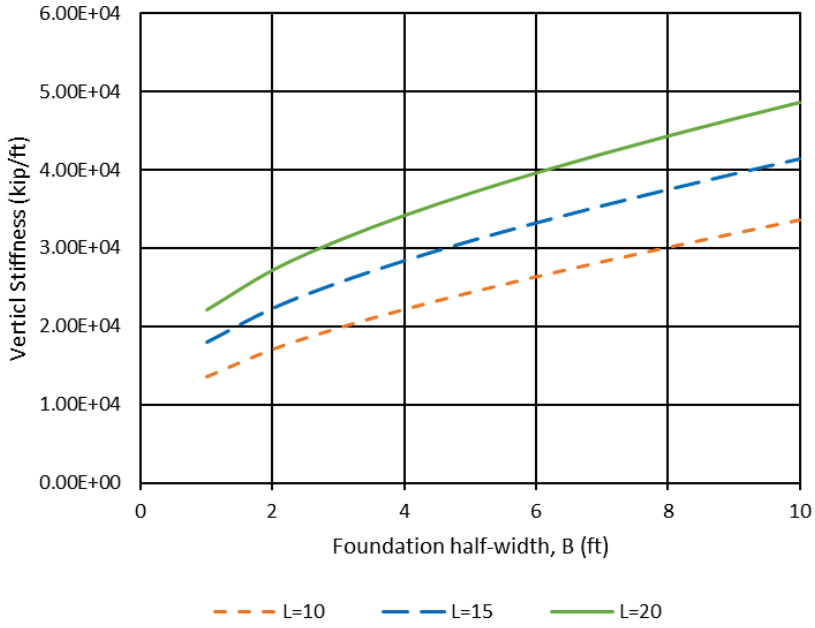

Figure 6-3 Variation of vertical stiffness with foundation dimensions.

Figure 6-4 shows the variation of strong-axis rotational stiffness $K_{yy,sur}$, with foundation dimensions, for the same parameters. As the width increases by 10, the stiffness increases by approximately 4. As the length increases by 2, the stiffness increases by approximately 5. As would be expected, the rotational stiffness is much more sensitive to the length than to width.

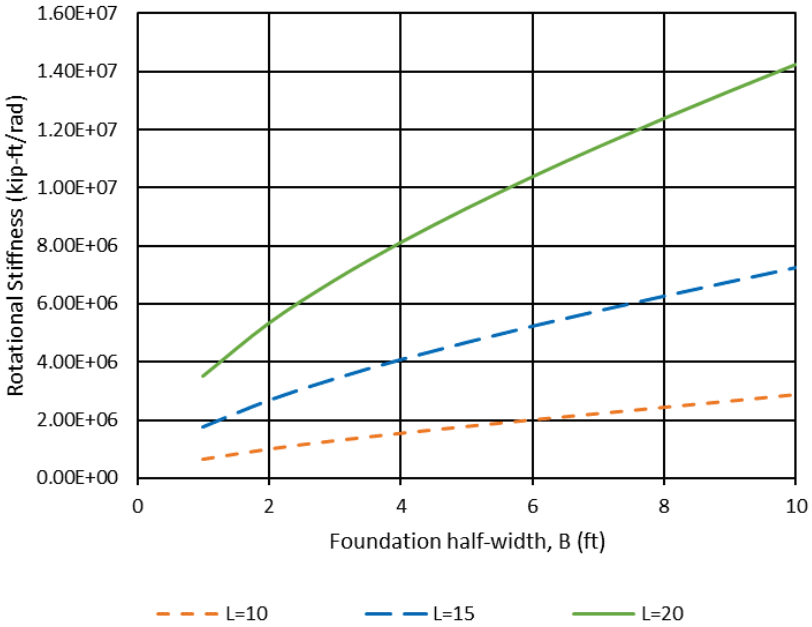

Figure 6-4 Variation of rotational stiffness with foundation dimensions.

Pais and Kausel (1988) provide modification factors to increase the values of stiffness for each degree of freedom based on the embedment of the foundation in the soil. These are presented below, for vertical (z-axis) stiffness and strong-axis (yy) rotation.

$$\eta_z = \left[1.0 + \left(0.25 + \frac{0.25}{L/B}\right)\left(\frac{D}{B}\right)^{0.8}\right]$$

$$\eta_{yy} = \left[1.0 + \frac{D}{B} + \left(\frac{1.6}{0.35 + (L/B)^4}\right)\left(\frac{D}{B}\right)^2\right]$$

Here, D is the depth from the ground surface to the bottom of the foundation. The net stiffness in each degree of freedom is the product of the applicable K and η values above.

Figure 6-5 shows the variation of the embedment modifier for vertical stiffness, η_z, with foundation dimensions, for example values of L (half-length) = 15 ft, B (half width) = 1 ft to 10 ft, D (depth) = 2 ft, 4 ft, and 6 ft. The modifier is essentially the same for values of L of 10 ft and 20 ft as it is for L of 15 ft. For small values of B and large values of D, the modifier can exceed 2, while as B increases, the modifier becomes less significant.

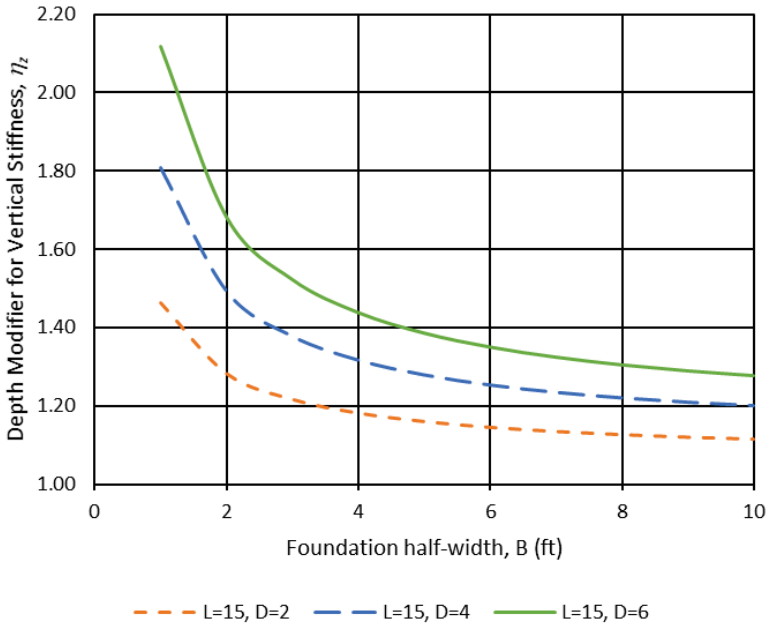

Figure 6-5 Variation of the embedment modifier vertical stiffness with foundation dimensions.

Figure 6-6 shows the variation of the embedment modifier for strong-axis rotational stiffness η_{yy}, with foundation dimensions, for the same parameters. The modifier is similar for values of L of 10 ft and 20 ft as it is for L of 15 ft. For small values of B and large values of D, the modifier can be as high as 7 for the cases illustrated here, while as B increases, the modifier becomes less significant. The rotational modifier is highly dependent on the term D/B.

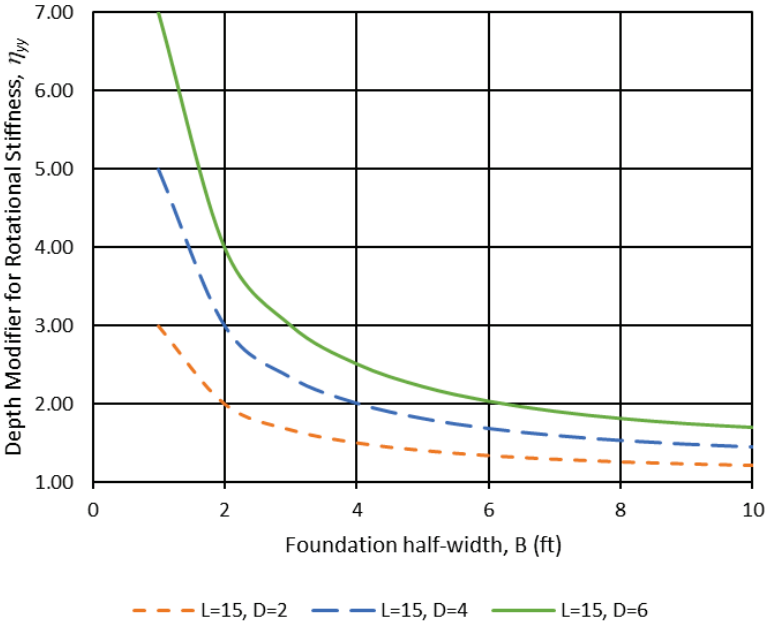

Figure 6-6 Variation of embedment modifiers for rotational stiffness with foundation dimensions.

6.3.2 Method 2 – Flexible Foundation and Nonlinear Flexible Soil

This method defines distributed springs representing the soil support as a discretized continuous medium, with the springs at each end of the footing increased in stiffness. This approach is recommended for nonlinear procedures where explicit coupling of axial and rotational stiffness is modeled with nonlinear springs. This method is explored in detail in Section 2.2.3 of NIST (2012a) and in Chapter 5 of FEMA P-2006 (FEMA, 2018), and is not discussed in detail here.

6.3.3 Method 3 – Flexible Foundation and Linear Flexible Soil

This method defines distributed springs representing the soil support as a discretized continuous medium, with a uniform value for the springs along the length of the footing. This method is best used when the flexibility of the structural elements of the foundation are modeled explicitly. ASCE/SEI 41-17 Equation 8-11 provides a recommended unit subgrade spring coefficient.

$$k_{sv} = \frac{1.3G}{B_f(1-\nu)}$$

Here, G is the effective shear modulus, described in Section 6.1, B_f is the full width of the foundation (not the half-width), and ν is Poisson's ratio, also described in Section 6.1. The subgrade spring coefficient, k_{sv}, has units of force per length cubed, or vertical stiffness per unit area. Where the foundation element is modeled as a line, the vertical stiffness per area is multiplied by the foundation width, cancelling the B_f quantity in the denominator, resulting in a stiffness per unit length that is independent of the foundation width. This is applicable if the foundation width was determined based on the total foundation load. A wider foundation having a higher total load results in a greater depth to which the soil stress extends. More soil under stress means more deformation and therefore lower stiffness.

Using the properties presented in Section 6.1, the value of this stiffness would be:

$$k_{sv}B_f = \frac{1.3(500 \text{ kip/ft}^2)}{(1-0.3)} = 929 \text{ kip/ft/ft}$$

It is also possible to employ the vertical stiffness from Section 6.3.1 divided by the foundation length as an alternative value of this quantity. Figure 6-7 presents examples of the resulting values for the properties discussed above, which range in general from 1 to 3 times the stiffness of that computed via Method 3 and is not independent of the foundation width.

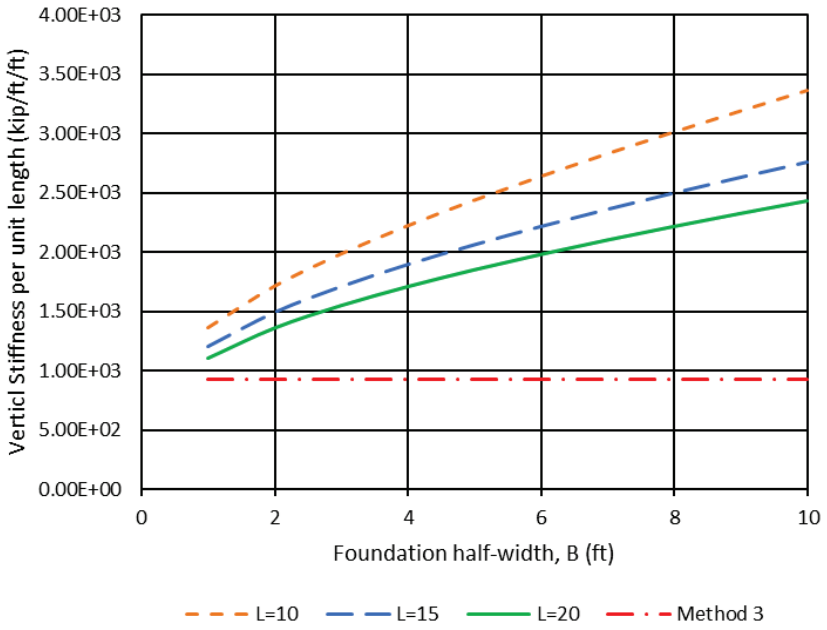

Figure 6-7 Vertical stiffness per unit length computed via Method 1, for various foundation half-lengths and half-widths, with stiffness computed by Method 3 for comparison.

The effect of the Method 3 stiffness may be compared to a rotational spring through the transformation below, adapted from Yim and Chopra (1984).

$$K_{yy} = \frac{2}{3} k_{sv} B_f L^3$$

For the case of L = 15 ft, the equivalent rotational stiffness is then

$$K_{yy} = \frac{2}{3}\left(929 \frac{\text{kip}}{\text{ft}^2}\right)(15 \text{ ft})^3 = 2.09 \times 10^6 \frac{\text{kip-ft}}{\text{rad}}$$

This value is on the lower end of the curve for L = 15 ft in Figure 6-4.

While Method 1 includes specific modifiers to account for the embedment depth, Method 3 does not. However, it may be appropriate to increase the Winkler stiffness developed in Method 3 in a manner similar to Method 1.

6.4 Horizontal Springs

ASCE/SEI 7-16 requires that the analytical model of the structure incorporate the horizontal flexibility of the soil, as well as the vertical and rotational flexibility. Generally, the horizontal flexibility will affect the behavior of the structure far less significantly than will the vertical and rotational flexibility. Nonetheless, all sources of flexibility must be considered.

Note that, unlike the vertical and rotational stiffness, which pertain only to the foundations supporting the individual seismic load resisting elements, the horizontal stiffness will usually include resistance from all foundation elements, including gravity-only footings. This will apply in most cases but may not apply if a building does not include a relatively rigid slab-on-grade or system of grade beams.

As is the case with the vertical and rotational springs, ASCE/SEI 7-16 provides no guidance regarding the development of horizontal springs parallel to the foundation length. There is a horizontal spring formula in ASCE/SEI 7-16 Section 19.3 as part of the radiation damping calculations. However, this formula is for horizontal movement parallel to the width of the foundation, not parallel to its length. Again, ASCE/SEI 41-17 Chapter 8 provides some guidance.

6.4.1 Method 1

Method 1 in ASCE/SEI 41-17 Chapter 8 provides recommendations for horizontal springs as well as for the vertical and rotational springs discussed in Section 6.3.1. The equations are again taken from NIST, with two alternative sets of equations included. The equation from Pais and Kausel (1988) for foundations at the ground surface for horizontal (x-axis) stiffness is presented below. This x-axis is parallel to L, the longer foundation half-dimension.

$$K_{x,sur} = \frac{GB}{2-\nu}\left[6.8\left(\frac{L}{B}\right)^{0.65} + 2.4\right]$$

Note that while the equations for foundation flexibility in Method 1 are indicated as applicable to conditions where the foundation is rigid relative to the soil, and the foundation's structural flexibility is not modeled explicitly, these limitations do not necessarily apply to the horizontal degrees of freedom. This is simply because there is essentially no structural flexibility of the foundation applicable to this direction of movement.

Figure 6-8 shows the variation of horizontal stiffness, $K_{x,sur}$, for the same foundation parameters and dimensions discussed above in Section 6.3.1. As the width increases by 10, the stiffness increases by approximately 2 ¾. As the length increases by a 2, the stiffness increases by approximately 1.5.

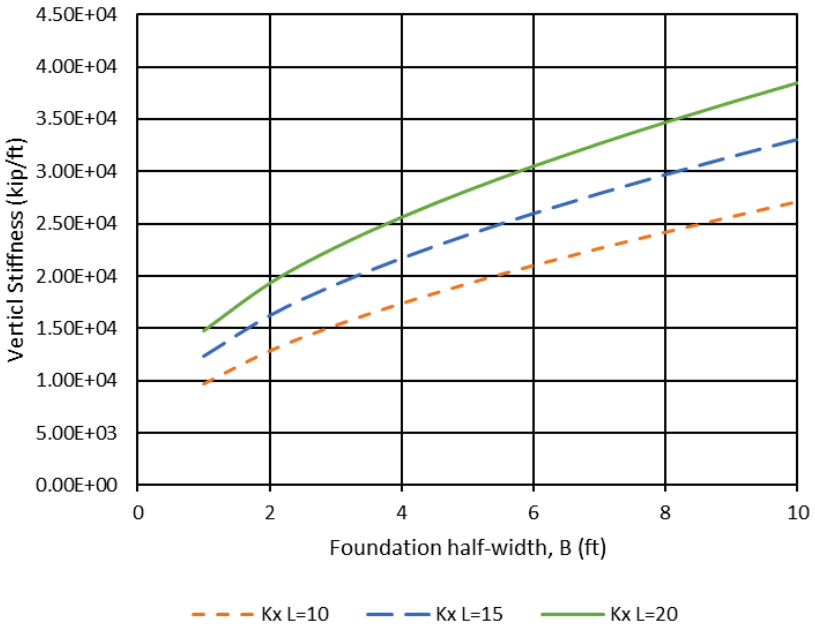

Figure 6-8 Variation of horizontal stiffness with foundation dimensions.

The Pais and Kausel (1988) modification factor to increase the value of horizontal stiffness based on the embedment of the foundation in the soil is presented below.

$$\eta_x = \left[1.0 + \left(0.33 + \frac{1.34}{1 + L/B}\right)\left(\frac{D}{B}\right)^{0.8}\right]$$

Again, D is the depth from the ground surface to the bottom of the foundation. The net stiffness is the product of K_x and η_x.

Figure 6-9 shows the variation of the embedment modifier for horizontal stiffness, η_x, for the same foundation parameters and dimensions discussed above in Section 6.3.1. Similar to the modifier for vertical stiffness, this modifier is essentially the same for values of L of 10 ft and 20 ft as it is for L of 15 ft. For small values of B and large values of D, the modifier can exceed 2, while as B increases, the modifier becomes less significant.

The horizontal spring values are limited by the maximum passive pressure and friction that can be developed. Section 6.4.2 of the *Guide* discusses passive pressure; Section 6.4.3 of the *Guide* discusses friction.

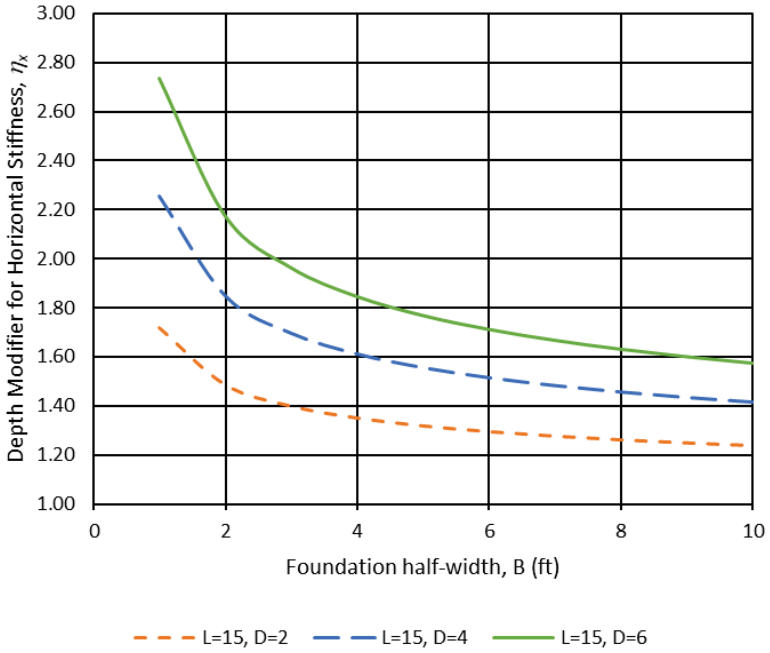

Figure 6-9 Variation of the embedment modifier horizontal stiffness with foundation dimensions.

6.4.2 Resistance due to Passive Pressure

Rather than using the horizontal stiffness formulae in Method 1 of ASCE/SEI 41-17 and in NIST (2012a), it is also possible to compute the horizontal stiffness by considering passive pressure on the sides of foundations based on the recommendations from the geotechnical engineer. Note that ultimate passive pressure is primarily applicable for assessment of the ultimate strength of the resistance provided by the soil, rather than the stiffness directly. A foundation's horizontal stiffness may be computed by dividing the passive pressure developed by the deformation at which it is developed, which can be estimated via a passive pressure mobilization curve. ASCE/SEI 41-17 provides a mobilization curve for passive pressure, which is reproduced in Figure 6-10. This figure presents the ratio of the passive pressure mobilized to the ultimate pressure (P/P_{ult}) as a function of the ratio of the lateral deformation to the depth of the footing (δ/H). This mobilization relationship can be approximated by the following equation, which has been fitted to the curve in the figure.

$$\frac{P}{P_{ult}} = 0.15 + 2.88\left(\frac{\delta}{H}\right)^{0.43}$$

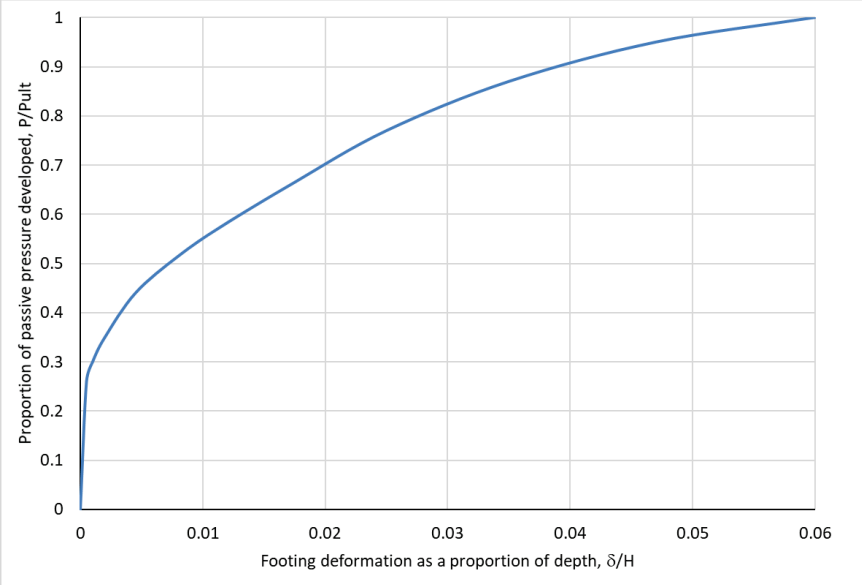

Figure 6-10 Passive pressure mobilization curve (reproduced from ASCE/SEI 41-17, Figure 8-6).

Note, however, that it may actually be more appropriate to use the stiffness from Section 6.4.1 for the initial part of the curve, then develop the larger-strain response as shown here.

6.4.3 Resistance due to Friction or Cohesion

Unlike the resistances discussed above, resistance due to friction between the structure and the soil depends on the weight of the supported structure and the foundation. Frictional resistance at the base of the foundation depends on the angle of internal friction of the soil and may be taken as ranging from 0.67 to 1 times the tangent of the angle of internal friction (Bowles, 2001).

Where foundation soils are cohesive, resistance may be developed by cohesion between the concrete foundation and the soil, which may be taken as 0.5 to 0.75 times the internal cohesion value of the soil (Bowles, 2001).

Resistance due to friction or cohesion occurs at very small deformations, so the precise computation of the resulting stiffness can be difficult. It is reasonable to consider that the frictional resistance will develop at a rate similar to that of the initial, steep portion of the passive pressure mobilization curve. Thus, the resistance due to friction can be added to that due to passive pressure for small deformations.

6.5 Bounding Analyses

ASCE/SEI 7-16 Sections 12.13.3 and 19.1.1 require the use of bounding analyses when considering the flexibility of foundations. ASCE/SEI 7-16 Section 12.13.3 requires consideration of a 50% increase and decrease in the computed soil stiffness for the use in dynamic analyses. ASCE/SEI 7-16 Section 19.1.1 references these bounds when soil-structure interactions are performed.

ASCE/SEI 41-17

ASCE/SEI 41-17 Section 8.4.2 includes a similar bounding requirement. The upper bound is stated as twice the calculated value and the lower bound to be half the calculated value.

See ASCE/SEI 41-17 Figure 8-1 for a graphical representation of this requirement. Note that the upper bound is higher than that indicated in ASCE/SEI 7-16.

The requirement for bounding analyses reflects recognition of the spatial variability and uncertainty of the soil's mechanical properties. In addition, while linear structural analyses may include foundation flexibility, soil behavior is highly nonlinear, which introduces further uncertainty in its behavior.

Another source of potential added flexibility and nonlinearity is the potential loss of contact between the structure and the soil due to rocking. In cases where such loss of contact is possible, the spring stiffness calculations discussed above will result in stiffer spring values that would be present if the loss of contact occurs. In nonlinear analyses, the loss of contact can be modeled explicitly and therefore more precisely. The degree to which the nonlinearity due to rocking can affect the rotational stiffness of a shallow foundation is addressed in Yim and Chopra (1984). In nonlinear analysis, it is important to include the loss of soil-structure contact in the elements at the base of the resisting elements so that this increased flexibility is considered.

6.6 Vertical and Rotational Spring Example

This section includes illustrative examples of vertical and rotational springs, based on the foundation of the transverse frame of the building in Appendix A. The foundation and soil in that example have the following dimensions and properties:

- Length, $2L = 38$ ft; $L = 19$ ft
- Width, $2B = 8$ ft; $B = 4$ ft
- Depth, $D = 5$ ft
- Effective shear modulus, $G = 538$ kip/ft^2
- Poisson's ratio, $\nu = 0.3$

The examples below will cover Methods 1 and 3 from ASCE/SEI 41-17. See FEMA P-2006 for an example of flexibility calculations according to Method 2.

6.6.1 Method 1

Following the Pais and Kausel (1988) equations presented in Section 6.3.1, the surface rotational stiffness is computed as follows:

$$K_{yy,sur} = \frac{GB^3}{1-\nu}\left[3.73\left(\frac{L}{B}\right)^{2.4} + 0.27\right]$$

$$K_{yy,sur} = \frac{\left(538\frac{\text{kip}}{\text{ft}^2}\right)(4\text{ ft})^3}{1-0.3}\left[3.73\left(\frac{19\text{ ft}}{4\text{ ft}}\right)^{2.4} + 0.27\right] = 7.733\times10^6\,\frac{\text{kip-ft}}{\text{rad}}$$

The surface stiffness is then modified to account for the foundation depth.

$$\eta_{yy} = \left[1.0 + \frac{D}{B} + \left(\frac{1.6}{0.35 + (L/B)^4}\right)\left(\frac{D}{B}\right)^2\right]$$

$$\eta_{yy} = \left[1.0 + \frac{5\text{ ft}}{4\text{ ft}} + \left(\frac{1.6}{0.35 + (19\text{ ft}/4\text{ ft})^4}\right)\left(\frac{5\text{ ft}}{4\text{ ft}}\right)^2\right] = 2.25$$

The stiffness of a single spring representing the rotational stiffness of the entire foundation is then computed as follows:

$$K_{yy} = K_{yy,sur}\eta_{yy} = \left(7.733\times10^6\,\frac{\text{kip ft}}{\text{rad}}\right)(2.25) = 17.399\times10^6\,\frac{\text{kip-ft}}{\text{rad}}$$

6.6.2 Method 3

The uniform vertical spring providing rotational resistance at the base of the foundation is computed by ASCE/SEI 41-17 Method 3 as follows:

$$k_{sv}B_f = \frac{1.3G}{(1-\nu)}$$

$$k_{sv}B_f = \frac{1.3(538\text{ kip}/\text{ft}^2)}{(1-0.3)} = 1{,}000\text{ kip/ft/ft}$$

A comparative uniform spring, based on the Method 1 vertical stiffness spread over the foundation length, is computed as follows.

$$K_{z,sur} = \frac{GB}{1-\nu}\left[3.1\left(\frac{L}{B}\right)^{0.75} + 1.6\right]$$

$$K_{z,sur} = \frac{\left(538\frac{\text{kip}}{\text{ft}^2}\right)(4\text{ ft})}{1-0.3}\left[3.1\left(\frac{19\text{ ft}}{4\text{ ft}}\right)^{0.75} + 1.6\right] = 35{,}583\frac{\text{kip}}{\text{ft}}$$

This can be converted to a uniform surface spring per unit length by dividing by the total foundation length, $2L$.

$$K_{z,unif,sur} = \frac{K_{z,sur}}{2L} = \frac{35{,}583\frac{\text{kip}}{\text{ft}}}{2(19\text{ ft})} = 936\text{ kip/ft/ft}$$

The value of this Winkler spring is within 5% of that computed by Method 3. Note that neither of these computations include a modification for the depth of the foundation, as this is not addressed in Method 3.

6.7 Horizontal Spring Example

This section includes illustrative examples of horizontal springs, also based on the foundation of the transverse frame of the building in Appendix A. The properties of the foundation and soil are as described in Section 6.6, above.

As above, the examples below will cover Method 1 from ASCE/SEI 41-17 as well as resistance due to passive pressure on the face of the footing and friction at the base of the footing.

6.7.1 Method 1

Following the Pais and Kausel (1988) equations presented in Section 6.3.1, the surface rotational stiffness is computed as follows:

$$K_{x,sur} = \frac{GB}{2-\nu}\left[6.8\left(\frac{L}{B}\right)^{0.65} + 2.4\right]$$

$$K_{x,sur} = \frac{\left(538\frac{\text{kip}}{\text{ft}^2}\right)(4\text{ ft})}{2-0.3}\left[6.8\left(\frac{19\text{ ft}}{4\text{ ft}}\right)^{0.65} + 2.4\right] = 26{,}738\text{ kip/ft}$$

The surface stiffness is then modified to account for the foundation depth.

$$\eta_x = \left[1.0 + \left(0.33 + \frac{1.34}{1+L/B}\right)\left(\frac{D}{B}\right)^{0.8}\right]$$

$$\eta_x = \left[1.0 + \left(0.33 + \frac{1.34}{1+(19\text{ ft}/4\text{ ft})}\right)\left(\frac{5\text{ ft}}{4\text{ ft}}\right)^{0.8}\right] = 1.67$$

The stiffness of a single spring representing the horizontal stiffness foundation is then computed as follows:

$$K_x = K_{x,sur}\eta_x = \left(26{,}738\frac{\text{kip}}{\text{ft}}\right)(1.67) = 44{,}735\frac{\text{kip}}{\text{ft}} = 3{,}728\frac{\text{kip}}{\text{in}}$$

6.7.2 Passive Pressure and Friction

The following structural information is also required to compute the horizontal stiffness of the transverse frame from the building in Appendix A:

- Imposed gravity load (two columns), $W = 152$ kips. The gravity load used here is based on the load combination $D + 0.25L$, where L is the unreduced live load, as described in ASCE/SEI 41-17 Section 7.2.2.
- Passive pressure = 1.6 kip/ft^2, acting on the leading face of the footing.
- Friction coefficient = 0.35.

Note that, for some sites, the geotechnical engineer will recommend that the passive pressure be computed based on a triangular distribution or may recommend that the upper portion of the footing face be neglected for this calculation.

The frictional resistance at the base of the foundation is

$$(0.35)(152 \text{ kip}) = 53.2 \text{ kip}$$

The fully mobilized passive pressure resistance is

$$\left(1.6\frac{\text{kip}}{\text{ft}^2}\right)(8 \text{ ft})(5 \text{ ft}) = 64 \text{ kip}$$

In this example, the total horizontal force to be resisted by this single footing is 68 kips. The frictional resistance is developed at a very small deformation, resulting in a net force to be resisted by passive pressure of

$$68 \text{ kip} - 53.2 \text{ kip} = 14.8 \text{ kip}$$

The deformation at which this level of resistance occurs can be determined by solving the fitted equation to the passive-pressure mobilization curve.

$$\frac{P}{P_{ult}} = \frac{14.8 \text{ kip}}{64 \text{ kip}} = 0.23 = 0.15 + 2.88\left(\frac{\delta}{H}\right)^{0.43}$$

$$\left(\frac{0.34 - 0.15}{2.88}\right)^{1/0.43} = \frac{\delta}{H} = 0.00025$$

$$\delta = 0.00025\left(H = 60 \text{ in}\right) = 0.015 \text{ in}$$

The horizontal stiffness of the soil-foundation interface computed in this way is then

$$K_x = 68 \text{ kip} / 0.015 \text{ in} = 4{,}550 \text{ kip/in}$$

This value is 22% higher than that computed by Method 1. Please note that the stiffness computed in this manner is highly dependent on the magnitude of the force resisted, due to the shape of the passive pressure mobilization curve.

Chapter 7
Period Lengthening

7.1 Overview

Chapter 6 discusses how vertical and horizontal springs are used to model soil flexibility. Consideration of that flexibility in lateral analysis produces longer fundamental periods and generally increases the degree of mass participation in fundamental modes. The shift to a longer fundamental period always increases displacement response and can increase or decrease acceleration response.

The key equation used to address period lengthening also includes the effect of foundation damping. Consideration of foundation damping is discussed in Chapter 8; this chapter uses the typical damping ratio of 0.05 so that the period lengthening effect can be isolated.

These effects of period lengthening on acceleration and displacement response are a consequence of the basic shape of acceleration and displacement spectra. Figure 7-1 shows a smooth acceleration design spectrum and the corresponding displacement spectrum. The spectral displacement ordinates, S_d, are computed from the spectral acceleration ordinates, S_a, using a following fundamental equation of structural dynamics.

$$S_d = S_a \frac{T^2}{4\pi^2} g$$

For increasing period, spectral acceleration increases to a peak value (at approximately 0.5 seconds in this example) and then decreases for longer periods. Spectral displacement generally increases with increasing period. As a result, period lengthening will result in corresponding changes to the acceleration and displacement response. Figure 7-1 shows the possible effects for Structure "X" and Structure "Y." For Structure X, increasing the period increases both spectral acceleration and spectral displacement. For Structure Y, increasing the period decreases spectral acceleration and increases spectral displacement.

Period Lengthening

Description: Soil flexibility leads to period lengthening in the superstructure, changing seismic demands.

Requirements:

- Two models must be prepared: one that considers the structure to be fixed at its base, and another where the load-deformation characteristics of the foundation-soil system (including lower- and upper-bound variations) are represented explicitly.
- Seismic response coefficients C_s and $\tilde{C}_s$ computed using the fixed-base fundamental period, T, and flexible-base fundamental period, $\tilde{T}$, respectively.
- Seismic weight, which can be taken as either the effective seismic weight, W, or the weight corresponding to the mass participating in the fundamental mode, $\overline{W}$.

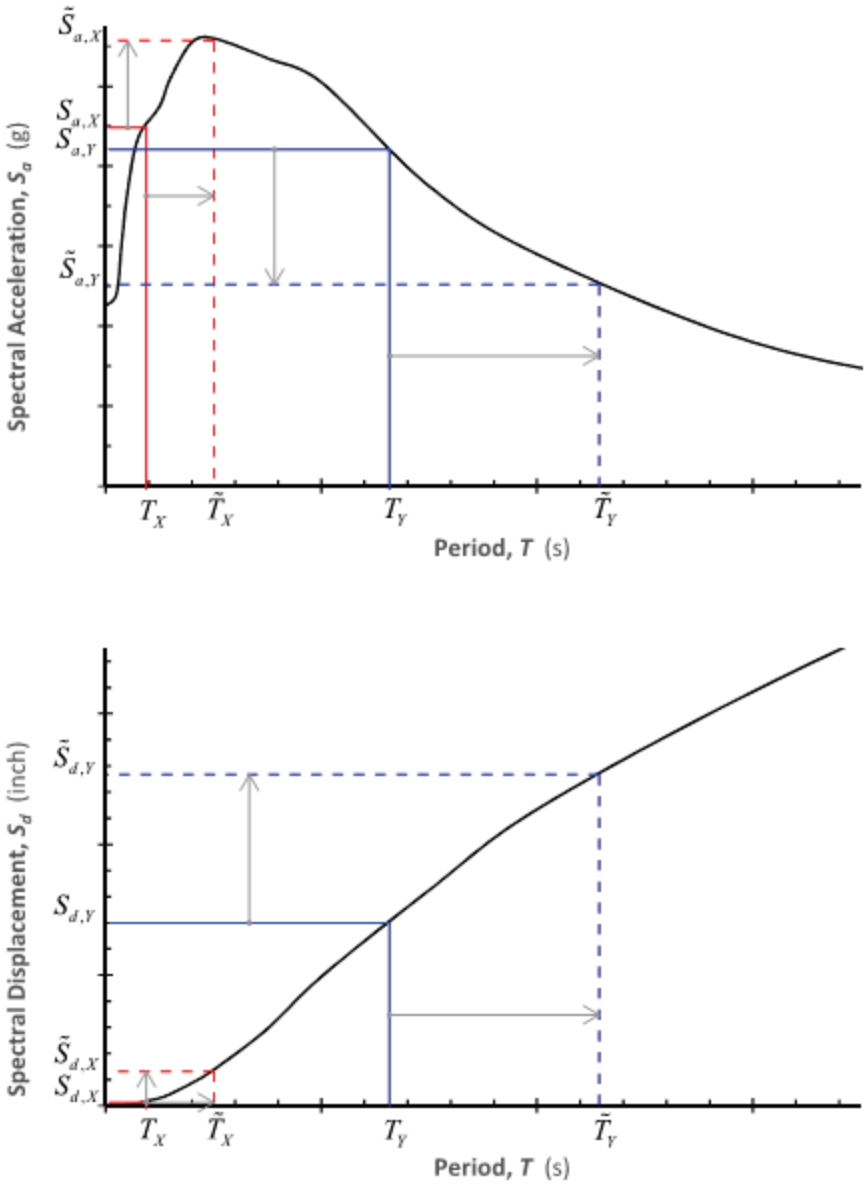

Figure 7-1 Example acceleration and displacement spectra.

7.2 Key Equation

The effect of period lengthening on the design base shear is determined by comparing the fundamental periods and corresponding seismic response coefficients for the fixed-base and flexible-base models. ASCE/SEI 7-16 Equation 19.2-2 is used to compute the base shear adjustment due to SSI, ΔV.

$$\Delta V = \left(C_s - \frac{\tilde{C}_s}{B_{SSI}} \right) \overline{W}$$

where:

C_s = the seismic response coefficient determined in accordance with ASCE/SEI 7-16 Section 12.8.1.1 assuming a fixed structural base at the foundation-soil interface.

$\tilde{C}_s$ = the seismic response coefficient determined in accordance with ASCE/SEI 7-16 Section 12.8.1.1 assuming flexibility of the structural base at the foundation-soil interface in accordance with ASCE/SEI 7-16 Section 19.1.1 using $\tilde{T}$ as the fundamental period of the structure in lieu of the fundamental period of the structure, T, as determined by ASCE/SEI 7-16 Section 12.8.2.

B_{SSI} = the factor to adjust the design response spectrum and MCE_R response spectrum in accordance with ASCE/SEI 7-16 Sections 11.4.6 and 11.4.7 or a site-specific response spectrum for damping ratios other than 0.05. (B_{SSI} is taken as 1.0 in this chapter, i.e., the typical, default damping ratio of 0.05 is assumed.)

W = weight caused by the effective modal mass in the fundamental mode, alternatively taken as the effective seismic weight in accordance with ASCE/SEI 7-16 Section 12.7.2.

T = fundamental period of the structure determined in accordance with ASCE/SEI 7-16 Section 12.8.2 based on a mathematical model with a fixed base condition. The upper bound limitation of $C_u T_a$ on the fundamental period from ASCE/SEI 7-16 Section 12.8.2 shall not apply, and the approximate structural period, T_a, shall not be used.

$\tilde{T}$ = fundamental period of the structure using a model with a flexible base in accordance with ASCE/SEI 7-16 Section 19.1.1. The upper bound limitation of $C_u T_a$ on the fundamental period from ASCE/SEI 7-16 Section 12.8.2 shall not apply, and the approximate structural period, T_a, shall not be used.

The key equation for period lengthening calls for computation of seismic response coefficients in accordance with ASCE/SEI 7-16 Section 12.8.1.1 for both fixed-base and flexible-base models. The intent is to better reflect the changes in dynamic characteristics of the system (due to period elongation and foundation damping). ASCE/SEI 7-16 Equations 12.8-2, 12.8-3, and 12.8-4 define seismic response coefficients that correspond to the constant acceleration, constant velocity, and constant displacement portions of the design response spectrum, respectively. To illustrate the important changes in dynamic response due to period lengthening as clearly as possible, the

examples in Section 7.3 use the smooth spectra directly—modified by $1/R$ for strength demands and by C_d/R for drift demands. The example in Section 7.4 uses the equations in ASCE/SEI 7-16 Sections 12.8.1.1 and 19.2.1, which produce results that differ from the pure dynamic calculations.

ASCE/SEI 7-16 Equations 12.8-5 and 12.8-6 set forth code minima that are independent of both the dynamic characteristics of the system and the basic spectral shape. Although the adjustment of structural demands to reflect SSI in accordance with ASCE/SEI 7-16 Section 19.2 is expressed as modifications to the base shear for the fixed-base structure computed in accordance with ASCE/SEI 7-16 Section 12.8.1, it is not intended that SSI modify the code minima reflected in ASCE/SEI 7-16 Equations 12.8-5 and 12.8-6.

Limited Reduction Due to Foundation Damping

The intent of ASCE/SEI 7-16 Equation 19.2-3 is to limit base shear reductions caused by foundation damping, but as formulated in ASCE/SEI 7-16 reductions due to period lengthening are also affected. A change proposal for the next edition of ASCE/SEI 7 has been submitted to address this issue.

ASCE/SEI 7-16 Equations 19.2-1 and 19.2-3 are used to limit the reduction in base shear due to SSI. While earlier editions of ASCE/SEI 7 limit the base shear reduction to 30%, ASCE/SEI 7-16 limits the reduction as a function of the response modification factor, R. According to the *Commentary* this reflects "the limited understanding of how the effects of SSI interact with the R factor" and the concern that damping caused by structural yielding could make foundation damping less effective. The limits are computed as follows:

$$\tilde{V} = V - \Delta V \geq \alpha V \qquad \text{(ASCE 7-16 Eq. 19.2-1)}$$

$$\alpha = \begin{cases} 0.7 & \text{for } R \leq 3 \\ 0.5 + R/15 & \text{for } 3 < R < 6 \\ 0.9 & \text{for } R \geq 6 \end{cases} \qquad \text{(ASCE 7-16 Eq. 19.2-3)}$$

where:

$\tilde{V}$ = the base shear adjusted for soil-structure interaction

V = the fixed-base structure base shear computed in accordance with ASCE/SEI 7-16 Section 12.8.1

α = the coefficient that accounts for the reduction in base shear caused by foundation damping SSI

R = the response modification coefficient

Unfortunately, this approach does not distinguish between period lengthening and foundation damping effects. It would be possible to recast ASCE/SEI 7-16 Section 19.2.1 so that the α coefficient applies only to the portion of SSI reduction that results from foundation damping. See Section 10.5.1 of this *Guide* for a recommended code change.

7.3 Examples to Illustrate Dynamic Response

To illustrate important changes in dynamic response due to period lengthening, calculations are performed for three example buildings, as follows:

- 3-story special reinforced concrete shear wall building
- 10-story special reinforced concrete shear wall building
- 10-story steel special moment frame building

The examples in this section reflect only the dynamic effects computed using the best available tools—without consideration of limitations imposed by ASCE/SEI 7-16. The fixed-base buildings, which do not have basements, have been realistically proportioned to satisfy strength and drift requirements of ASCE/SEI 7-16. Table 7-1 shows the fundamental mode dynamic properties computed for both fixed-base models and flexible base models.

Table 7-1 Fundamental Mode Dynamic Properties for Example Buildings

Example Building	Fixed-base Condition		Flexible-base Condition	
	Period, T (s)	Fundamental Mode Mass Participation	Period, $\tilde{T}$ (s)	Fundamental Mode Mass Participation
3-story reinforced concrete shear wall	0.193	76.5%	0.492	91.%
10-story reinforced concrete shear wall	1.32	65.0%	2.28	76.0%
10-story steel special moment frame	2.04	80.3%	2.40	82.1%

As expected, introducing foundation flexibility (represented by vertical and horizontal springs) results in period lengthening and increase in fundamental mode mass participation. The introduction of a concentrated source of (foundation) flexibility at the base of a structure has an effect similar to seismic isolation, which allows more of the superstructure mass to participate in the adjusted fundamental mode. Figure 7-2 highlights the changes in fundamental mode properties and response on the acceleration and displacement spectra.

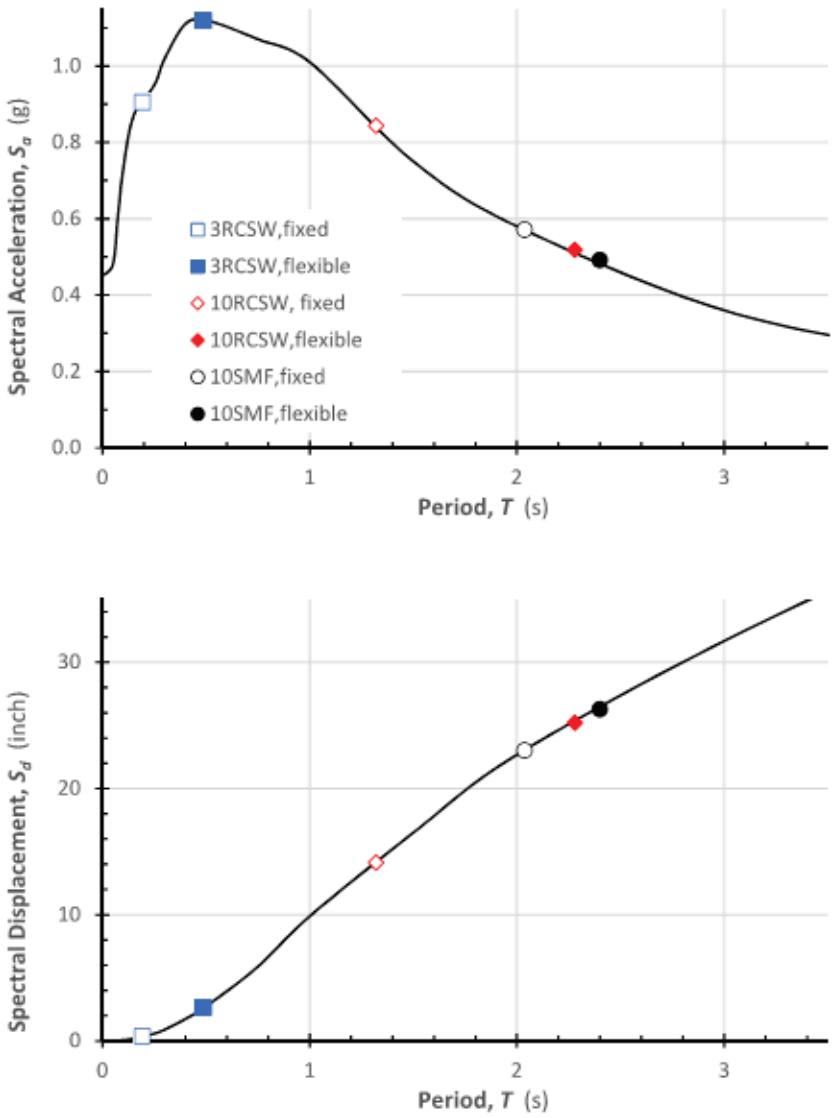

Figure 7-2 Example acceleration and displacement spectra, including points for each example building.

Key lessons that can be drawn from Figure 7-2 are as follows:

- Because the fixed-base period for the 3-story reinforced concrete shear wall building is less than the period with maximum spectral acceleration, period lengthening leads to an increase in the spectral acceleration (which would be associated with increase strength demands).
- Because the fixed-base periods for the 10-story example buildings are greater than the period with maximum spectral acceleration, period lengthening leads to a decrease in spectral acceleration (which would be associated with reduced strength demands).
- Period lengthening always results in increased spectral displacement (which would be associated with increased story drifts).

Although fundamental mode response is dominant, as can be seen from the mass participation factors in Table 7-1, the example buildings have additional modes of dynamic response. Figures 7-3, 7-4, and 7-5 show the global results of modal response spectrum analysis (MRSA) for the example buildings. The story shears, story moments, and story drifts follow the same trends that appear in the fundamental mode response illustrated in Figure 7-2.

Figure 7-5 shows story drift ratios greater than zero at the base for the flexible-base conditions. Because foundation springs are introduced in those models, the displacement at the base is non-zero. The base displacement is equal to the base "drift." Since Figure 7-5 shows story drift ratios, it is necessary to divide the story drift by a story height; story drift ratios are effectively a measure of story rotation angle. Taking a story height of zero at the base would result in undefined drift ratios (due to a divide by zero error), so the figure assumes a fictitious story height of 12'-6" below grade. As a result, for this building with uniform story heights, the drift ratio plot exactly mirrors the story drift plot, which would show non-zero base drift. This method also illustrates the increased base rotation due to foundation (soil) flexibility.

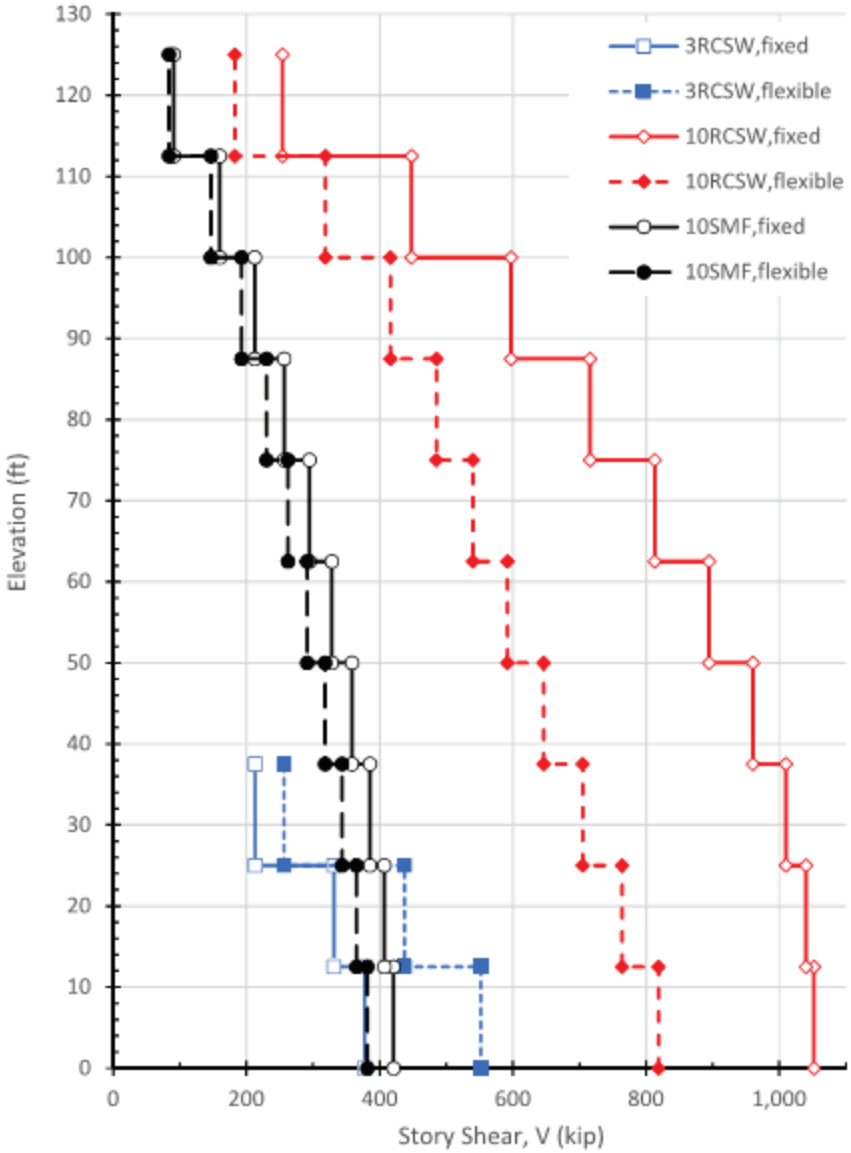

Figure 7-3 Story shears for example buildings.

The effects of adding foundation flexibility on global structural demands (story shear and moment) are more pronounced for the inherently stiffer reinforced concrete shear wall structures. The changes in global structural demands for the inherently flexible steel moment frame structure are more modest.

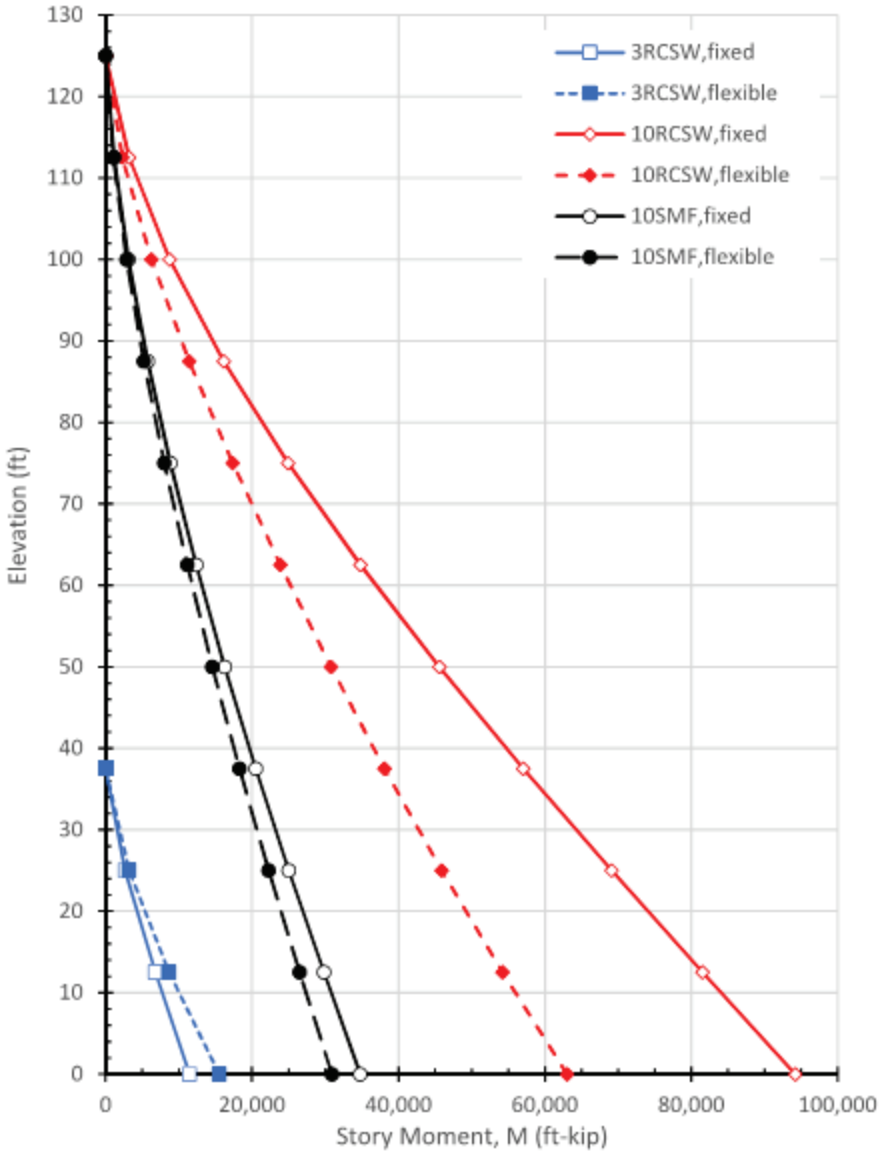

Figure 7-4 Story moments for example buildings.

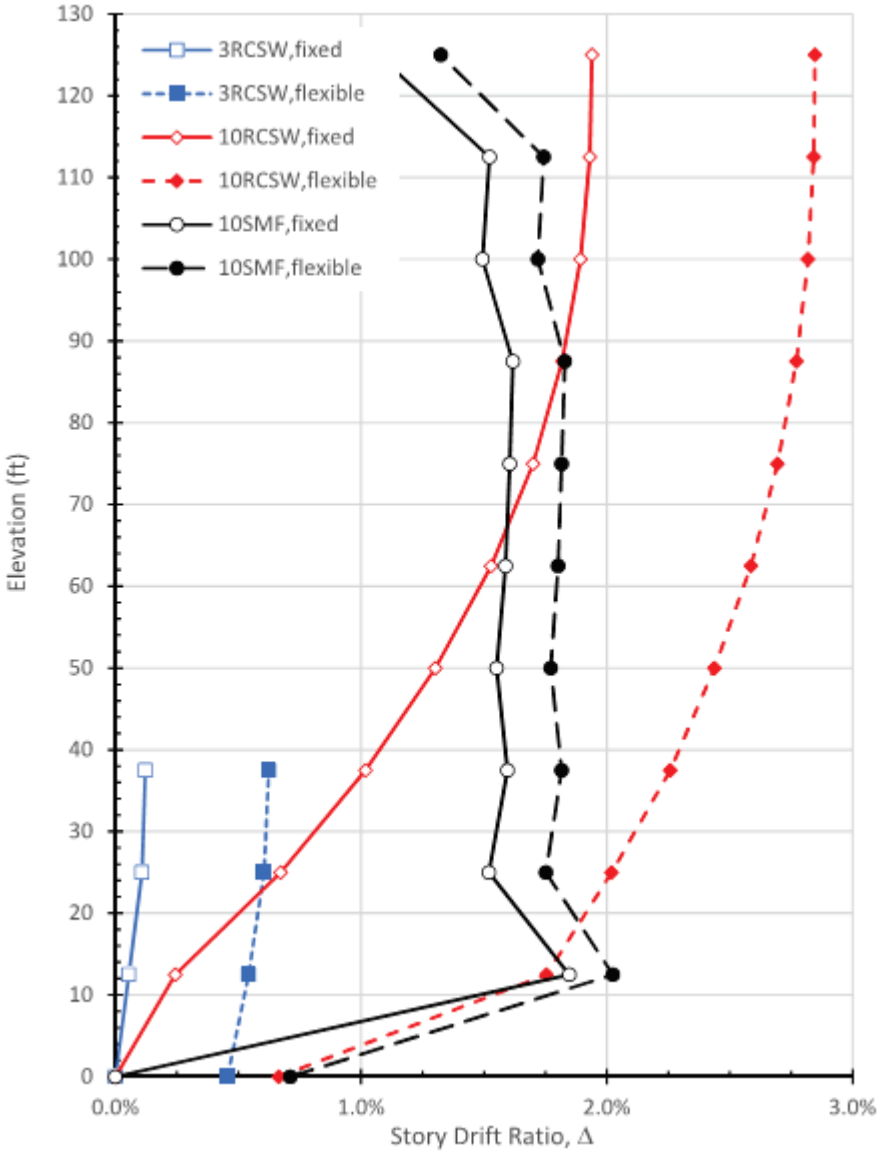

Figure 7-5 Story drift ratios for example buildings.

A few lessons can be learned from Figure 7-5, as follows:

- Foundation (soil) flexibility leads to displacement at the base.
- Rocking response of the 10-story reinforced concrete shear wall building produces greater changes in story drift ratio in the lower half of the building.
- Where story drift ratios for the fixed-base 10-story steel moment frame structure are less than the allowable story drift (2%) set forth in ASCE/SEI 7-16 Table 12.12-1, the flexible-base structure slightly exceeds the allowable story drift at Level 2.

- Although the story drift ratios for the fixed-base 10-story reinforced concrete shear wall building are below the allowable story drift ratio, consideration of foundation flexibility results in story drifts that exceed the limit considerably—due to rotation at the base. Since the rotation about the base of the wall is largely rigid body rotation, there is very little shear distortion in the upper levels of the wall. However, as illustrated in Figure 7-6 the gravity framing and nonstructural systems are subject to shear distortion corresponding to the full story drift.

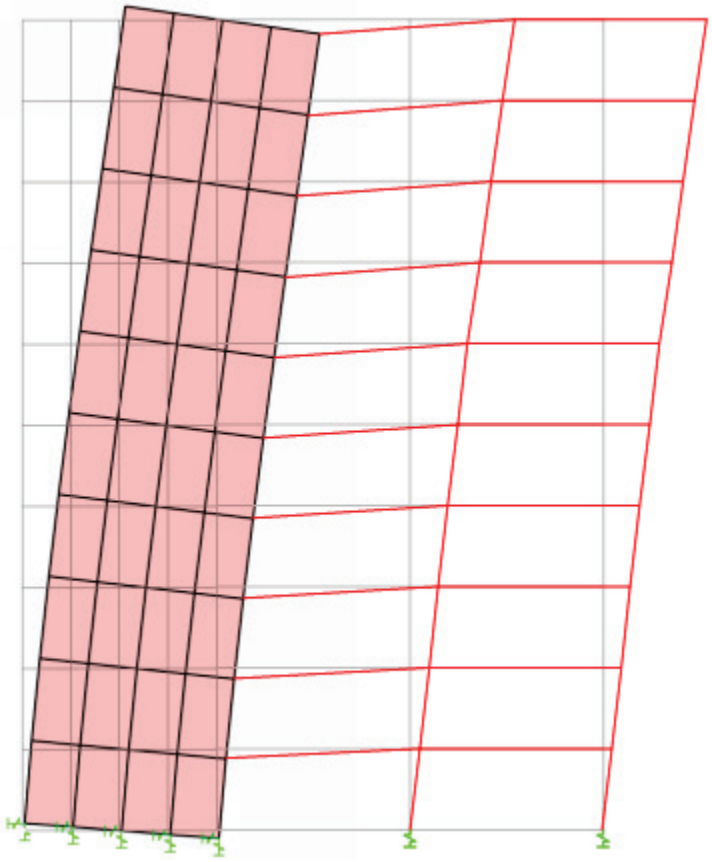

Figure 7-6 Displaced shape for flexible-base, 10-story RCSW building.

7.4 Example Using Code Equations

Application of several provisions in ASCE/SEI 7-16 affect the way that soil structure interaction impacts design—beyond the basic dynamic effects discussed above. These include short period spectral minima, upper limits on the fundamental period, minimum base shear equations, scaling of MRSA results to achieve the base shear values from equivalent lateral force procedure (ELF), and limits on foundation damping.

An example application is used to illustrate the calculation of the period lengthening effect in accordance with ASCE/SEI 7-16 Section 19.2 as

modifications to the ELF procedure of Section 12.8 and the modal response spectrum analysis design requirements of Section 12.9.1.

The example building has plan dimensions of 120 ft in both directions, ten stories at 12 ft 6 in story height, no basement, and perimeter steel special moment frames. The seismic weight tributary to each perimeter moment frame, W, is 7,000 kip. The response modification factor, R, is 8. The seismic importance factor, I_e, is 1.0.

The building is located in a high seismic area with S_{DS} = 1.39 and S_{D1} = 1.16. Figure 7-7 shows the design response spectrum.

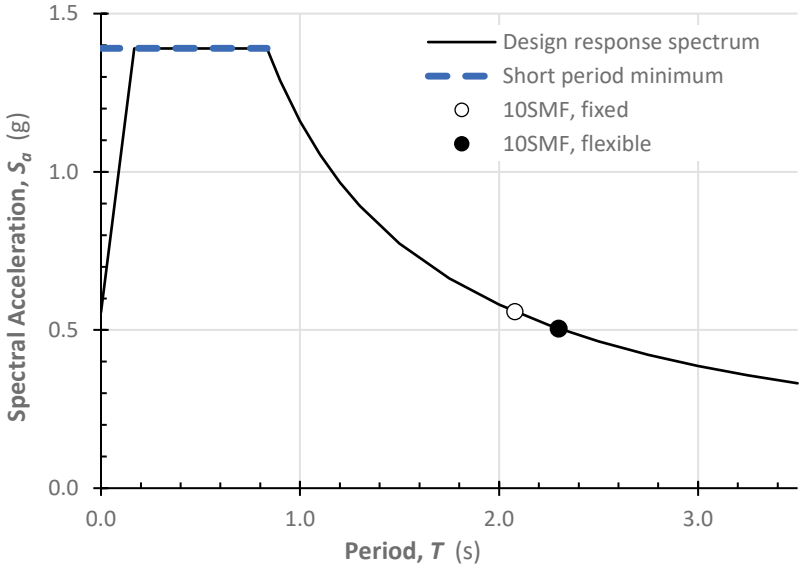

Figure 7-7 Design response spectrum for the example building.

7.4.1 Calculations for the Fixed-Base Condition

The fundamental period from modal analysis for the model with pin supports at the base of each column is 2.04 seconds (with 80.3% of the system mass participating in this mode).

The approximate period is computed using ASCE/SEI 7-16 Equation 12.8-7, with values of C_t and x taken from Table 12.8-2 for steel moment-resisting frames resisting 100% of the required seismic force, as:

$$T_a = C_t h_n^x = 0.028(125)^{0.8} = 1.33 \text{ s}$$

The upper limit period is computed in accordance with ASCE/SEI 7-16 Section 12.8.2 as:

$$C_u T_a = 1.4 \times 1.33 = 1.87 \text{ s}$$

Since this period is shorter than that computed in the analysis, the upper limit period is used in subsequent calculations for the fixed-base condition.

The seismic response coefficient (for the constant acceleration portion of the design spectrum) is computed using ASCE/SEI 7-16 Equation 12.8-2 as follows:

$$C_s = \frac{S_{DS}}{\left(\frac{R}{I_e}\right)} = \frac{1.39}{\left(\frac{8}{1.0}\right)} = 0.174$$

Note that the portion of the design spectrum extending from zero period to the plateau may not be used in computing the base shear. Instead, ASCE/SEI 7-16 Equation 12.8-2 enforces the short period minimum shown in Figure 7-7.

However, the seismic response coefficient need not be taken greater than the value computed using ASCE/SEI 7-16 Equation 12.8-3 or 12.8-4, as applicable. Since $T = 1.87$ seconds $< T_L$, Equation 12.8-3 applies as follows:

$$C_s = \frac{S_{D1}}{T\left(\frac{R}{I_e}\right)} = \frac{1.16}{1.87\left(\frac{8}{1.0}\right)} = 0.0775$$

The minimum seismic response coefficient is computed using ASCE/SEI 7-16 Equation 12.8-5 as follows:

$$C_s = 0.044 S_{DS} I_e = 0.044(1.39)(1.0) = 0.0612$$

ASCE/SEI 7-16 Equation 12.8-3 controls, so the seismic base shear (for each frame) is computed using ASCE/SEI 7-16 Equation 12.8-1 as follows:

$$V = C_s W = 0.0775(7{,}000) = 543 \text{ kip}$$

The base shear from modal analysis for the fixed-base condition is $V_t = 433$ kips. Design force values from modal analysis would require scaling by the factor $V/V_t = 543/433 = 1.25$ in accordance with ASCE/SEI 7-16 Section 12.9.1.4.1.

7.4.2 Calculations for the Flexible-Base Condition

The fundamental period from modal analysis for the model with vertical and horizontal spring supports at the base of each column is 2.40 seconds (with 82.1% of the system mass participating in this mode). This reflects a period lengthening ratio, $\tilde{T}/T = 2.40/2.04 = 1.18$.

As noted in the definitions of T and $\tilde{T}$ in ASCE/SEI 7-16 Section 19.1.3, where the provisions of Chapter 19 are used for SSI, the upper bound limitation of $C_u T_a$ does not apply. Instead, the computed periods, T and $\tilde{T}$ are used directly.

The seismic response coefficient for the fixed-base condition (where that condition will be adjusted in accordance with ASCE/SEI 7-16 Section 19.2) is controlled by ASCE/SEI 7-16 Equation 12.8-3 computed using $T = 2.04$ s as follows:

$$C_s = \frac{S_{D1}}{T\left(\frac{R}{I_e}\right)} = \frac{1.16}{2.04\left(\frac{8}{1.0}\right)} = 0.0711$$

The corresponding fixed-base base shear (using T, since $C_u T_a$ doesn't apply), is computed as 0.0711 times 7,000 kips, which equals 498 kips.

The seismic response coefficient for the flexible-base condition computed using ASCE/SEI 7-16 Equation 12.8-3 is as follows:

$$\tilde{C}_s = \frac{S_{D1}}{\tilde{T}\left(\frac{R}{I_e}\right)} = \frac{1.16}{2.40\left(\frac{8}{1.0}\right)} = 0.0604$$

However, since that flexible-base value of $\tilde{C}_s$ is less than the minimum seismic response coefficient computed using ASCE/SEI 7-16 Equation 12.8-5 (0.0612, as shown above), the minimum value controls and the seismic base shear (for each frame) is computed using ASCE/SEI 7-16 Equation 12.8-1 as follows:

$$\tilde{V} = \tilde{C}_s W = 0.0612(7{,}000) = 428 \text{ kip}$$

Adjustment of the design base shear to account for SSI effects using linear analysis is in accordance with ASCE/SEI 7-16 Section 19.2.1. This example, which focuses on period lengthening, neglects reductions due to damping, which are discussed in Chapter 8; the value of B_{SSI} is taken as 1.0 (corresponding to 5% of critical damping).

The base shear adjustment, ΔV, is computed using Equation 19.2-2.

$$\Delta V = \left(C_s - \frac{\tilde{C}_s}{B_{SSI}}\right)\bar{W} = \left(0.0711 - \frac{0.0612}{1.0}\right)7{,}000 = 69.3 \text{ kip}$$

Note that this permitted reduction is affected by application of the minimum seismic response coefficient, which governs the design base shear.

The value of effective seismic weight used in this calculation, W , could be taken as the "weight caused by the effective modal mass in the fundamental mode," which would be $0.821W$, based on the fundamental mode mass participation factor. However, ASCE/SEI 7-16 permits the direct use of the full effective seismic weight, W. The latter approach is taken as it allows a greater reduction in base shear, without being unconservative since the fixed-base base shear being reduced is computed using the full effective seismic weight.

The limitation on base shear reduction is quantified by the α factor computed in accordance with ASCE/SEI 7-16 Equation 19.2-3. For this system $R = 8$, so $\alpha = 0.9$.

The final base shear adjusted for SSI is computed in accordance with ASCE/SEI 7-16 Equation 19.2-1 as follows:

$$\tilde{V} = V - \Delta V \geq \alpha V$$

$$\tilde{V} = V - \Delta V = 498 - 69.3 = 429 \text{ kip}$$

$$\geq \alpha V = 0.9(498) = 448 \text{ kip} \quad \leftarrow \text{ controls}$$

The final design base shear computed in accordance with ASCE/SEI 7-16 Chapter 19 reflects only a 10% reduction from the fixed-base base shear (without the $C_u T_a$ period limit). This reduction is controlled by application of the limitation for foundation damping, reflected by α, even though no reduction for foundation damping was included in the calculations. This illustrates a flaw in the formulation of ASCE/SEI 7-16 Section 19.2.1, which does not distinguish between reductions due to period lengthening and reductions due to foundation damping. However, this is still an 18% reduction of the base shear used for a truly fixed-base design, where the $C_u T_a$ period limit applies.

The base shear from modal analysis for the flexible-base condition is $\tilde{V}_t = 384$ kips . Design force values from modal analysis would require scaling by the factor $\tilde{V} / \tilde{V}_t = 448 / 384 = 1.17$ in accordance with ASCE/SEI 7-16 Sections 19.2.2 and 12.9.1.4.1.

7.4.3 Summary of Design Demands

Table 7-2 summarizes design demands for the example building. These demands differ from the pure spectral values in several ways. For the fixed-base condition the upper limit on period, $C_u T_a$, defined in ASCE/SEI 7-16 Section 12.8.2 controls. For the flexible-base condition the period independent minimum base shear applies since it is larger than the base shear computed

using the calculated period. However, the design base shear is governed by the maximum reduction permitted by ASCE/SEI 7-16 Section 19.2.1.

Table 7-2 Summary of Design Demands for Example Building

	Fixed-base condition	Flexible-base condition
Computed period	T = 2.04 s	$\tilde{T}$ = 2.40 s
Upper limit on period	$C_u T_a$ = 1.87 s	--
Base shear, ASCE/SEI 7-16 Equation 12.8-3	V = 543 kips (using $C_u T_a$)	$\tilde{V}$ = 423 kips (using $\tilde{T}$)
Minimum base shear, ASCE/SEI 7-16 Equation 12.8-5	V = 428 kips	$\tilde{V}$ = 428 kips
Base shear limited by ASCE/SEI 7-16 Section 19.2.1	--	$\tilde{V}$ = 448 kips
Design base shear	V = 543 kips	$\tilde{V}$ = 448 kips
Base shear from MRSA	V_t = 433 kips	$\tilde{V}_t$ = 384 kips
Scale factor for MRSA design forces, per ASCE/SEI 7-16 Section 12.9.1.4.1	1.25	1.17

Chapter 8
Foundation Damping

8.1 Overview

Inertial interaction is the dynamic interaction between the structure, its foundation, and the surrounding soil caused by the foundation input motion. **Period lengthening** is one inertial interaction effect. It results in an increase in the building period due to foundation flexibility. Period lengthening is covered in Chapter 7. This chapter covers **foundation damping**, a second inertial interaction effect. There are two contributors to foundation damping: **soil damping** and **radiation damping**.

Soil damping is the hysteretic (material) damping of the soil. It is similar to inherent viscous damping in the superstructure, but it is independent of the flexible-base period of the structure.

Radiation damping is the damping in the soil-structure system caused by the generation and propagation of waves away from the foundation, which are caused by dynamic displacements of the foundation relative to the free-field displacements. Radiation damping is larger when the structure-to-soil stiffness ratio is larger. The structure-to-soil stiffness ratio is described in Chapter 3.

Foundation damping is less commonly applied in practice than other types of SSI effects, such as period lengthening and kinematic interaction. NIST (2012a) and Givens et al. (2016) provide an analysis framework for foundation damping that clearly distinguishes the separate contributions from soil damping and radiation damping from different types of foundation vibration. This is convenient for application because the soil damping component of foundation damping is easy to implement. The adiation damping component of foundation damping, on the other hand, is considerably more complex.

ASCE/SEI 7-16 Section 19.3 provides provisions, modified from NIST (2012a), for both the soil and radiation components of foundation damping. Foundation damping can be combined with the effective viscous damping in the superstructure, increasing the damping used, and leading to a reduction in spectral demands. More sophisticated models can incorporate damping effects as dashpots directly into the analytical model. Chapter 9 shows some

Foundation Damping

Description: Foundation damping is an inertial SSI effect. There are two types: soil damping and radiation damping.

Requirements for Soil Damping

- Design spectral response acceleration parameter at short periods, S_{DS}
- Site class
- Fundamental period in a fixed base model, T
- Fundamental period in a flexible base model, $\tilde{T}$
- Response modification coefficient, R
- Overstrength factor, Ω_0
- Expected ductility demand, μ, which is permitted to be taken as R / Ω_0

Additional Requirements for Radiation Damping

- Foundation geometry
- Average effective shear wave velocity, v_s
- Average low strain shear wave velocity, v_{so}
- Average unit weight of soil, γ
- Poisson's ratio, ν

conceptual examples of how dashpots can be incorporated in various modeling approaches; Section 4.3 of NIST (2012a) provides more details. This chapter focuses on the approach in ASCE/SEI 7-16 Section 19.3.

8.2 Foundation Damping Requirements

In order to use foundation damping, the foundation system of the building has to meet the requirements in ASCE/SEI 7-16 Section 19.3.1. Foundation damping is not permitted for the following three cases.

> *[Case 1]: A foundation system consisting of discrete footings that are not interconnected and that are spaced less than the larger dimension of the supported lateral force-resisting element in the direction under consideration.*
>
> *[Case 2]: A foundation system consisting of, or including, deep foundations such as piles or piers.*
>
> *[Case 3]: A foundation system consisting of structural mats interconnected by concrete slabs that are characterized as flexible in accordance with [ASCE/SEI 7-16] Section 12.3.1.3 or that are not continuously connected to grade beams or other foundation elements.*

For Case 1, the commentary in ASCE/SEI 7-16 Section C19.3 notes that:

> *The radiation damping procedure … could be potentially unconservative where wall and frame elements are close enough so that waves emanating from distinct foundation components destructively interfere with each other across the period range of interest. That is why the limit of spacing of the vertical lateral force-resisting elements is imposed on the use of these provisions.*

Figure 8-1 illustrates an example where a pair of discrete, unconnected shear walls and their foundations are too close together. The spacing between the two shear wall footings is s = 14 ft. Although this is greater than the narrower shear wall with width of b_{w2} = 10 ft, it is less than the wider shear wall with a width of b_{w1} = 18 ft. It is the larger wall that governs per the provision. There is additional discussion of this case in FEMA 440 Section 8.3 (FEMA, 2005), which notes that such cases can "effectively decrease the energy dissipated in the soil material, and … could overestimate the related damping."

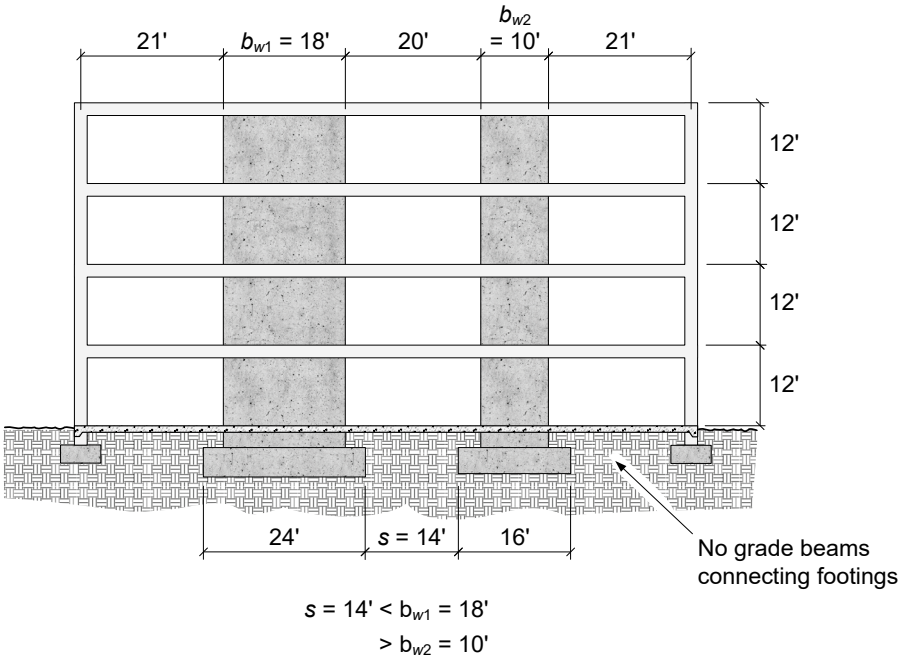

Figure 8-1 Example of a foundation and superstructure where foundation damping is not permitted because the unconnected footings are too close.

For Case 2, the commentary in ASCE/SEI 7-16 Section C19.3 notes that the equations for foundation damping are for shallow foundations.

> *This is not to say that radiation damping does not occur with deep (pile or caisson) foundation systems, but the phenomenon is more complex. Soil layering and group effects are important, and there are the issues of the possible contributions of the bottom structural slab and pile caps. Because the provisions are based on the impedance produced by a rigid plate in soil, these items cannot be easily taken into account. Therefore, more detailed modeling of the soil and the embedded foundations is required to determine the foundation impedances. The provisions permit such modeling but do not provide specific guidance for it. Guidance can be found for example in NIST GCR 12-917-21 [NIST, 2012a] and its references.*

In Case 3, the concern is that a lack of adequate coupling, either through a rigid diaphragm or through continuous grade beams, means the vertical elements of the lateral force-resisting system, such as braced frames or shear walls, may be too weakly coupled and use of the provisions, which are based on the full width of the structure would be potentially unconservative. ASCE/SEI 7-16 Section 19.3.1.1 refers to ASCE/SEI 7-16 Section 12.3.1.3 for evaluation of the flexibility of the slab-on-grade linking footings.

ASCE/SEI 7-16 Section 12.3.1.3 is used in general to characterize slabs as rigid or flexible. A slab is characterized as flexible if $\delta_{MDD} / \Delta_{ADVE} > 2$, with terms defined as shown in Figure 8-2.

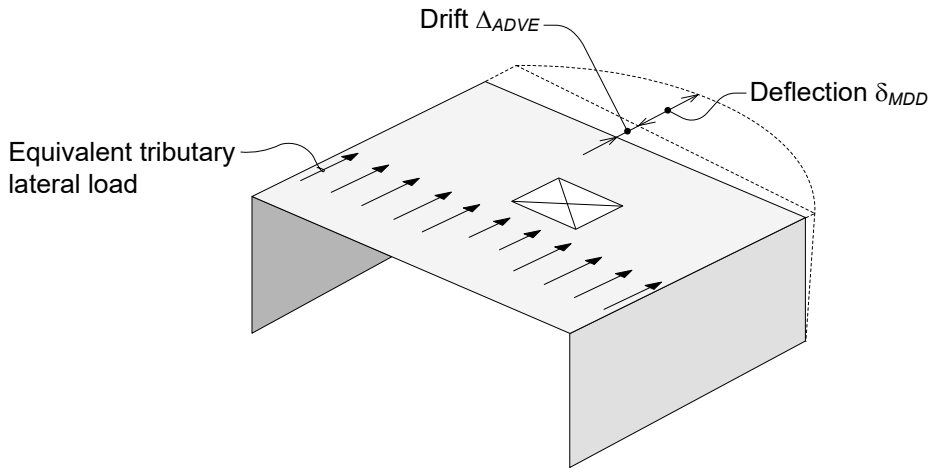

Figure 8-2 Determining slab-on-grade in-plane flexibility (from ASCE/SEI 7-16 Figure 12.3-1).

8.3 Effective Damping Ratio

Typically, seismic code demands for linear procedures are based on an equivalent viscous damping ratio for the structure of 5%. When foundation damping SSI is considered, the goal is to determine an effective damping ratio for the soil-structure system that incorporates contributions from both the structure and the foundation-soil interaction. This is captured in ASCE/SEI 7-16 Equations 19.3-1, 19.3.2, and 19.3.3 shown below.

$$\beta_0 = \beta_f + \frac{\beta}{\left(\frac{\tilde{T}}{T}\right)_{eff}^2} \leq 0.20 \qquad \text{(ASCE/SEI 7-16 Eq. 19.3-1)}$$

where:

β_0 = effective damping ratio of the soil-structure system

β_f = effective viscous damping ratio relating to foundation-soil interaction

β = effective viscous damping ratio of the structure, taken as 5% unless otherwise justified by analysis.

$(\tilde{T}/T)_{eff}$ = effective period lengthening ratio defined in ASCE/SEI 7-16 Equation 19.3-2.

$$\left(\frac{\tilde{T}}{T}\right)_{eff} = \left\{1 + \frac{1}{\mu}\left(\left(\frac{\tilde{T}}{T}\right)^2 - 1\right)\right\}^{0.5}$$

where:

μ = effective ductility demand. For equivalent lateral force or modal response spectrum analysis procedures, μ is the maximum base shear divided by the elastic base shear capacity; alternatively, μ is permitted to be taken as R / Ω_0, where R and Ω_0 are per ASCE/SEI 7-16 Table 12.2-1. This is based on the assumption that R can be considered as the product of ductility and overstrength, so dividing R by Ω_0 results in an estimate of ductility. For response history analysis procedures, μ is the maximum displacement divided by the yield displacement of the structure measured at the highest point above grade.

$$\beta_f = \left[\frac{\left(\frac{\tilde{T}}{T}\right)^2 - 1}{\left(\frac{\tilde{T}}{T}\right)^2}\right]\beta_s + \beta_{rd} \text{ (ASCE/SEI 7-16 Eq. 19.3-3)}$$

where:

β_s = soil hysteretic damping ratio

β_{rd} = radiation damping ratio

The effective damping ratio of the soil-structure system, β_o, is then used in lieu of β when applying damping factors. There is a limit of up to 20% for β_0, or effectively a limit of 15% on β_f. Even so, large values of β_f and β_0 can lead to large reductions in demand.

Note that when a site has a deep softer surface layer over a very stiff layer with a shear wave velocity of twice that of the surface layer, then ASCE/SEI 7-16 Equation 19.3-3 is replaced with Equation 19.3-4 (not reproduced here).

8.4 Soil Damping

8.4.1 Discussion

Soil damping, or soil hysteretic damping, occurs because of shearing within the soil and at the soil–foundation interface. Values of the soil hysteretic damping ratio, β_s, to model the soil hysteretic damping can be obtained from site response analysis as determined by a geotechnical engineer or directly from ASCE/SEI 7-16 Table 19.3-3 as shown in Table 8-1.

Table 8-1 Soil Hysteretic Damping Ratio, β_s (from ASCE/SEI 7-16 Table 19.3-3)

Site Class	Effective Peak Acceleration, $S_{DS}/2.5$[1]			
	$S_{DS}/2.5 = 0$	$S_{DS}/2.5 = 0.1$	$S_{DS}/2.5 = 0.4$	$S_{DS}/2.5 \geq 0.8$
C	0.01	0.01	0.03	0.05
D	0.01	0.02	0.07	0.15
E	0.01	0.05	0.20	[2]
F	[2]	[2]	[2]	[2]

[1] Use straight-line interpolation for intermediate values of $S_{DS}/2.5$.

[2] Site-specific geotechnical investigation and dynamic site response analyses shall be performed.

8.4.2 Soil Damping Example

As an example of soil damping, assume the following.

- The design spectral response acceleration parameter at short periods at the site is S_{DS} = 1.0g; then the effective peak acceleration is S_{DS} / 2.5 = 0.4.
- The site is characterized as Site Class E; then β_s = 0.20 per Table 8-1. Review of the values in Table 8-1 indicates that softer soils and higher ground shaking levels lead to higher values of soil damping.
- The building is Risk Category II, so I_e = 1.0.
- The lateral force-resisting system is a special concentrically braced frame structure with a seismic response or base shear coefficient governed by ASCE/SEI 7-16 Equation 12.8-2 of $V / W = C_s = S_{DS} / (R / I_e)$ = 1.0 / (6 / 1.0) = 0.167.
- The effective viscous damping ratio of the structure is the typical 0.05.
- The equivalent lateral force procedure is being used for design.

In order to implement soil damping and determine its impact on design forces, several steps are required.

Step 1: The effective viscous damping ratio related to foundation-soil interaction, β_f, must be calculated, and this depends on the ratio ($\tilde{T}/T$). This in turn requires modeling the building with soil springs to compare fixed-base and flexible-base periods. This is described in Chapters 6 and 7. Say that the results of this exercise lead to a ratio ($\tilde{T}/T$) = 1.2. Entering the values into ASCE/SEI 7-16 Equation 19.3-3 yields the following, assuming zero for radiation damping.

$$\beta_f = \left[\frac{\left(\frac{\tilde{T}}{T}\right)^2 - 1}{\left(\frac{\tilde{T}}{T}\right)^2}\right]\beta_s + \beta_{rd} = \left[\frac{\left((1.2)^2 - 1\right)}{(1.2)^2}\right](0.20) + 0 = 0.06$$

Step 2: Calculate the expected ductility demand, μ. For a special concentrically braced frame, $R = 6$ and $\Omega_0 = 2$. μ is permitted to be taken as $R / \Omega_0 = 6 / 2 = 3$.

Step 3: Calculate the effective period lengthening ratio per ASCE/SEI 7-16 Equation 19.3-2.

$$\left(\frac{\tilde{T}}{T}\right)_{eff} = \left\{1 + \frac{1}{\mu}\left(\left(\frac{\tilde{T}}{T}\right)^2 - 1\right)\right\}^{0.5}$$

$$= \left\{1 + \left(\frac{1}{3}\right)\left((1.2)^2 - 1\right)\right\}^{0.5} = 1.071$$

Step 4: Calculate the effective viscous damping ratio of the soil-structure system per ASCE/SEI 7-16 Equation 19.3-1.

$$\beta_0 = \beta_f + \frac{\beta}{\left(\frac{\tilde{T}}{T}\right)^2_{eff}} \le 0.20 = 0.06 + \left(\frac{0.05}{(1.071)^2}\right) = 0.06 + 0.04 = 0.10 < 0.20$$

Thus, in this example, soil damping doubles the effective damping from 0.05 for the effective viscous damping ratio of the structure to 0.10 for the effective damping ratio of the soil-structure system.

Step 5: Determine the factor to adjust the design response spectrum, B_{SSI} per ASCE/SEI 7-16 Equation 19.2.4.

$$B_{SSI} = 4 / [5.6 - \ln (100\ \beta_0)] = 4 / [5.6 - \ln (100 \times 0.10)] = 1.21$$

Step 6: For the equivalent lateral force procedure, determine the reduction in base shear per a modified version of ASCE/SEI 7-16 Equation 19.2.2 to compare the base shear coefficient $V / W = C_s$ directly. For this short structure, it is assumed that the flexible base period does not lengthen sufficiently to change the governing base shear, and $C_s = \tilde{C}_s = 0.167$.

$$\Delta C_s = C_s - \frac{\tilde{C}_s}{B_{SSI}} = 0.167 - \frac{0.167}{1.213} = 0.167 - 0.138 = 0.029$$

Step 7: Determine the ratio of the base shear adjusted for SSI vs. the base shear from a fixed base model per a modified version of ASCE/SEI 7-16 Equation 19.2.1: 0.138 / 0.167 = 0.826.

Step 8: Compare with the limits in ASCE/SEI 7-16 Equation 19.2-3. With $R = 6$, there is a floor on the reduction $\alpha = 0.9$. This is higher than the 0.826 ratio calculated in Step 7, so the $\alpha = 0.9$ floor governs, and ASCE/SEI 7-16 limits the reduction due to soil damping to 10%.

8.5 Radiation Damping

8.5.1 Discussion

Radiation damping is discussed in NIST (2012a) and the equations in ASCE/SEI 7-16 are a simplification of those in NIST (2012a). Radiation damping provisions for rectangular footings are in ASCE/SEI 7-16 Section 19.3.3. Section 19.3.4 provides provisions for circular footings, which have been a traditional focus of research, but are rarely needed in practice since circular footings are rarely found in actual buildings. This *Guide* focuses on rectangular footings. Even with the simplifications in ASCE/SEI 7-16, calculations for radiation damping are involved. In addition, the order in which the equations are given in ASCE/SEI 7-16 does not follow the sequence that is needed to perform the calculations. As such, a step by step example is given in Section 8.5.2 to illustrate the proper sequence.

For rectangular footings, the long direction is defined as $2L$, and the narrow direction is defined as $2B$, in keeping with the traditional approach used in the geotechnical literature. Earthquake movement can occur parallel to either axis. Movement parallel to the long direction is called movement in the strong direction. Movement parallel to the narrow direction is called movement in the weak direction. NIST (2012a) provides equations to allow calculating radiation damping for translational and rotational movement in both the strong direction and weak direction.

In the development process for the SSI provisions in ASCE/SEI 7-16, the desire for simplification led code writers to include only the translational and rotational stiffness values that result in the lower values of damping which are associated with movement in the weak direction parallel to the narrow direction of the footing. They are purposely conservative. This is not stated in the ASCE/SEI 7-16 provisions or commentary. The engineer could, with more effort, use the more refined equations that are in NIST (2012a). In fact, it would be more rational in many cases since the long direction of the footing is typically associated with the primary direction of resistance of the

vertical lateral-force resisting element that the footing supports. The long direction will also typically produce more radiation damping.

8.5.2 Radiation Damping Example

The example of radiation damping here is taken from Appendix A.6, except that more background is provided here. The resulting impact on the base shear coefficient is determined, similar to the soil damping example in Section 8.4.2. In the appendix, the design implications on member sizes of the base shear reduction are studied. Assumptions for the example are as follows.

- The design spectral response acceleration parameter at short periods at the site is S_{DS} = 1.57g.
- The site is characterized as Site Class D.
- The building is Risk Category II, so I_e = 1.0.
- The lateral force-resisting system is a buckling-restrained braced frame structure on spread footings with a seismic response or base shear coefficient governed by ASCE/SEI 7-16 Equation 12.8-2 of $V / W = C_s = S_{DS} / (R / I_e) = 1.57 / (8 / 1.0) = 0.196$.
- The effective viscous damping ratio of the structure is the typical 0.05.
- Spread footings under the braced frames are 38 ft long by 8 ft wide by 5 ft deep, not connected to one another, and are far enough apart to satisfy ASCE/SEI Section 19.3.1.1. The top of the footing is 1'0" below the top of the slab-on-grade.
- The slab-on-grade is 5" thick, and overpoured above the footings.
- Equivalent lateral force (ELF) procedure is being used for design.
- Figure A-1 presents the soil profile at the site.

In order to implement radiation damping and determine its impact on design forces, a number of steps are required. Initial steps focus on determining the appropriate geometry, followed by determining soil properties under the footings, including the shear wave velocity, then the stiffness properties, then the damping coefficients, then the foundation damping ratio, and finally the effective reduction in base shear. Note that these soil, stiffness, and damping properties are all particular to the radiation damping computations.

Step 1: Determine the L and B dimensions to use. In a mat foundation, or a foundation connected by grade beams, the dimensions for entire structure footprint are used, so that L is half the larger dimension of the base of the structure and B is half the smaller dimension of the base of the structure. For

this example, however, the braced frames are on discrete spread footings that are not connected to one another. The radiation damping comes in part from rotation of the individual footings in the soil. The commentary of ASCE/SEI 7-16 Section C19.3 recommends use of the individual footing dimensions in this case. Thus $2L$ = 38 ft for the long direction of the footing parallel to the braced frame and $2B$ = 8 ft for the narrow direction of the footing perpendicular to the braced frame, so L = 19 ft and B = 4 ft. The value of B = 4 ft is key in the next steps.

Step 2: Calculate the average low strain shear wave velocity, v_{so}. Note that the shear wave velocity here is not v_s , the value used to determine the site class. Here, v_s is considered for the upper soil layer, over the depth from base of footing at 1'0" for the slab-on-grade and overpour plus the 5'0" footing at Elevation -6'0" to B = 4 ft below to Elevation -10'0". The use of $\overline{v_s}$ for site class determination is intended to account for the average soil stiffness in the upper 100 ft (30 m); the use of v_s for the upper soil layer is intended to capture the effects of the upper soils that more directly affect the damping at the soil-structure interface. The shear wave velocity between Elevation -6'0" and Elevation -10'0" is 653 ft/s, per Figure A-1. Note that a profile of shear wave velocity vs. depth is thus needed in the geotechnical report, not simply the $\overline{v_s}$ value.

Step 3: Calculate the average effective shear wave velocity, v_s. This value represents the reduction in velocity from the average low strain velocity as the soil softens and yields at higher strains during earthquake shaking. It is thus dependent on the earthquake shaking level. This calculation uses ASCE/SEI 7-16 Table 19.3-1 and the design spectral response acceleration parameter at short periods, S_{DS}. For this site, S_{DS} =1.57. Thus, the effective peak acceleration is S_{DS} / 2.5 = 0.628. This is in between the columns for S_{DS} / 2.5 = 0.4 and S_{DS} / 2.5 ≥ 0.8 in Table 19.3-1, so interpolation is used. For Site Class D and S_{DS} / 2.5 = 0.4, the effective shear wave velocity ratio, [v_s / v_{so}] = 0.71. For S_{DS} / 2.5 ≥ 0.8, the effective shear wave velocity ratio, [v_s / v_{so}] = 0.32. Interpolating at S_{DS} / 2.5 = 0.628 yields [v_s / v_{so}] = 0.488. Thus $v_s = v_{so}$ [v_s / v_{so}] = 653 ft/s (0.488) = 318.664 ft/s = 319 ft/s.

Step 4: Calculate the average shear modulus for the soils beneath the foundation, G_0. This also applies to the soil from Elevation -6'0" to Elevation -10'0". Figure A-1 shows the soil density in this region, γ, to be 120 to 125 lb/ft^3. Use an average value of 122.5 lb/ft^3. From the ASCE/SEI 7-16 Section 19.3.3 definition, the soil shear modulus at small strain levels, G_0, is computed as

$$G_0 = \gamma \frac{v_{so}^2}{g} = (122.5)\left(\frac{653^2}{32.174}\right) = 1{,}609 \ \frac{\text{kip}}{\text{ft}^2}$$

Step 5: Calculate the effective shear modulus, G. Like the average effective shear wave velocity in Step 3, G represents the reduction in shear modulus from the shear modulus based on average low strain velocity as the soil softens and yields at higher strains during earthquake shaking. This calculation uses ASCE/SEI 7-16 Table 19.3-2 and the design spectral response acceleration parameter at short periods, S_{DS}. For this site, per above S_{DS} / 2.5 = 0.628. This is in between the columns for S_{DS} / 2.5 = 0.4 and S_{DS} / 2.5 ≥ 0.8 in Table 19.3-2, so interpolation is used. For Site Class D and S_{DS} / 2.5 = 0.4, the effective shear modulus ratio, $[G/G_0] = 0.50$. For S_{DS} / 2.5 ≥ 0.8, the effective shear modulus ratio, $[G/G_0] = 0.10$. Interpolating at S_{DS} / 2.5 = 0.628 yields $[G/G_0] = 0.272$. Thus $G = G_0\ [G/G_0]$ = 1,609 kip/ft^2 (0.272) = 441.597 kip/ft^2 = 442 kip/ft^2.

Step 6: Calculate the period lengthening ratio, $(\tilde{T}/T)$, where $\tilde{T}$ is the flexible-base period and T is the fixed-base period. These values come from models without and with springs. The value of $(\tilde{T}/T)$ is computed as 0.532 s / 0.466 s = 1.142.

Step 7: Calculate the expected ductility demand, μ. For a buckling-restrained braced frame, R = 8 and Ω_0 = 2.5. μ is permitted to be taken as R / Ω_0 = 8 /2.5 = 3.2.

Step 8: Calculate the effective period lengthening ratio, $(\tilde{T}/T)_{eff}$. It depends on the period lengthening ratio $(\tilde{T}/T)$ =1.142 from Step 6 and the system ductility, μ = 3.2 from Step 7. The effective period lengthening ratio is then computed according to ASCE/SEI 7-16 Equation 19.3-2.

$$\left(\frac{\tilde{T}}{T}\right)_{eff} = \left\{1 + \frac{1}{\mu}\left(\left(\frac{\tilde{T}}{T}\right)^2 - 1\right)\right\}^{0.5}$$

$$= \left\{1 + \left(\frac{1}{3.2}\right)\left((1.142)^2 - 1\right)\right\}^{0.5} = 1.046$$

Step 9: Calculate the translational foundation stiffness, K_y. This represents the horizontal stiffness of the foundation moving horizontally within the soil. It requires the effective shear modulus G = 442 kip/ft^2 from Step 5, B = 4 ft, a Poisson's ratio of ν = 0.3 (for the sandy soil), and the plan dimensionless ratio (L/B) = (38 ft / 8 ft) = 4.75. The translational foundation stiffness is calculated per ASCE/SEI 7-16 Equation 19.3-8.

$$K_y = \frac{GB}{2-\nu}\left[6.8\left(\frac{L}{B}\right)^{0.65} + 0.8\left(\frac{L}{B}\right) + 1.6\right]$$

$$= \left[\frac{(441{,}597)(4)}{1.7}\right]\left[18.722 + 3.8 + 1.6\right] = 2.506 \times 10^7 \text{ lb/ft}$$

Step 10: Calculate the rotational foundation stiffness, K_{xx}. This represents the rotational stiffness of the frame and footing rocking in the soil. The rocking foundation stiffness is calculated per ASCE/SEI Equation 19.3-9.

$$K_{xx} = \frac{GB^3}{1-\nu}\left[3.2\left(\frac{L}{B}\right) + 0.8\right]$$

$$= \left[\frac{(441{,}597)(4)^3}{0.7}\right]\left[15.2 + 0.8\right] = 6.460 \times 10^8 \left(\frac{\text{ft} - \text{lb}}{\text{rad}}\right)$$

Step 11: Calculate the dimensionless frequency, a_0, per ASCE/SEI Equation 19.3-11.

$$a_0 = \frac{2\pi B}{\tilde{T}v_s} = \frac{\left[(2)(\pi)(4)\right]}{\left[(0.532)(319)\right]} = 0.1489$$

Step 12: Calculate the dimensionless factor, ψ, per ASCE/SEI Equation 19.3-13.

$$\psi = \sqrt{\frac{2(1-\nu)}{1-2\nu}} = \left[\frac{(2)(1-0.3)}{1-0.6}\right]^{0.5} = 1.871 \le 2.5, \text{ use } 1.871$$

Step 13: Calculate the dimensionless factor, α_{xx}, per ASCE/SEI Equation 19.3-14.

$$a_{xx} = 1.0 - \left[\frac{\left(0.55 + 0.01\sqrt{\left(\frac{L}{B}\right) - 1}\right)a_0^2}{\left(2.4 - \frac{0.4}{\left(\frac{L}{B}\right)^3}\right) + a_0^2}\right]$$

$$= 1.0 - \left[\frac{\left(0.55 + 0.01(1.936)\right)(0.148)^2}{\left[(2.4 - 0.0037) + (0.148)^2\right]}\right] = 0.995$$

Step 14: Calculate the effective structure height, h^*. As indicated in the ASCE/SEI 7-16 Section 19.3.3 definitions, this is the vertical distance from the foundation to the centroid of the first mode shape for multistory structures. Alternatively, h^* is permitted to be approximated as 70% of the total structural height for multistory structures or as the full height of the structure for one-story structures. The alternate formulation is 0.70 × (12.5 ft first story + 12.5 ft second story) = 17.5 ft. The more precise formulation comes from analyzing the first mode shape output from computer results. This is described in Appendix A and results in $h^* = 0.677$ (25 ft) = 16.92 ft.

Step 15: Calculate the fundamental translational period, T_y. The fundamental translational period of the damping system is computed based on the computed stiffness, K_y, and the effective modal mass, M^*. The effective modal mass comes from computer results. As described in Appendix A, the effective modal mass, M^*, is the building seismic mass, multiplied by the first modal mass participation factor (in this case, 0.87), divided by the number of frames in the direction under consideration (4). The modal mass participation factor expresses the proportion of the total mass excited in the first natural mode of vibration. It can be found as part of the computer modal results. In this case, $M^* = 3.26 \times 10^4$ lb-sec^2/ft.

The translational period, T_y, is computed according to ASCE/SEI 7-16 Equation 19.3-6. Note again that the fundamental translational period (and the fundamental rotational period) is particular to the damping computations and is not directly related to the fixed base and flexible base periods from the structural analyses.

$$T_y = 2\pi\sqrt{\frac{M^*}{K_y}} = (2)(\pi)\left(\frac{32{,}600}{25{,}060{,}000}\right)^{0.5} = 0.227 \text{ sec}$$

Step 16: Calculate the fundamental rotational period, T_{xx}. Note that this is incorrectly identified as the fundamental translational period in the ASCE/SEI 7-16 Section 19.1.3 definitions. The fundamental rotational period, T_{xx}, is computed according to ASCE/SEI 7 Equation 19.3-7.

$$T_{xx} = 2\pi\sqrt{\frac{M^* h^{*2}}{\alpha_{xx} K_{xx}}} = (2)(\pi)\left[\frac{(32{,}600)(16.92)^2}{(0.995)(646{,}000{,}000)}\right]^{0.5} = 0.757 \text{ sec}$$

Step 17: Calculate the translational foundation damping coefficient, β_y. per ASCE/SEI 7-16 Equation 19.3-10.

$$\beta_y = \left[\frac{4\left(\frac{L}{B}\right)}{\frac{K_y}{GB}}\right]\left[\frac{a_0}{2}\right] = \left[\frac{(4)(4.75)}{\frac{25{,}060{,}000}{(441{,}597)(4)}}\right]\left[\frac{0.148}{2}\right] = 0.099$$

Step 18: Calculate the rotational foundation damping coefficient, β_{xx}. per ASCE/SEI 7-16 Equation 19.3-12.

$$\beta_{xx} = \left[\frac{\left(\frac{4\psi}{3}\right)\left(\frac{L}{B}\right)a_0^2}{\left(\frac{K_{xx}}{GB^3}\right)\left[2.2 - \frac{0.4}{\left(\frac{L}{B}\right)^3} + a_0^2\right]}\right]\left[\frac{a_0}{2\alpha_{xx}}\right]$$

$$= \left[(4)\left(\frac{1.871}{3}\right)(4.75)(0.148)^2 / \left((646{,}000{,}000)/(441{,}597)(4)^3\right)\right]\left[\left(2.2 - \frac{0.4}{(4.75)^3}\right) + (0.148)^2\right]\left[\frac{0.148}{(2)(0.995)}\right]$$

$$= 0.000383$$

Note that the translational damping is a much more significant effect than the rotational damping ($\beta_y = 0.0998 > \beta_{xx} = 0.00383$), although the elastic behavior of the building is more significantly affected by the rotation.

Step 19: Calculate the effective radiation damping ratio, β_{rd}, per ASCE/SEI 7-16 Equation 19.3-5.

$$\beta_{rd} = \frac{1}{\left(\frac{\tilde{T}}{T_y}\right)^2}\beta_y + \frac{1}{\left(\frac{\tilde{T}}{T_{xx}}\right)^2}\beta_{xx}$$

$$= \left(\frac{1}{\left(\frac{0.532}{0.228}\right)^2}\right)(0.0998) + \left(\frac{1}{\left(\frac{0.532}{0.761}\right)^2}\right)(0.000389)$$

$$= 0.0183 + 0.00080 = 0.019$$

Step 20: Calculate the foundation damping ratio, β_f. This can include the effect of both soil damping and radiation damping. The foundation damping ratio is calculated per ASCE/SEI 7-16 Equation 19.3-3. Since this example focuses on radiation damping, assume that soil damping is zero. Typically, they would be included together, and they are for the example in Appendix

A. For the assumption here that soil damping is zero, ASCE/SEI 7-16 Equation 19.3-3 simplifies to:

$$\beta_f = \left[\frac{\left(\frac{\tilde{T}}{T}\right)^2 - 1}{\left(\frac{\tilde{T}}{T}\right)^2} \right] \beta_s + \beta_{rd} = 0 + 0.019 = 0.019$$

Step 21: Calculate the effective viscous damping ratio of the soil-structure system per ASCE/SEI 7-16 Equation 19.3-1.

$$\beta_0 = \beta_f + \frac{\beta}{\left(\frac{\tilde{T}}{T}\right)^2_{eff}} \leq 0.20$$

$$= 0.019 + \left(\frac{0.05}{(1.046)^2} \right) = 0.019 + 0.046 = 0.065 < 0.20$$

Thus, in this example, radiation damping increases the effective damping from 0.05 for the effective viscous damping ratio of the structure to 0.065 for the effective damping ratio of the soil-structure system.

Step 22: Determine the factor to adjust the design response spectrum, B_{SSI} per ASCE/SEI 7-16 Equation 19.2.4.

$$B_{SSI} = 4 / [5.6 - \ln (100\ \beta_0)] = 4 / [5.6 - \ln (100 \times 0.065)] = 1.073$$

Step 23: For the equivalent lateral force procedure, determine the reduction in base shear per a modified version of ASCE/SEI 7-16 Equation 19.2.2 to compare the base shear coefficient $V / W = C_s$ directly. For this short structure, it is assumed that the flexible base period does not lengthen sufficiently to change the governing base shear, and $C_s = \tilde{C}_s = 0.196$.

$$\Delta C_s = C_s - \frac{\tilde{C}_s}{B_{SSI}} = 0.196 - \frac{0.196}{1.073} = 0.196 - 0.183 = 0.013$$

Step 24: Determine the ratio of the base shear adjusted for SSI vs. the base shear from a fixed base model per a modified version of ASCE/SEI 7-16 Equation 19.2.1: 0.183 / 0.196 = 0.933.

Step 25: Compare with the limits in ASCE/SEI 7-16 Equation 19.2-3. With $R = 8$, there is a floor on the reduction of $\alpha = 0.9$. This is lower than the 0.933 ratio calculated in Step 23, so the 0.933 value governs, and radiation damping results in a 7% reduction in the base shear for this example.

Step 26: Incorporate soil damping, if calculated. Soil damping and radiation damping are typically implemented together. In this example, if the reduction in base shear from soil damping were more than 3%, then the combined effect of soil damping and radiation damping would be more than 10%, and the 10% floor of ASCE/SEI 7-16 Equation 19.2-3 would govern for this $R = 8$ building.

8.6 Limitations and Issues

8.6.1 Limitations on the Influence of Radiation Damping

As the examples for soil damping and radiation damping show, there are several limitations that have been incorporated into the ASCE/SEI 7-16 provisions. These include:

- In ASCE/SEI 7-16 Section 19.3.2, the limit on the effective damping ratio including both the effective viscous damping ratio of the structure and the effective viscous damping ratio related to foundation-soil interaction is 20%. It is possible to reach this limit on soft soils, particularly when both soil damping and radiation damping are calculated.
- In ASCE/SEI 7-16 Section 19.3.1, there is a 10% limit on the reduction in base shear for systems with a response modification coefficient, $R \geq 6$. This will often govern when foundation damping is incorporated. The ASCE/SEI 7-16 Section C19.3 commentary notes that there is limited understanding of how the effects of SSI interact with the *R*-factor. It goes on to say:

  > *For higher R factors systems, where significant damping caused by structural yielding is expected, the contribution of foundation damping is assumed to have little effect on the reduction of the response. Some reduction is permitted because of (1) an assumed period lengthening resulting from the incorporation of base flexibility, (2) potential reduction in mass participation in the fundamental mode because two additional degrees of freedom are present caused by translation and rotation of the base, and (3) limited foundation damping interacting with the structural damping.*

8.6.2 Potential Code Changes Related to Foundation Damping

As part of the code development process for the next edition of ASCE/SEI 7, editorial proposals are under consideration related to foundation damping. They cover two issues:

- **Reordering equations:** A minor recommended revision is to reorder equations such that they appear in the order in which they need to be calculated, similar to the step by step process illustrated by the design examples in Sections 8.4.2 and 8.5.2 above.
- **Shear wave velocity and shear modulus definitions:** There are several similar shear wave velocity parameters in ASCE/SEI 7-16 in Chapters 19 and 20. ASCE/SEI 7-16 is not consistent with the terms. An editorial proposal is under consideration to explicitly define the shear wave velocity and shear modulus to be used for radiation damping and make it clearer the soil depth over which it should apply.

Chapter 9
How to Model a Basement

9.1 Overview

ASCE/SEI 7-16 (ASCE, 2017a) does not provide explicit direction on how to model a basement. There are several strategies that practicing engineers use. In *Soil-Structure Interaction for Building Structures* (NIST, 2012a), relatively simple approaches were evaluated against models with sophisticated soil-structure interaction (SSI) effects, and recommendations were developed. This chapter provides recommendations and examples for modeling of basements when grade is relatively level around the entire building and when grade slopes so that there is unbalanced soil pressure on the building.

Modeling of Basements

This chapter provides recommendations for modeling of basements for two conditions:

- Buildings on level grade
- Buildings on sloping grade

9.2 Past Analytical Comparisons of Different Models

9.2.1 Models Studied

NIST (2012a) documents surveys of practitioners regarding typical models they used and the analytical studies that were undertaken to compare various models against the most sophisticated substructure model. Figure 9-1 shows an example building with a one-story basement, and Figure 9-2 shows the different models that were studied. Figure 9-3 shows a more detailed image of Model 4 in Figure 9-2.

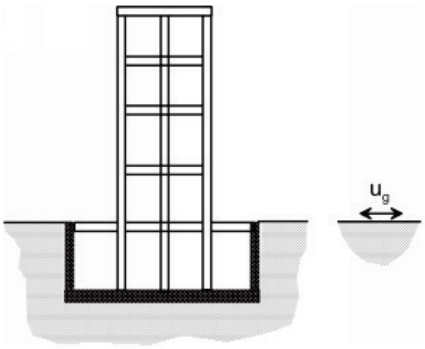

Figure 9-1 Illustration of an embedded building configuration with a basement surrounded by soil and a level grade on all sides [from Figure 6-1 in NIST (2012a)]. u_g represents the free field motion.

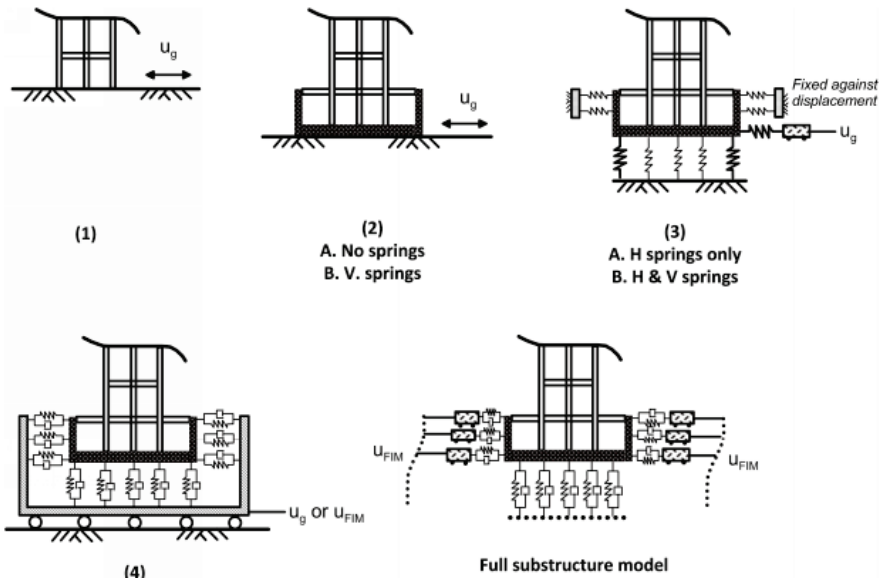

Figure 9-2 Modeling approaches for buildings with basements [from Figure 6-2 in NIST (2012a)]. u_g represents the free field motion, and u_{FIM} represents the foundation input motion. In Model 3 and the full substructure model, the little boxcars are sliders to which the free-field motion is applied. They do not have mass. The mass of the soil is included in the calculation of the free-field motions (and, as applicable, its depth-dependence).

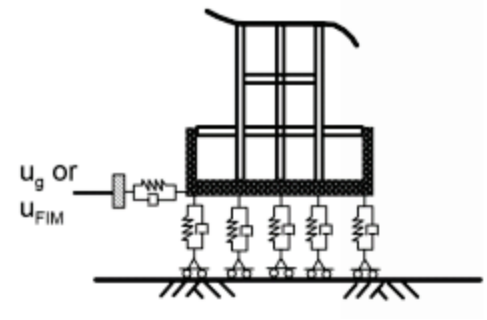

Figure 9-3 Simplified version of Model 4 in Figure 9-2 [from Figure 4-6d in PEER (2017)]. u_g represents the free field motion, and u_{FIM} represents the foundation input motion.

A summary of the models is as follows:

- **Model 1.** In this approach, the building is assumed to be fixed at the ground level, and no SSI effects are considered. Reactions are calculated at the base of the model at grade, and then applied to the foundation in a separate model. This approach is used occasionally by some engineers, and frequently by others. Some believe this model is more appropriate for moment frame and braced frame buildings, and less appropriate for shear wall buildings. Others would only use this model if there were no "back-stay effects." Back-stay effects occur when the lateral system of the superstructure does not align with the full footprint of the foundation.

An example of such a configuration is a superstructure with a concrete shear wall core system founded on a wider basement podium structure with perimeter walls. Backstay effects involve the transfer of lateral forces in the superstructure into additional elements that exist within the basement, typically through one or more floor diaphragms. This force transfer helps tall buildings resist overturning effects and is referred to as the backstay effect because of its similarity to the back-span of a cantilever beam. The added stiffness of the retaining walls, and the relative rigidity of the walls and diaphragms comprising the basement, can lead to larger shear forces in the basement levels than in the superstructure. Modeling of the in-plane flexibility of the basement diaphragms can provide more rational results for this effect. When the lateral force-resisting system of the superstructure covers the full footprint of the basement, the backstay effect is reduced or eliminated.

- **Model 2.** In this approach, the soil on the sides of the retaining walls is ignored, but the basement structure is explicitly included in the model. The lowest basement level is taken as the base of the model. It is argued that the amount of movement required to develop passive pressure of any significance far exceeds the amount of movement anticipated in the basement retaining walls, so the retained earth can be conservatively ignored. One variation of this model (Model 2A) has a fixed base. A second variation of this model (Model 2B) has vertical springs under the foundation. Model 2A is occasionally used, though limited by some to the preliminary design phases of their projects. Model 2B is used more frequently, though some use both Model 1 and Model 2B to bound their analyses for design.
- **Model 3.** In this approach, horizontal springs are used to capture the effect of the surrounding soil. The ends of the springs are fixed against translation, and ground motion is input at the base of the model. When this modeling approach is used, it is used in pushover analyses. One variation of this model (Model 3A) is fixed vertically. A second variation of this model (Model 3B) includes vertical springs. Model 3A is used occasionally by some, while Model 3B is used more frequently. Some engineers never use either version of this modeling approach.
- **Model 4.** In this approach, horizontal springs are attached to rigid walls (referred to as a "bathtub"), and the ground motion is applied to the bathtub so that the ends of the horizontal springs all move together with the input motion. This modeling approach is rarely used, although it is recommended in the *Guidelines for Performance-Based Seismic Design of Tall Buildings, Version 2.03* (PEER, 2017). A simplified version of

Model 4 taken from PEER (2017) is shown in Figure 9-3. As noted in PEER (2017):

> *The bathtub model [Model 4] applies the same ground motion to the ends of soil foundation interaction elements at the foundation level and across the embedded depth of the structure. To apply the same ground motion at these depths requires the use of rigid elements (for the ends of interaction elements opposite the foundation), which can create numerical difficulties in some structural engineering software packages. An option that can be considered to overcome this problem is to use interaction elements at the foundation level only [Figure 9-3]. When interaction elements are used only at the foundation level, they should in aggregate reproduce the cumulative stiffness of the embedded foundation as given in NIST [2012a] or similar documents. (This stiffness is higher than that of the base slab alone as a result of embedment effects.)*

- **Full Substructure Model (Baseline Model).** This represents a comprehensive modeling approach in which dashpots are used to address soil damping variation, foundation rotation is considered, and multi-support excitation is applied through the horizontal springs so that the inputs vary up the height of the basement walls. This model is not currently used in practice.

9.2.2 Recommended Models

Based on the analyses done for the NIST (2012a) report, the following findings were observed for two detailed case studies. These findings are based on comparisons of dynamic response analysis results (e.g., story drift profiles) between simplified models and the full substructure model (Baseline Model) shown in Figure 9-2.

- For design of a building with a moment frame superstructure, Model 1 and Model 2 lead to comparable or slightly conservative results to the Baseline Model and thus represent reasonable and practical design alternatives.
- For design of buildings with shear wall superstructures, Model 4 provides more consistent results to the Baseline Model, though Model 2 typically conservatively bounds the Baseline Model results and is thus a reasonable and practical design alternative. Model 1 results are more variable, less of a match, and conservative for several parameters, but not all.
- Model 3 showed the least agreement with the Baseline Model.

Based on these findings, Model 1, Model 2, and the simplified version of Model 4 as shown in Figure 9-3 are recommended.

9.3 Models for Buildings on Relatively Level Grade

9.3.1 Example Building

A section cut through an example building is shown in Figure 9-4. It is a four-story buckling-restrained braced frame building above grade with a one-story basement.

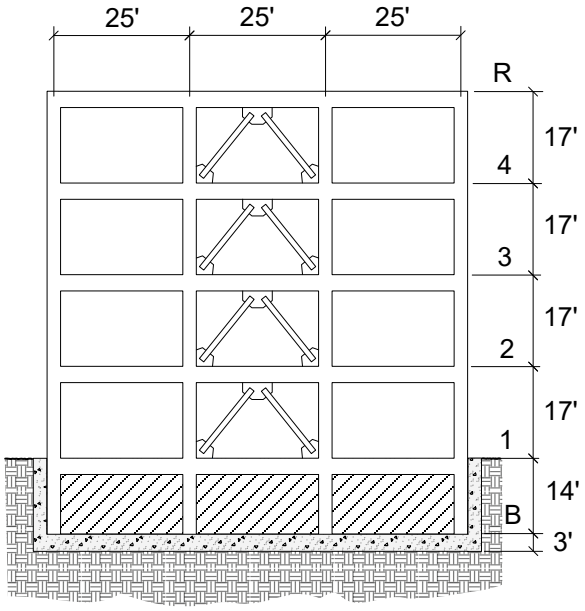

Figure 9-4 Example building with basement and relatively level grade.

The example building is 75 feet in the transverse direction (between column centerlines) as shown in Figure 9-4 and 346.5 feet in the longitudinal direction. It has concrete fill on metal deck floors and a roof on steel framing. The steel columns continue down to the mat foundation, but the braced frames stop at grade at Level 1. Lateral forces are transferred out from the braced frames through the Level 1 diaphragm to concrete shear walls in the basement.

9.3.2 Model 1 for Example Building

The first approach for seismic analysis of the example building in Figure 9-4 is to use the fixed based Model 1 approach shown schematically in Figure 9-2(1) and the equivalent lateral force procedure of ASCE/SEI 7-16 Section 12.8. The dynamic base of the building is set at grade which aligns with Level 1. Table 9-1 shows the story force distribution from an equivalent lateral force procedure static analysis. The top portion of Figure 9-5 shows

free body diagrams for the forces Table 9-1. Those forces are then applied to the basement story in a separate model for design of the basement and foundation. The seismic weight of the building, W, is 24,498 kip. The spectral acceleration, S_a, is 1.11g. The response modification coefficient, R, is 8 for the buckling-restrained braced frames. The building is a Risk Category III structure, so the Seismic Importance Factor, I_e, is 1.25. The governing equation for base shear is ASCE/SEI 7-16 Equation 12.8-1 which yields $V = C_s W = (S_a / R) \times I_e = (1.11 / 8) \times 1.25W = 0.173W =$ 0.173(24,498 kip) = 4,240 kip. The base shear of 4,240 kip is the story shear between Level 1 and Level 2.

Table 9-1 Model 1 Distribution of Forces

Diaphragm	Story (ft)	Height, h_i (ft)	Weight, w_i (kip)	Static Analysis	
				Force (kip)	Story Shear (kip)
Roof		68	7,620	2,047	
	4				2,047
4		51	5,626	1,113	
	3				3,160
3		34	5,626	726	
	2				3,886
2		17	5,626	354	
	1				4,240
1 (Base)		0			
Total			24,498	4,240	4,240

Notes:

1. For Model 1, the dynamic base is set at grade (Level 1).
2. The ASCE/SEI 7-16 Equation 12.8-1 base shear is $V = C_s W = 0.173W$.

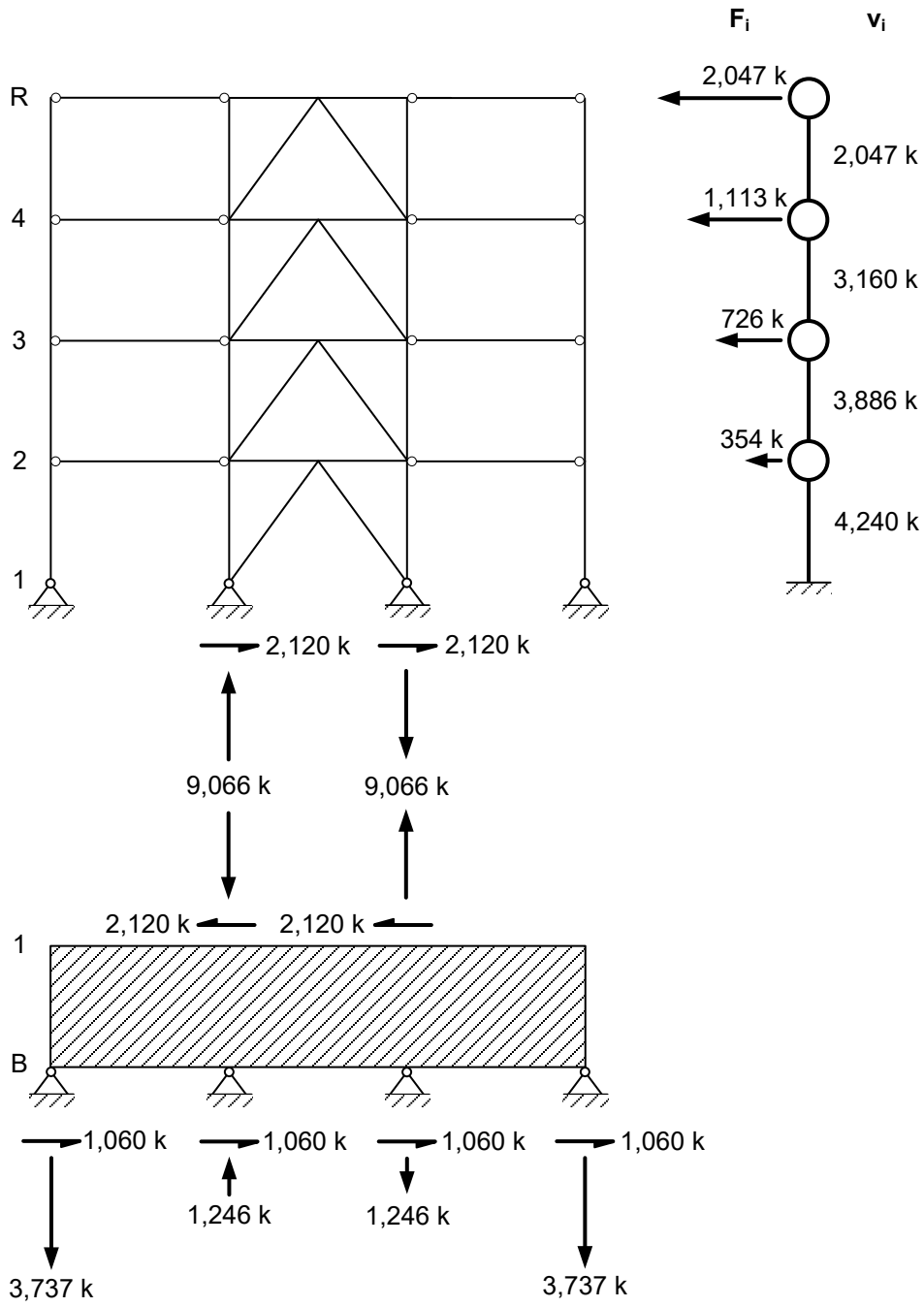

Figure 9-5 Model 1 distribution of forces for example building.

9.3.3 Model 2 for Example Building

The second approach to modeling the example building uses Model 2A from Figure 9-2(2) and model response spectrum analysis of ASCE/SEI 7-16 Section 12.9.1. The soil flexibility from using vertical springs in Model 2B is not included. It would have lengthened the building fundamental period and might have impacted the resulting design forces. In Model 2A, the

dynamic base is set at the bottom of the building, which is the basement level. More specifically, for this example, it is set at the bottom of the mat where it contacts the soil. The soil surrounding the basement is ignored. The mass of Level 1 is included in the model. A dynamic analysis is run. Due to the stiffness of the retaining walls in the basement, relatively little of the Level 1 mass impacts the forces at the upper floors. Table 9-2 shows how the initial dynamic analysis forces are scaled. Per ASCE/SEI 7-16 Section 12.9.1.4.1, the dynamic analysis forces from the modal response spectrum analysis are scaled to the full value from the equivalent lateral force procedure. For this example, this is done for the story shear between Level 1 and Level 2. The story shear for the dynamic analysis is 3,660 kip, and the story shear (or base shear) for the static analysis is 4,240 k. The scale factor is thus 4,240 kip / 3,660 kip = 1.1585. The initial dynamic analysis values are multiplied by 1.1585 to produce the final scaled dynamic analysis values used in design. Figure 9-6 shows this graphically.

Table 9-2 Model 2 Distribution of Forces

Diaphragm	Story (ft)	Height, h_i (ft)	Weight, w_i (kip)	Dynamic Analysis		Static Analysis		Scaled Dynamic Analysis	
				Force (kip)	Story Shear (kip)	Force (kip)	Story Shear (kip)	Force (kip)	Story Shear (kip)
Roof		85	7,620	1,809		2,047		2,096	
	4				1,809		2,047		2,096
4		68	5,626	886		1,113		1,026	
	3				2,695		3,160		3,122
3		51	5,626	602		726		697	
	2				3,297		3,886		3819
2		34	5,626	363		354		421	
	1				**3,660**		**4,240**		**4,240**
1		17	9,685	144				167	
	Basement				3,804				4,407
Basement		0							
Total			34,183	3,804	3,804	4,240	4,240	4,407	4,407

Notes:

1. For Model 2, the dynamic base is set at the basement floor.
2. The ASCE/SEI 7-16 Equation 12.8-1 equivalent lateral force procedure base shear is $V = C_s W = 0.173W$.
3. The scale factor is taken at the bottom story for the static analysis (Story 1) where the story shear for the dynamic analysis is 3,660 kip and the story shear (or base shear) for the static analysis is 4,240 kip. This produces a scale factor of 4,240 kip / 3,660 kip = 1.1585.
4. The dynamic analysis values are scaled by the scale factor to produce the scaled dynamic analysis values.

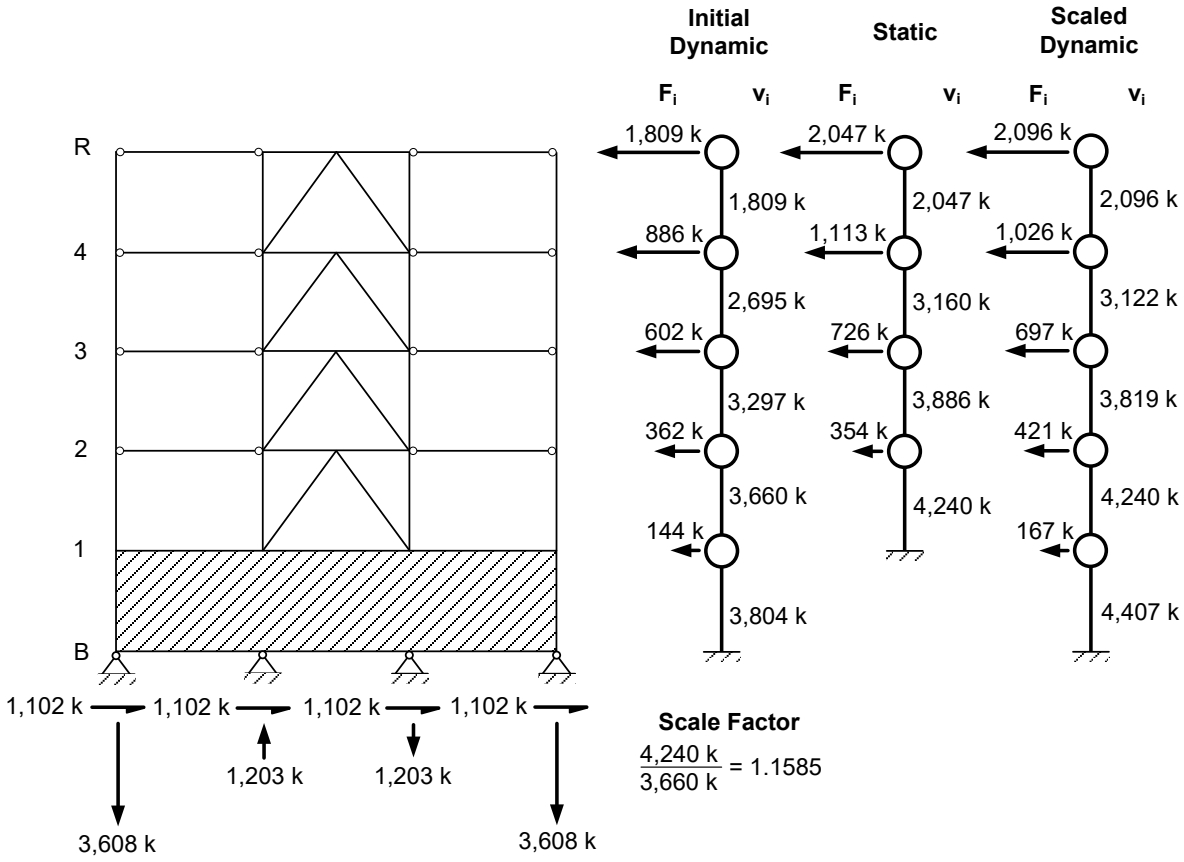

Figure 9-6 Model 2 distribution of forces for example building.

9.4 Models for Buildings on Sloping Grade

9.4.1 Example Building

When buildings are on a sloping grade that creates a retaining wall, soil pressure is exerted on the building. In addition, during an earthquake, the soil exerts an additional "seismic increment" of pressure on the structure. These pressures are typically provided by the project geotechnical engineer. To illustrate how to model a building on a sloping grade, the example building in Section 9.3 on a level site has been moved to a sloping site as shown in Figure 9-7. The basement floor aligns with the lower grade level on the left; the Level 1 floor aligns with the higher grade on the right.

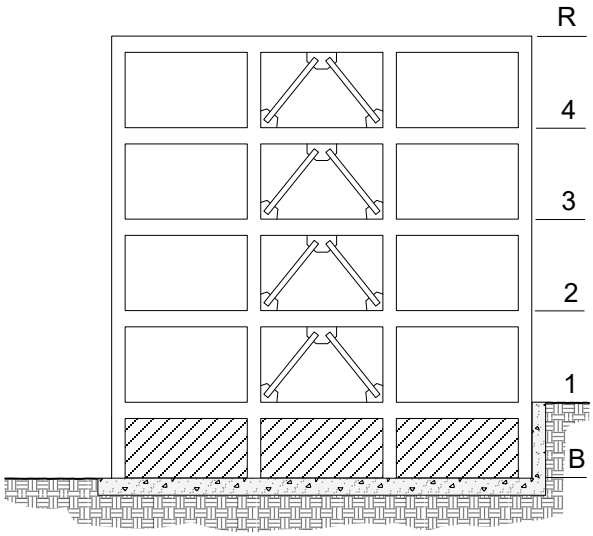

Figure 9-7 Example building on a sloping site.

9.4.2 Model 2 for Example Building

In this approach, seismic loads from the design of the superstructure are combined with those from the soil by linear superposition. The dynamic base is set at the bottom of the mat. Figure 9-8 shows the scaled dynamic forces from Figure 9-6 applied to the building. It also shows the derivation of the earth pressure loads. For this example, there is the "static" or "active" soil pressure component of 40 pcf of equivalent fluid pressure plus the seismic increment of 20 pcf of equivalent fluid pressure. Both are given at the factored level so they can be directly combined with the factored loads from the superstructure. The values to be used for actual projects will vary depending on the soil conditions and geotechnical engineer's approach. It is important to make sure there is a clear understanding of the assumed load level that underlies the geotechnical engineer's design recommendations. They are sometimes given for the allowable stress design level, rather than the factored level. For this simple example, the resistance that may exist from passive pressure due to shallow embedment of the mat in Figure 9-7 is not included in the free body diagram in Figure 9-8.

Note that this seismic pressure increment should be a consequence of the SSI that is the subject of this *Guide*, not a prescribed quantity. This is a significant logic gap in analysis procedures currently used in practice. The way that this pressure should be derived is to provide springs, conduct a response analysis, and then obtain the spring forces. FEMA (2020b) provides a resource paper current thinking in retaining wall pressures.

For this example, it is interesting to note that the base shear that the basement and foundation must resist is substantially increased due to the unbalanced

soil pressure. It rises from 4,407 kip from the building seismic inertial weight alone to 4,407 kip + 1,001 kip + 2,002 kip = 7, 410 kip or a 1.68 increase. On the other hand, because the centroid of the applied soil loading is relatively low, the overturning load at the ends of the structure of the only rises from 3,608 kip to 3,812 kip or an increase of 1.06.

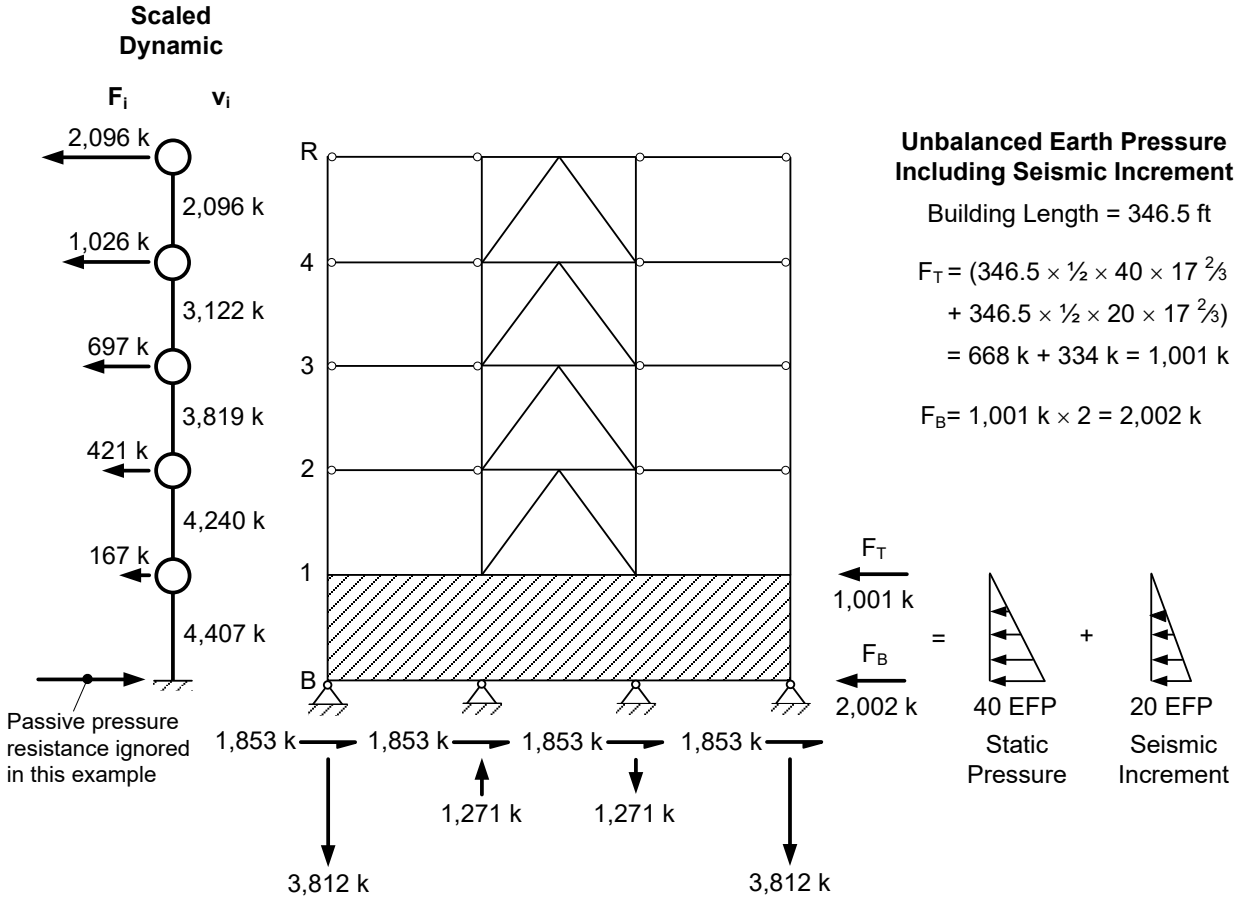

Figure 9-8 Model 2 distribution for example building on a slope.

Chapter 10

Conclusions and Recommendations

10.1 Overview

Soil-structure interaction (SSI) can make a substantial difference in how buildings behave during earthquake shaking and how they should be designed, and yet there is relatively little implementation of SSI effects by practicing engineers. Provisions are available in Chapter 19 of ASCE/SEI 7-16 *Minimum Design Loads and Associated Criteria for Buildings and Other Structures* (ASCE, 2017a) and in Chapter 8 of ASCE/SEI 41-17 *Seismic Evaluation and Retrofit of Existing Buildings* (ASCE, 2017b) that can be used to address SSI. The overall goal of this *Guide* is to present information regarding SSI as implemented in code provisions but in an easy-to-understand, concise format. It is directed towards practicing engineers to help them determine when SSI effects are of importance and to show them examples of how to implement SSI in design.

10.2 Conclusions

- SSI is not that difficult to implement.
- SSI is typically iterative, so it may require additional rounds of analysis, as compared to a fixed base analysis, to converge on the final solution.
- Inertial SSI typically reduces the seismic force demands that are used for design, but there are unusual cases with site-specific response spectra where force demands can increase because period elongation may lead to climbing up the response spectrum with increasing levels of spectral acceleration at short periods. Displacement demands—in particular, drift—always increase when SSI is considered as compared to when it is not.
- Adding foundation flexibility to a model can dramatically affect how the building behaves in some situations, particularly where foundation flexibility would lead to rocking of shear walls or braced frames in the superstructure.
- Effective shear wave velocity, v_s, is a key parameter in several SSI equations and techniques. The effective shear wave velocity differs from

the low-strain shear wave velocity, v_{so}, used for site classification in ASCE/SEI 7-16 Chapter 21. Modifications are made based on site class, site spectral acceleration, and the depth of importance.

- There are several code provisions, both in ASCE/SEI 7-16 Chapter 12 and Chapter 19, that can limit the extent of SSI reductions that can be utilized.
- Although ASCE/SEI 7-16 is the standard that is referenced and used in this *Guide*'s design examples, ASCE/SEI 41-17 has a similar set of SSI provisions. In some cases, ASCE/SEI 41-17 has more relaxed requirements and limitations regarding the use of SSI.

10.3 Other Helpful Resources

In addition to the examples in this *Guide* in Chapters 3 through 9, Appendix A, and Appendix B, there are other resource documents that provide practical SSI advice and worked examples. These are summarized in Appendix C.

10.4 Comparison of SSI Provisions

It is useful to compare the SSI provisions in ASCE/SEI 7-16 Chapter 19 with those in ASCE/SEI 41-17 Chapter 8. The provisions in the two standards are similar, but the ASCE/SEI 41-17 provisions have fewer limitations, except in a couple of cases. Table 10-1 provides a comparison.

10.5 Recommendations

Based on project studies and the design example development process for this *Guide*, revisions to code provisions and further studies regarding SSI provisions are needed.

10.5.1 Recommendations for Code Developers

General recommendations are made here to code developers, such as the Building Seismic Safety Council Provisions Update Committee that develops the NEHRP *Recommended Seismic Provisions for New Buildings and Other Structures* and the ASCE Minimum Design Loads on Buildings and Other Structures Standards Committee that develops ASCE/SEI 7. Both technical and editorial revisions are recommended. At the time of writing of this *Guide* in October 2020, several code change proposals had been developed and were under consideration in the code development process. Other proposals were considered, but they did not find sufficient support to proceed. Both are indicated below.

Table 10-1 Comparison of SSI Provisions

Issue	ASCE/SEI 7-16	ASCE/SEI 41-17	Comment/Justification
Site Class	No Class A or B for any SSI (§19.1)	Class C, D, E for kinematic (§8.5.1.1)	SSI effects in Class A and B assumed minimal (ASCE/SEI 7-16 §C19.1)
Kinematic SSI (base slab averaging and embedment)	Only permitted for Nonlinear Response History Analysis (NRHA)	Permitted for any method	No equivalent lateral force procedure or response spectrum studies (ASCE/SEI 7-16 §C19.2)
Kinematic reduction floor	$RRS_{bsa} \times RRS_e \geq 0.7$ (§19.4)	$RRS_{bsa} \times RRS_e \geq 0.5$ (§8.5.1.1)	To be conservative (ASCE/SEI 7-16 §C19.4)
Kinematic connectivity	Mat, grade beam, connected slab (§19.4.1)	Mat, grade beam, connected slab (§8.5.1.1)	Further study is needed
Kinematic restrictions	$T \geq 0.2$ and $b_e < 260$ ft (§19.4.1)	$b_e < 260$ ft (§8.5.1.1)	No studies of larger b_e
Embedment depth limit	20 ft (§19.4.2)	20 ft (§8.5.1.2)	No case study over 20 ft
Equivalent lateral force procedure reduction floor	Capped at 0.9 if $R > 6$ (§19.2)	Not applicable	Limited studies on interaction of SSI and *R*-factor (ASCE/SEI 7-16 §C19.2)
Overall SSI reduction floor	None	0.7 x non-SSI results for procedures besides NRHA	No justification given
Minimum base shear	Chapter 12 minimums	No minimum	Limits SSI in tall buildings
Upper and lower bounds	Required (§19.1.1, 12.13.3)	Required (§8.4.2)	Further study is needed
When SSI is required	Optional (§19.1.1)	Required if longer period increases S_a (§7.2.7)	Provisions are typically ignored in practice

Notes:

RRS_{bsa} = Ratio of response spectra factor for base slab averaging

RRS_e = Ratio of response spectra factor for embedment

T = Fundamental period of the building

b_e = Effective foundation size

R = Response modification coefficient

Technical Revisions

- **Require SSI unless it can be shown not including SSI is conservative:** There are some cases, such as short period structures with site-specific response spectra that are not capped at short periods all the way to the zero period, where the increase in period from inclusion of foundation flexibility will lead to climbing up the response spectrum and an increase in design forces. This situation can occur for short period structures when a site-specific response spectrum is used. This is already required by ASCE/SEI 41-17 Section 7.2.7. A proposal was considered to change ASCE/SEI 7-16 Section 12.7.1 as follows:
  - ***Current Text:*** **Section 12.7.1 Foundation Modeling.** For the purposes of determining seismic loads, it is permitted to consider the

structure to be fixed at the base. Alternatively, where foundation flexibility is considered, it shall be in accordance with Section 12.13.3 or Chapter 19.

- ***Proposed Text:*** **Section 12.7.1 Foundation Modeling.** For the purposes of determining seismic loads and analytical results, foundation flexibility shall be considered in accordance with Section 12.13.3 or Chapter 19, unless it can be shown that this flexibility does not substantially change the analytical results.

The proposal did not find sufficient support to proceed.

- **Remove limit without charging language:** ASCE/SEI 7-16 Equation 19.4-4 has a limitation on the average effective shear wave velocity of $200 \leq v_s \leq 500$ m/s in the base slab averaging provisions, but since this parameter is not used in the equations, it is unclear how it should be interpreted. Can base slab averaging only be used if v_s is within those limits? At the time of writing of this *Guide* in October 2020, a proposal was under review to remove this requirement, as base slab averaging is already restricted to Site Classes C, D, and E, and a v_s value less than 200 m/s should not reduce the effects of base slab averaging.
- **Revise the limitation on the equivalent lateral force procedure:** ASCE/SEI 7-16 Section 19.2.1 included a revision in the limits for SSI reductions that unintentionally limited the reduction in the equivalent lateral force procedure base shear due to period elongation as a function of the structure's response modification coefficient, when the original intent was to apply the limit only to foundation damping. At the time of writing of this *Guide* in October 2020, a code change proposal was under review to correct this. A maximum reduction of 30% is imposed due to the effects of period elongation. The effect of the revision does not alter the results for foundation damping reductions.

Editorial Revisions

- **Shear wave velocity definitions:** There are several similar shear wave velocity parameters in ASCE/SEI 7-16 in Chapters 19 and 20. ASCE/SEI 7-16 is not consistent with the terms. This should be clarified.
  - In ASCE/SEI 7-16 Chapter 20, $\overline{v}_s$ is the "average shear wave velocity." It is taken over the top 30 m of soil. This is often designated as V_{s30} for 30 m. Both $\overline{v}_s$ and V_{s30} are the *low strain* shear wave velocity, though this is never stated in ASCE/SEI 7-16 Chapter 20. This should be clarified.

- In ASCE/SEI 7-16 Chapter 19, v_{so}, is the "average low strain shear wave velocity over a depth of B (half the smaller dimension of the base of the structure)" for damping considerations and the "average low strain shear wave velocity over the embedment" for embedment considerations. If the embedment depth were 30 m, it would be the same as $\overline{v}_s$. When the embedment depth is shallower, they are not the same. Clarification is also needed that v_{so} is determined using ASCE/SEI 7-16 Equation 20.4-1, and that the sum of d_i in Equation 20.4-1 is the depth in question noted above.
- In ASCE/SEI 7-16 Chapter 19, the *low strain* shear wave velocity needs to be modified by ASCE/SEI 7-16 Table 19.3-1 to obtain the *average effective* shear wave velocity, v_s.

A code change proposal for ASCE/SEI 7-16 Chapter 19 is under review to use specific variables to define the terms to help address the above inconsistencies. Similar revisions are proposed for the shear modulus to clarify the appropriate depth of soil to apply to consider for different SSI effects.

- **Clarifying when SSI can be used for linear procedures:** The current provisions have overlapping requirements in ASCE/SEI 7-16 Chapters 12, 16, and 19 regarding which SSI provisions can be used with linear procedures. Explicit statements and reordering of text are being considered to assist in clarity. An example is the linear analysis that is required to accompany a nonlinear response history analysis (NRHA) covered by ASCE/SEI 7-16 Section 16.1.2. The linear analysis is to be conducted in accordance with one of the linear methods in ASCE/SEI Chapter 12 (equivalent lateral force procedure, modal response spectrum analysis, and linear response history analysis). The ASCE/SEI Chapter 19 spectral modifications for kinematic effects (base slab averaging and embedment) are not permitted for linear analyses, including the Chapter 16 required linear analysis. The effects of inertial SSI (foundation flexibility and foundation damping) can be used for linear analyses, including the Chapter 16 required linear analyses. A code change proposal is under review to make this intent clearer.
- **Reordering equations:** A minor recommended revision is to reorder equations such that they appear in the order in which they need to be calculated. A code change proposal with the appropriate reordering is under review.

10.5.2 Recommendations for Further Study

As part of the project that included development of this *Guide*, detailed case studies were performed to investigate various SSI issues. The case study analyses used what is termed the "direct analysis" approach where the soil and building are both modeled with nonlinear finite elements. The ground motion inputs included spatial variability so that the effects of this variability on foundation input motions could be compared with semi-empirical models used in current procedures such as NIST (2012a).

Case studies covered both instrumented buildings and archetype buildings. Recordings from instrumented buildings were compared with results from analytical models to help validate and calibrate the modeling techniques and assumptions. Since there are very limited recorded data from ground shaking at the design earthquake or maximum considered earthquake levels, archetype buildings, based on those in Appendices A and B, were used together with records scaled to large shaking levels. Archetype building parameter studies included varying the level and spatial variability of ground shaking, the soil-to-structure interface assumptions, and nonlinearity in the soil and superstructure.

The studies revealed a variety of issues with the assumptions and methods used in direct analyses and the challenges in simulating realistic ground motions throughout the soil column profile. The direct analysis case studies generally show a reduction in short period spectral response of the foundation as compared to free field motion, but results were highly sensitive to modeling assumptions, soil properties, and soil nonlinearity. Building response appears to be more sensitive to soil nonlinearity than to spatial variability of ground motion. Further checking and validation of these findings is needed before the results could be used to inform recommendations for application. Although definitive conclusions were not reached regarding potential revisions to code SSI provisions, such as the response spectral modification factor for kinematic interaction, the work provides an excellent starting point that includes a large body of preliminary results, an outline of the approach and issues, and recommendations on the next steps that are needed for further study. Jeremic, et al. (2020) provide a summary of the case studies that were conducted.

This project was limited in terms of time and funding and could not address all of the issues that had been originally raised. Because of this, further study is recommended for the following topics:

- **Kinematic interaction models:** The database used to develop current kinematic interaction models is approximately 25 years old. This work

should be revisited because (1) the scope of the database (e.g., range of conditions, numbers of recordings) will be broader; and (2) the quality of modern recordings is much better than recordings from the 1980s-1990s, which can significantly improve the resolution with which kinematic effects can be resolved.

- **Direct analysis:** Direct analyses conducted for this study generally show a reduction in short period spectral response of the foundation as compared to free field motion, but results are highly sensitive to modeling assumptions, soil properties, and soil nonlinearity. Study is needed for a greater range of soil conditions, building structural systems and geometries, and ground motion variability including spatial variability, and soil nonlinearity and contact properties with the foundation. Future work should begin by continuing the validation of direct analyses against available data, and then extend to conditions for which data is not available, such as higher ground motion levels.
- **Deconvolution**: More detailed investigation is needed of what is called "deconvolution," which involves the process of simulating ground motions at depth to produce the desired free field motions at the ground surface.
- **Shear wave conversions:** A study should evaluate whether the conversions from average low strain shear wave velocity to effective shear wave velocity in ASCE/SEI 7-16 Table 19.3-1 should always be based on S_{DS}, or whether S_{D1} be used for longer periods. Regardless of the decision, the revisions must account for the differences between the Design Earthquake and MCE_R ground motion levels. A code change proposal has been submitted to correct this error.
- **Limitations on use of kinematic SSI provisions:** ASCE/SEI 41-17 permits use of kinematic SSI provisions for all analysis methods; ASCE/SEI 7-16 limits their use to only NRHA. Analysis is needed to investigate whether there is analytical justification for relaxing the ASCE/SEI 7-16 provisions. This should include the limits on embedment depth (20 ft), effective foundation size, b_e (260 ft), and average effective shear wave velocity (650 ft/s $\leq v_s$) that are now somewhat dated.
- **Limitations on the reduction in design forces from SSI:** ASCE/SEI 7-16 Section 19.2.1 correlates the amount of reduction in base shear permitted with SSI to the response modification coefficient, R, for the lateral force-resisting system of the superstructure. Systems with higher R factors and more ductility have more significant limitations because

SSI research has primarily been based on linear elastic superstructure models. The Section 19.2.1 provisions should be studied to determine if they are justified by carefully examining the interaction of superstructure nonlinearity and SSI effects.

- **Foundation interconnectivity for use of kinematic SSI provisions:** ASCE/SEI 7-16 Section 19.4.1 limits the use of base slab averaging for structures with a full mat foundation, a grid of grade beams, or a slab-on-grade connected to the footings by overpours and dowels. Detailed case studies are needed to investigate differences in response to foundations for those cases and those where the slab-on-grade is separated from the top of the footings by soil but is either poured tight to the columns or separated by a typical sealant gap for crack control.
- **Bounding of soil properties:** ASCE/SEI 7-16 Sections 12.13.3 and 19.1.1 require bounding of soil stiffnesses when flexible base models are used, with a 50% increase and decrease in soil stiffness. The worst case results are to be used. This leads to substantial analytical work. Further study of this requirement is recommended to determine the variability of the results on design and on performance to determine if the effort is warranted.
- **Seismic earth pressures on basement walls:** Current procedures for analysis of seismic earth pressures on basement walls do not consider the inertial and kinematic SSI effects that are the subject of this *Guide*. Recent research has provided a more rational SSI-based framework for characterizing the seismic increment of earth pressure as discussed in FEMA (2020b). These new procedures should be vetted through case studies of buildings, with participation of practicing geotechnical and structural engineers. The aim of these studies would be to advance the detailed implementation of the procedures to an extent where code change proposals could be considered in future cycles.

Appendix A
Two-Story Building Example

A.1 Overview

This chapter provides an example of application of the foundation damping provisions and base slab averaging provisions of ASCE/SEI 7-16 Chapter 19. The example applies the provisions to a two-story steel-frame building with buckling-restrained braced frames and shallow foundations. The example building is based on the three-story steel braced-frame building evaluated in Chapter 9 of FEMA P-2006 (FEMA, 2018). The gravity framing and plan dimensions of this example are the same as those in the FEMA P-2006 example. The site conditions, ground motions, number of stories, and bracing type have been changed for this example to better illustrate the provisions.

The soil-structure interaction (SSI) computations illustrated in this example depend on the foundation geometry and the dynamic properties of the structure; it is therefore necessary to begin by preparing a conventional design as a starting point. This starting point is based on ASCE/SEI 7-16, employing the equivalent lateral force (ELF) method, without consideration of soil-structure interaction (Section A.4).

In Sections A.5 and A.6, the dynamic properties and foundation geometry determined based on the conventional analysis are employed to compute the foundation springs, flexible-base analysis and reductions in demand due to foundation damping, as permitted in ASCE/SEI 7-16. Section A.7 presents an updated design with smaller brace areas and foundation sizes, which is verified to produce dynamic behavior and demand reductions consistent with the design input.

Section A.8 then explores the soil-structure interaction reductions without consideration of the limitations in ASCE/SEI 7-16, allowing more significant reductions due to foundation damping and including the additional reduction due to base slab averaging, which is not permitted for linear analysis methods in ASCE/SEI 7-16.

This example is not a complete design of the structure. The example focuses on selected elements of the design that are essential to the application of the provisions being illustrated.

Example Summary

Building Type: 2-story steel-frame building with buckling-restrained braced frames

Foundation Type: Spread footings

Analysis Method: Equivalent Lateral Force (ELF) method, with modal analysis as required for damping computations.

SSI Topics Covered:

- Foundation flexibility (vertical and lateral)
- Reductions in loading due to soil damping, radiation damping, and base slab averaging
- Impacts of limitations imposed by ASCE/SEI 7-16 provisions

A.1.1 Outline of the Example

This example includes the following:

- Section A.2: Site description, including ground motion parameters and soil properties
- Section A.3: Building description, including geometry, gravity framing, seismic force-resisting system and foundations
- Section A.4: Initial design, including buckling-restrained brace core areas, column sizes, and foundation sizes
- Section A.5: Flexible-base analysis, including vertical springs under foundations that allow the frames to rock as well as lateral springs
- Section A.6: Foundation damping, including the computations for reductions in seismic demand according to ASCE/SEI 7-16 Section 19.3
- Section A.7: Design for SSI-reduced base shear per ASCE/SEI 7-16 Chapter 19, including reduced brace and foundation sizes
- Section A.8: Alternative design for full theoretical SSI-reduced base shear, including reductions due to base slab averaging

A.1.2 Limitations in ASCE/SEI 7-16 Chapter 19

This example employs the ELF procedure for design, employing dynamic modal analysis as a tool to assess the damping, which depends on period lengthening due to foundation flexibility. ASCE/SEI 7-16 Chapter 19 allows the application of the foundation damping provisions to buildings designed with the ELF procedure, but only allows application of base slab averaging (and other kinematic effects) with the nonlinear response history analysis. ASCE/SEI 7-16 Chapter 19 also places limits on the permissible reduction in lateral forces due to soil-structure interaction. Sections A.4 through A.7 present a design complying strictly with the requirements in ASCE/SEI 7-16 Chapter 19 (limiting the design force reduction and not including base slab averaging). Section A.8 presents an alternative (non-compliant) design based on the design force reductions computed without the limitations and including the reductions due to base slab averaging.

A.2 Site Description

For the purpose of this example, this fictitious building is located at the site of the VA Loma Linda Healthcare System building in San Bernardino County, California (Latitude 34.049601, Longitude -117.250073). The site soils comprise sands and gravels, loose at the surface and increasing in density with depth. Figure A-1 shows the generalized soil profile. The

average shear wave velocity in the upper 100 feet is 950 ft/s, resulting in a site classification as Site Class D. The ground motion parameters according to the ATC Hazards by Location web application (available at https://hazards.atcouncil.org/, last accessed October 15, 2020) are as follows:

- S_S = 2.355g
- S_1 = 0.943g
- S_{MS} = 2.355g
- S_{DS} = 1.57g

The values of S_{M1} and S_{D1} are not specified by the ATC Hazards by Location web application, which points to ASCE/SEI 7-16 Section 11.4.8, which requires a site response analysis. An exception in ASCE/SEI 7-16 Section 11.4.8 allows consideration of a conservative spectral shape with C_S taken as the value determined by ASCE/SEI 7-16 Equation 12.8-2 for periods up to $1.5T_S$ (1.02 s) and taken as 1.5 times the value computed by ASCE/SEI 7-16 Equation 12.8-3 for longer periods considering F_v = 1.7. The effect of the modified spectral shape is to elongate the short-period plateau, pushing the descending branch of the spectrum to the right. The design response spectrum is shown in Figure A-2, along with the spectrum based on the mapped values without the increases required by ASCE/SEI 7-16 Section 11.4.8 for comparison. Note that the short period of the example building will not require consideration of the descending portion of the response spectrum. The longest period computed in this example (for 50% decreased soil springs and reduced brace sizes) is 0.62 s, which remains less than T_s = 0.68 s and considerably less than 1.5 T_s = 1.02 s.

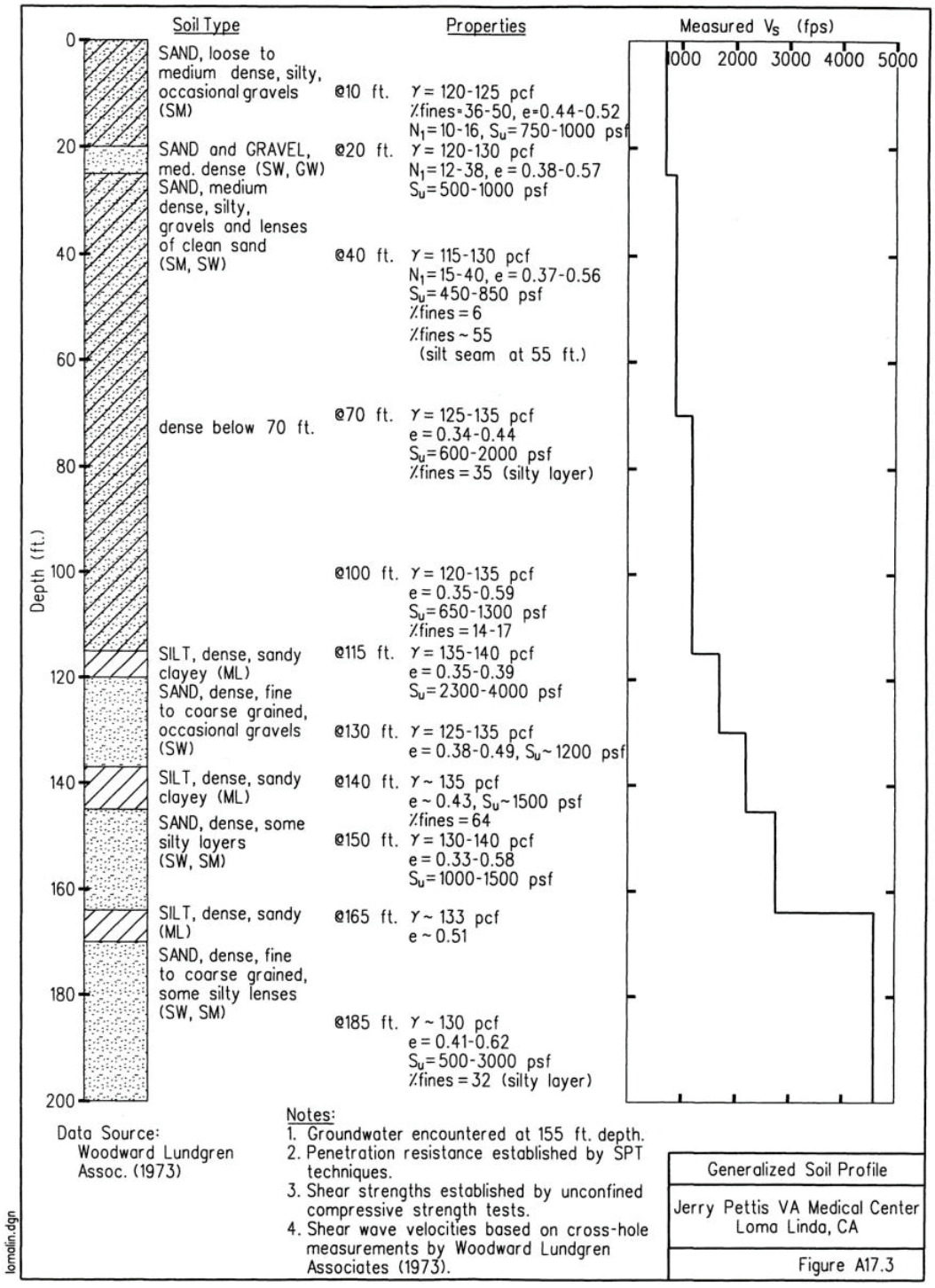

Figure A-1 Generalized soil profile for the Loma Linda Site, taken from Stewart and Stewart (1997) UCB/EERC-97/01.

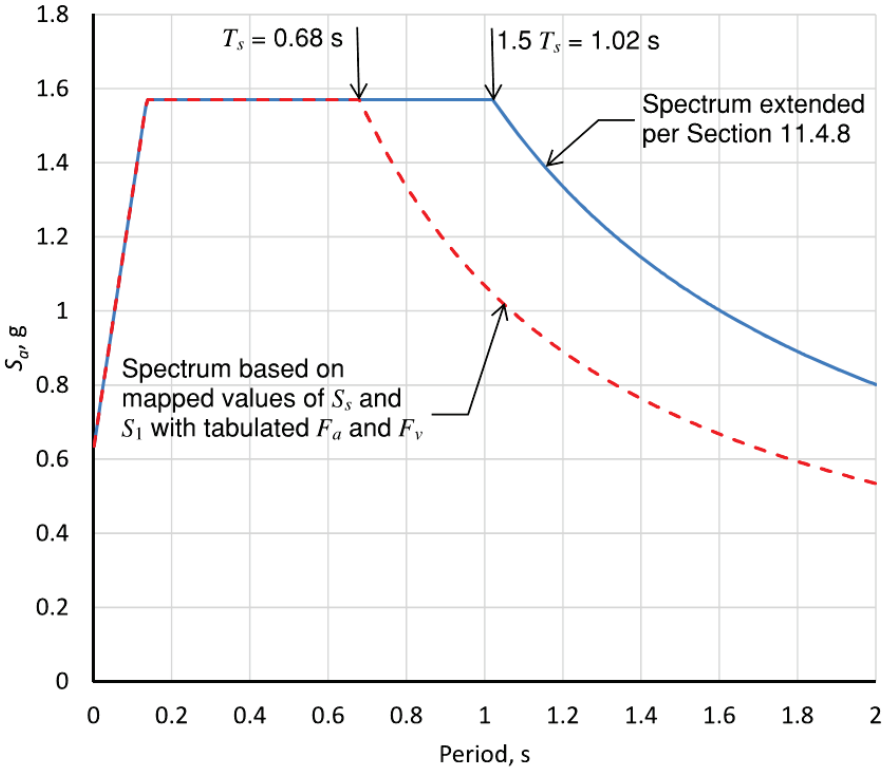

Figure A-2 Design acceleration response spectrum per ASCE/SEI 7-16 Chapters 11 and 12.

A.3 Building Description

The example building is a two-story office building. (For the purpose of this example, the original FEMA P-2006 example was reduced from three stories to two.) An overall building view, a typical floor plan, and the foundation plan are shown in Figures A-3, A-4, and A-5, respectively. The building is rectangular in plan, with five 30-foot bays in the north-south (transverse) direction and seven 30-foot bays in the east-west (longitudinal) direction. Each story height is 12'-6". Discussion of the loading in these two directions uses the terminology "transverse" and "longitudinal."

A.3.1 Gravity Framing

The roof and second floor are constructed of 3¼ in structural lightweight concrete fill over 3 in composite steel deck, supported by steel wide-flange beams at 10-foot spacing and wide-flange girders at 30-foot spacing. The gravity framing is supported on W14 columns at the grid intersections.

A.3.2 Lateral Framing

The building resists lateral loading with a system of single-bay buckling-restrained braced frames, arranged symmetrically on the perimeter, with two

frames on each of the short sides acting in the transverse direction and three frames on each of the longer sides acting in the longitudinal direction.

A.3.3 Gravity Loads and Seismic Weight

Dead loads and seismic weights are given in Table A-1 for the roof and Table A-2 for the typical floor. Live loads are 20 lb/ft^2 for the roof and 50 lb/ft^2 for the typical floor.

The total seismic weight at the roof level is 2,385 kip at the roof and 2,449 kip at the second floor, resulting in a total seismic weight of 4,834 kip, as indicated in Table A-3.

Table A-1 Flat Loads on Roof

Component	Dead Load (lb/ft^2)	Seismic Weight (lb/ft^2)
Roofing	5.0	5.0
Insulation	3.0	3.0
Steel deck and concrete fill	46.4	46.4
Steel framing (beams and columns)	7.0	7.0
Ceiling	3.0	3.0
Partitions	0.0	5.0
Exterior walls, MEP, miscellaneous components, extra concrete for deck deflection	4.6	4.6
Total	69.0	74.0

Table A-2 Flat Loads on Second Floor

Component	Dead Load (lb/ft^2)	Seismic Weight (lb/ft^2)
Floor Covering	1.0	1.0
Steel deck and concrete fill	46.4	46.4
Steel framing (beams and columns)	11.0	11.0
Ceiling	3.0	3.0
Partitions	15.0	10.0
Exterior walls, MEP, miscellaneous components, extra concrete for deck deflection	4.6	4.6
Total	81.0	76.0

Table A-3 Summary of Seismic Weights

Level	East-West Dimension (ft)	North-South Dimension (ft)	Area (ft^2)	Flat Load (lb/ft^2)	Total Weight (kip)
Roof	212	152	32,224	74	2,385
Second Floor	212	152	32,224	76	2,449
Total					4,834

A.3.4 Foundation System

The building is supported on a system of spread and continuous footings, with square spread footings at each gravity column and continuous strip footings at each braced frame, encompassing both frame columns and extending beyond each column to provide overturning resistance.

The slab-on-grade is designed as an interconnecting diaphragm, with Z-dowels cast into each footing. The slab is underlain by a moisture barrier. Frictional resistance between the slab and the soil is neglected.

The foundation design is based on the LRFD (strength) design provisions in ASCE/SEI 7-16 Section 12.13.5. The geotechnical engineer has provided a nominal bearing strength of 10 kip/ft^2, to which a resistance factor of 0.45 applies per ASCE/SEI 7-16 Table 12.13-1 for a design strength of 4.5 kip/ft^2.

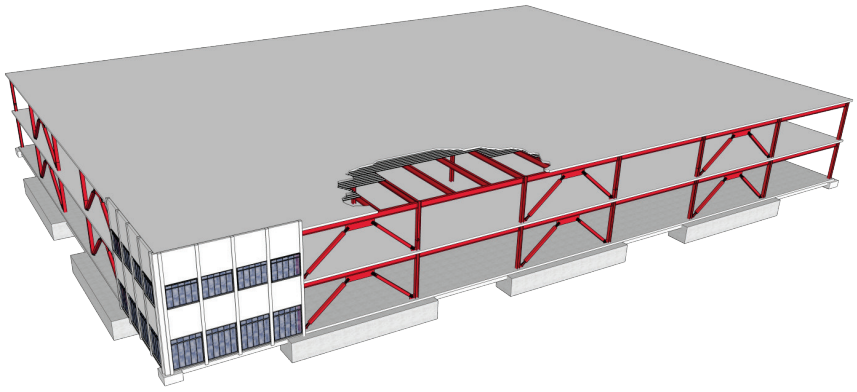

Figure A-3 Overall view.

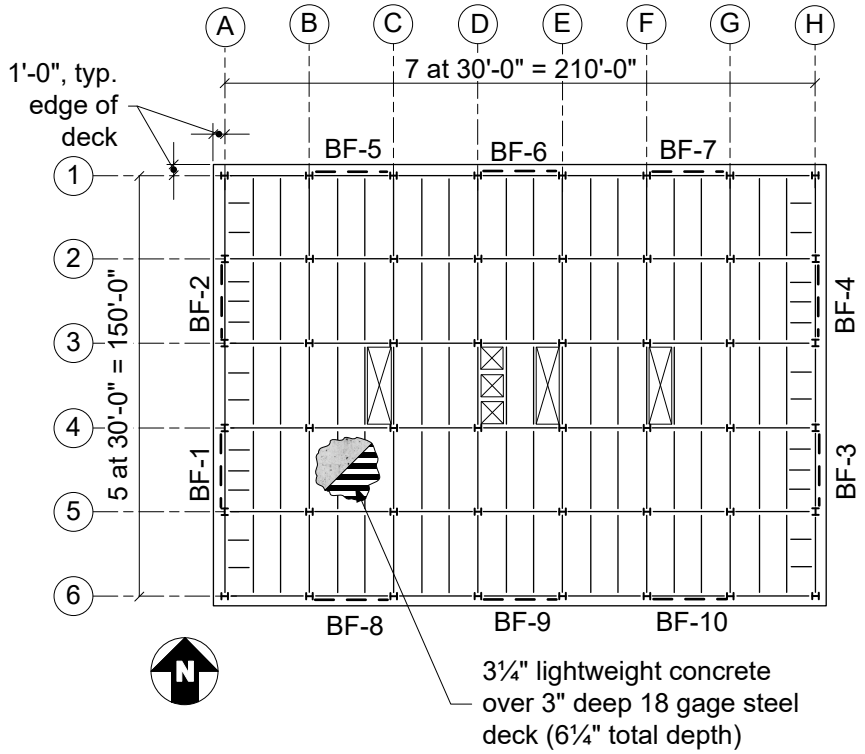

Figure A-4 Typical floor framing plan (roof framing similar).

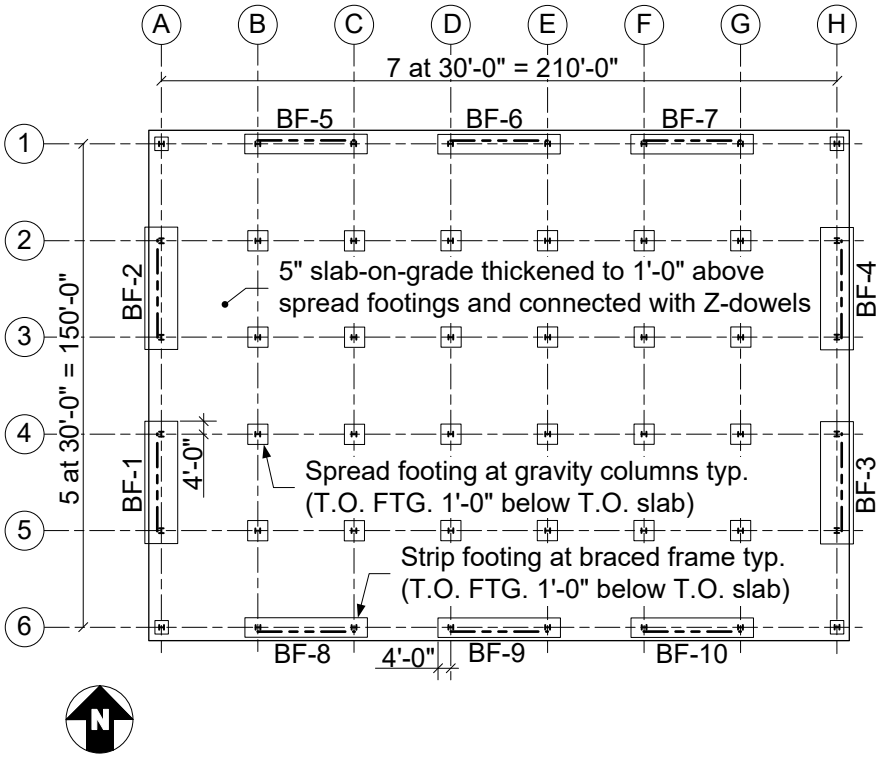

Figure A-5 Foundation plan.

A.4 Initial Design

Design incorporating soil-structure interaction requires a more iterative approach than traditional fixed-base design, because determination of the design-force reductions applicable to the building depend on the foundation sizes and on both the fixed-base and flexible-base building periods. This section presents the design of the structure and foundations without consideration of any reductions in seismic loading due to soil-structure interaction. The SSI reductions are then computed in subsequent sections, based on the structure dynamics and foundation geometry of the initial design.

A.4.1 Base Shear per ASCE/SEI 7-16 Chapter 12 Equivalent Lateral Force Procedure

The initial design is based on the ELF procedure of ASCE/SEI 7-16 Section 12.8. In this procedure, the base shear is computed considering the building to be fixed at the base, and forces are distributed over the height to find the story shears used to compute the required brace sizes and foundation overturning demands.

The fundamental period of the building for determination of the base shear, T_a, is computed according to ASCE/SEI 7-16 Section 12.8.2.

$$T_a = C_t h_n^x = (0.03)(25)^{0.75} = 0.34 \text{ s} \quad \text{(ASCE/SEI 7-16 Eq. 12.8-7)}$$

Where h_n is 25 feet and C_t and x are determined from ASCE/SEI 7-16 Table 12.8-2.

Because T_a is less than 1.5 T_s, the base shear, V, is calculated according to ASCE/SEI 7-16 Equations 12.8-1 and 12.8-2 as follows:

$$V = C_S W \quad \text{(ASCE/SEI 7-16 Eq. 12.8-1)}$$

where:

$$C_S = \frac{S_{DS}}{\left(\frac{R}{I_e}\right)} \quad \text{(ASCE/SEI 7-16 Eq. 12.8-2)}$$

R = 8 for Buckling-restrained braced frames

I_e = 1.0 for Risk Category II

V = (C_s=0.196)(W=4,834 kip) = 949 kip

Distribute the seismic forces over the building height according to ASCE/SEI 7-16 Section 12.8.3, as indicated in Table A-4.

Table A-4 Vertical Distribution of Seismic Forces

Level	w_x (kip)	h_x (ft)	C_{vx}	F_x (kip)
Roof	2,385	25	0.66	627
Second Floor	2,449	12.5	0.34	322
Total	4,834			949

A.4.2 Brace Design

For the purpose of this example, application of accidental torsion according to ASCE/SEI 7-16 Section 12.8.4.3 is not considered. This simplifies the computations that are not related to the concepts being illustrated.

Determination of the required brace areas for the buckling restrained braces requires that the total story shears be divided by the number of braces in each direction, multiplied by the ratio of the brace length to the half-bay-width (1.30), and divided by the design yield strength of the brace core material, which in this case is (0.9) 42 ksi = 37.8 ksi. The computed brace areas are then rounded up to the nearest quarter of a square inch for fabrication convenience. The brace core areas are shown in Tables A-5 and A-6. Note that the brace demands in the longitudinal direction are two thirds of those in the transverse direction, since the only difference between the two calculations is the number of braces in each direction.

Table A-5 Transverse Brace Core Areas

Level	Number of braces	Brace Force (kip)	Computed Core Area (in^2)	Specified Core Area (in^2)
Below Roof	8	102	2.98	3.00
Below Second Floor	8	154	4.51	4.75

Table A-6 Longitudinal Brace Core Areas

Level	Number of braces	Brace Force (kip)	Computed Core Area (in^2)	Specified Core Area (in^2)
Below Roof	12	68	1.99	2.00
Below Second Floor	12	103	3.01	3.25

The columns in each frame are designed to resist the amplified factored overturning demands, which are 461 kip for the transverse frames and 351 kip for the longitudinal direction. The smallest seismically compact W10 column section, W10×68, is used with an axial compression capacity of 687 kip for the building's story height.

A.4.3 Foundation Design

The foundations for the frames are designed to resist gravity loads along with seismic overturning demands. Two LRFD load combinations are considered to capture minimum and maximum gravity loads that ASCE/SEI 7-16 considers applicable in concert with earthquake demands. The load combinations from ASCE/SEI 7-16 Section 2.3.6 are employed below:

$$1.2D + E_v + E_h + 0.5L + 0.2S \qquad \text{(ASCE/SEI 7-16 Sec. 2.3.6, Eq. 6)}$$

$$0.9D - E_v - E_h \qquad \text{(ASCE/SEI 7-16 Sec. 2.3.6, Eq. 7)}$$

where E_v is $0.2S_{DS}D$, as defined in ASCE/SEI 7-16 Section 12.4.2.2. With S_{DS} for the site equal to 1.57g, this is an added or reduced dead load of $0.314D$. Note that Exception 2b of this section indicates that the vertical seismic load effect, E_v, may be taken as zero in (ASCE/SEI 7-16 Sec. 2.3.6 Equation 7, where determining overturning demands on the soil-structure interface of foundations, so the reduction of $0.314D$ need not be considered in in the equation when determining the foundation stability and soil pressures.

Although the frame columns are designed to incorporate the amplified loading due to overstrength, there is no requirement to consider the amplified loading for the foundation design.

Since the frames and their loading are symmetrical, the total gravity loading can be considered to act at the frame centerline. The weight of the foundation is included in the dead load, D. The snow load, S, is zero. The live load, L, is the reduced live loading acting on the second floor. The factor of 0.5 on the live load is according to Exception 1 in ASCE/SEI 7-16 Section 2.3.6. Roof live load is not considered to act with the earthquake load.

Consider a continuous foundation with a depth of 5 ft, extending four feet beyond the center of each column, resulting in a foundation length of 38 ft. Determine foundation width by trial and adjustment in order to provide overturning stability and soil pressures remaining less than the design strength of 4.5 kip/ft^2. Because the tributary areas are the same between the two frame types, the superstructure gravity loads on each frame column are the same for both types of frames.

The live load reduction is computed according to ASCE/SEI 7-16 Section 4.7.2, with the tributary area, A_T of 480 ft^2 and K_{LL} taken as 4, per ASCE/SEI 7-16 Table 4.7-1.

$$L = L_0\left(0.25 + \frac{15}{\sqrt{K_{LL}A_T}}\right) = \left(L_0 = 50 \text{ lb/ft}^2\right)\left(0.59\right) = 29.6 \text{ lb/ft}^2$$

(ASCE/SEI 7-16 Eq. 4.7-1)

The gravity column loads at the foundation are as follows:

$$D = \left(480 \text{ ft}^2\right)\left(69 \text{ lb/ft}^2 + 81 \text{ lb/ft}^2\right) = 72 \text{ kip}$$

$$L = \left(480 \text{ ft}^2\right)\left(29.6 \text{ lb/ft}^2\right) = 14.2 \text{ kip}$$

The overturning demand is reduced by 25% for stability and soil pressure design, as permitted by ASCE/SEI 7-16 Section 12.13.4.

A.4.3.1 Transverse Frame Foundation

The foundation dead load for a foundation width of 8 feet is computed as (5 ft)(38 ft)(8 ft)(0.15 k/ft^3) = 228 kip. When the weight of the slab overpour of 1 ft is added for (1 ft)(38 ft)(8 ft)(0.15 k/ft^3) = 45.6 kip, the total foundation weight is 273.6 kip.

As indicated in Section A.5.2, below, in computation of the lateral soil springs, resistance to shear at the base of the frames is mobilized by all of the building footings acting together and interconnected by the slab-on-grade. It is necessary to confirm this assumption by verifying the capacity of the slab-on-grade and its connections to the footings. Grade beam ties may be necessary in addition to the slab. About 90% of the resistance to any single frame's lateral loading acts through the slab-on-grade. The remaining 10% of the resistance acts on the face of the frame footing through passive pressure or at its base through friction. The resultant resistance acts at or near the top of the footing, which is also the point from which the bottom story height is defined. Accordingly, the story heights employed in the overturning computations below are the same as the nominal story heights defined above. Moments are summed about point "A" as indicated in Figure A-6.

The reduced overturning demand on each of the four frames in the transverse direction is:

M_{OT} = (1/4) [(626.7 kip)(25 ft) + (321.8 kip)(12.5 ft)] (1-0.25) = 3,692 kip-ft

The resisting moment is computed separately for each factored load combination. Table A-7 shows the sum of gravity loads for each combination, along with the resisting moment and the factor of safety against overturning.

Figure A-6 shows a free-body diagram of the transverse frame and foundation, indicating the 25%-reduced overturning demands and the maximum gravity loads on the frame (ASCE/SEI 7-16 Section 2.3.6 Equation 6).

The factored foundation weight shown in Figure A-6, per ASCE/SEI 7-16 Section 2.3.6 Equation 6 is:

$$P_u = 1.2 + \left[0.2(S_{DS} = 1.57)\right] 273.6 \text{ kip} = 414.2 \text{ kip}$$

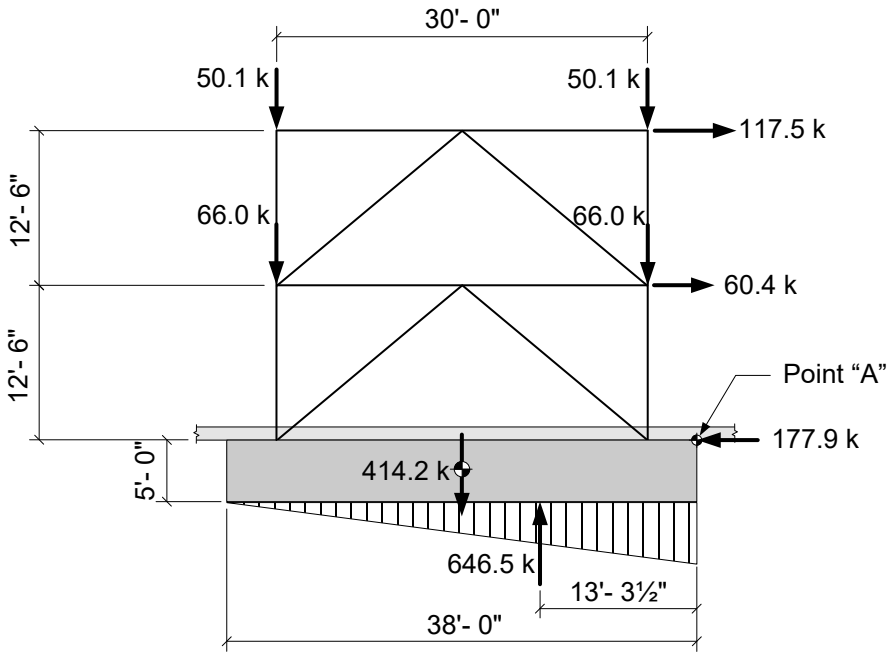

Figure A-6 Free-body diagram of a typical transverse frame showing the 25%-reduced overturning demands and the maximum factored gravity loads.

Table A-7 Resisting Moments

ASCE/SEI 7-16 Section 2.3.6 Equation	Total Weight (kip)	Resisting Moment (kip-ft)	Factor of Safety Against Overturning
Eq. 6 (Maximum gravity load)	647	12,282	3.3
Eq. 7 (Minimum gravity load)	376	7,141	1.9

Table A-8 shows the resulting distance from the end of the footing to the centroid of the soil reaction, *a*, along with the computed maximum and minimum soil pressures for each case.

The controlling case is the maximum gravity load combination, which results in a nearly triangular soil pressure distribution with almost no pressure at the back (uplifting) end of the foundation. The maximum pressure is less than

the design soil bearing pressure (4.0 kip/ft^2 < 4.5 kip/ft^2), so this foundation size is acceptable.

Table A-8 Soil Pressures

ASCE/SEI 7-16 Section 2.3.6 Equation No.	*a* (ft)	Maximum Soil Pressure (kip/ft^2)	Minimum Soil Pressure (kip/ft^2)
Eq. 6 (Maximum gravity load)	13.3	4.0	0.21
Eq. 7 (Minimum gravity load)	9.2	3.4	0.0

A.4.3.2 Longitudinal Frame Foundation

There are six longitudinal frames sharing the same seismic load as the four transverse frames, while the gravity loading is the same. As a result, narrower foundations are possible. The foundation length and depth are kept the same.

Foundation dead load for a foundation width of 5.5 feet is computed as (5 ft)(38 ft)(5.5 ft)(0.15 kip/ft^3) = 157 kip. When the weight of the slab overpour of 1 ft (1 ft)(38 ft)(5.5 ft)(0.15 kip/ft^3) = 31 kip is added the total foundation weight is 188 kip.

The reduced overturning demand considering six frames in the longitudinal direction is:

$$M_{OT} = (1/6)\ [\ (626.7\ \text{kip})(25\ \text{ft}) + (321.8\ \text{kip})(12.5\ \text{ft})\ ]\ (1\text{-}0.25) = 2{,}461\ \text{kip-ft}$$

The resisting moment about the foundation tip is computed separately for each load combination. Table A-9 shows the sum of gravity loads for each combination, along with the resisting moment and the factor of safety against overturning.

Table A-9 Resisting Moments

ASCE/SEI 7-16 Section 2.3.6 Equation	Total Weight (kip)	Resisting Moment (kip-ft)	Factor of Safety Against Overturning
Eq. 6 (Maximum gravity load)	517	9,823	4.0
Eq. 7 (Minimum gravity load)	299	5,679	2.3

Table A-10 shows the resulting distance from the end of the footing to the centroid of the soil reaction, *a*, along with the computed maximum and minimum soil pressures for each case.

Table A-10 Soil Pressures

ASCE/SEI 7-16 Section 2.3.6 Equation No.	*a* (ft)	Maximum Soil Pressure (k/ft²)	Minimum Soil Pressure (k/ft²)
Eq. 6 (Maximum gravity load)	14.2	4.3	0.62
Eq. 7 (Minimum gravity load)	10.8	3.4	0.00

The controlling case is again the maximum gravity load combination, which results in a nearly triangular soil pressure distribution very low pressure at the back (uplifting) end of the foundation. The maximum pressure is less than the design soil bearing pressure, so this narrower foundation size is acceptable.

A.4.4 Fixed-base Modal Analysis

Although the analyses in this section employ the ELF method, it is necessary to compute the periods of vibration for the structure for the fixed-base condition. This allows comparison of the dynamic behavior of the fixed-base and flexible-base conditions, as will be required to compute radiation damping.

The braces are modeled in ETABS 2016 (CSI, 2016)as prismatic rectangular members, extending from node to node, with stiffness modification factors of 1.28 to account for the larger stiffness of the connection elements that occur near the brace ends.

The fixed-base modal analysis results in primary modes of vibration of 0.466 s and 0.459 s due to movement in the transverse direction and longitudinal direction, respectively. The transverse direction is slightly more flexible than the longitudinal direction. While the brace areas in the two directions are proportional to the story shear divided by the number of frames (rounded), the column sizes are the same. The longitudinal frames are effectively stiffer because there are six columns resisting overturning as opposed to four.

A.5 Flexible-base Analysis

The soil-structure interaction calculations require determination of the behavior of the building with a flexible base. This is for two reasons. First, it is necessary to consider the change in dynamic behavior between the fixed-base and the flexible-base conditions in order to compute the radiation damping reductions, which rely on the ratio of the fixed-base to flexible-base periods. Second, ASCE/SEI 7-16 Section 19.1 requires that all elements of foundation flexibility must be considered to be permitted to consider soil

structure interaction. This includes horizontal, vertical, and rotational foundation and soil flexibility.

ASCE/SEI 7-16 Section 12.13.3 requires a 50% increase and decrease in the values of the soil springs for analysis. This requires that the maximum and minimum spring values be computed as 1.5 times and 0.5 times the best estimates.

For the flexible-base analysis, it is necessary to include vertical springs under each of the strip footings under the frames, as well as lateral springs representing resistance to sliding due to passive pressure on the foundation faces and friction at the bottoms of the footings under gravity load.

A.5.1 Vertical Springs

Vertical soil springs are computed according to ASCE/SEI 41-17 Section 8.4.2.5 Method 3. This method employs a uniform spring along the length of the footing based on some flexibility of the concrete foundation element relative to the soil. The method is considered applicable because the continuous footings extend as cantilevers beyond the frame columns, producing flexibility in the foundation structure, and the flexibility of the footings is included explicitly in the model. See Chapter 6 for a detailed discussion of foundation flexibility, including the effects of footing embedment in the soil. The spring values are based on the shear modulus of the soil, G, and Poisson's ratio, ν. These may be estimated by the geotechnical engineer or determined according to the definitions in ASCE/SEI 7-16 Section 19.3.3. For the purpose of the vertical soil spring computations, the geotechnical engineer has recommended the use of $\nu = 0.3$ and G=538 kip/ft^2, which are employed in ASCE/SEI 41-17 Equation 8-11 to compute the vertical soil springs.

$$k_{sv} = \frac{1.3G}{B_f\left(1-\nu\right)} = \frac{1.3\left(538 \text{ kip/ft}^2\right)}{B_f\left(1-0.3\right)} = \frac{1{,}000}{B_f} \text{ kip/ft}^3$$

(ASCE/SEI 41-17 Eq. 8-11)

The soil stiffness intensity is expressed as kip/ft^3, which is stiffness (kip/ft) per unit area (ft^2). Note that in this formulation the stiffness intensity by area is inversely related to the foundation width—as the footing gets wider, its stiffness intensity decreases, due to a larger volume of soil being subject to compression. As a result, the stiffness intensity per unit length is independent of the foundation width. So, multiplying through by a unit footing width, the linear spring value in kip/ft^2 is the same as the spring value per area in kip/ft^3. The unit spring value of 1,000 kip/ft per linear ft is then

employed for any foundation width. This is modeled in ETABS as a vertical line spring with the stiffness of 1,000 / $(12)^2$ = 6.94 kip/in per linear inch.

The approach outlined in ASCE/SEI 41-17 is only one method of developing the soil springs. Other methods, such as that in NIST GCR 12-917-21 (NIST, 2012a) may also be applicable. This method results in spring values that are not independent of the footing width. A geotechnical engineer should be consulted regarding the appropriateness of these and other methods.

A.5.2 Lateral Springs

The lateral resistance of the building at the base includes two components: passive pressure on the sides of footings, and friction at the base of the footings. Because the building has a continuous slab-on-grade that is connected to the braced frame footings and the individual gravity footings, the entire building base is considered to act as a unit, such that all footings are mobilized to resist lateral loads.

The geotechnical engineer has provided a recommended value for the passive pressure that can be developed at each footing, which is 1.6 kip/ft^2, spread uniformly over the face of the footing which is developed according to the relative displacement of the footing face and the soil according to ASCE/SEI 41-17 Figure 8-6, which is reproduced in Figure A-7. The proportion of the ultimate passive pressure that is developed, P/P_{ult}, is a function of δ/H, where δ is the lateral displacement and H is the depth of the footing. This mobilization relationship can be approximated by the following equation, which has been fitted to the curve in the figure.

$$\frac{P}{P_{ult}} = 0.15 + 2.88\left(\frac{\delta}{H}\right)^{0.43}$$

The geotechnical engineer has also provided a friction coefficient of 0.35, to be applied to the gravity load at each footing. This friction is developed at very small displacement. For the purpose of these calculations the mobilization of friction is presumed to occur at zero displacement.

The friction is proportional to the gravity load on the footings, which can vary depending on which load combination is selected. Since the springs developed in this manner are intended to be best estimates, the gravity load used here is based on the load combination $D + 0.25L$, where L is the unreduced live load, as described in ASCE/SEI 41-17 Section 7.2.2.

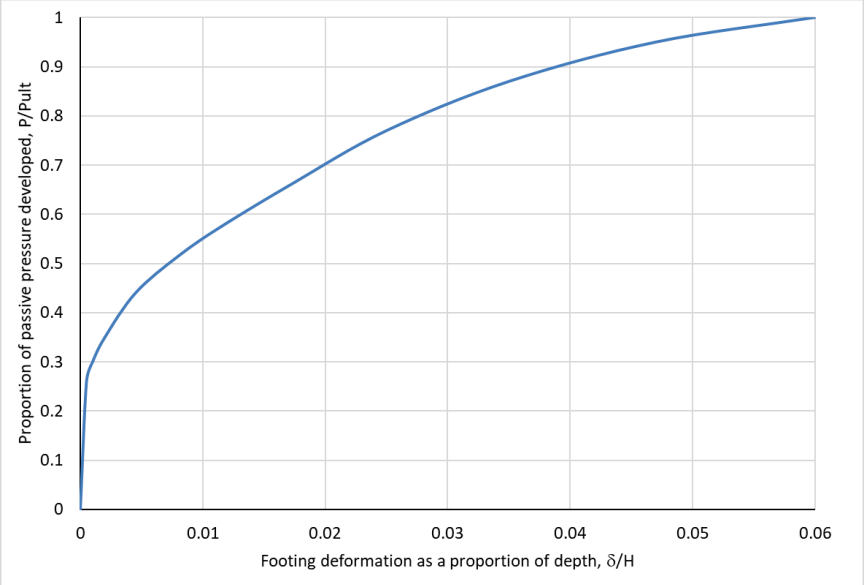

Figure A-7 Passive pressure mobilization curve (reproduced from ASCE/SEI 41-17, Figure 8-6).

Because of the shape of the passive pressure mobilization curve, the lateral springs at the base of the building are nonlinear. In order to perform a flexible-base linear analysis, a secant stiffness is developed based on the expected value of base shear resistance. This is not the nominal base shear computed in Section A.4.1, which includes the response modification factor, R. Since the passive pressure resistance is nonlinear (and the frictional resistance is effectively constant), it is appropriate to base this calculation on an estimate of the actual demand rather than the demand reduced for design purposes. ASCE/SEI 7-16 uses the overstrength factor, Ω_0, as a multiplier on the nominal base shear to approximate the real seismic load. Accordingly, the best estimate for the base shear to be resisted is taken as $\Omega_0 V$, which is $(\Omega_0 = 2.5)(V = 949 \text{ kip}) = 2{,}371$ kip.

The total lateral resistance is computed by trial and adjustment to find the displacement that produces the desired resistance of 2,371 kip. For ease of spreadsheet calculations, Tables A-11 and A-12 show the total resistance developed at each column type, with each column in the braced frames considered separately (with foundations of half the total length). In each of these tables, the passive resistance for the frames parallel to the load considers only one passive face per frame (not one per column), while the passive pressure developed in the frame footings perpendicular to the load engages the half-length of the foundation at both columns in the frame.

Table A-11 Total Lateral Resistance - Transverse Direction at Displacement of 0.015 in

Column Type	No. Each	Depth (ft)	Width (ft)	Axial Load (kip)	Friction Each (kip)	Passive Developed Each (kip)	Total Resistance (kip)
Corner	4	2	4	38	13	3	67
Interior	24	**3**	**8**	151	53	**10**	1,500
Transverse Frame friction	8			76	27		213
Transverse Frame passive	4	5	8			15	59
Longitudinal Frame	12	5	19	76	27	35	741
TOTAL							2,580

Table A-12 Total Lateral Resistance - Longitudinal Direction at Displacement of 0.035 in

Column Type	No. Each	Depth (ft)	Width (ft)	Axial Load (kip)	Friction Each (kip)	Passive Developed Each (kip)	Total Resistance (kip)
Corner	4	2	4	38	13	4	70
Interior	24	3	8	151	53	12	1541
Transverse Frame	8	5	19	76	27	21	375
Longitudinal Frame friction	12			76	27		319
Longitudinal Frame passive	6	5	5.5			6	71
TOTAL							2,376

An example computation for the passive resistance at a typical interior footing, which is 8 ft by 8 ft in plan and 3 ft deep at 0.015 inches displacement is shown below:

Ultimate passive resistance = (3 ft)(8 ft)(1.6 kip/ft^2) = 38.4 kip.

$$\delta/H = 0.015/36 = 0.00042$$

The value P/P_{ult} may be computed according to the curve-fit equation above as follows:

$$\frac{P}{P_{ult}} = 0.15 + 2.88\left(0.00042\right)^{0.43} = 0.25$$

Passive pressure developed = (38.4)(0.25) = 10 kip

These example values are shaded in Table A-11.

The total displacement required in the transverse direction is lower than that required for the longitudinal direction, because of the broader total passive width provided by the longitudinal frame footings when they are pushed perpendicular to their length.

The lateral spring stiffness is computed as the total resistance provided divided by the displacement at which it is developed. The best estimate spring value computed for the transverse direction is computed as (2,580 kip)/(0.015 in) = 172,026 kip/in, which is divided by 4 (43,006 kip/in) to be applied in the model at each corner of the slab. The longitudinal lateral spring is computed similarly.

There will be some additional flexibility in the ground floor slab as it and deforms in flexure and shear due to the resistance developed within the span of the slab between the frames, which are on the edges of the building. There will also be additional stiffness developed due to the friction between the slab and the ground, although this friction will be mitigated by the presence of the vapor barrier between the slab and the ground. These two refinements are not considered in this example. They are small and will produce opposing effects.

A.5.3 Flexible-base Modal Analysis

As required by ASCE/SEI 7-16 Section 12.13.3, flexible-base analyses incorporating three estimates for each spring must be performed, these include a 50% increase and a 50% decrease in the best estimate spring values. Table A-13 shows the values of spring stiffnesses employed in the three flexible-base models.

ASCE/SEI 41

Note that in ASCE/SEI 41, sensitivity analysis requirements differ: the upper bound spring values are twice the best estimate values. The lower bound values in both standards are the same.

Table A-13 Spring Values

Spring	Lower Bound	Best Estimate	Upper Bound
Vertical linear springs	3.47 kip/in/in	6.94 kip/in/in	10.42 kip/in/in
Transverse lateral springs (each building corner)	21,503 kip/in	43,006 kip/in	64,510 kip/in
Longitudinal lateral springs (each building corner)	8,485 kip/in	16,970 kip/in	25,456 kip/in

The lateral springs are very stiff and do not significantly affect the behavior, but the vertical springs under each frame foundation produce a rotation of each frame and its foundation and the primary mode of behavior.

Table A-14 presents the fundamental modes for the fixed-base model and the three versions of the flexible-base model. Figure A-8 shows the first-mode displaced shape of one transverse frame. Note the vertical displacement of the ends of the footings due to the vertical foundation springs.

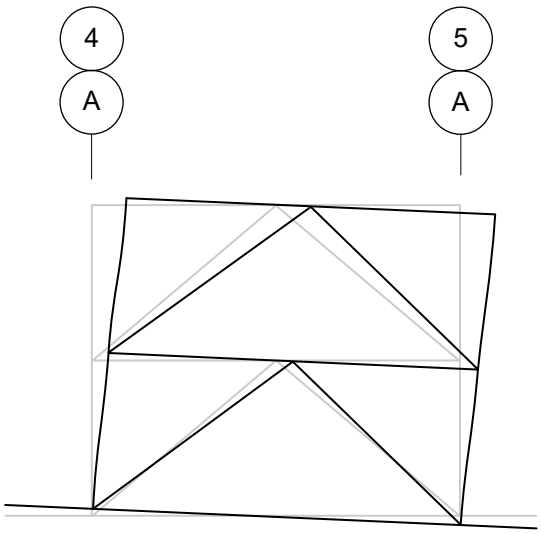

Figure A-8 First-mode displaced shape of a typical frame with foundation flexibility included.

Table A-14 Fundamental Periods for Fixed- and Flexible-Base Models

Model	Transverse first mode period (s)	Longitudinal first mode period (s)
Fixed base (for comparison)	0.466	0.459
Flexible-base upper bound	0.510	0.493
Flexible-base best estimate	0.532	0.509
Flexible-base lower bound	0.592	0.554

The first mode periods increase by 27% in the transverse direction and 21% in the longitudinal direction between the fixed-base and the lower bound flexible-base models.

A.6 Foundation Damping

With the analyses complete, soil-structure interaction reductions due to foundation damping are computed. There are two categories of damping to be considered: soil hysteretic damping and radiation damping. These are addressed in the following sections. Note that foundation damping is not permitted per ASCE/SEI 7-16 Section 19.3.1.1 when the foundation system consists of discrete footings that are both (1) not interconnected and that (2) are spaced less than the larger dimension of the supported lateral force-resisting element in the direction under consideration. In this example

building, the slab-on-grade is reinforced and thickened over footings and connected to them as shown in Figure A-5. This is considered to provide sufficient interconnectivity to engage all footings to move together. Thus, foundation damping is permitted. However, if the footings were not interconnected, they would be too closely spaced to use the foundation damping provisions: the braced frames are 30'0" wide and the spread footings supporting them are 38'0" long parallel to the brace, leaving a space of 22'0" between footings. More details are in Chapter 8. However, in order to illustrate the application of the foundation damping provisions, this limitation is ignored in the following calculations.

A.6.1 Soil Hysteretic Damping

This effect is simple to address; it depends only on the site class and the value of S_{DS} for the site. The applicable value is taken directly from ASCE/SEI 7-16 Table 19.3.3. For Site Class D, the tabular values of 0.07 for $S_{DS}/2.5 = 0.4$ and 0.15 for $S_{DS}/2.5 = 0.8$ are tabulated. For this site, with S_{DS} of 1.57, $S_{DS}/2.5$ is 0.628, the soil hysteretic damping ratio, β_s, is 0.116.

A.6.2 Radiation Damping

Radiation damping is considerably more complex. The initial inputs pertain to the soil at the site: the soil density and the shear wave velocity. Note that the shear wave velocity here is not $\overline{v}_s$, the value used to determine the site class. Here, v_s is considered for the upper soil layer, over a depth B from the base of the foundation. Here, B is half the width of the foundation under consideration. The use of $\overline{v}_s$ for site class determination is intended to account for the average soil stiffness in the upper 100 ft (30m); the use of v_s for the upper soil layer is intended to capture the effects of the upper soils that more directly affect the damping at the soil-structure interface.

Figure A-1 shows the soil density in the upper soils, γ, to be 120 to 125 lb/ft^3. Use an average value of 122.5 lb/ft^3. Scale the shear wave velocity from the profile in Figure A-1 as 653 ft/s. This is v_{so}. Then use ASCE/SEI 7-16 Table 19.3-1 to compute the effective shear wave velocity, v_s. The modification factor is interpolated in a manner like that used for the soil hysteretic damping ratio, as 0.488, which results in an effective shear wave velocity, v_s, of 319 ft/s.

The soil shear modulus at small strain levels, G_o, is computed as:

$$G_o = \gamma \frac{v_{so}^2}{g} = 1,624 \text{ kip/ft}^2$$

(ASCE/SEI 7-16 Sec. 19.3.3 definition)

where g is the acceleration of gravity.

ASCE/SEI 7-16 Table 19.3-2 is used to compute the effective shear modulus, *G*. The modification factor is interpolated in a manner like that used for the soil hysteretic damping ratio, as 0.272, which results in an effective shear modulus, *G*, of 442 kip/ft^2. This is slightly lower than the value recommended by the geotechnical engineer for the vertical soil spring calculation. The value computed according to ASCE/SEI 7-16 Section 19.3 is used here for consistency with the other formulations within this section.

The following computations are then followed for each loading direction, for the three estimates of the soil spring values. The values shown in the paragraphs below are for the best estimate in the transverse direction. The results for both directions and all three spring value estimates are tabulated at the end of this section.

Since the foundations under consideration behave independently, compute the radiation damping for one frame in each direction. For the transverse direction, the foundation plan dimensions are $2L$ = 38 ft by $2B$ = 8 ft. The plan dimensional ratio, *L/B* is 4.75.

The first computation is the period lengthening ratio, $\tilde{T} / T$, where $\tilde{T}$ is the flexible-base period and T is the fixed-base period. The value of $\tilde{T} / T$ is computed as 0.532/0.466 = 1.142.

The effective period-lengthening ratio, which depends on the system ductility, μ, is computed. ASCE/SEI 7-16 indicates in the definition of μ that it may be taken as the ratio of the response modification factor, *R*, and the overstrength factor, Ω_0, to be 8/2.5 = 3.2. *R* can be considered as the product of ductility and overstrength, so dividing *R* by the overstrength results in an estimate of the ductility. The effective period lengthening ratio is then computed according to ASCE/SEI 7-16 as

$$\left(\frac{\tilde{T}}{T}\right)_{eff} = \left\{1+\frac{1}{\mu}\left(\left(\frac{\tilde{T}}{T}\right)^2 - 1\right)\right\}^{0.5} = 1.046$$

(ASCE/SEI 7-16 Eq. 19.3-2)

The translational stiffness, K_y, and rotational stiffness, K_{xx}, are then computed according to ASCE/SEI 7-16 Equation 19.3-8 and 19.3-9, respectively. Here, ν is Poisson's ratio, taken as 0.3 for sandy soil, according to definitions in ASCE/SEI 7-16 Section 19.3. Note that these stiffness equations are particular to the damping computations. See Chapter 6 for further information regarding foundation flexibility. The geometry and

direction of movement implicit in these equations are based on the weak-axis movement of a rectangular foundation, which in this case results in a conservative assessment of the damping. These stiffness equations are not directly related to the stiffness from the structural analyses in ETABS.

$$K_y = \frac{GB}{2-\nu}\left[6.8\left(\frac{L}{B}\right)^{0.65} + 0.8\left(\frac{L}{B}\right) + 1.6\right] = 2.506\times10^{7} \text{ lb/ft}$$

(ASCE/SEI 7-16 Eq. 19.3-8)

$$K_{xx} = \frac{GB^3}{1-\nu}\left[3.2\left(\frac{L}{B}\right) + 0.8\right] = 6.46\times10^{8} \left(\text{ft-lb/rad}\right)$$

(ASCE/SEI 7-16 Eq. 19.3-9)

In order to compute the damping values, three dimensionless constants, a_0, Ψ, and α_{xx}, are computed according to ASCE/SEI 7-16 Equations 19.3-11, 19.3-13, and 19.3-14, respectively.

$$a_0 = \frac{2\pi B}{\tilde{T} v_s} = 0.148 \qquad \text{(ASCE/SEI 7-16 Eq. 19.3-11)}$$

$$\psi = \sqrt{\frac{2(1-\nu)}{1-2\nu}} = 1.871 \quad \text{(ASCE/SEI 7-16 Eq. 19.3-13)}$$

(ψ must not exceed 2.5)

$$\alpha_{xx} = 1.0 - \left[\frac{\left(0.55 + 0.01\sqrt{(L/B)-1}\right)a_0^2}{\left(2.4 - \frac{0.4}{(L/B)^3}\right) + a_0^2}\right] = 0.995$$

(ASCE/SEI 7-16 Eq. 19.3-14)

The fundamental translational period and fundamental rotational period of the damping system are computed based on the computed stiffness, the effective modal mass, M^*, and the effective structure height, h^*. The effective modal mass, M^*, is the building seismic mass, multiplied by the first modal mass participation factor (in this case, 0.87), divided by the number of frames in the direction under consideration (4). The modal mass participation factor expresses the proportion of the total mass excited in the first natural mode of vibration. It can be found as part of the ETABS (or similar analysis program) modal results. In this case, $M^* = 3.26\times10^4$ lb-sec^2/ft. The effective structure height, h^*, is computed from the displaced shape of the first mode or may be taken as 0.7 times the building height. A more explicit computation based on the actual first mode shape results in 0.68 times the building height, 16.92 ft. The first mode shape for this two-

story building is defined by two points—the lateral displacements of the second story and of the roof in the first mode, with each displacement considered at the height of the associated diaphragm. The effective height may be computed as the centroid of the polygon defined by these two points and the ground. For the two-story building under consideration, the effective height may be computed as follows:

$$h^* = \frac{\left(\frac{2}{3}h_2 + h_1\right)\left(\frac{(\delta_2 - \delta_1)}{2}h_2\right) + \left(\frac{h_2}{2} + h_1\right)(\delta_1 h_2) + \left(\frac{2}{3}h_1\right)\left(\frac{\delta_1}{2}h_1\right)}{\frac{\delta_1 h_1}{2} + \frac{(\delta_1 + \delta_2)h_2}{2}} = 16.92 \text{ ft}$$

Where h_1 and h_2 are the first and second story heights, respectively, and δ_1 and δ_2 are the lateral displacements of the second story and roof in the first mode, which in this case are 0.48 and 1.0. The translational period, T_y, and rotational period, T_{xx}, are then computed according to ASCE/SEI 7-16 Equations 19.3-6 and 19.3-7, respectively. Note again that these values are particular to the damping computations and are not directly related to the periods from our structural analyses.

$$T_y = 2\pi\sqrt{\frac{M^*}{K_y}} = 0.227 \sec \quad \text{(ASCE/SEI 7-16 Eq. 19.3-6)}$$

$$T_{xx} = 2\pi\sqrt{\frac{M^* h^{*2}}{\alpha_{xx} K_{xx}}} = 0.757 \sec \quad \text{(ASCE/SEI 7-16 Eq. 19.3-7)}$$

The translational damping coefficient, β_y and the rotational damping coefficient, β_{xx}, are now computed according to ASCE/SEI 7-16 Equations 19.3-10 and 19.3-12, respectively.

$$\beta_y = \left[\frac{4(L/B)}{K_y/GB}\right]\left[\frac{a_0}{2}\right] = 0.099$$

(ASCE/SEI 7-16 Eq. 19.3-10)

$$\beta_{xx} = \frac{(4\psi/3)(L/B)a_0^2}{\left(\frac{K_{xx}}{GB^3}\right)\left[\left(2.2 - \frac{0.4}{(L/B)^3}\right) + a_0^2\right]}\left[\frac{a_0}{2\alpha_{xx}}\right] = 3.827 \times 10^{-4}$$

(ASCE/SEI 7-16 Eq. 19.3-12)

Note that the translational damping is a much more significant effect than the rotational damping ($\beta_y = 0.099 > \beta_{xx} = 3.287 \times 10^{-4}$), although the elastic behavior of the building is more significantly affected by the rotation. The radiation damping ratio, β_{rd}, is computed according to ASCE/SEI 7-16 Equation 19.3-5.

$$\beta_{rd} = \frac{1}{\left(\tilde{T}/T_y\right)^2}\beta_y + \frac{1}{\left(\tilde{T}/T_{xx}\right)^2}\beta_{xx} = 0.018 + 7.75\times10^{-4} = 0.019$$

(ASCE/SEI 7-16 Eq. 19.3-5)

Next, the foundation damping ratio, β_f, is computed and includes both the radiation damping computed here and the hysteretic damping (Section A.6.1), according to ASCE/SEI 7-16 Equation 19.3-4, and the effective damping ratio, β_0, according to ASCE/SEI 7-16 Equation 19.3-1.

$$\beta_f = \left[\frac{\left(\tilde{T}/T\right)^2 - 1}{\left(\tilde{T}/T\right)^2}\right]\beta_s + \beta_{rd} = 0.046$$

(ASCE/SEI 7-16 Eq. 19.3-4)

$$\beta_0 = \beta_f + \frac{\beta}{\left(\tilde{T}/T\right)^2_{eff}} = 0.091$$

(ASCE/SEI 7-16 Eq. 19.3-1)

(must not exceed 0.20)

where β is the effective viscous damping ratio of the structure, taken as 5% as recommended in ASCE/SEI 7, and the effective period lengthening ratio is computed above.

A.6.3 Adjusted Base Shear

With this effective damping ratio, the response adjustment factor, B_{SSI}, is computed from ASCE/SEI 7-16 Equation 19.2-4, the reduction in base shear, ΔV, from ASCE/SEI 7-16 Equation 19.2-2, and the adjusted base shear from ASCE/SEI 7-16 Equation 19.2-1.

$$B_{SSI} = \frac{4}{\left[5.6 - \ln\left(100\beta_0\right)\right]} = 1.181$$

(ASCE/SEI 7-16 Eq. 19.2-4)

For ease of comparison, the reduction in seismic response coefficient, ΔC_s, is computed rather than computing the reduction in base shear, ΔV.

$$\Delta C_s = C_S - \frac{\tilde{C}_s}{B_{SSI}} = 0.196 - \frac{0.196}{1.181} = 0.196 - 0.166 = 0.03$$

(modified ASCE/SEI 7-16 Eq. 19.2-2)

Here C_s is the fixed-base response coefficient, computed in Section A.4.1, and $\tilde{C}_s$ is the value of the response coefficient computed based on the

flexible-base period. In this case, the value is the same as that computed at the fixed-base period, since all fundamental periods are within the flat top (acceleration controlled) region of the response spectrum.

Accordingly, the updated value of C_s is computed as 0.196 - 0.03 = 0.166. This value is 87% of the ASCE/SEI 7-16 Chapter 12 value of 0.196. Similar reductions are computed for the other directions and stiffness values, as indicated in Table A-15.

Table A-15 Tabulation of Reduced Seismic Response

Model	C_s Transverse (g)	C_s Longitudinal (g)
Fixed base (for comparison)	0.196	
Upper bound springs	0.168	0.175
Best estimate springs	0.166	0.172
Lower bound springs	0.162	0.167

A.6.4 Code-limited Adjusted Base Shear

The largest value of C_s computed is for the upper bound soil springs in the longitudinal direction, which is 0.175g. In the transverse direction, the largest value is 0.168g. ASCE/SEI 7-16 Section 19.2.1 places limitation on the reduction in demand. For structures with R factors greater than or equal to 6, the adjusted response coefficient must be at least 90% of the ASCE/SEI 7-16 Chapter 12 value: (0.9) (0.196g) = 0.177g.

A.7 Design for SSI-Reduced Base Shear per ASCE/SEI 7-16 Chapter 19

Now that the reduced base shear is computed, the structure is redesigned employing the lower design forces. This will result in smaller brace areas, and narrower foundations. Following that redesign, the reductions in seismic response coefficient are recomputed to compare with the starting point of 0.177. If the resulting value is smaller than this value, the reduced sizes remain applicable. If the resulting seismic response coefficient is larger than 0.177, a further iteration is required with the larger coefficient and larger resulting sizes.

A.7.1 Brace Design

Brace areas are computed in the same manner as in Section A.4.2. Tables A-16 and A-17 show the brace sizes required for the reduced seismic demands. Column sizes remain unchanged, as they were already the smallest compact W10 sections available.

Table A-16 Transverse Brace Core Areas

Level	Number of braces	Brace Force (kip)	Computed Core Area (in^2)	Specified Core Area (in^2)
Below roof	8	92	2.69	2.75
Below second floor	8	139	4.07	4.25

Table A-17 Longitudinal Brace Core Areas

Level	Number of braces	Brace Force (kip)	Computed Core Area (in^2)	Specified Core Area (in^2)
Below Roof	12	61	1.79	2.00
Below Second Floor	12	93	2.71	2.75

In general, the brace areas are reduced in rough proportion to the seismic demand. However, due to rounding, the braces below the roof in the longitudinal direction remain the same size.

A.7.2 Foundation Design

With the reduced demands, the overturning moment reduces, but the gravity load remains the same, so the effect on the foundation sizes is not a linear reduction. The foundation sizes are determined in the same manner as in Section A.4.3, above. The lengths and depths of the foundations remain the same. Trial and adjustment result in width reductions from 8 ft to 7 ft for the transverse frame and from 5.5 ft to 4 ft for the longitudinal frame. These reduced widths are the minimum sizes (rounded up to the nearest half foot) that produce acceptable soil pressures.

A.7.3 Fixed-base Modal Analysis

The smaller brace sizes result in a softer structure. The primary modal period in the transverse direction increases from 0.466 s to 0.489 s. The primary modal period in the longitudinal direction increases from 0.459 s to 0.483 s.

A.7.4 Flexible-base Modal Analysis

The vertical linear springs are not dependent on the footing width, so those values do not change with the narrower foundations. The lateral spring values include the passive pressure, which does depend on the foundation sizes, but the widths of the frame foundations are not a significant factor. The base shear is lower, however, and this affects the lateral spring properties by reducing the anticipated displacement. Table A-18 shows the

updated spring values used in the flexible-base analysis. Table A-19 shows the updated flexible-base fundamental periods.

Table A-18 Updated Spring Values

Spring	Lower Bound	Best Estimate	Upper Bound
Vertical linear springs	3.47 kip/in/in (unchanged)	6.94 kip/in/in (unchanged)	10.42 kip/in/in (unchanged)
Transverse lateral springs (each building corner)	32,079 kip/in	64,158 kip/in	96,238 kip/in
Longitudinal lateral springs (each building corner)	21,406 kip/in	42,811 kip/in	64,217 kip/in

Table A-19 Updated Fundamental Periods for Fixed-base and Flexible-base Models

Model	Transverse first mode period (s)	Longitudinal first mode period (s)
Fixed base (for comparison)	0.489	0.483
Flexible-base upper bound	0.531	0.515
Flexible-base best estimate	0.552	0.530
Flexible-base lower bound	0.610	0.573

A.7.5 Check of Base Shear

Based on the updated foundation sizes and dynamic properties, recompute the damping properties and resulting seismic response coefficient using the same approach outlined in Section A.6, above. The resulting seismic response coefficients are shown in Table A-20.

Table A-20 Tabulation of Reduced Seismic Response

Model	Reduced C_s Transverse (g)	Reduced C_s Longitudinal (g)
Upper bound springs	0.171	0.177
Best estimate springs	0.171	0.175
Lower bound springs	0.164	0.169

The highest value of the seismic response coefficient computed with the reduced brace sizes and the reduced foundation widths is the same as our starting value of 0.177g, indicating that no further iteration is required and the design including soil-structure interaction is acceptable.

A.8 Design for Full Theoretical SSI-Reduced Base Shear

ASCE/SEI 41

Note that the restrictions in ASCE/SEI 7 are not present in ASCE/SEI 41. Accordingly, the reductions computed in this section would be applicable for an ASCE/SEI 41 analysis of an existing structure.

This section explores extending the reductions in design loads beyond those permitted by the ASCE/SEI 7. This allows larger reductions due to foundation damping as well as the further reduction due to base slab averaging, which is not permitted by ASCE/SEI 7-16 for linear analyses.

A.8.1 Base Slab Averaging

Base slab averaging is one of the two kinematic soil-structure interaction effects covered in ASCE/SEI 7-16 Section 19.4. The embedment effect, addressing buildings with basements, is not addressed in this example, but is covered in Appendix B.

Base slab averaging is an effect that addresses the incoherence of ground motions over a building's footprint. If the building base is large enough and the foundation system has sufficient interconnection and lateral rigidity, the effect of earthquake ground motions will be reduced. This effect is more pronounced for buildings with shorter periods of vibration and for those with larger base extents. These two quantities alone determine the reduction due to base slab averaging, termed RRS_{bsa}.

The effective foundation size, b_e, depends on the building base area A_{base}, which is the extent of the ground-level slab.

$$A_{base} = (150 \text{ ft})(210 \text{ ft}) = 31{,}500 \text{ ft}^2$$

$$b_e = \sqrt{A_{base}} = 177 \text{ ft}$$

(ASCE/SEI 7-16 Equation 19.4-4)

The computed value of b_e shall not exceed 260 ft. ASCE/SEI 7-16 requires that the shear wave velocity of the soil, v_s, be in the range of 650 to 1,650 ft/s. In this case, v_s is taken as the average value over a depth equal to the effective foundation size, b_e. Referring back to Figure A-1, the average shear wave velocity for this site is clearly within that range.

The reduction due to base slab averaging is dependent on b_e and on the building period. The reduction is computed according to ASCE/SEI 7-16 Equations 19.4-1, 19.4-2, and 19.4-3. The values shown below pertain to the flexible-base period in the transverse direction for the best estimate soil springs ($T = 0.532$ s).

$$b_0 = 0.00071\left(\frac{b_e}{T}\right) = 0.236$$

(ASCE/SEI 7-16 Equation 19.4-3)

Where the period, T, shall not be taken as less than 0.2 s. ASCE/SEI 7-16 Equation 19.4-2 for B_{bsa}, has two forms, depending on the value of b_0. The first form (for $b_0 \leq 1$) is applicable:

$$B_{bsa} = 1 + b_0^2 + b_0^4 + \frac{b_0^6}{2} + \frac{b_0^8}{4} + \frac{b_0^{10}}{12} = 1.06$$

(ASCE/SEI 7-16 Eq. 19.4-2(a))

The second form, (for $b_0 > 1$) is

$$B_{bsa} = \exp\left(2b_0^2\right)\left[\frac{1}{\sqrt{\pi b_0}}\left(1 - \frac{1}{16b_0^2}\right)\right]$$

(ASCE/SEI 7-16 Eq. 19.4-2(b))

The reduction is computed as follows.

$$RRS_{bsa} = 0.25 + 0.75\left\{\frac{1}{b_0^2}\left[1 - \left(\exp\left(-2b_0^2\right)\right)B_{bsa}\right]\right\} = 0.98$$

(ASCE/SEI 7-16 Eq. 19.4-1)

This reduction is applied to the value of C_s in Section A.6.3 of 0.166g. The updated value of C_s is then (0.98)(0.166g) = 0.163g. Table A-21 presents the values of C_s for each direction and each soil spring estimate for with and without the base slab averaging reduction.

Table A-21 Tabulation of Reduced Seismic Response with and without Base Slab Averaging

Model	C_s Transverse (No BSA) (g)	C_s Transverse (w/ BSA) (g)	C_s Longitudinal (No BSA) (g)	C_s Longitudinal (w/ BSA) (g)
Fixed base (for comparison)	0.196			
Upper bound springs	0.168	0.164	0.175	0.164
Best estimate springs	0.166	0.163	0.172	0.164
Lower bound springs	0.162	0.159	0.167	0.159

Note that the reductions due to base slab averaging are more significant in the longitudinal direction, due to the shorter periods. The upper bound spring estimates result in the largest values of C_s, 0.164g.

Figure A-9 shows the base slab averaging reductions for three values of b_e: 100 ft, 177 ft (this example), and 260 ft (maximum permitted). Note that the reductions are limited to the values computed at periods of 0.2 s.

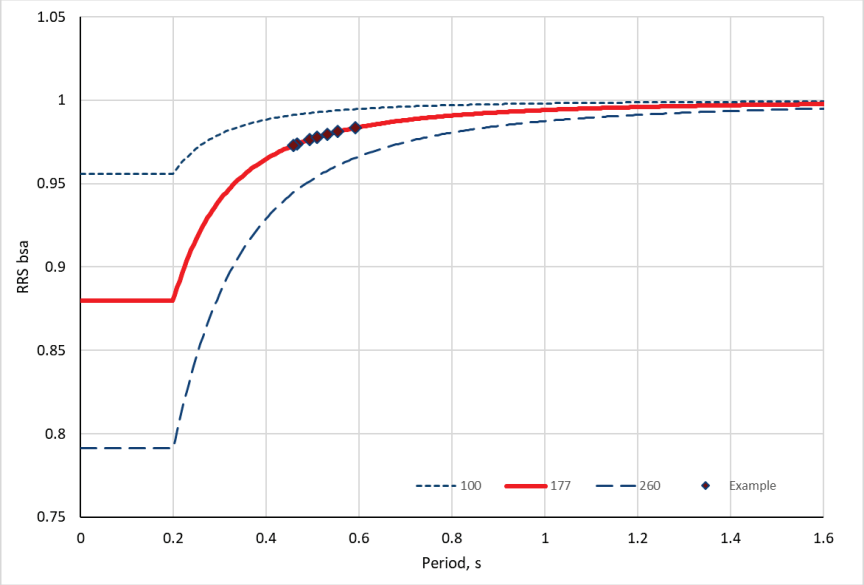

Figure A-9 Reductions for base slab averaging relative to building period for three values of effective foundation size.

As in Section A.7, above, redesigning the structure employing the lower design forces will result in smaller brace areas, and narrower foundations. Following that redesign, the reductions in seismic response coefficient are recomputed to compare with our starting point of 0.164g. If the resulting value is smaller than this value, the reduced sizes remain applicable. If the resulting seismic response coefficient is larger than 0.164g, a further iteration is required with the larger coefficient and larger resulting sizes.

A.8.2 Brace Design

Brace areas are computed in the same manner as in Section A.4.2. Tables A-22 and A-23 show the brace sizes required for the reduced seismic demands, with the original (unreduced) sizes and the code-limited reduced sizes shown for comparison.

In general, brace areas are reduced in rough proportion to the seismic demand. However, due to rounding, the braces below the second floor in the longitudinal direction remain the same size.

Table A-22 Transverse Brace Core Areas

Level	Unreduced Core Area (in^2)	Code-Limited Reduced Core Area (in^2)	Fully Reduced Core Area (in^2)
Below Roof	3.00	2.75	2.50
Below Second Floor	4.25	4.25	4.00

Table A-23 Longitudinal Brace Core Areas

Level	Unreduced Core Area (in^2)	Code-Limited Reduced Core Area (in^2)	Fully Reduced Core Area (in^2)
Below Roof	2.00	2.00	1.75
Below Second Floor	3.25	2.75	2.75

A.8.3 Foundation Design

With the reduced demands, the overturning moment reduces, but the gravity load remains the same, so the effect on the foundation sizes is not a linear reduction. The foundation sizes are determined in the same manner as in Sections A.4.3 and A.7.2, above. The foundation plan dimensions remain the same as those computed in Section A.7.2 for the code-limited reductions. The foundation depths are reduced from 5 feet to 4 feet.

A.8.4 Fixed-base Modal Analysis

The smaller brace sizes result in a softer structure. The primary modal period in the transverse direction increases further from 0.489 s. to 0.506 s. The primary modal period in the longitudinal direction increases further from 0.483 s to 0.496 s.

A.8.5 Flexible-base Modal Analysis

The lateral spring values are again adjusted based on the lower base shear and resulting lower anticipated displacement. Table A-24 shows the updated flexible-base fundamental periods.

Table A-24 Updated Fundamental Periods for Fixed-base and Flexible-base Models

Model	Transverse first mode period (s)	Longitudinal first mode period (s)
Fixed base (for comparison)	0.506	0.496
Flexible-base upper bound	0.545	0.524
Flexible-base best estimate	0.564	0.538
Flexible-base lower bound	0.618	0.577

A.8.6 Check of Base Shear

The seismic response coefficient is recomputed based on the updated dynamic properties using the same approach outlined above. The resulting seismic response coefficients are shown in Table A-25.

Table A-25 Tabulation of Reduced Seismic Response

Model	Reduced C_s Transverse (g)	Reduced C_s Longitudinal (g)
Upper bound springs	0.169	0.168
Best estimate springs	0.167	0.166
Lower bound springs	0.163	0.162

The highest values of the seismic response coefficients computed are 0.168g and 0.169g, compared to the starting value of 0.164g, indicating that the structure designed for the fully reduced loads no longer produces the same amount of reduction in loads. Accordingly, a redesign using the higher computed loads is required.

A.8.7 Redesign (Iteration)

The affected structural elements are redesigned for the higher value of C_s = 0.169g. Small changes in some elements of the design are required. These are an increase in the transverse brace size below the roof to 2.75 in^2 and an increase in the transverse foundation depth to 5 ft. (These are the same values of these elements as in the SSI-reduced design as limited by ASCE/SEI 7.)

A.8.8 Reanalysis

The fixed-base and flexible-base models are reanalyzed incorporating the updated design. The periods in the longitudinal direction are essentially unchanged, since the design modifications did not affect these frames. Table A-26 shows the updated dynamic properties.

Table A-26 Updated Fundamental Periods for Fixed-base and Flexible-base Models

Model	Transverse first mode period (s)	Longitudinal first mode period (s)
Fixed base (for comparison)	0.498	0.496
Flexible-base upper bound	0.537	0.524
Flexible-base best estimate	0.556	0.538
Flexible-base lower bound	0.611	0.578

A.8.9 Check of Base Shear

The seismic response coefficient is recomputed based on the updated dynamic properties using the same approach outlined above. The resulting seismic response coefficients are shown in Table A-27.

Table A-27 Tabulation of Reduced Seismic Response

Model	Reduced C_s Transverse (g)	Reduced C_s Longitudinal (g)
Upper bound springs	0.168	0.168
Best estimate springs	0.166	0.166
Lower bound springs	0.162	0.162

The highest values of the seismic response coefficients computed are 0.168g, just slightly lower than the starting value of 0.169g, indicating that the modified structure produces the same amount of reduction in loads as used in computing the member and foundation sizes. Therefore, this design is internally consistent, although it is not permitted by ASCE/SEI 7, as it includes base slab averaging reductions with the ELF procedure and does not consider the limitation on the amount of design force reduction.

Appendix B
Twelve-Story Building Example

B.1 Overview

This example is based on the structure designed in Chapter 10 of FEMA P-1051 (FEMA, 2016), with deep foundations similar to those illustrated in FEMA P-1051 Section 7.2. This is a 12-story reinforced concrete office building in Antioch, California with some retail shops on the first floor. The building is assigned to Risk Category II with seismic importance factor, I_e = 1.0.

Four variations of structural configuration and boundary conditions are considered in this example, as follows:

- Model 1: Base case building, with basement and fixed base
- Model 2: Base case building, with basement and flexible base
- Model 3: Building modified by removing the basement, fixed base
- Model 4: Building modified by removing the basement, flexible base

The aspects of soil-structure interaction considered in this example include spectral modifications for kinematic SSI (base slab averaging and embedment), adjustments to structural demands due to period elongation and foundation damping, and the impacts of limitations imposed by ASCE/SEI 7-16 provisions, including the following:

- Minimum base shear per ASCE/SEI 7-16 Equations 12.8-5 and 12.8-6
- Consideration of $C_u T_a$ for T and $\tilde{T}$
- Coefficient α that limits reduction in base shear caused by foundation damping
- Analysis procedures permitted to include various aspects of SSI
- Foundation types permitted to use simple damping procedures in ASCE/SEI 7-16 Section 19.3
- Consideration of bounding stiffnesses for foundation/soil system

Example Summary

Building Type: 12-story concrete building with moment frame in one direction and dual system in the other.

Foundation Type: Drilled piles.

SSI Topics Covered:

- Spectral modifications for kinematic interaction, including base slab averaging and embedment effects.
- Adjustments to demands from period elongation and foundation damping.
- Impacts of limitations imposed by ASCE/SEI 7-16 provisions.

B.1.1 Outline of the Example

This example includes the following:

- Section B.2: Site description
- Section B.3: Building description
- Section B.4: Initial design (Model 1)
- Section B.5: Spectral modifications for kinematic SSI
- Section B.6: SSI adjusted structural demands
- Section B.7: Design variations

B.2 Site Description

B.2.1 Geotechnical Properties

Table B-1 outlines the geotechnical characteristics of the example site.

Table B-1 Site Characteristics

Depth	Geotechnical Parameters	Nominal Unit Capacities
0 to 5 ft	**Loose sand/fill** effective unit weight, γ = 110 pcf effective friction angle = 28 deg soil modulus parameter, k = 25 pci low-strain shear wave velocity, v_{so} = 580 ft/s	neglect skin friction neglect end bearing
5 to 30 ft	**Soft clay** effective unit weight, γ = 110 pcf undrained shear strength, s_u = 700 psf soil modulus parameter, k = 25 pci strain at 50% of maximum stress, ε_{50} = 0.01 low-strain shear wave velocity v_{so} = 700 ft/s	skin friction = 0.40 ksf neglect end bearing
30 to 100 ft	**Medium dense sand** effective unit weight, γ = 120 pcf effective friction angle = 36 deg soil modulus parameter, k = 50 pci low-strain shear wave velocity v_{so} = 1,040 ft/s	skin friction = 3.0 ksf end bearing = 100 ksf
Pile cap resistance	300 pcf, ultimate passive pressure	

Using the equations and definitions in ASCE/SEI 7-16 Section 20.4.1, the site is assigned to Site Class D based on $\overline{v}_s$ = 896 ft/s, based on the following calculation:

$$\overline{v}_s = \frac{\sum_{i=1}^{n} d_i}{\sum_{i=1}^{n} \frac{d_i}{v_{si}}} = \frac{5+25+70}{\frac{5}{580}+\frac{25}{700}+\frac{70}{1{,}040}} = 896 \text{ ft/s}$$

B.2.2 Seismic Ground Motion Parameters

For this example site, located at 38.0021°N, 121.7976°W, the mapped ground motion parameters are S_S = 1.537, S_1 = 0.525, and T_L = 8 seconds. Based on ASCE/SEI 7-16 Sections 11.4 and 21.3, the short-period and long-period site coefficients are F_a = 1.0 and F_v = 2.5.

Using the site-specific ground motion procedures of ASCE/SEI 7-16 Chapter 21 (not shown in detail here), the following design acceleration parameters, which satisfy the minima prescribed in Section 21.3, are determined as S_{DS} = 1.0 and S_{D1} = 0.7. For the purpose of this example, the free-field, surface, design response spectrum is taken as the generalized spectral shape consistent with these values. Figure B-1 compares the design spectra computed in accordance with ASCE/SEI 7-16 Section 21.3 to the site-specific, free-field spectrum. It may be seen that the site-specific, free-field spectrum does not fall below the minimum spectrum defined in Section 21.3. The site-specific spectrum is used for all designs in this appendix.

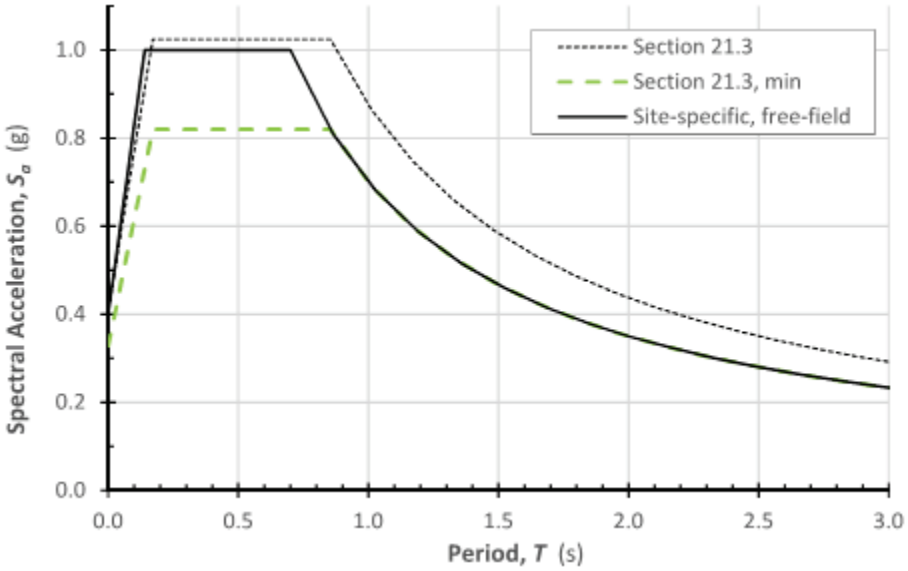

Figure B-1 Design response spectra for the example building.

B.3 Building Description

B.3.1 Framing Systems

Gravity. The basic structural configuration is shown in Figures B-2 and B-3. The building has 12 stories above grade and one basement level. The section of a variation on this building, with no basement, is shown in Figure B-3b. The typical bays are 30 feet long in the north-south (N-S) direction and either 40 or 20 feet long in the east-west (E-W) direction.

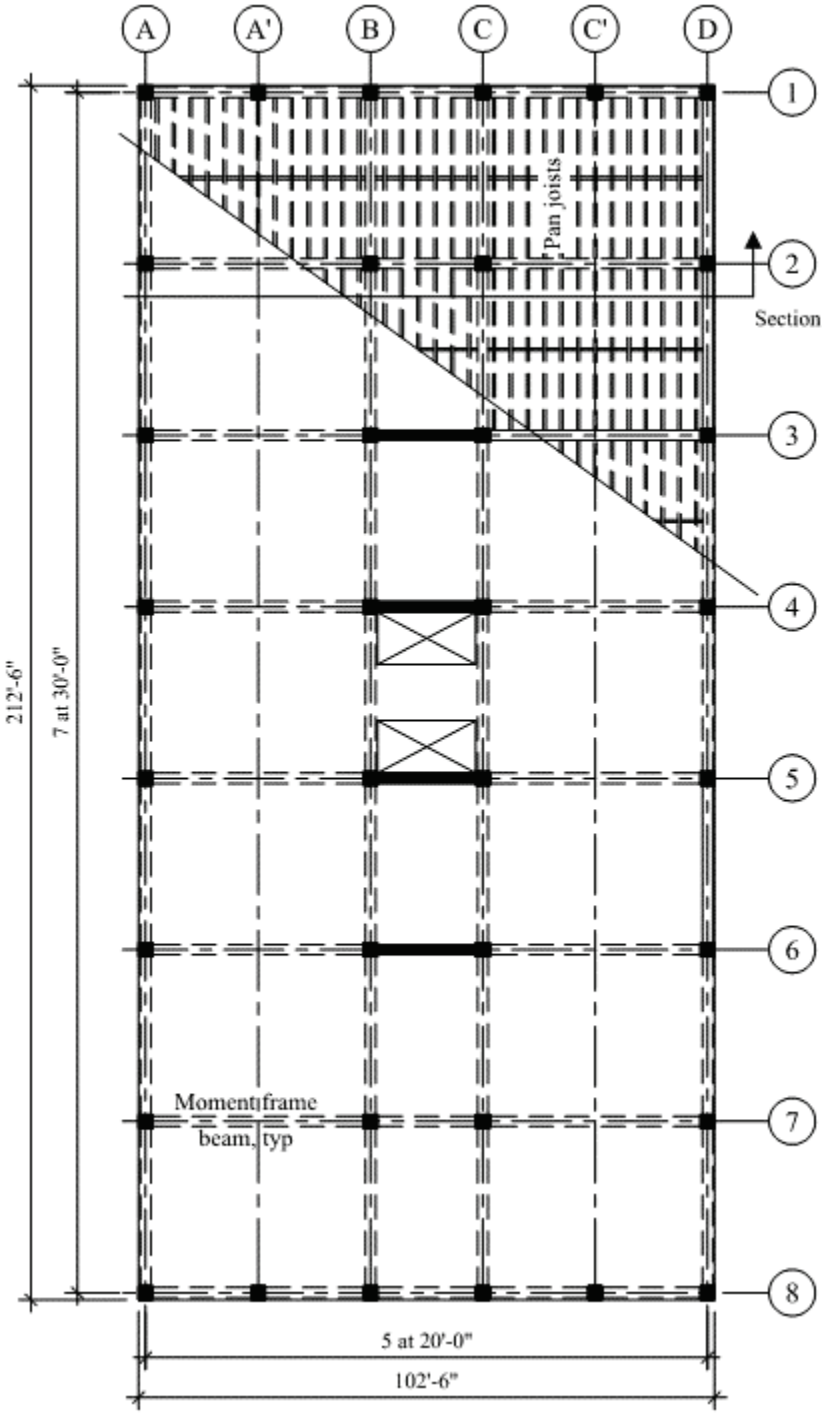

Figure B-2 Typical floor plan of the example building (after FEMA P-1051, 2016).

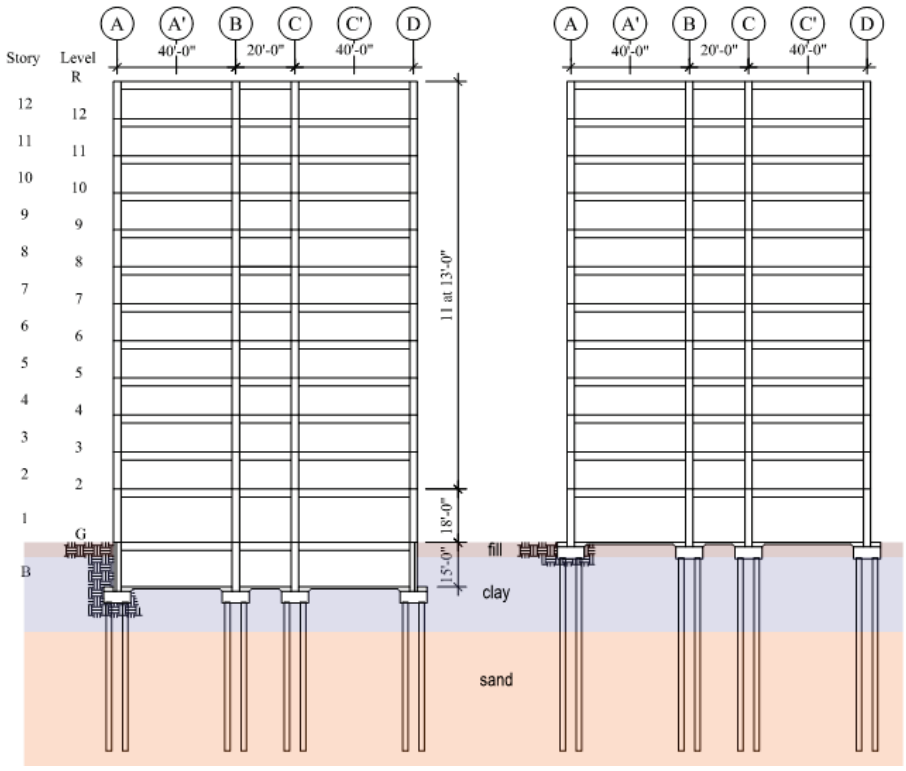

(a) Section for building with basement

(b) Section for building without basement

Figure B-3 Typical sections of the example building (after FEMA P-1051, 2016).

The main gravity framing system consists of seven continuous 30-foot spans of pan joists. These joists are spaced at 36 inches on center and have an average web thickness of 6 inches and a depth below slab of 16 inches. Due to fire code requirements, a 4-inch-thick floor slab is used, giving the joists a total depth of 20 inches. The joists are supported by concrete beams running in the E-W direction. The building is constructed of normalweight concrete.

12-inch-thick concrete walls are located around the entire perimeter of the basement level.

Lateral. The seismic force-resisting system in the N-S direction consists of four 7-bay special moment-resisting frames. In the E-W direction, the seismic force-resisting system is a dual system composed of a combination of moment frames and walls integrated into a moment-resisting frame. Along Grids 1 and 8, the frames have five 20-foot bays. Along Grids 2 and 7, the frames consist of two exterior 40-foot bays and one 20-foot interior bay. At Grids 3, 4, 5, and 6, the interior bay consists of shear walls infilled between the interior columns. The exterior bays of these frames are similar to Grids 2 and 7. Hereafter, frames are referred to by their gridline designation (e.g.,

Frame 1 is located on Grid 1). Table B-2 summarizes the response modification coefficient, R, overstrength factor, Ω_0, and deflection amplification factor, C_d, for the lateral framing system. Figure B-4 shows the analytical model for the base building.

Table B-2 Response Modification Coefficient, Overstrength Factor, and Deflection Amplification Factor for Structural Systems Used

Response Direction	Building Frame Type	R	Ω_0	C_d
N-S	Special moment frame	8	3	5.5
E-W	Dual system incorporating special moment frame and special shear wall	7	2.5	5.5

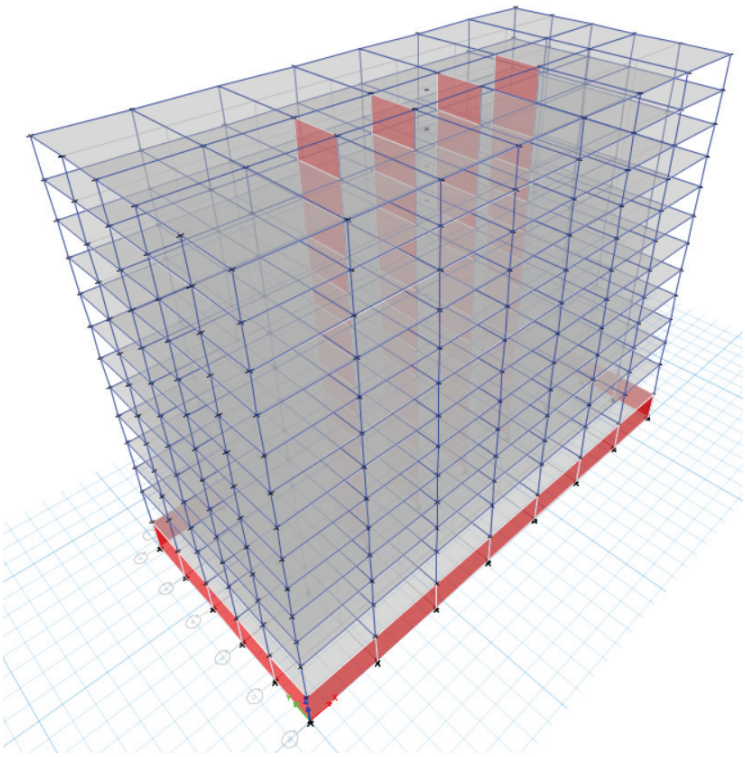

Figure B-4 Analytical model for base case building (Model 1).

Foundation. Figure B-5 shows the foundation plan for this example building. The deep foundations consist of a 4-pile group at each column or shear wall boundary element. ASCE/SEI 7-16 Section 12.13.7.2 requires ties between individual pile groups, which are provided in this example by a system of tie beams; it would also be permitted to design the basement slab to perform that function.

Each pile group consists of four 22-inch diameter drilled shafts, located 5’-6” on center in each direction, extending at least 3 inches into a 9’-2”×9’-2”×4’-

0” deep pile cap, as illustrated in Figure B-6. The top of the pile cap is located 1’-0” below top of slab on grade.

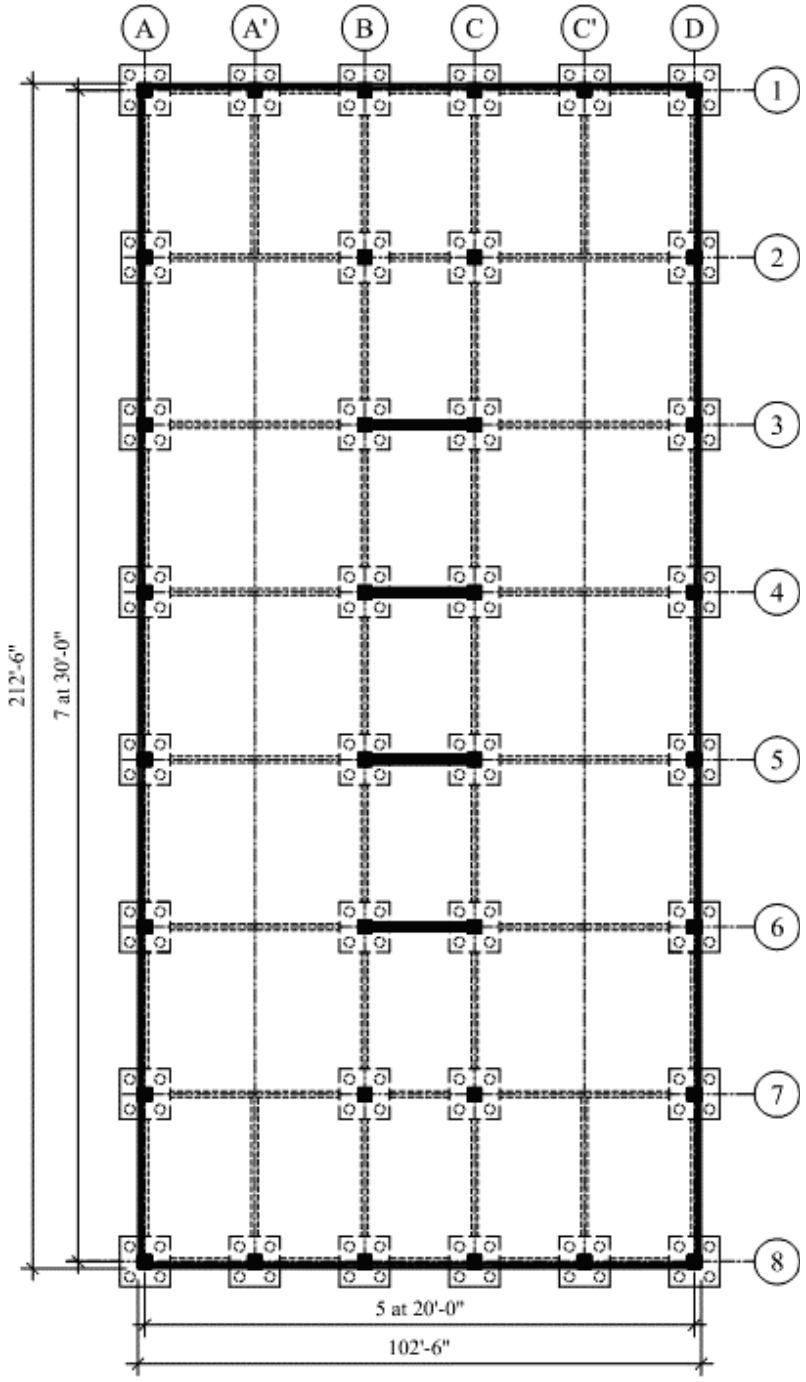

Figure B-5 Foundation plan for the example building.

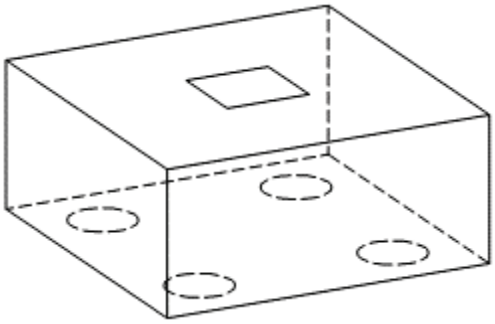

Figure B-6 Arrangement of piles and columns or boundary elements at each pile group (after FEMA P-1051, 2016).

B.3.2 Material Properties and Modeling Criteria

Normalweight concrete of 5,000 psi strength is used everywhere. All reinforcement has a specified yield strength of 60 ksi.

The building is analyzed with a three-dimensional mathematical model using the ETABS software (CSI, 2019). Typical practice is to use a reduced moment of inertia for the beams, columns, and walls based on the expected level of cracking. This example utilizes the following effective moments of inertia, I_{eff}, which are slightly different from those in ACI 318:

- Beams: $I_{eff} = 0.3I_{gross}$
- Columns: $I_{eff} = 0.5I_{gross}$
- Walls: $I_{eff} = 0.5I_{gross}$

The effective stiffness of the moment frame elements is based on the recommendations in NIST GCR 16-917-40 (NIST, 2016) and ASCE/SEI 41-17 Table 10-5 and account for the expected axial loads and reinforcement levels in the members. The value for the structural walls is based on the recommendations in NIST GCR 11-917-11 (NIST, 2011) and ASCE/SEI 41-17 Table 10-5 for cracked concrete structural walls.

The following are other significant aspects of the mathematical model that should be noted:

- The structure is modeled with 12 levels above grade and one level below grade. The perimeter basement walls are modeled as shear panels as are the main structural walls. For the primary analyses, the walls are assumed to be fixed against translation at nodes located at the center of each boundary element at the basement level. Piles, pile caps, and tie-beams are not included in the analytical model. A second series of analyses are performed using foundation springs at the base.

- All floor diaphragms are modeled as infinitely rigid in plane and infinitely flexible out-of-plane, consistent with common practice for a regular-shaped concrete diaphragm.
- Beams, columns, and structural wall boundary members are represented by two-dimensional frame elements. The beams are modeled as T-beams using the effective slab width per ACI 318.
- The structural walls are modeled as a combination of boundary columns and shear panels with composite stiffness.
- Beam-column joints are modeled in accordance with NIST GCR 16-917-40, which references the procedure in ASCE/SEI 41-17. Both the beams and columns are modeled with end offsets based on the geometry, but the beam offset is modeled as 0 percent rigid, while the column offset is modeled as 100 percent rigid. This provides effective stiffness for beam-column joints consistent with the expected behavior of the joint: strong column-weak beam condition.
- P-delta effects are neglected in the analysis for simplicity. This assumption was verified, but it is not shown in this example.
- Although the base of the model is located at the basement level, the seismic base for determination of forces is assumed to be at the first floor, which is at the exterior grade. As a result, Table B-3 neglects the weight at Level 1.

B.3.3 Gravity Loads and Seismic Mass

In addition to the building structural weight, the following superimposed dead loads are assumed:

- Roofing = 10 psf
- Partition = 10 psf
- Ceiling and M/E/P = 10 psf
- Curtain wall cladding = 10 psf (on vertical surface area)

Building mass includes contributions from the various members of the seismic force-resisting system, as sized in the source example in FEMA P-1051. It is assumed that all columns and structural wall boundary elements are 30 inches by 30 inches, beams are 24 inches wide by 32 inches deep (including slab thickness), and the panel of the structural wall is 16 inches thick. It has already been established that pan joists are spaced at 36 inches on center, have an average web thickness of 6 inches, and are 20 inches deep, inclusive of the 4-inch-thick slab.

Based on the above member sizes and superimposed dead load, the individual story weights and masses are listed in Table B-3.

Table B-3 Story Weights and Masses

Level	Weight (kip)	Mass (kip-s^2/inch)
Roof	3,352	8.68
12	3,675	9.52
11	3,675	9.52
10	3,675	9.52
9	3,675	9.52
8	3,675	9.52
7	3,675	9.52
6	3,675	9.52
5	3,675	9.52
4	3,675	9.52
3	3,675	9.52
2	3,817	9.88
Total	43,919	113.75

In the ETABS model, these masses are applied as uniform distributed masses across the extent of the floor diaphragms in order to provide a realistic distribution of mass in the dynamic model. The structural framing is modeled using massless elements since their mass is included with the floor mass.

B.4 Initial Design (Model 1)

B.4.1 Base Shear per Chapter 12 ELF

The seismic base shear for structural design is determined in accordance with ASCE/SEI 7-16 Section 12.8.1, and is taken as the product of the seismic weight, W, and the seismic response coefficient, C_s. That base shear is used directly for the equivalent lateral force (ELF) procedure and for scaling the results of modal response spectrum analysis (MRSA).

ASCE/SEI 7-16 Equations 12.8-2, 12.8-3, and 12.8-4 define seismic response coefficients that correspond to the constant acceleration, constant velocity, and constant displacement portions of the design response spectrum, respectively. ASCE/SEI 7-16 Equations 12.8-5 and 12.8-6 set forth code minima that are independent of both the dynamic characteristics of the system and the basic spectral shape.

The SSI procedures set forth in ASCE/SEI 7-16 Chapter 19 are intended to modify the shape of the design spectrum (due to base slab averaging and embedment) or better reflect the dynamic characteristics of the system (due to period elongation and foundation damping). Although the adjustment of structural demands to reflect SSI in accordance with ASCE/SEI 7-16 Section 19.2 is expressed as modifications to the base shear for the fixed-base structure computed in accordance with ASCE/SEI 7-16 Section 12.8.1, it is not intended that SSI modify the code minima reflected in ASCE/SEI 7-16 Equations 12.8-5 and 12.8-6.

Base Shear in the N-S Direction. The fundamental period in the N-S direction from modal analysis is 2.18 seconds.

The approximate period is computed using ASCE/SEI 7-16 Equation 12.8-7, with values of C_t and x taken from ASCE/SEI 7-16 Table 12.8-2 for concrete moment-resisting frames resisting 100% of the required seismic force, as:

$$T_a = C_t h_n^x = 0.016(161)^{0.9} = 1.55 \text{ sec}$$

The upper limit period is computed in accordance with ASCE/SEI 7-16 Section 12.8.2 as:

$$C_u T_a = 1.4 \times 1.55 = 2.17 \text{ sec}$$

Since this period is shorter than that computed in the analysis, the upper limit period is used in subsequent calculations.

The seismic response coefficient (for the constant acceleration portion of the design spectrum) is computed using ASCE/SEI 7-16 Equation 12.8-2 as follows:

$$C_s = \frac{S_{DS}}{\left(\frac{R}{I_e}\right)} = \frac{1.0}{\left(\frac{8}{1.0}\right)} = 0.125$$

However, it need not be taken greater than the value computed using ASCE/SEI 7-16 Equation 12.8-3 or 12.8-4, as applicable. Since $T = 2.17$ seconds $< T_L$:

$$C_s = \frac{S_{D1}}{T\left(\frac{R}{I_e}\right)} = \frac{0.7}{2.17\left(\frac{8}{1.0}\right)} = 0.040$$

The minimum seismic response coefficient is computed using ASCE/SEI 7-16 Equation 12.8-5 as follows:

$$C_s = 0.044 S_{DS} I_e = 0.044(1.0)(1.0) = 0.044$$

This minimum controls, so the seismic base shear in the N-S direction is computed using ASCE/SEI 7-16 Equation 12.8-1 as follows:

$$V_{N-S} = C_s W = 0.044(43{,}919) = 1{,}932 \text{ kip}$$

Base Shear in the E-W Direction. The fundamental period in the E-W direction from modal analysis is 1.49 seconds.

The approximate period is computed using ASCE/SEI 7-16 Equation 12.8-7, with values of C_t and x taken from ASCE/SEI 7-16 Table 12.8-2 for "all other structural systems" since the concrete moment-resisting frames resist less than 100% of the required seismic force in this direction, as:

$$T_a = C_t h_n^x = 0.020(161)^{0.75} = 0.90 \text{ sec}$$

The upper limit period is computed in accordance with ASCE/SEI 7-16 Section 12.8.2 as:

$$C_u T_a = 1.4 \times 0.090 = 1.27 \text{ sec}$$

Since this period is shorter than that computed in the analysis, the upper limit period is used in subsequent calculations.

The seismic response coefficient (for the constant acceleration portion of the design spectrum) is computed using ASCE/SEI 7-16 Equation 12.8-2 as follows:

$$C_s = \frac{S_{DS}}{\left(\frac{R}{I_e}\right)} = \frac{1.0}{\left(\frac{7}{1.0}\right)} = 0.143$$

However, it need not be taken greater than the value computed using ASCE/SEI 7-16 Equation 12.8-3 or 12.8-4, as applicable. Since T = 1.27 seconds < T_L:

$$C_s = \frac{S_{D1}}{T\left(\frac{R}{I_e}\right)} = \frac{0.7}{1.27\left(\frac{7}{1.0}\right)} = 0.079$$

The minimum seismic response coefficient is computed using ASCE/SEI 7-16 Equation 12.8-5 as follows:

$$C_s = 0.044 S_{DS} I_e = 0.044(1.0)(1.0) = 0.044$$

The seismic response coefficient (for the constant velocity portion of the design spectrum) from ASCE/SEI 7-16 Equation 12.8-3 controls, so the

seismic base shear in the E-W direction is computed using ASCE/SEI 7-16 Equation 12.8-1 as follows:

$$V_{E-W} = C_s W = 0.079(43{,}919) = 3{,}470 \text{ kip}$$

B.4.2 Fixed-Base Modal Analysis

Where ELF is used, the base shears computed above would be distributed vertically in accordance with ASCE/SEI 7-16 Section 12.8.3. Where MRSA is used, these base shears are used for scaling design forces in accordance with ASCE/SEI 7-16 Section 12.9.1.4.1. That section requires scaling MRSA results to 100% of the ELF base shear; earlier editions of ASCE/SEI 7-16 permitted scaling to 85% of the ELF base shear.

Although the base shear is identical for both methods, MRSA typically results in smaller overturning moments and design story drifts. The following sections compare ELF and MRSA story shears, story moments, and story drifts.

B.4.3 Story Shears and Moments

Figure B-7 compares story shears and moments for the base building (Model 1) analyzed using ELF and MRSA. The vertical force distribution prescribed for the ELF procedure tends to produce story shears at mid-height and story moments at the base that are slightly larger than those computed using MRSA.

B.4.4 Story Drifts

For drift checks, the minimum seismic response coefficient computed using ASCE/SEI 7-16 Equation 12.8-5 does not apply, and periods are not limited to $C_u T_a$. Design story drifts are taken as the drift from the elastic analysis multiplied by C_d. In the N-S (moment frame) direction, ELF produces drifts at mid-height that are slightly larger than those from MRSA. In the E-W (dual system) direction, ELF drifts are nearly 50% larger than those from MRSA. Proportioning for strength demands controls the design in both directions, so drifts are well below the drift limit.

B.4.5 Foundation Design

For typical deep foundation systems resistance to lateral loads is provided by both piles and pile cap. Although the behavior of foundation and superstructure are closely related, they typically are modeled independently. Earthquake loads are applied to a model of the superstructure, which is assumed to have fixed or spring supports. Then the support reactions are seen as demands on the foundation system. A similar substructure technique is usually applied to the foundation system itself, whereby the behavior of pile cap and piles are considered separately.

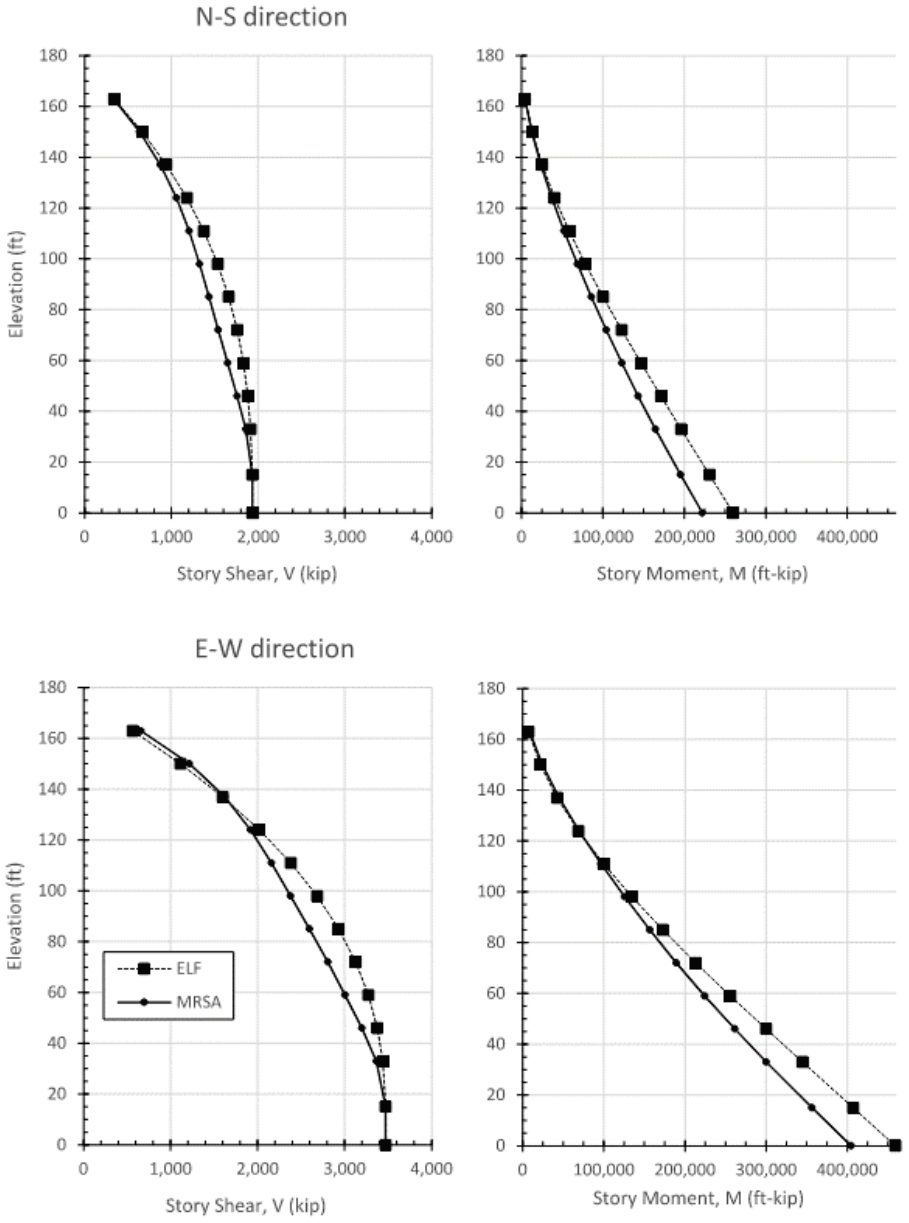

Figure B-7 Story shears and moments for Model 1, ELF vs. MRSA.

The response of individual piles to lateral loads is highly nonlinear. It has become increasingly common to consider that nonlinearity directly. Based on extensive testing of full-scale specimens and small-scale models for a wide variety of soil conditions, researchers have developed empirical relationships for the nonlinear *p-y* response of piles that are suitable for use in design. The *p-y* response is sensitive to pile size; soil type and properties; and, in the case of sands, vertical stress, which increases with depth. Pile response to lateral loads is usually computed using computer programs such as LPile (ENSOFT, 2018). For this example, LPile is used to analyze 22-inch diameter piles for the soil layering shown in Table B-1.

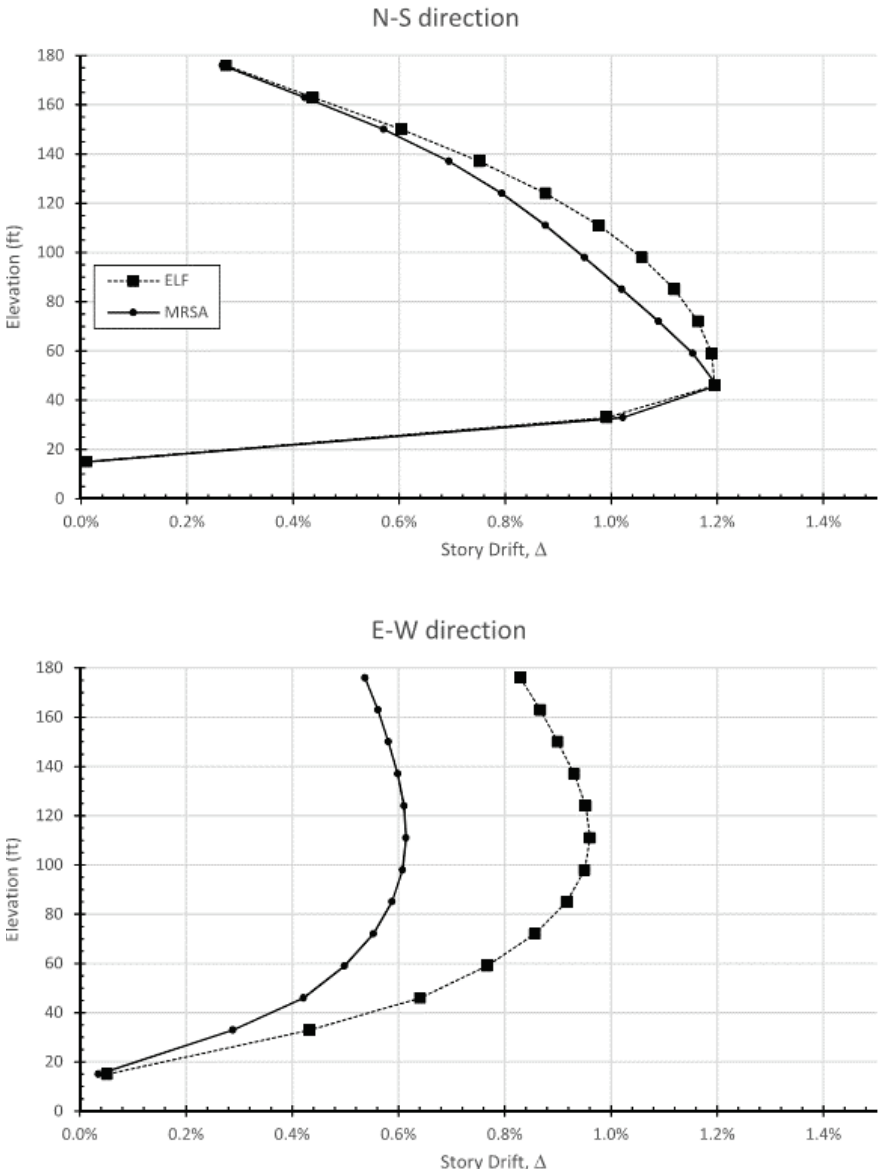

Figure B-8 Story drifts for Model 1, ELF vs. MRSA.

Pile caps contribute to the lateral resistance of a pile group in two important ways: directly as a result of passive pressure on the face of the cap that is being pushed into the soil mass and indirectly by producing a fixed head condition for the piles, which can significantly reduce displacements for a given applied lateral load, thus improving economy of the design. Similar to the *p-y* response of piles, the passive pressure resistance of the cap is nonlinear.

The response of a group of piles to lateral loading will differ from that of a single pile due to pile-soil-pile interaction. In this example *p*-multipliers of 0.5 are used for group effects on these shafts spaced 3 diameters center to center.

Figure B-9 shows the shear, moment, and displacement versus depth response for an applied lateral load of 32 kip.

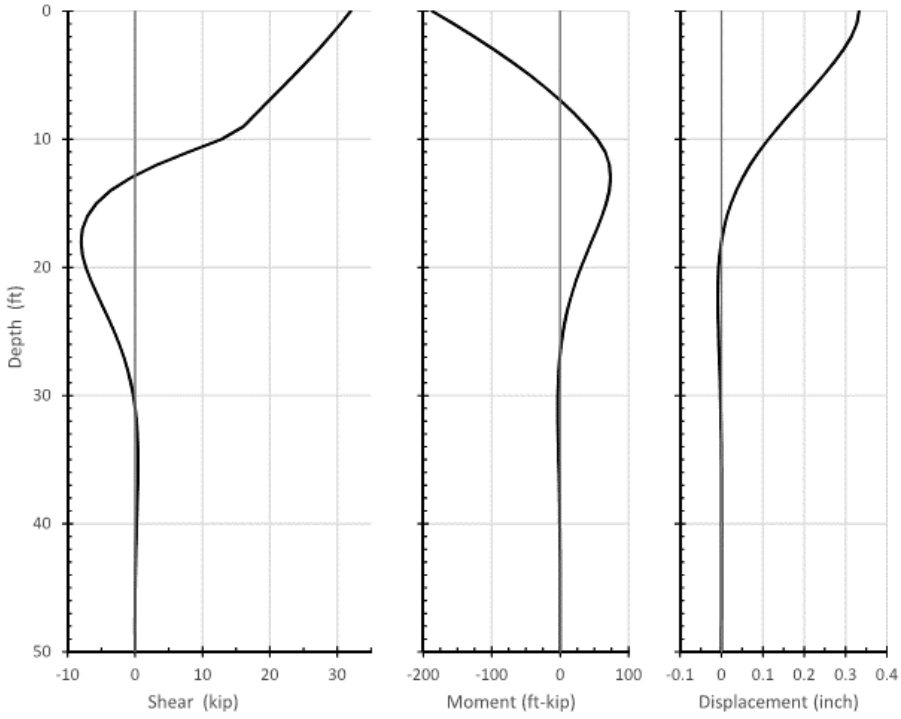

Figure B-9 Lateral pile analysis results vs. depth (applied lateral load is 32 kip).

Group stiffness includes four drilled shafts plus passive pressure on the leading face. Passive pressure mobilization is computed in accordance with ASCE/SEI 41-17 Figure 8-6, which can also be computed using the following expression, which is fitted to the curve in the figure:

$$\frac{P}{P_{ult}} = 0.15 + 2.88\left(\frac{\delta}{H}\right)^{0.43}$$

As a point of reference, for a lateral displacement of 0.33 inches the total lateral load is 144 kip, including 32 kip in each of four drilled shafts and 16 kip of passive pressure resistance. Figure B-10 shows the total lateral load versus head displacement for eight points in a range of loads. P_{ult} is computed considering that the top of cap is 1 ft below the top of the slab on grade. Although the response is slightly nonlinear, a straight line provides a reasonable fit that can be used to estimate lateral stiffness. In this case the central value can be estimated as 425 kip/inch, with reasonable lower and upper bounds of 300 kip/inch and 600 kip/inch, based on field measurements of dynamic soil properties. These lower- and upper-bound variations, which are required by ASCE/SEI 7-16 Section 12.13.3, are discussed in more detail in Section B.7.3.

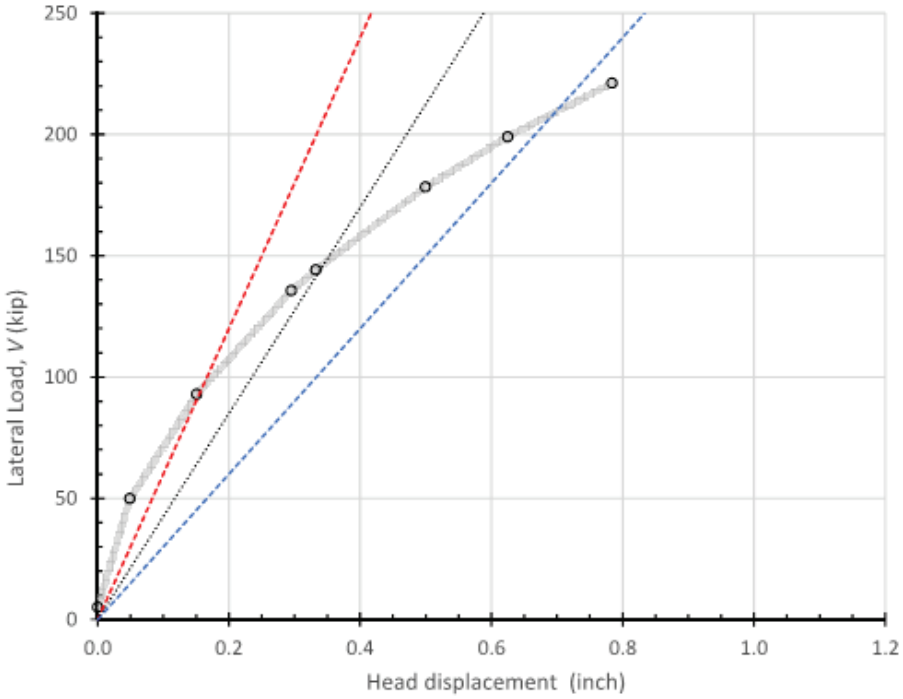

Figure B-10 Pile group lateral stiffness for Models 1 and 2.

B.5 Spectral Modifications for Kinematic SSI

The average effective shear wave velocity used in SSI calculations is based on a reduction of the average low strain shear wave velocity due to seismically induced demands. Using ASCE/SEI 7-16 Table 19.3-1 for Site Class D with $S_{DS}/2.5 = 1.0/2.5 = 0.4$, the effective shear wave velocity ratio, $v_s/v_{so} = 0.71$.

B.5.1 Base Slab Averaging

Spectral modifications due to base slab averaging depend on the area of interconnected foundation. For this example,

L = half the larger dimension of the base of the structure
= 212.5 ft / 2 = 106.25 ft

B = half the smaller dimension of the base of the structure
= 102.5 ft / 2 = 51.25 ft

A_{base} = the area of the base of the structure
= 2L×2B = 202.5 × 102.5 = 21,781 ft^2

Using ASCE/SEI 7-16 Equation 19.4-4, $b_e = \sqrt{A_{base}} \le 260 \text{ ft} = 147.6 \text{ ft}$.

The v_s limits in ASCE/SEI 7-16 Section 19.4.1 should be based on the average effective shear wave velocity in Section 19.3 computed over a depth

of B below the base of the structure. Using the values in Table B-1, the average low strain shear wave velocity over a depth of B = 51.25 ft below the base of the structure, v_{so}, is 791 ft/s, which is computed using ASCE/SEI 7-16 Equation 20.4-1 as follows:

$$v_{so} = \frac{\sum_{i=1}^{n} d_i}{\sum_{i=1}^{n} \frac{d_i}{v_{si}}} = \frac{5 + 25 + 21.25}{\frac{5}{580} + \frac{25}{700} + \frac{21.25}{1{,}040}} = 791 \text{ ft/s}$$

The average effective shear wave velocity, $v_s = 0.71 \times 791$ ft/s = 562 ft/s. This value is less than the lower limit shown in the inequality immediately after ASCE/SEI 7-16 Equation 19.4-4 (650 ft/s). Although that inequality indicates the range of effective shear wave velocity considered in the source research on base slab averaging, since v_s is not used in computing base slab averaging there is no consequence for this structure that otherwise satisfies the charging requirements of Section 19.4.1.

ASCE/SEI 7-16 Equations 19.4-1 through 19.4-3 are used to compute the period-dependent modification factor RRS_{bsa}. The period used in this calculation may not be taken less than 0.20 s per ASCE/SEI 7-16 Section 19.4.1, which produces a floor on the spectral reduction. Chapter 4 of this *Guide* illustrates the process of computing modification factors for base slab averaging.

B.5.2 Embedment

Spectral modifications due to embedment depend on the depth of embedment (subject to a maximum of 20 ft per ASCE/SEI 7-16 Section 19.4.2) and the average effective shear wave velocity over the embedment depth (which is the depth of basement for this condition). For this example,

e = foundation embedment depth = 15 ft

Using the values in Table B-1, the average low strain shear wave velocity over the embedment depth of the foundation (e = 15 ft), v_{so}, is 655 ft/s, which is computed using ASCE/SEI 7-16 Equation 20.4-1 as follows:

$$v_{so} = \frac{\sum_{i=1}^{n} d_i}{\sum_{i=1}^{n} \frac{d_i}{v_{si}}} = \frac{5 + 10}{\frac{5}{580} + \frac{10}{700}} = 655 \text{ ft/s}$$

The average effective shear wave velocity, $v_s = 0.71 \times 655$ ft/s = 465 ft/s. This value is less than the lower limit of 650 ft/s, so a value of v_s = 650 ft/ is used in computing the modification factor for embedment.

ASCE/SEI 7-16 Equation 19.4-5 is used to compute the period-dependent modification factor RRS_e. The period used in this calculation may not be taken less than 0.20 s, which produces a floor on the spectral reduction. Chapter 5 of this *Guide* illustrates the process of computing modification factors for embedment.

Figure B-11 shows the kinematic SSI spectral modification factors RRS_{bsa} and RRS_e as well as the free-field and modified design response spectra. As expected kinematic SSI has substantial effects only in the short period range.

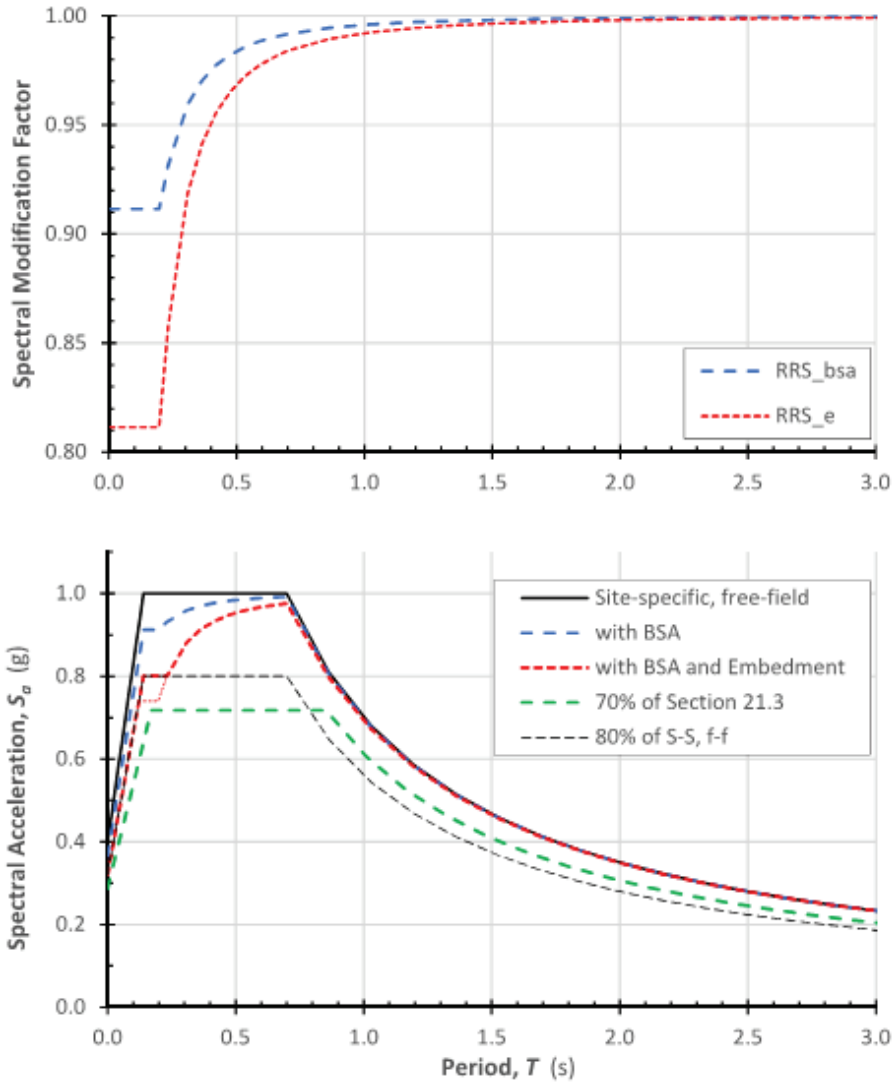

Figure B-11 Kinematic SSI spectral modification factors and design response spectra for the example building.

According to ASCE/SEI 7-16 Section 19.2.3 Item 3, the site-specific response spectrum modified for kinematic SSI cannot be taken less than 80% of the site-specific free-field response spectrum. Where the product of RRS_{bsa} and RRS_e is less than 0.8 (periods between 0 and 0.23 s), this limit

controls. Although ASCE/SEI 7-16 Section 19.4 specifies that the product of RRS_{bsa} and RRS_e not be taken less than 0.7, Section 19.2.3 Item 3 (which limits that product to 0.8) always controls. ASCE/SEI 7-16 Section 19.2.3 Item 4 requires that the site-specific response spectrum modified for kinematic interaction not be taken less than 70% of the response spectrum computed in accordance with ASCE/SEI 7-16 Chapter 11 (using S_{DS} = 1.025 and S_{D1} = 0.875 per ASCE/SEI 7-16 Section 21.3, for the mapped values and tabulated site response factors in this case). Figure B-11b shows this limit, confirming that the 70% criterion is satisfied.

Although the process illustrated above results in design spectra modified for kinematic SSI, those spectra may not be used for design using the ELF procedure, MRSA, or linear response history analysis. ASCE/SEI 7-16 Section 19.4 clearly limits use of the design spectra modified for kinematic SSI to nonlinear response history analysis, where they may serve as target spectra for ground motion selection and scaling.

B.6 SSI Adjusted Structural Demands

B.6.1 Period Elongation Due to Flexible Base

Since spectral acceleration generally reduces at longer periods (particularly in the constant velocity and constant displacement portions of the spectrum), accounting for period elongation due to foundation flexibility can reduce seismic design loads. On the other hand, spectral displacements increase with increasing period (in the constant acceleration and constant velocity portions of the spectrum). Therefore, ASCE/SEI 7-16 Section 19.1.1 requires that the analytical model directly incorporate horizontal, vertical, and rotational foundation, and soil flexibility where soil-structure interaction effects are considered.

In recognition of more detailed modeling, ASCE/SEI 7-16 Section 19.1.3 indicates that the upper bound limitation of C_uT_a on the fundamental period does not apply to T or $\tilde{T}$ for the flexible base condition. The corresponding modeling direction provided in ASCE/SEI 7-16 Section 12.13.3 does not address whether the C_uT_a limitation is lifted where that section is applied. However, since it relies on and is consistent with Chapter 19 for various parameters and procedures, the limitation is interpreted to not apply.

Section B.4.5 illustrates the estimation of lateral stiffness for the pile groups typical of this example. Similarly, vertical stiffness can be computed considering the springs-in-series stiffness corresponding to axial shortening of the drilled shafts and the displacement required to mobilize expected skin friction and end bearing capacity. For the typical pile group in this example

(with 50-ft-long piles), lower-bound, best estimate, and upper-bound pile group stiffnesses are estimated by the geotechnical consultant, based on field measurements of dynamic soil properties, as 2,00 kip/inch, 3,000 kip/inch, and 3,800 kip/inch. If lower and upper bounds are established without field measurements, ASCE/SEI 7-16 Section 12.13.3 requires a 50% decrease and increase in stiffness. Figure B-12 shows Model 2, which is a refinement of Model 1 to include lateral and vertical springs at each pile group.

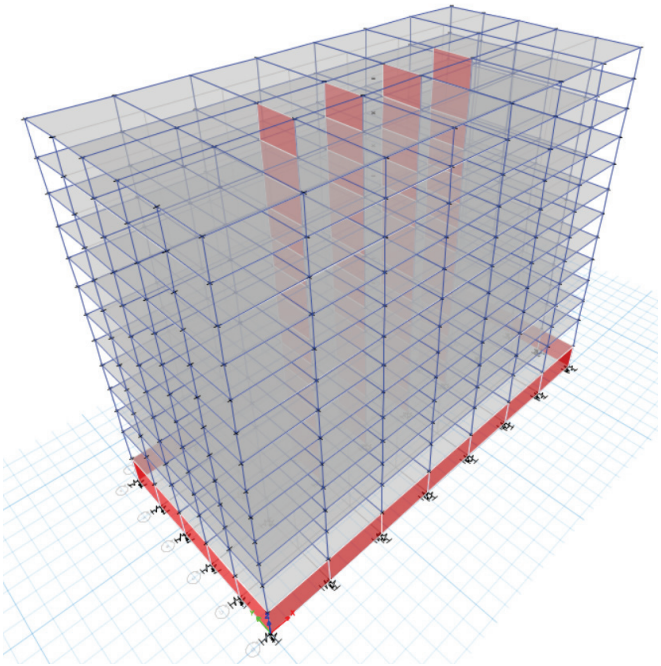

Figure B-12 Analytical model for the example building, with spring supports (Model 2).

Table B-4 compares the fundamental periods from the fixed-base and flexible-base models, T and $\tilde{T}$, respectively and tabulates $\tilde{T}/T$, which is used in subsequent calculations.

Table B-4 Fundamental Periods for Model 1 (Fixed-Base) and Model 2 (Flexible-Base)

Response Direction	T	$\tilde{T}$	$\tilde{T}/T$
N-S	2.177s	2.259s	1.038
E-W	1.491s	1.765s	1.184

B.6.2 Foundation Damping

Once the period elongation effect has been quantified, foundation damping effects can be computed in accordance with ASCE/SEI 7-16 Section 19.3. Item 2 in ASCE/SEI 7-16 Section 19.3.1 indicates that the simple procedures of this section are not permitted to be used where a foundation system

includes deep foundations. Instead, the section would require "direct incorporation of soil hysteretic damping and radiation damping in the mathematical model of the structure." This interpretation is borne out by the Commentary in Section C19.3 of ASCE/SEI 7-16, which indicates, "The provisions in this section provide simplified ways to approximate these effects. However, they are complex phenomena and there are considerably more detailed methods to predict their effects on structures. … The equations in Sections 19.3.3 and 19.3.4 are for shallow foundations. This is not to say that radiation damping does not occur with deep (pile or caisson) foundation systems, but the phenomenon is more complex. Soil layering and group effects are important, and there are the issues of the possible contributions of the bottom structural slab and pile caps. Because the provisions are based on the impedance produced by a rigid plate in soil, these items cannot be easily taken into account. Therefore, more detailed modeling of the soil and the embedded foundations is required to determine the foundation impedances. The provisions permit such modeling but do not provide specific guidance for it. Guidance can be found for example in NIST GCR 12-917-21 [NIST 2012a] and its references." However, for the purposes of this example, calculations are performed using Section 19.3.1. The calculations are presented in the required order of computation, which is the opposite of the order of presentation in ASCE/SEI 7-16.

Table B-4 shows the period lengthening ratio, $\tilde{T}/T$. Since reductions are more pronounced for larger values of $\tilde{T}/T$, the E-W direction is illustrated in the following calculations.

Next, the soil hysteretic damping ratio, β_s in determined. Using ASCE/SEI 7-16 Table 19.3-3 for Site Class D with $S_{DS}/2.5 = 0.4$, $\beta_s = 0.07$.

Since this section does not provide a method to compute radiation damping effects for deep foundations, β_{rd} is conservatively taken as 0.

The foundation damping ratio, β_f, is computed using ASCE/SEI 7-16 Equation 19.3-3.

$$\beta_f = \left[\frac{\left(\tilde{T}/T\right)^2 - 1}{\left(\tilde{T}/T\right)^2}\right]\beta_s + \beta_{rd} = \left[\frac{(1.184)^2 - 1}{(1.184)^2}\right](0.07) + 0.0 = 0.020$$

As permitted in the notes following ASCE/SEI 7-16 Equation 19.3-2, the expected ductility demand, μ, is computed based on the values of R and Ω_0 provided in ASCE/SEI 7-16 Table 12.2-1.

$$\mu = R/\Omega_0 = 7/2.5 = 2.8$$

The effective period lengthening ratio is computed using ASCE/SEI 7-16 Equation 19.3-2.

$$\left(\frac{\tilde{T}}{T}\right)_{eff} = \left\{1+\frac{1}{\mu}\left[\left(\frac{\tilde{T}}{T}\right)^2 - 1\right]\right\}^{0.5} = \left\{1+\frac{1}{2.8}\left[(1.184)^2 - 1\right]\right\}^{0.5} = 1.069$$

As permitted in the notes following ASCE/SEI 7-16 Equation 19.3-1, the effective viscous damping ratio of the structure, β, is taken as 0.05.

The effective damping ratio of the soil-structure system is computed using ASCE/SEI 7-16 Equation 19.3-1.

$$\beta_0 = \beta_f + \frac{\beta}{\left(\tilde{T}/T\right)^2_{eff}} = 0.020 + \frac{0.05}{(1.069)^2} = 0.064 < 0.20$$

B.6.3 ELF Base Shear Adjusted for SSI

Having quantified the period elongation effect and the effective damping ratio of the soil-structure system, the reduced ELF base shear is computed in accordance with ASCE/SEI 7-16 Section 19.2.1.

The adjustment factor for damping ratios other than 0.05 is computed using ASCE/SEI 7-16 Equation 19.2-4.

$$B_{SSI} = 4\Big/\left[5.6 - \ln\left(100\beta_0\right)\right] = 4\Big/\left[5.6 - \ln\left(100(0.064)\right)\right] = 1.067$$

The seismic response coefficient is computed including soil flexibility, $\tilde{C}_s$, using the equations in ASCE/SEI 7-16 Section 12.8.1 but substituting $\tilde{T}$ for T. With $\tilde{T} = 1.765$ seconds per Table B-4, the controlling value, using ASCE/SEI 7-16 Equation 12.8-3, is $\tilde{C}_s = 0.057$, calculated as follows:

$$\tilde{C}_s = \frac{S_{D1}}{\tilde{T}\left(\frac{R}{I_e}\right)} = \frac{0.70}{1.765\left(\frac{7}{1.0}\right)} = 0.057$$

The base shear adjustment, ΔV, is computed using ASCE/SEI 7-16 Equation 19.2-2.

$$\Delta V = \left(C_s - \frac{\tilde{C}_s}{B_{SSI}}\right)\overline{W} = \left(0.079 - \frac{0.057}{1.067}\right)43{,}919 = 1{,}123 \text{ kip}$$

This would result in a 32% reduction of the fixed-base base shear from 3,470 kip to 2,347 kip. It is worth noting that 966 kip of this reduction is due to period elongation (taking B_{SSI} = 1.0) and 157 kip is due to the slight increase in damping.

The limitation on base shear reduction quantified by the α factor computed in accordance with ASCE/SEI 7-16 Equation 19.2-3 is checked. For this system with $R = 7$, so $\alpha = 0.9$.

The final base shear adjusted for SSI is computed in accordance with ASCE/SEI 7-16 Equation 19.2-1.

$$\tilde{V} = V - \Delta V \geq \alpha V$$

$$\tilde{V} = V - \Delta V = 3{,}470 - 1{,}123 = 2{,}347$$
$$\geq \alpha V = 0.9(3{,}470) = 3{,}123 \text{ kip} \leftarrow \text{controls}$$

The final design base shear computed in accordance with ASCE/SEI 7-16 Chapter 19 reflects only a 10% reduction from the fixed-base base shear. Both the text and commentary indicate that the α limitation computed in accordance with ASCE/SEI 7-16 Equation 19.2-3 reflects concern that damping caused by structural yielding could make foundation damping less effective. However, in this example, most of the computed reduction is due to period elongation, so the validity of that concern is questionable.

By comparison, analysis that includes foundation load-deformation characteristics in accordance with ASCE/SEI 7-16 Section 12.13.3 would be permitted to realize all of the period elongation effect. (Sensitivity to the required consideration of lower-bound and upper-bound foundation stiffness is discussed further in Section B.7.3.) Table B-5 compares the design base shear from the fixed-base condition to that from the flexible-base condition determined in accordance with ASCE/SEI 7-16 Chapter 19 or Section 12.13.3. Response in the N-S direction is controlled by minimum base shear in ASCE/SEI 7-16 Equation 12.8-5, which is independent of period and damping, so no reduction due to SSI can be realized.

Table B-5 Design Base Shear for Model 1 (Fixed-Base) and Model 2 (Flexible-Base), Using Best-Estimate Springs

Response Direction	Model 1 Fixed-base	Model 2 Flexible-base, ASCE/SEI 7-16 Chapter 19	Model 2 Flexible-base, ASCE/SEI 7-16 Section 12.13.3
N-S	1,932 kip	1,932 kip	1,932 kip
E-W	3,470 kip	3,123 kip	2,488 kip

B.6.4 Story Shears, Moments, and Drifts

Figure B-13 compares the story shears and moments for Model 1 (fixed-base) and Model 2 (flexible-base), where the flexible base model can satisfy either the limitations in ASCE/SEI 7-16 Chapter 12 or in Chapter 19. These results are from MRSA using the site-specific free-field spectrum, since

ASCE/SEI 7-16 Section 19.4 does not permit modification of the response spectrum for kinematic SSI effects for ELF or MRSA. As discussed above, no reductions due to SSI may be realized in the N-S direction. In the E-W direction the process in ASCE/SEI 7-16 Chapter 12 results in base shear and base overturning moment that are 28% and 31% lower, respectively, than for Model 1; the reductions using the Chapter 19 process are only 10% and 13%, respectively.

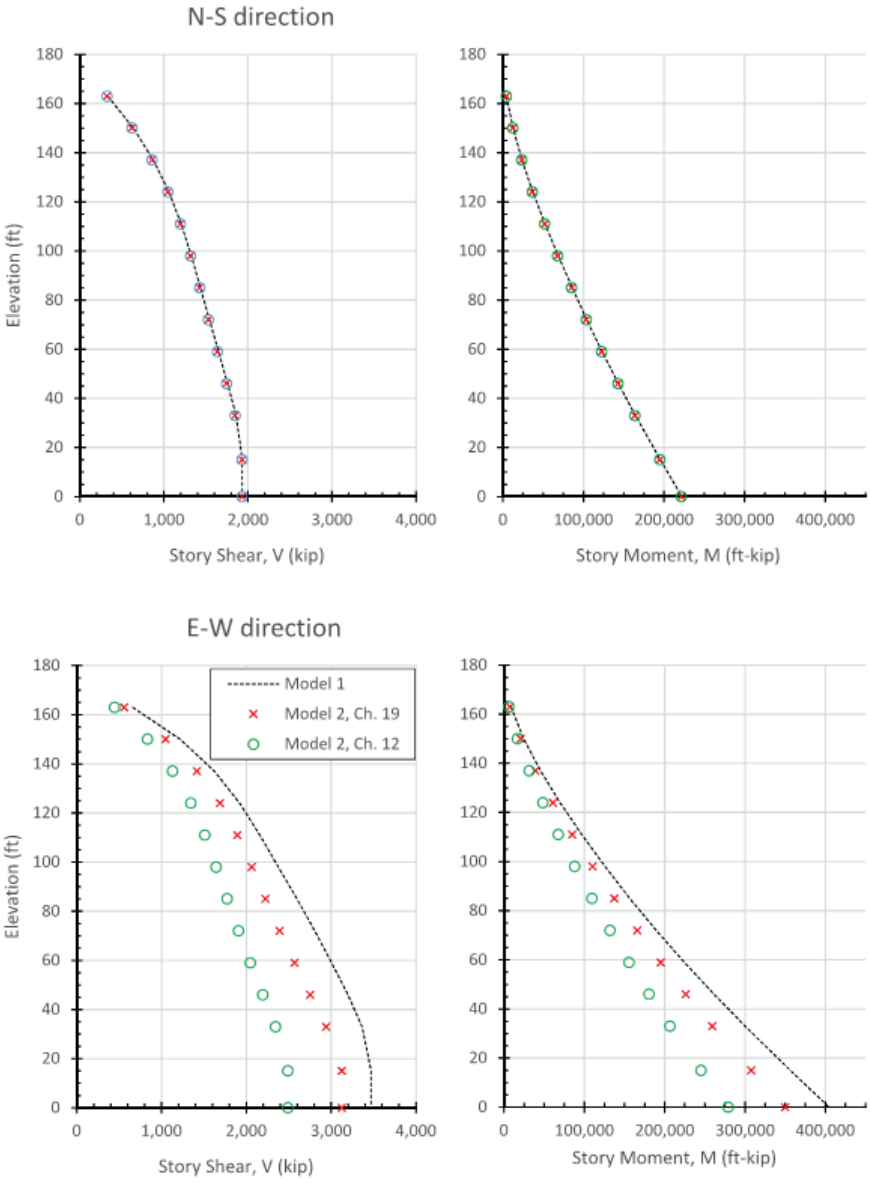

Figure B-13 Story shears and moments for Models 1 and 2.

Figure B-14 shows story drifts for Models 1 and 2, which are computed from MRSA using the site-specific free-field spectrum. Since the value of C_s used in design is not controlled by ASCE/SEI 7-16 Equation 12.8-6, drifts are not subject to scaling, so the base shear limitations defined in Section 19.2.1 do

not apply to drift calculations. Although drifts are not subject to scaling, the drifts for Model 2 still differ slightly depending on whether ASCE/SEI 7-16 Chapter 12 or Chapter 19 procedures are used since Section 19.2.2.2 allows the site-specific spectrum to be adjusted for the slightly beneficial effect of increased damping. Although the design forces for Model 2 are less than those for Model 1 in the E-W direction, story drifts are greater. This is due to period elongation and base rotation for the shear walls. It is possible for inclusion of SSI to increase drifts enough that the design must be revised to satisfy drift limits.

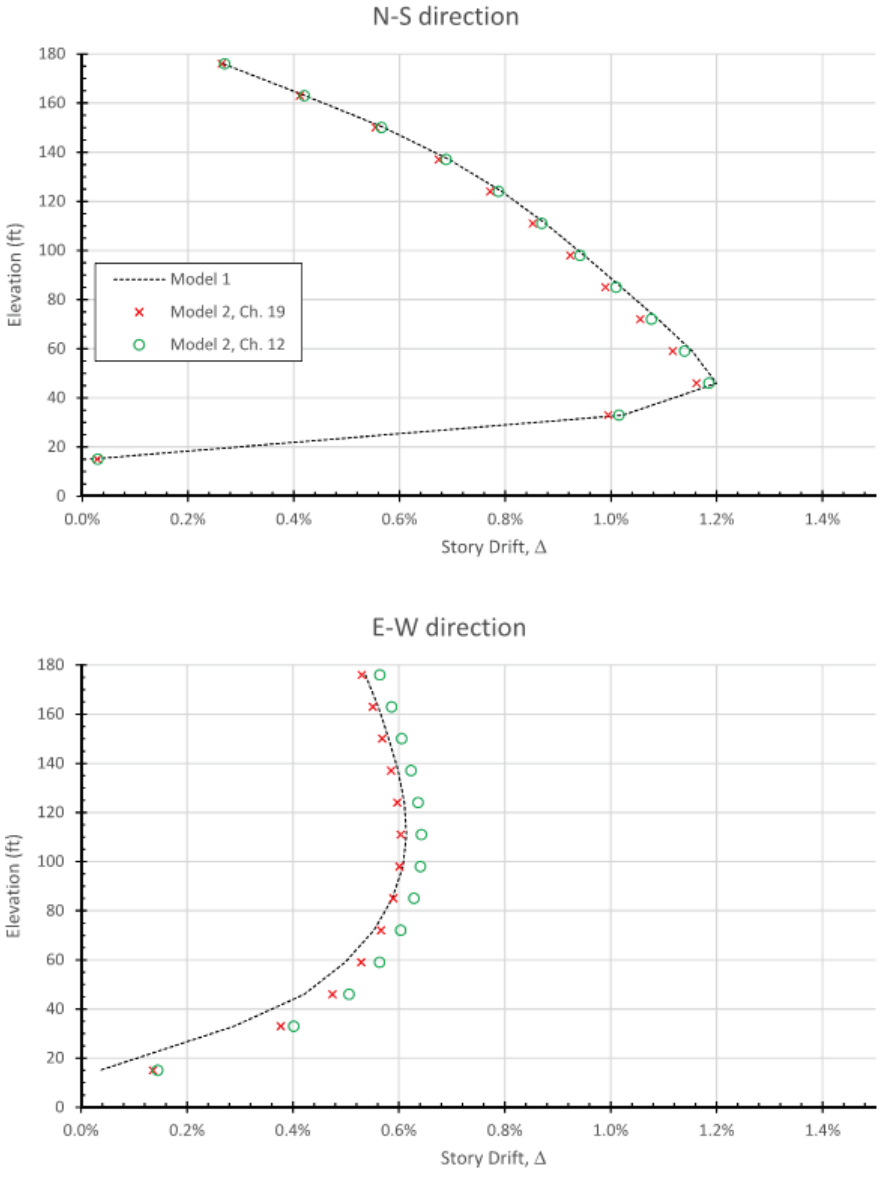

Figure B-14 Story drifts for Models 1 and 2.

B.7 Design Variations

B.7.1 Building Without Basement, Fixed Base (Model 3)

To investigate further the sensitivity of the design seismic demands, the base building is reanalyzed with the basement removed and assuming a fixed base condition (Model 3). Figure B-15 shows this model.

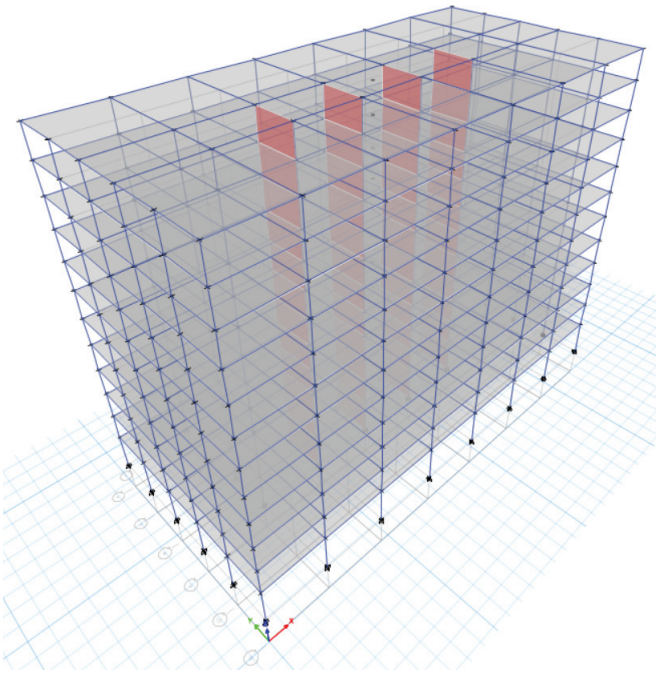

Figure B-15 Analytical model of the example building, with basement removed and fixed base (Model 3).

Because the flexibility in the basement is removed from this model, the fundamental periods are slightly shorter than for Model 1. However, since the base shear in the N-S direction is governed by the minimum base shear from ASCE/SEI 7-16 Equation 12.8-5 and the period used for design of the fixed-base structure in the E-W direction is controlled by the upper limit period, $C_u T_a$, the design base shears are unchanged from those for Model 1.

B.7.2 Building Without Basement, Flexible Base (Model 4)

The response of individual piles to lateral loads is highly nonlinear. It has become increasingly common to consider that nonlinearity directly. Based on extensive testing of full-scale specimens and small-scale models for a wide variety of soil conditions, researchers have developed empirical relationships for the nonlinear *p-y* response of piles that are suitable for use in design. The *p-y* response is sensitive to pile size; soil type and properties; and, in the case of sands, vertical stress, which increases with depth. Pile response to lateral loads is usually computed using computer programs such

as LPile (ENSOFT, 2018). For this example, LPile is used to analyze 22-inch diameter piles for the soil layering shown in Table B-1.

Since the drilled shafts extend into the soft soils near the ground surface, the pile group lateral stiffness for Model 4 shown in Figure B-16 is considerably less than that for Model 2. As a point of reference, for a lateral displacement of 0.49 inches the total lateral load is 146 kip, including 32 kip in each of four drilled shafts and 18 kip of passive pressure resistance. Figure B-17 shows the total lateral load versus head displacement for a range of loads. In this case the best estimate linear stiffness is estimated as 300 kip/inch, with reasonable lower and upper bounds of 215 kip/inch and 430 kip/inch. Axial stiffnesses are the same as those computed for the Model 2.

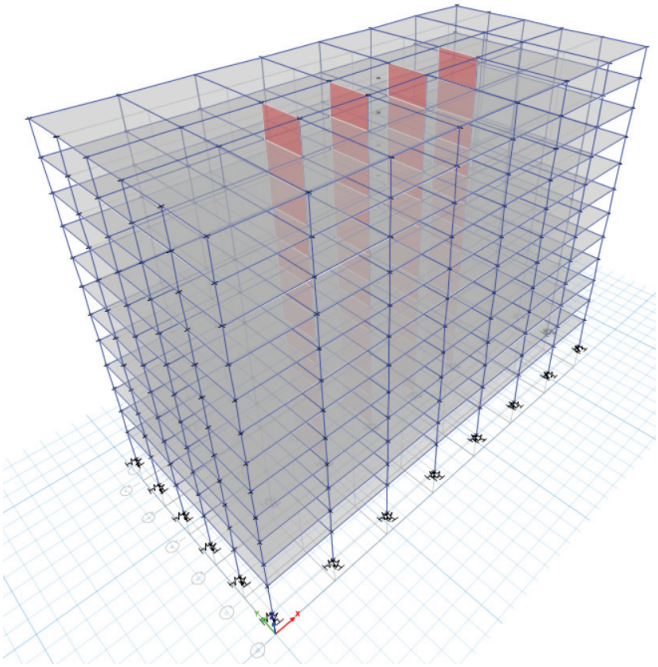

Figure B-16 Analytical model of the example building, with basement removed and flexible base (Model 4).

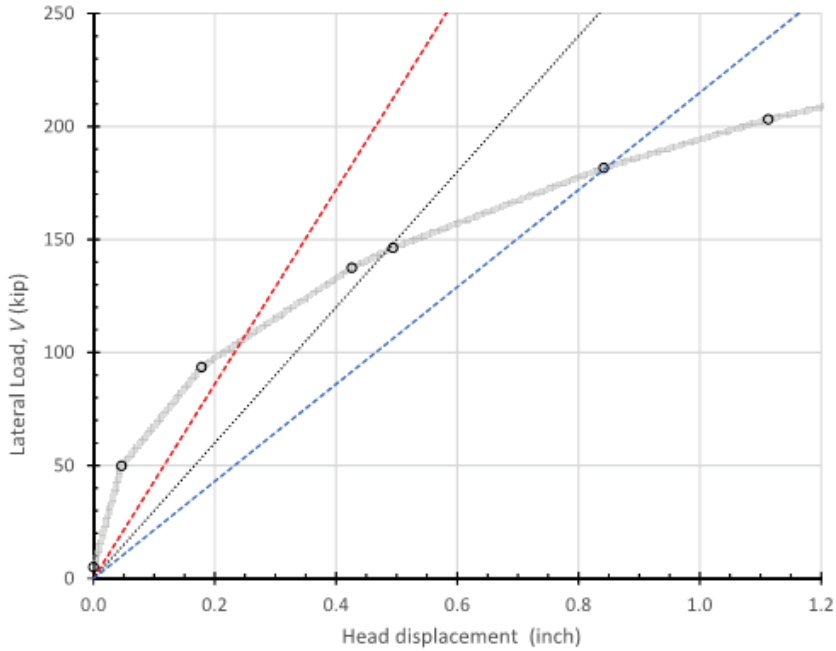

Figure B-17 Pile group lateral stiffness for Models 3 and 4.

B.7.3 Sensitivity to Lower-Bound and Upper-Bound Spring Stiffnesses

Where foundation flexibility is included for linear analysis, ASCE/SEI 7-16 Section 12.13.3 requires use of best estimate "equivalent linear stiffness using soil properties that are compatible with the soil strain levels associated with the design earthquake motion," and consideration of lower-bound and upper-bound variations in stiffness, with the largest values of response being used in design. Similarly, ASCE/SEI 7-16 Section 19.1.1 requires that "both upper and lower bound estimates for the foundation and soil stiffnesses per Section 12.13.3 … be considered." The detailed example calculations and analyses above use best estimate soil springs. The lower- and upper-bound stiffnesses used in this appendix presume they were provided by a geotechnical consultant, based on field measurements of dynamic soil properties. If lower and upper bounds are established without field measurements, ASCE/SEI 7-16 Section 12.13.3 requires a 50% decrease and increase in stiffness. This differs from what ASCE/SEI 41-17 Section 8.4.3 requires (dividing and multiplying by 1 + the coefficient of variation, C_v, but not less than 1.5). Table B-6 summarizes periods and base shears in the E-W direction for all models, including spring stiffness variations for Models 2 and 4. For comparison it also tabulates base shears three variations of the flexible-base conditions: using ASCE/SEI 7-16 Chapter 19 (which reflects period elongation and foundation damping, with limits on maximum reductions per ASCE/SEI 7-16 Equation 19.2-3), using ASCE/SEI 7-16 Section 12.13.3 (which reflects only period elongation), and using ASCE/SEI Chapter 19 but ignoring the limitation computed using ASCE/SEI 7-16 Equation 19.2-3.

Table B-6 Summary of Periods and Base Shears for All Models, E-W Direction

Model	Springs	T (s)	V (kip)	V_{SSI} (kip)	V_{SSI}/V
1	—	1.491	3,470		
2, using ASCE/SEI 7-16 Chapter 19	UB	1.717		3,123	90%
	BE	1.765		3,123	90%
	LB	1.839		3,123	90%
2, using ASCE/SEI 7-16 Section 12.13.3	UB	1.717		2,558	74%
	BE	1.765		2,488	72%
	LB	1.839		2,388	69%
2, using ASCE/SEI 7-16 Chapter 19, no α	UB	1.717		2,414	70%
	BE	1.765		2,331	67%
	LB	1.839		2,216	64%
3	—	1.366	3,470		
4, using ASCE/SEI 7-16 Chapter 19	UB	1.992		3,123	90%
	BE	2.074		3,123	90%
	LB	2.181		3,123	90%
4, using ASCE/SEI 7-16 Section 12.13.3	UB	1.992		2,205	64%
	BE	2.074		2,118	61%
	LB	2.181		2,104	61%
4, using ASCE/SEI 7-16 Chapter 19, no α	UB	1.992		1,993	57%
	BE	2.074		1,907	55%
	LB	2.181		1,807	52%

Although the upper-bound spring stiffnesses used in this example are approximately twice the lower-bound values, the periods and base shears vary by less than 10%. A wider range of bounds would increase this variation, but the work presented here demonstrates relative insensitivity of results.

As discussed above where ASCE/SEI 7-16 Section 12.13.3 is used to account for period elongation effects, design base shear is less than would be computed using ASCE/SEI 7-16 Chapter 19, which limits the total reduction due to SSI. In this example the period elongation effect dominates—making the Chapter 12 process result in more economical designs.

Unfortunately, the manner in which ASCE/SEI 7-16 Section 19.2.1 limits the reduction due to SSI does not distinguish between period elongation and foundation damping. It would be possible to recast Section 19.2.1 so that the α coefficient applies only to the portion of SSI reduction that results from foundation damping. A code change proposal is under consideration to make this clarification.

Appendix C

Helpful Resources

Several documents are recommended as helpful resources for practicing engineers to better understand soil-structure interaction (SSI) and to see additional examples. They include the following, in approximate order of likely interest and value to practicing engineers.

- NIST GCR 12-917-21, *Soil-Structure Interaction for Building Structures*, (NIST, 2012a): This is a comprehensive compilation of SSI information and forms much of the underlying basis of the SSI provisions in both ASCE/SEI 7-16 (ASCE, 2017a) and ASCE/SEI 41-17 (ASCE, 2017b). It discusses the underlying technical basis and includes several significant cases study examples and comparisons of different modeling techniques.
- ASCE/SEI 41-17, *Seismic Evaluation and Retrofit of Existing Buildings*, (ASCE, 2017b): Chapter 8 of this standard covers foundation evaluation and retrofit design. Procedures to develop vertical and horizontal springs are in ASCE/SEI 41-17 Section 8.4. SSI provisions are in ASCE/SEI 41-17 Section 8.5. There are no design examples.
- FEMA P-2006, *Example Application Guide for ASCE/SEI 41-13 Seismic Evaluation and Retrofit of Existing Buildings with Additional Commentary for ASCE/SEI 41-17*, (FEMA, 2018): This document provides design examples for many of the provisions and building types in ASCE/SEI 41-13 (ASCE, 2014) and ASCE/SEI 41-17 (ASCE, 2017b). Chapter 5 discusses the foundation chapter of ASCE/SEI 41-13 including the various methods for modeling the foundation and soil springs. Chapter 9 is a design example of a steel braced frame building, and the example includes a comparison of results between a fixed base and a flexible base model. Chapter 11 is a design example for a nonlinear static analysis of a concrete shear wall building, and the example addresses both kinematic interaction and foundation damping.
- FEMA P-1051, 2015 *NEHRP Recommended Seismic Design Provisions: Design Examples*, (FEMA, 2016): This document provides a series of design examples for the 2015 NEHRP Provisions that form the basis of those adopted into ASCE/SEI 7. Chapter 8 covers SSI and includes

detailed design examples for foundation damping, base slab averaging, and embedment effects.

- *Guidelines for Performance-Based Seismic Design of Tall Buildings, Version 2.03* (PEER, 2017): Section 4.5 of this document addresses foundation modeling and soil-structure interaction. Although the document focuses on tall buildings in general, the discussion is relevant to buildings of all heights.
- ATC-40, *The Seismic Evaluation and Retrofit of Concrete Buildings*, (ATC, 1996): This report addresses the capacity spectrum method for seismic evaluation and design. Chapter 10 covers foundation modeling and evaluation, including vertical and horizontal springs.
- *NEHRP Seismic Design Technical Brief No. 7: Seismic Design of Reinforced Concrete Mat Foundations: A Guide for Practicing Engineers* (NIST, 2012b): Sections 3 and 4 of this document provide a very brief overview of SSI issues as they apply to mat foundations. It references NIST (2012a) for more detailed information.

References

ACI, 2014, *Building Code Requirements for Structural Concrete and Commentary*, ACI 318-14, American Concrete Institute, Farmington Hills, Michigan.

ASCE, 2014, *Seismic Evaluation and Retrofit of Existing Buildings*, ASCE/SEI 41-13, Structural Engineering Institute of American Society of Civil Engineers, Reston, Virginia.

ASCE, 2017a, *Minimum Design Loads and Associated Criteria for Buildings and Other Structures*, ASCE/SEI 7-16, Structural Engineering Institute of American Society of Civil Engineers, Reston, Virginia.

ASCE, 2017b, *Seismic Evaluation and Retrofit of Existing Buildings*, ASCE/SEI 41-17, Structural Engineering Institute of American Society of Civil Engineers, Reston, Virginia.

ATC, 1996, *The Seismic Evaluation and Retrofit of Concrete Buildings*, Applied Technology Council, ATC-40 Report, Redwood City, California.

Boore, D., Thompson, E., and Cadet, H., 2011, "Regional correlations of V_{S30} and velocities averaged over depths less than and greater than 30 meters," *Bulletin of the Seismological Society of America*, Vol. 101, No. 6, pp. 3046–3059, December, doi: 10.1785/0120110071.

Bowles, J.E., 2001, *Foundation Analysis and Design*, Fifth Edition, McGraw-Hill, New York, New York.

CSI, 2016, *SAP2000 Version 18.2*, Computers and Structures, Inc., Walnut Creek, California.

CSI, 2019, ETABS, Computers and Structures, Inc., Walnut Creek, California

ENSOFT, 2018, *LPile 2018 Using Data Format Version 10*, developed by W.M. Isenhower, S-T. Wang, and L.G. Vasquez for ENSOFT, Inc, Austin, Texas.

FEMA, 2005, *Improvement of Nonlinear Static Seismic Analysis Procedure*, FEMA 440, prepared by the Applied Technology Council for the Federal Emergency Management Agency, Washington, D.C.

FEMA, 2016, 2015 *NEHRP Recommended Seismic Design Provisions: Design Examples*, FEMA P-1051, prepared by the Building Seismic Safety Council of the National Institute for Standards and Technology for the Federal Emergency Management Agency, Washington, D.C.

FEMA, 2018, *Example Application Guide for ASCE/SEI 41-13 Seismic Evaluation and Retrofit of Existing Buildings with Additional Commentary for ASCE/SEI 41-17*, FEMA P-2006, prepared by the Applied Technology Council for the Federal Emergency Management Agency, Washington, D.C.

FEMA, 2019, *FEMA P-2006 Training Steel Braced Frame*, training presentation to accompany FEMA P-2006 *Example Application Guide for ASCE/SEI 41-13 Seismic Evaluation and Retrofit of Existing Buildings with Additional Commentary for ASCE/SEI 41-17*, prepared by the Applied Technology Council for the Federal Emergency Management Agency, Washington, D.C.

FEMA, 2020a, 2020 *NEHRP Recommended Seismic Design Provisions for New Buildings and Other Structures, Volume I: Part 1 Provisions, Part 2 Commentary*, FEMA P-2082-1, prepared by the Building Seismic Safety Council for the Federal Emergency Management Agency, Washington, D.C.

FEMA, 2020b, 2020 *NEHRP Recommended Seismic Design Provisions for New Buildings and Other Structures, Volume II: Part 3 Resource Papers*, FEMA P-2082-2, prepared by the Building Seismic Safety Council for the Federal Emergency Management Agency, Washington, D.C.

Gazetas, G., 1991, "Foundation vibrations," *Foundation Engineering Handbook*, 2nd Edition, Chapter 15, H.-Y. Fang, ed., Chapman and Hall, New York, New York.

Givens, M.J., Mylonakis, G., and Stewart, J.P., 2016, "Modular analytical solutions for foundation damping in soil-structure interaction applications," *Earthquake Spectra*, Vol. 32, No. 3, pp. 1749-1768.

Jeremic, B., Yang, H., Wang, H., Lizundia, B., 2020, *Direct Analysis Soil-Structure Interaction Case Studies for the ATC-144 Project*.

Kim, S., and Stewart, J.P., 2003, "Kinematic soil-structure interaction from strong motion recordings," *Journal of Geotechnical and Geoenvironmental Engineering*, Vol. 129, No. 4, pp. 323-335.

Mylonakis, G., Nikolaou, S., and Gazetas, G., 2006, "Footings under seismic loading: Analysis and design issues with emphasis on bridge foundations," *Soil Dynamics and Earthquake Engineering*, Vol. 26, pp. 824-853.

NIST, 2011, *NEHRP Seismic Design Technical Brief No. 4: Nonlinear Structural Analysis for Seismic Design: A Guide for Practicing Engineers*, NIST GCR 11-917-11, prepared by the Applied Technology Council and the Consortium of Universities for Research in Earthquake Engineering for the National Institute of Standards and Technology, Gaithersburg, Maryland.

NIST, 2012a, *Soil-Structure Interaction for Building Structures*, NIST GCR 12-917-21, prepared by the Applied Technology Council and the Consortium of Universities for Research in Earthquake Engineering for the National Institute of Standards and Technology, Gaithersburg, Maryland.

NIST, 2012b, *NEHRP Seismic Design Technical Brief No. 7: Seismic Design of Reinforced Concrete Mat Foundations: A Guide for Practicing Engineers*, NIST GCR 12-917-22, prepared by the Applied Technology Council and the Consortium of Universities for Research in Earthquake Engineering for the National Institute of Standards and Technology, Gaithersburg, Maryland.

NIST, 2016, N*EHRP Seismic Design Technical Brief No. 1: Seismic Design of Reinforced Concrete Special Moment Frames: A Guide for Practicing Engineers, Second Edition*, NIST GCR 16-917-40, prepared by the Applied Technology Council for the National Institute of Standards and Technology, Gaithersburg, Maryland.

Pais, A., and Kausel, E., 1988, "Approximate formulas for dynamic stiffnesses of rigid foundations," *Soil Dynamics and Earthquake Engineering*, Vol. 7, No. 4, pp. 213-227.

PEER, 2017, *Guidelines for Performance-Based Seismic Design of Tall Buildings, Version 2.03*, Report No. 2017/06, developed by the Pacific Earthquake Engineering Research Center (PEER) as part of the Tall Buildings Initiative (TBI), Berkeley, California.

Yim, C-S, and Chopra, A.K., 1984, "Earthquake response of structures with partial uplift on Winkler foundation," *Earthquake Engineering and Structural Dynamics*, Vol. 12, pp. 263-281.

Glossary

This *Guide* uses terminology consistent with the definitions in ASCE/SEI 7-16. Where ASCE/SEI 7-16 does not have explicit definitions, other sources are used and are identified below.

Base slab averaging: Kinematic SSI of a shallow (nonembedded) foundation caused by wave incongruence over the base area.

Direct analysis approach: An approach to SSI modeling where the soil and structure are included within the same model and analyzed as a complete system. The soil is often represented as a continuum (e.g., finite elements) along with foundation and structural elements, transmitting boundaries at the limits of the soil mesh, and interface elements at the edges of the foundation (adapted from NIST, 2012a).

Embedment effects: Kinematic SSI embedment effects in which foundation-level motions are reduced as a result of ground motion reduction with depth below the free surface in structures with embedded foundations (adapted from NIST, 2012a).

Foundation and soil flexibility: The vertical, horizontal, and rotational flexibility of foundation elements and the soil. Incorporation of foundation and soil flexibility typically increases the flexible-base fundamental period of building as compared to the fixed-based period where foundation and soil flexibility are not included.

Foundation input motion: Motion that effectively excites the structure and its foundation.

Free-field motion: Motion at ground surface in absence of structure and its foundation.

Inertial SSI (or inertial interaction): The dynamic interaction between the structure, its foundation, and the surrounding soil caused by the foundation input motion.

Kinematic SSI (or kinematic interaction): The modification of free-field ground motion caused by nonvertical incident seismic waves and spatial incoherence; the modification yields the foundation input motion.

Per FEMA (2018), "it is important to distinguish between rigid (fixed) or flexible foundations and rigid or flexible footings… A rigid base (also known as fixed base) or flexible base foundation refers to the flexibility of the structural footing and soil system as a boundary condition of the building, whereas a rigid or flexible footing refers to the structural footing element itself relative to the supporting soil stiffness. Therefore, the foundation may be modeled and evaluated with a combination of foundation and footing flexibility. For instance, a structure can have a rigid footing with a flexible foundation where the flexibility of the soil is modeled with springs." Figure 5-1 of FEMA (2018) illustrates three potential combinations: (1) rigid footing with rigid (fixed base) foundation where there are no springs for soil flexibility; (2) rigid footing with a flexible foundation where there are springs for soil flexibility; and (3) flexible footing with a flexible foundation where there are also springs for soil flexibility.

Radiation damping: The damping in the soil-structure system caused by the generation and propagation of waves away from the foundation, which are caused by dynamic displacements of the foundation relative to the free-field displacements.

Shear wave velocity: The effective shear wave velocity, v_s, is defined as $v_s = (G / \rho_s)^{1/2}$, where G is the effective soil shear modulus and ρ_s is the soil mass density. Effective shear wave velocity is calculated over different depths in ASCE/SEI 7-16 Sections 19.3 and 19.4 depending on how the parameter is used, and it is influenced by the level of ground shaking. (Adapted from NIST, 2012a).

Shear wave: An *S* wave, or shear wave, is a seismic body wave that shakes the ground back and forth perpendicular to the direction the wave is moving. (From https://earthquake.usgs.gov/learn/glossary/?term=S%20wave, last accessed November 5, 2020).

Soil damping: The hysteretic (material) damping of the soil.

Structure-to-Soil Stiffness Ratio: A ratio defined as $h' / (v_s T)$, where h' is the effective height of the structure, v_s is the effective shear wave velocity over the depth of interest, and T is the fundamental period of the structure. See Chapter 3 for details. (Adapted from NIST, 2012a).

Substructure Approach: An approach to SSI modeling where the SSI problem is partitioned into distinct parts that are combined to formulate the complete solution. Proper consideration of SSI effects in a substructure approach requires: (1) an evaluation of free-field soil motions and corresponding soil material properties; (2) an evaluation of transfer functions

to convert free-field motions to foundation input motions; (3) incorporation of springs and dashpots (or more complex nonlinear elements) to represent the stiffness and damping at the soil foundation interface; and (4) a response analysis of the combined structure spring/dashpot system with the foundation input motion applied. (Adapted from NIST, 2012a).

Symbols

This *Guide* uses symbols and notations consistent with referenced standards, primarily ASCE/SEI 7-16. This section presents a list of symbols and notations used in this *Guide* and their definitions as presented in the referenced standards. The list is not exhaustive; for comprehensive definition of symbols and notation, please refer to the referenced standards identified within the sections of the *Guide*.

If a symbol or notation is referenced in ASCE/SEI 7-16, this is not indicated in the list below, as this constitutes most of the entries. If a symbol or notation is from a different reference document, a citation is provided.

A_{base} Area of foundation footprint if the foundation components are interconnected laterally

A_T Tributary area

B Width of footing, typically taken as the dimension perpendicular to the direction of seismic force unless noted otherwise

B_{bsa} Bessel function used to compute base slab averaging effects

B_f Width of footing, typically taken as the dimension perpendicular to the direction of seismic force D unless noted otherwise

B_{SSI} Factor to adjust the design response spectrum and MCE_R response spectrum

C_d Deflection amplification factor

C_s Seismic response coefficient

C_t Coefficient from ASCE/SEI 7-16 Table 12.8-2 that depends on the structural system

D Depth from the ground surface to the bottom of the foundation

F_a Factor to adjust spectral acceleration in the short period range for site class

F_v Factor to adjust spectral acceleration at 1 s for site class

F_x Pseudo-seismic force applied at floor level x

G Soil shear modulus

G_0 Initial or maximum soil shear modulus

$[G/G_0]$ The effective shear modulus ratio beneath the foundation over a depth specified in ASCE/SEI 7-16 Section 19.3 and used in ASCE/SEI 7-16 Table 19.3-2

I_e Importance Factor

K_{sur} Stiffness at ground surface

K_{xx} Rotational foundation stiffness

K_y Translational foundation stiffness

L Length

M^* Effective mass for the first mode

M_{OT} Total overturning moment induced on the element by seismic forces applied at and above the level under consideration

P Passive pressure

P_{ult} Ultimate pressure

R Response modification coefficient

RRS_{bsa} Ratio of response spectra factor for base slab averaging

RRS_e Ratio of response spectra factor for embedment

S_1 Spectral response acceleration parameter at a 1-second period, obtained from response acceleration contour maps

S_a Spectral response acceleration

S_d Spectral displacement

S_{D1} Design, 5% damped, spectral response acceleration parameter at a period of 1 s

S_{DS} Design, 5% damped, spectral response acceleration parameter at short periods

S_{MS} the MCE_R, 5% damped, spectra response acceleration parameter at short periods adjusted for site class effects

T Fundamental period of the building in the direction under consideration

$\tilde{T}$ Fundamental period of the building using a model with a flexible base

T_a Approximate fundamental period of the building

T_{xx} Fundamental translational period of SSI system

T_y Fundamental translational period of SSI system

W Effective seismic weight of a building, including total dead load and applicable portions of other gravity loads

b_0 Parameter relating effective foundation area to building period

b_e Effective foundation size, ft

d_i Thickness of any soil or rock layer i between 0 and 100 ft

e Foundation embedment depth

h' Effective structure height, measured from base of foundation to the center of mass of the fundamental mode

h^* Effective height of building

h_n Height above base to roof level

h_x Height from base to floor level x

k Soil modulus parameter

k_{sv} Winkler spring stiffness in vertical direction, expressed as force/unit displacement/unit area

r Effective depth for foundation rotation

v_s The average effective shear wave velocity over a depth specified in ASCE/SEI 7-16 Sections 19.3 and 19.4 specific to the SSI effect being computed determined using v_{so} and ASCE/SEI 7-16 Table 19.3-1 or a site-specific geotechnical study

v_{so} The average shear wave velocity for soils beneath the foundation at small strain levels (10^{-3}% or less) over a depth specified in ASCE/SEI 7-16 Sections 19.3 and 19.4 specific to the SSI effect being computed. Note that the small strain shear wave velocity in ASCE/SEI 7-16 Chapter 19 is the same as the shear wave velocity used in ASCE/SEI 7-16 Chapter 20 for site class determination

$[v_s/v_{so}]$ The effective shear wave velocity ratio beneath the foundation over a depth specified in ASCE/SEI 7-16 Sections 19.3 and 19.4 and used in ASCE/SEI 7-16 Table 19.3-1

w_i Portion of the effective seismic weight located on or assigned to floor level *i*

z_p Effective profile depth from NIST (2012a)

Δ_{ADVE} Average drift of adjoining vertical elements of the seismic force-resisting system over the story below the diaphragm under consideration, under tributary lateral load equivalent to that used in the computation of δ_{MDD}

Ψ Dimensionless factor, function of Poisson's ratio

Ω_0 Overstrength factor

α Coefficient that accounts for the reduction in base shear caused by foundation damping SSI

α_{xx} Dimensionless factor, function of dimensionless frequency, a_0

β Effective viscous damping ratio of the structure, taken as 5% unless otherwise justified by analysis

β_0 Effective viscous damping ratio of the soil-structure system

β_f Effective viscous damping ratio relating to foundation-soil interaction

β_{rd} Radiation damping ratio

β_s Soil hysteretic damping ratio

β_{xx} Rotational foundation damping coefficient

β_y Translational foundation damping coefficient

γ Average unit weight of the soils over a depth of *B* below the base of the structure

δ_{MDD} Computed maximum in-plane deflection of the diaphragm under lateral load

μ Expected ductility demand

ν Poisson's ratio

Project Participants

FEMA Oversight

Mike Mahoney (Project Officer)
Federal Emergency Management Agency
500 C Street, SW
Washington, DC 20472

Robert D. Hanson (Subject Matter Expert)
Federal Emergency Management Agency
500 C Street, SW
Washington, DC 20472

ATC Management and Oversight

Jon A. Heintz (Program Executive, Program Manager)
Applied Technology Council
201 Redwood Shores Parkway, Suite 240
Redwood City, California 94065

Ayse Hortacsu (Project Manager)
Applied Technology Council
201 Redwood Shores Parkway, Suite 240
Redwood City, California 94065

Project Technical Committee

Bret Lizundia (Project Technical Director)
Rutherford + Chekene
375 Beale Street, Suite 310
San Francisco, California 94105

C.B. Crouse
AECom
1111 3rd Avenue, Suite 1600
Seattle, Washington 98101

Steve Harris
Simpson Gumpertz & Heger, Inc.
100 Pine Street, Suite 1600
San Francisco, California 94111

Boris Jeremic
Department of Civil and Environmental Engineering
University of California Davis
Davis, California 95616

Jonathan P. Stewart
Department of Civil and Environmental Engineering
University of California Los Angeles
5731 Boelter Hall
Los Angeles, California 90095

Michael Valley
Magnusson Klemencic Associates
909 Fifth Avenue, Unit 305
Seattle, Washington 98164

Project Review Panel

Peter Lee
Skidmore, Owings, Merrill
One Maritime Plaza
San Francisco, California 94111

Sissy Nikolaou
(ATC Board Representative)
WSP USA
One Penn Plaza
New York, New York 10119

Robert Pekelnicky
Degenkolb Engineers
375 Beale Street, Suite 500
San Francisco, California 94105

Payman Khalili Tehrani
SC Solutions
1261 Oakmead Parkway
Sunnyvale, California 94085

Working Group Members

Timothy D. Ancheta
RMS
7575 Gateway Blvd., Suite 300
Newark, California 94560

Laurel Jiang
Rutherford + Chekene
375 Beale Street, Suite 310
San Francisco, California 94105

Ricardo Henoch
Skidmore, Owings, Merrill
One Maritime Plaza
San Francisco, California 94111

Gyimah Kasali
Rutherford + Chekene
375 Beale Street, Suite 310
San Francisco, California 94105

Lisa M. Star
17664 Sarentina Court
Bellflower, California 90706

Christos Tokas
920 El Dorado Way
Sacramento, California 95819

Jiejing Zhou
Skidmore, Owings, Merrill
One Maritime Plaza
San Francisco, California 94111

FEMA

FEMA P-2091